NASA Conference Publication 10012
Part 3

NASA Workshop on Computational Structural Mechanics 1987

Nancy P. Sykes, *Editor*
Analytical Services and Materials, Inc.
Hampton, Virginia

Proceedings of a workshop sponsored by
the National Aeronautics and Space
Administration and held at
Langley Research Center
Hampton, Virginia
November 18–20, 1987

February 1989

(NASA-CP-10012-Pt-3) NASA WORKSHOP ON COMPUTATIONAL STRUCTURAL MECHANICS 1987, PART 3 (NASA. Langley Research Center) 419 p CSCL 20K

N89-29799
--THRU--
N89-29810
Unclas
H1/39 0211967

National Aeronautics and
Space Administration

Preface

This document contains the proceedings of the NASA Workshop on Computational Structural Mechanics, held at NASA Langley Research Center, November 18-20, 1987. The workshop was sponsored jointly by NASA Langley Research Center and NASA Lewis Research Center.

The purpose of the workshop was to allow participants in Langley's and Lewis' Computational Structural Mechanics (CSM) research programs to meet and to share research objectives and accomplishments. The intent was to encourage a cooperative Langley/Lewis CSM program in which Lewis concentrates on engine structures applications, Langley concentrates on airframe and space structures applications, and all participants share technology of mutual interest.

The workshop was organized into the following three sessions:

- I Concurrent Processing Methods and Applications
- II Advanced Methods & Testbed/Simulator Development
- III Computational Dynamics

Session I dealt with parallel processing methods and languages, new computer hardware, and software architecture to exploit parallel computers.

Session II dealt with the Langley CSM Testbed, the Lewis Engine Structures Computational Simulator, and Structural Analysis Technology involving finite elements, boundary elements, and probabilistic approaches.

Session III dealt with advanced methods for structural dynamics.

The use of trade names or names of manufacturers in this publication does not constitute an official endorsement of such products or manufacturers, either expressed or implied, by the National Aeronautics and Space Administration.

W. Jefferson Stroud

With the exception of a few adjustments made primarily for the purpose of uniformity, all papers have been published as received.

—Editor

CONTENTS

* Published under separate cover

Part 2*

SESSION II - ADVANCED METHODS & TESTBED/SIMULATOR DEVELOPMENT

* Published under separate cover

Part 3

SESSION III - COMPUTATIONAL DYNAMICS

N89
29800
UNCLAS

BOUNDARY ELEMENTS FOR STRUCTURAL ANALYSIS

Work carried ~~out in part~~
Under Contract NAS3-23697
NASA Program ~~Manager – C. C.~~ Chamis

Pratt & Whitney
Commercial Engine Business

This talk is intended to discuss the status of the boundary element method (BEM) for structural analysis, both in terms of the present and anticipated capabilities of the method and in terms of the incorporation of the method in the design/analysis process, particularly for gas turbine engine components.

The three-dimensional work discussed was carried out largely under the support of a National Aeronautics and Space Administration contract (NAS3-23697, "3D Inelastic Analysis Methods for Hot Section Components") with Dr. C. C. Chamis of NASA-Lewis Research Center as program manager. The BEST3D (Boundary Element Stress Technology - 3-Dimensional) code was developed jointly by Pratt & Whitney (R. B. Wilson and N. M. Miller) and the Civil Engineering Department of the State University of New York at Buffalo (P. K. Banerjee, S. Ahmad, D. Henry, G. Dargush, S. Raveendra). The two-dimensional work discussed represents a long period of development at Pratt & Whitney, originating in the work of Dr. T. A. Cruse and D. W. Snow in the mid-1970's, and more recently including the participation of Dr. Banerjee and his colleagues.

TOPICS

- Current 2D/axisymmetric capabilities
- BEST3D development effort
- Selected BEST3D analyses
- BEM incorporation in design/analysis process

It is not possible, in a brief talk, to give a comprehensive review of the BEM. After an extremely short review of the basis of the method, the talk will focus on the topics listed on this slide.

REVIEW

FOR A HOMOGENEOUS ELASTIC STRUCTURE

$$\mu\frac{\partial^2 u_i}{\partial x_j^2} + (\lambda + \mu)\frac{\partial^2 u_j}{\partial x_i \partial x_j} + f = 0$$

CAN BE MANIPULATED USING:

Reciprocal Work Theorem

Point Force (Kelvin) Solutions

Limiting Operations

TO OBTAIN

The BEM is based on the application of the Reciprocal Work Theorem with (for isotropic materials) the Kelvin point load solution and its derived traction solution integrated against the desired boundary displacements and tractions. Suitable limiting operations as the point of load application is moved to the boundary allow derivation of the boundary integral equation (BIE), a boundary constraint equation relating the surface displacements and tractions for any well-posed elasticity problem. Since this (singular) integral equation can not generally be solved in closed form, the practical application of the BEM is based on the solution of a numerical approximation to this equation. In currently available general purpose codes it is usual to model both the part geometry and the displacement and traction variation using isoparametric interpolation functions.

1. **INTERIOR DISPLACEMENT EQUATION**

$$u_j(\xi) = \int_S (t_i(x) G_{ij}(x,\xi) - F_{ij}(x,\xi) u_i)\, dS + \int_V G_{ij}(x,\xi) f_i(x)\, dV$$

2. **BOUNDARY INTEGRAL EQUATION**

$$(\delta_{ij} - c_{ij}) u_j(\xi_0) = \int_S (t_i(x) G_{ij}(x,\xi_0) - F_{ij}(x,\xi_0) u_i(x))\, dS + \int_V G_{ij}(x,\xi_0) f_i(x)\, dV$$

3. **INTERIOR STRESS (STRAIN) EQUATION**

	F/E	BEM
Primitive Variables	Displacements only	Displacements and tractions
Geometry Approximation	Throughout structure	Surface only
Dominant Cost	Equation solution	Surface integration

The computing and modelling characteristics of the BEM are fundamentally different from those of the finite element method. For elastic analysis the BEM models both displacements and tractions, on the surface of the body only, so that no interior geometric discretization is required. The dominant analysis cost for the BEM is the surface integration. This is due to the pairwise nature of the BIE - a complete surface integration must be done for each point which will contribute degrees of freedom to the final system equations. Typically, in a 3D BEM structural analysis, surface integration will require 60% to 75% of analysis time, while the solution of the system equations will consume only about 10% of the time.

The development of parallel processing computing environments can be expected to have a major impact on BEM analysis. Each substructure in a BEM analysis uses a distinct set of input data and generates a distinct set of output data. Questions of memory contention and/or data transfer conflict can be expected to be relatively minor - for either shared or local memory configurations. Exploitation of parallel computing is also possible within each substructure, although more code modification would be required.

2D/AXISYMMETRIC BEM CAPABILITIES

- **PRODUCTION**

  elastic, substructured analysis for isotropic, anisotropic, composite materials

  arbitrary geometry

  general boundary conditions (mixed displacement/traction, springs)

  plane strain/stress fracture mechanics capability

  body forces

The two-dimensional (plane stress and plane strain) and axisymmetric capabilities of the BEM codes presently in use at Pratt & Whitney are listed on this chart. The code is highly integrated within a graphics pre-/post-processing environment. Commercial packages are also available which possess many, but not all of the capabilities outlined.

thermal stress

- DEVELOPMENT/RESEARCH

  plasticity, creep

  natural frequency/mode shape determination

  material inhomogeneity

Advanced capabilities are presently being incorporated in the Pratt & Whitney code, and will become available in the production version over the next year.

2D STRESS CONCENTRATION CALIBRATION

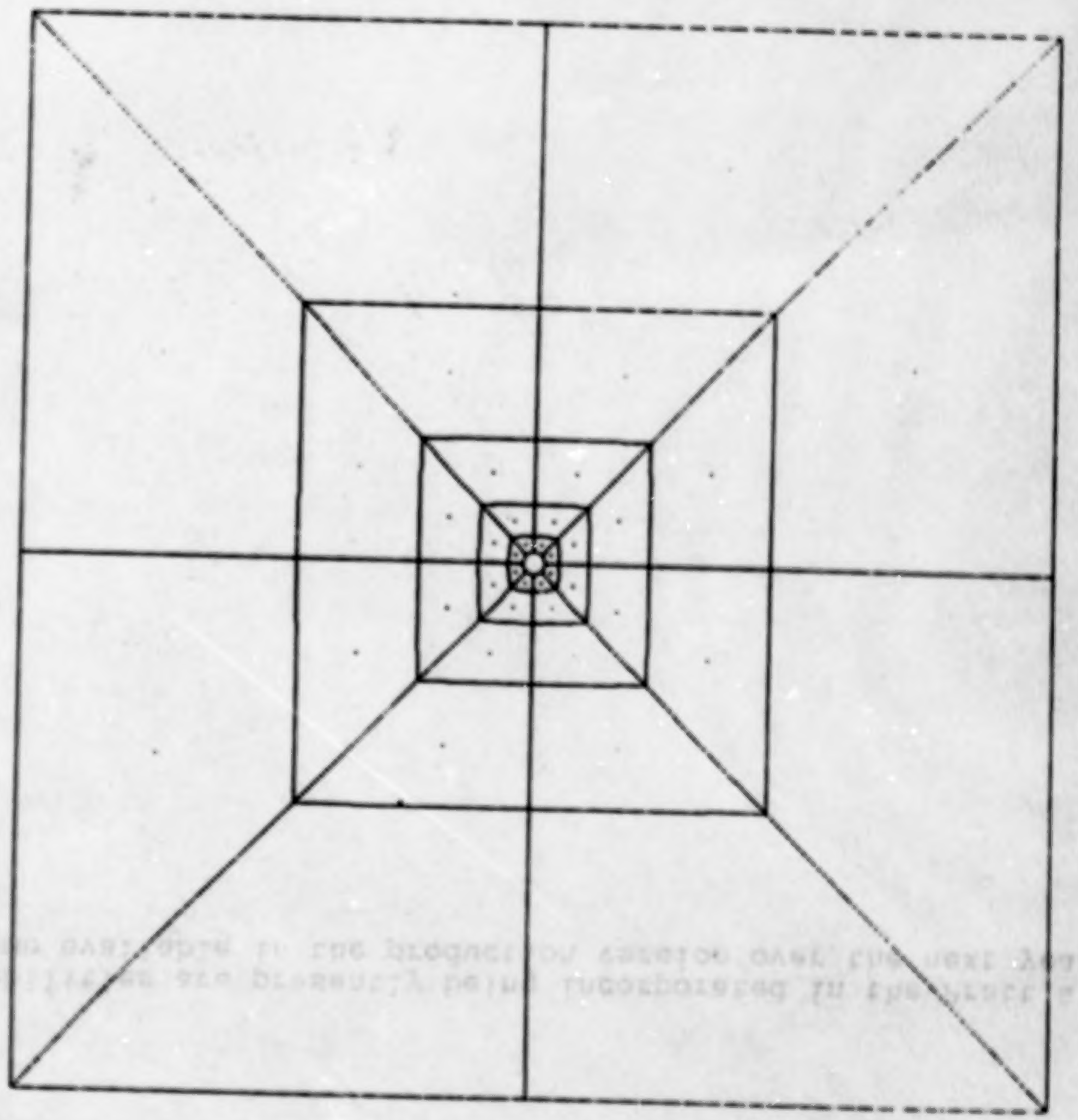

As an illustration of the advantages obtained through BEM use, for suitable problem types, consider a calibration study recently completed for the Pratt & Whitney code. An effectively infinite plate with a circular hole was subjected to a variety of loads, both remote and on the hole surface. Analyses were carried out using the P&W BEM code and the MARC finite element code (8 noded isoparametric plane stress elements). The meshes used two, four and eight elements per quadrant. Isotropic, orthotropic and layered composite materials were considered.

Plane Stress Orthotropic Plate with Hole
Normal Pressure

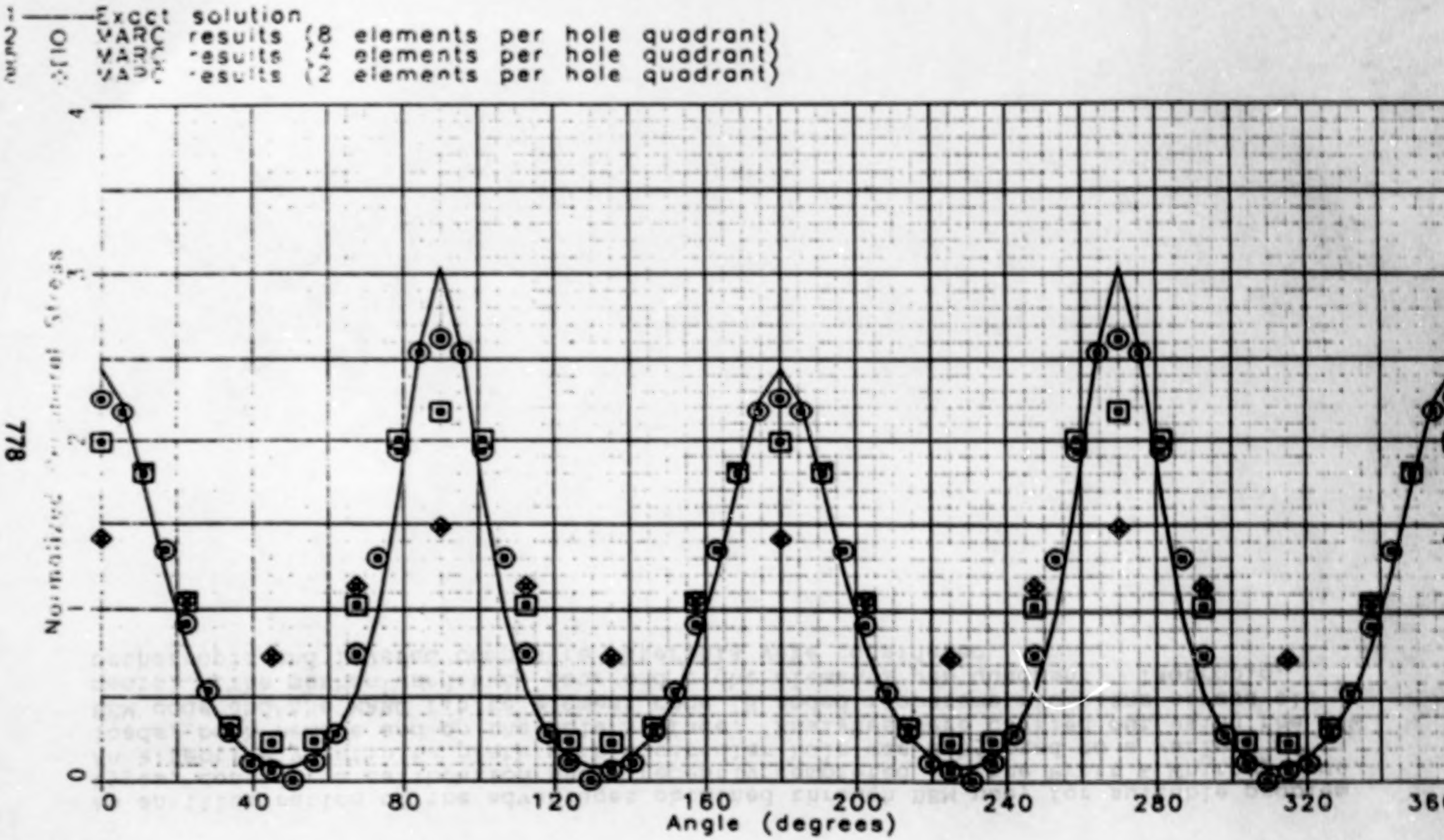

778

For an orthotropic material subject to a normal pressure on the hole surface, The MARC analyses underpredict the peak tangential stress by 50%, 20% and 12% respectively, compared to the exact solution in Lekhnitski. For an isotropic material the same models give somewhat better accuracies of 20%, 5% and 2% respectively. For this problem the anisotropic material produces a significant change in the result, since for an isotropic material the tangential stress on the hole is unity at all locations.

Plane Stress Orthotropic Plate with Hole
Normal Pressure

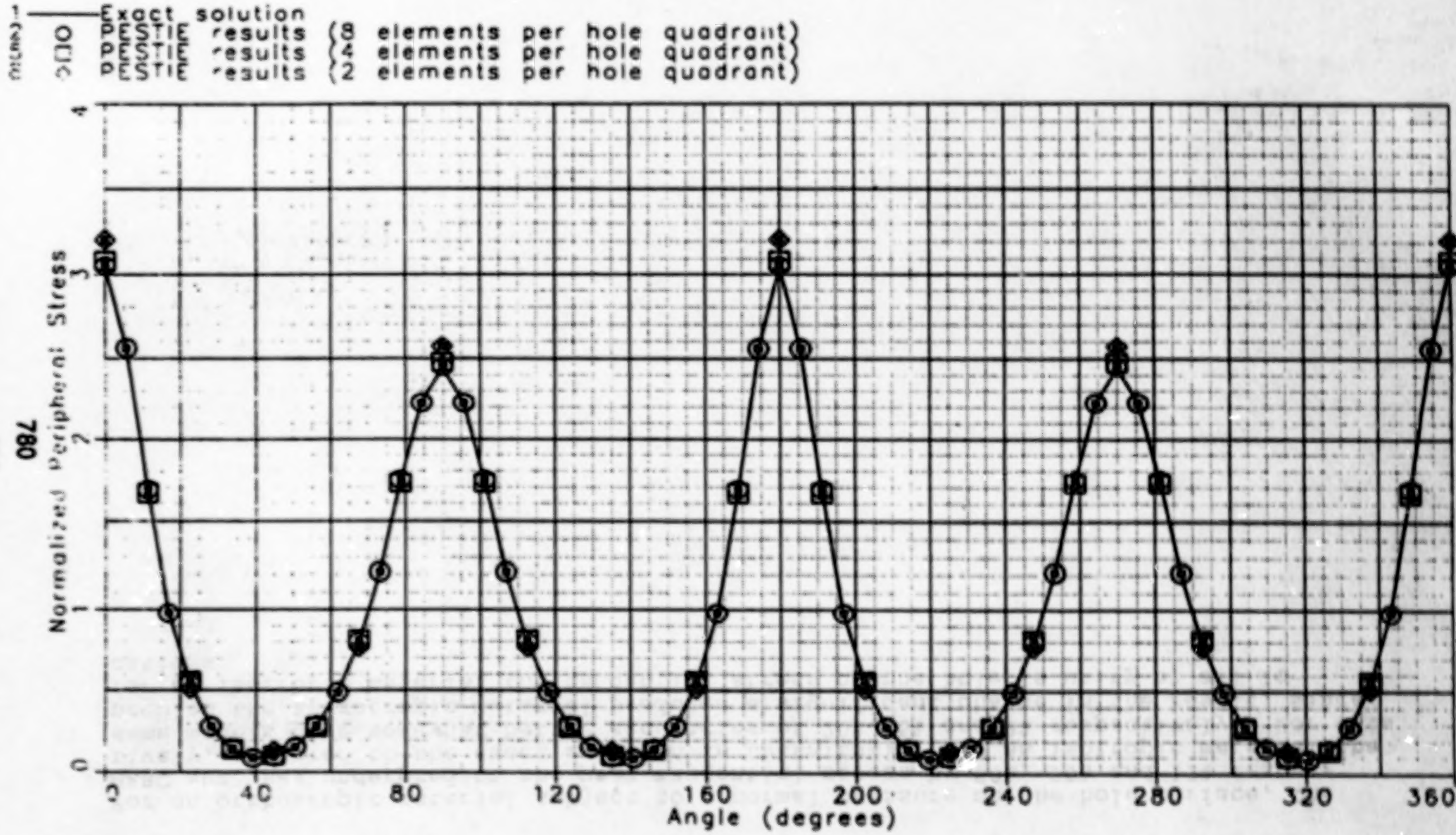

The corresponding BEM models give accuracies of 7%, 3% and 1%, respectively (extremely close to the 6%, 1.5% and .4% obtained for the isotropic case). Significantly, no modification of the BEM model is required to maintain accuracy as the complexity of the material changes.

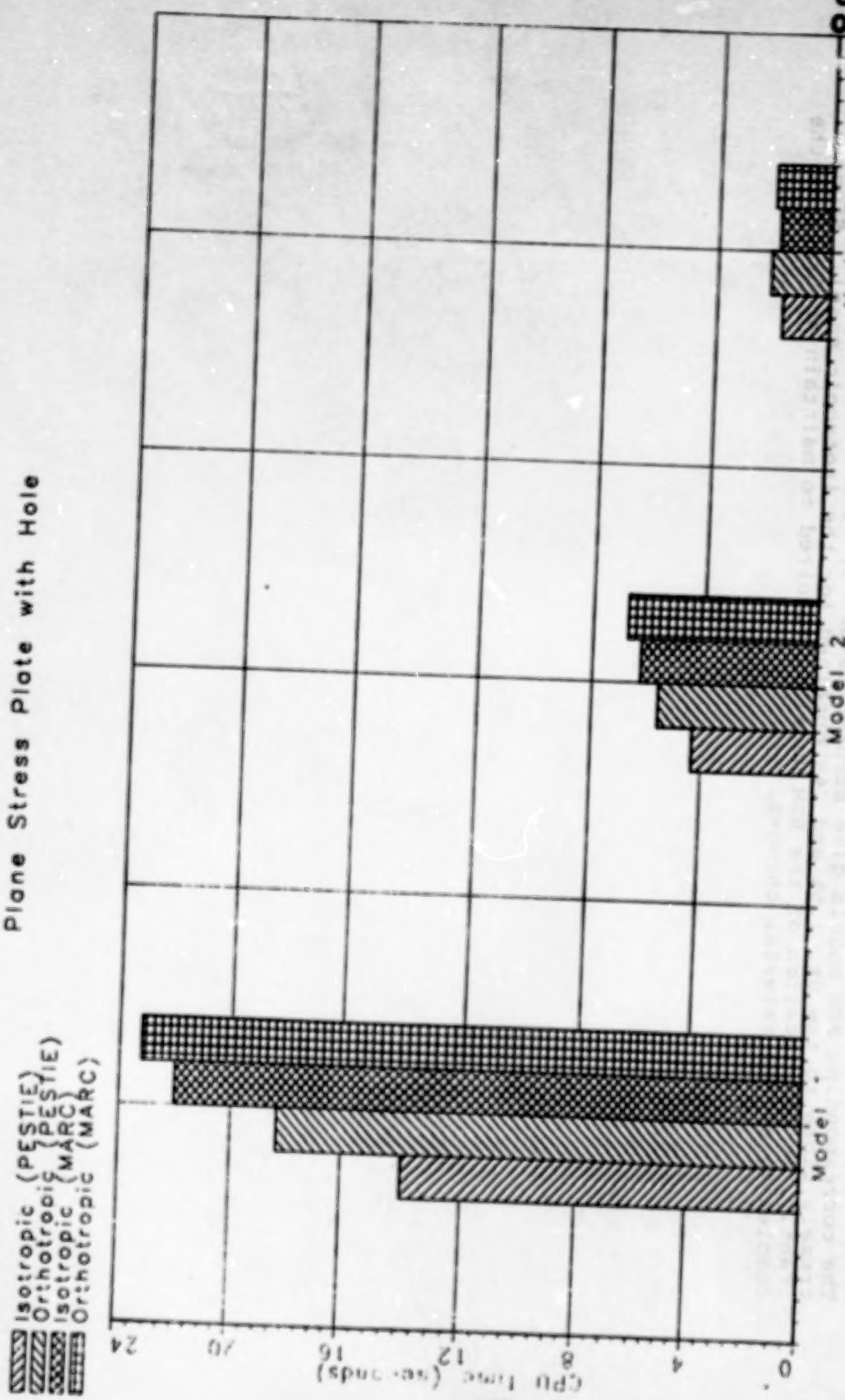
Plane Stress Plate with Hole
Isotropic (PESTIE)
Orthotropic (PESTIE)
Isotropic (MARC)
Orthotropic (MARC)
Model 1
Model 2
Model 3
0
4
8
12
16
20
24
CPU Time (seconds)

Computing times for the coarse model were essentially equal for the BEM and finite element analyses. For the finest mesh the finite element orthotropic analysis took 1.3 times as long as the BEM analysis. More importantly, the coarse BEM model gave better accuracy than the finest finite element model, yielding a CPU time ratio of better than 11 to 1 for (not quite) equivalent accuracy.

This problem illustrates the significant advantages obtainable with the BEM, both in analysis time and, equally significantly, in the fact that the BEM analysis gave consistent results for all materials.

BEST3D GOALS

- Develop structural analysis tool distinct from, and complementary to, the finite element method.
- Address wide range of problem types - elastic, inelastic, dynamic, vibration.

BOUNDARY ELEMENT METHOD (BEM) SELECTION

- Applicability to various problem types established.
- BEM suitable for complex geometries.
- Attractive for resolution of high gradients.

BEST3D is a general purpose BEM structural analysis code developed by Pratt & Whitney and the State University of New York at Buffalo under NASA contract NAS3-23697.

Major goals of the program were:

1. Development of a general purpose structural analysis tool applicable to problems not amenable to finite element solution

2. Development of analysis calibration capability for problems in which experimental data is lacking.

Previous experience with the BEM indicated that it was the most promising basis for developing this alternative method.

BEST3D (Boundary Element Stress Technology - 3D)

STRATEGY

- o Consider general geometry and boundary conditions
- o Organize code to accommodate all problem types within one structure
- o Make code expandable
- o Aim for machine independence
- o Avoid competition with professionals in pre-/post-processing and linear algebra

BEST3D development was planned to produce a single general purpose structural analysis code. Major emphasis was placed on the treatment of general geometry and boundary conditions and on the development of fundamental analysis capabilities. No major work was undertaken in the areas of pre-/post-processing.

BEST3D OVERVIEW

- 42,000 lines of new source code (FORTRAN 77)
- Implemented on HP, VAX, CRAY and IBM systems
- Major capabilities include:
  - elastic and inelastic analysis
  - forced response analysis
  - transient elastodynamics
  - natural frequency/mode shape calculations
  - substructuring for all problem types

BEST3D is a large code, but is written in standard Fortran 77. It has been successfully implemented on a variety of computing systems. Major capabilities are summarized on the chart.

MAJOR ADVANCES

- Time embedded dynamic formulation
- Complex variable forced response calculation
- 3D, real variable eigenvalue calculation
- Application of particular integrals to thermal stress, plasticity
- BEM variable stiffness plasticity

Major advances have been made during the development of BEST3D, both in the creation of new BEM analysis capabilities and in the incorporation of available capabilities (for the first time) in a general purpose code. Of particular importance is the fact that the all capabilities are made available for substructured analysis, a necessity for practical utilization of the program.

BEST3D PLASTICITY

- o Representation of initial stress/strain
  - Volume cells
  - Particular solutions
- o Solution algorithms
  - Iterative
  - Variable stiffness

A major feature of BEST3D is the provision of a very complete plasticity capability for substructured analysis. In BEM analysis of problems with material nonlinearity it is necessary to provide a description of the variation of plastic strain in the interior of the part. Two different techniques for this description are available in BEST3D, as are two different solution algorithms. Both the use of particular solutions in plasticity and the variable stiffness solution algorithm are new developments carried out as part of the NASA contract referred to previously.

The availability of a variety of independent plasticity algorithms within BEST3D allows calibration of the code by running the same problem using different solution sequences.

PERFORATED PLATE

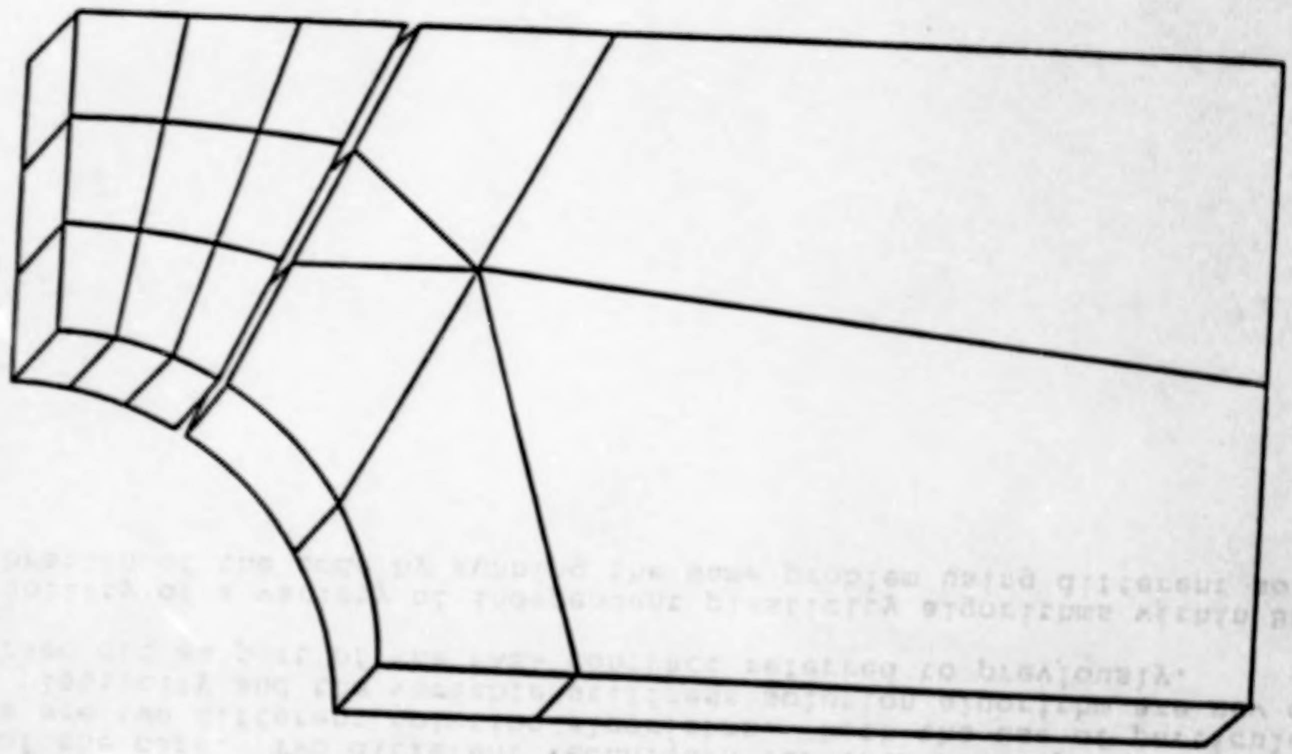

The classical problem of a tension loaded perforated plate was analyzed using the two region BEST3D model shown. Plastic strain distribution was modelled only in the region near the root of the notch, since the other region remains elastic. The model shown represents one quarter of the physical specimen because of symmetry considerations.

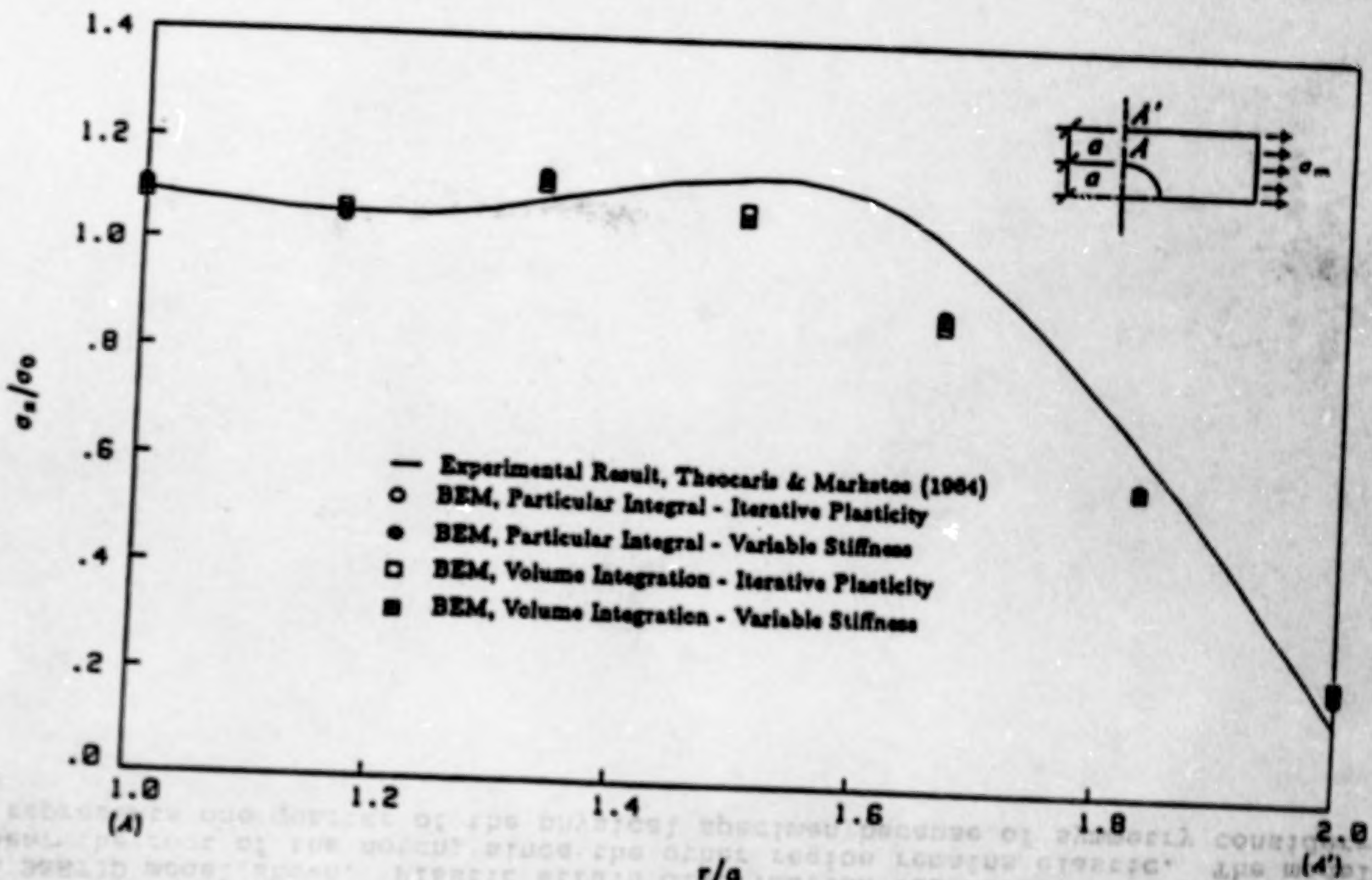

1.4
1.2
1.0
.8
.6
.4
.2
.0
σ_s/σ_0
1.0
(A)
1.2
1.4
1.6
1.8
2.0
(A')
r/a
a
a
A
A'
σ_m
Experimental Result, Theocaris & Marketos (1964)
BEM, Particular Integral - Iterative Plasticity
BEM, Particular Integral - Variable Stiffness
BEM, Volume Integration - Iterative Plasticity
BEM, Volume Integration - Variable Stiffness

The stress distribution at the root of the notch is shown for all four possible combinations of plastic strain representation and solution strategy. For the load applied the plastic front is 60% of the way from the hole surface to the free surface of the specimen. There is excellent agreement among all four solutions. Departures from the experimental data are due primarily to lack of detailed knowledge of the plastic properties of the actual material used. The BEM results are essentially identical to finite element results obtained using a variable stiffness algorithm and the same material properties as those used in the BEM analyses.

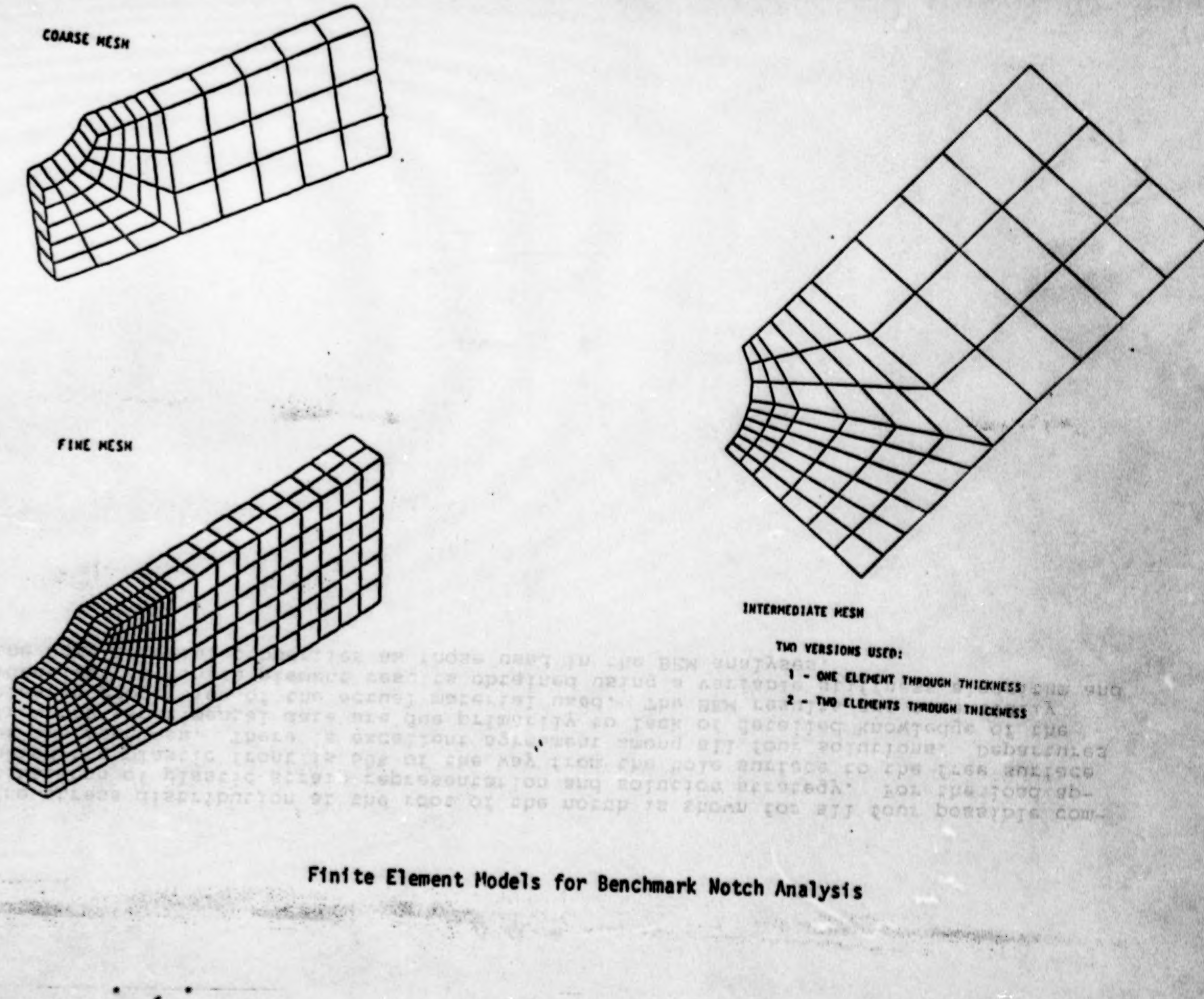

Finite Element Models for Benchmark Notch Analysis

A variety of finite element models were used for the nonlinear (MARC and MHOST) analysis of the NASA Benchmark Notch specimen. The specimen notch is typical of those found in turbine attachments. Use of the finest model shown was required to obtain good agreement with cyclic experimental data.

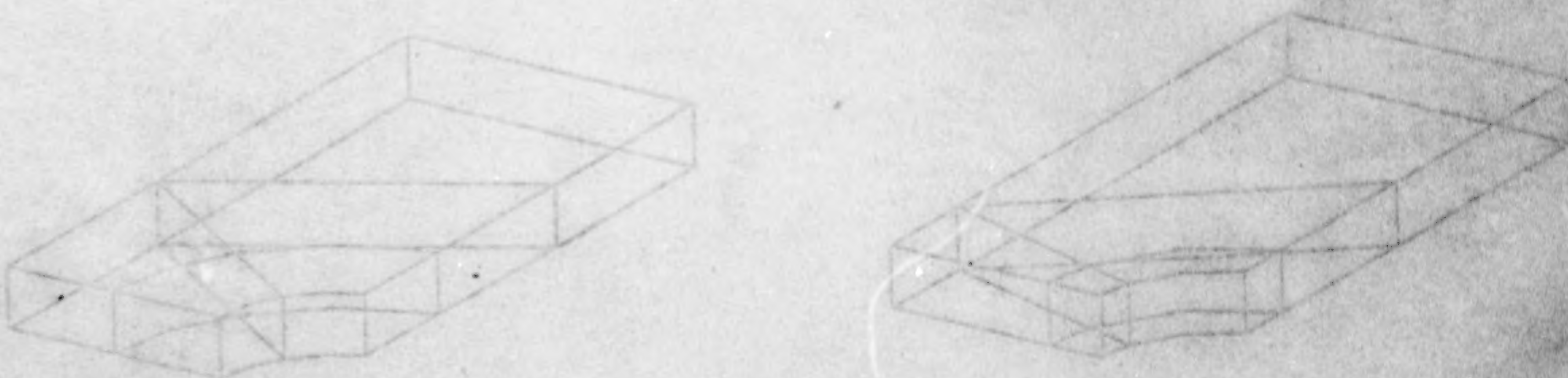

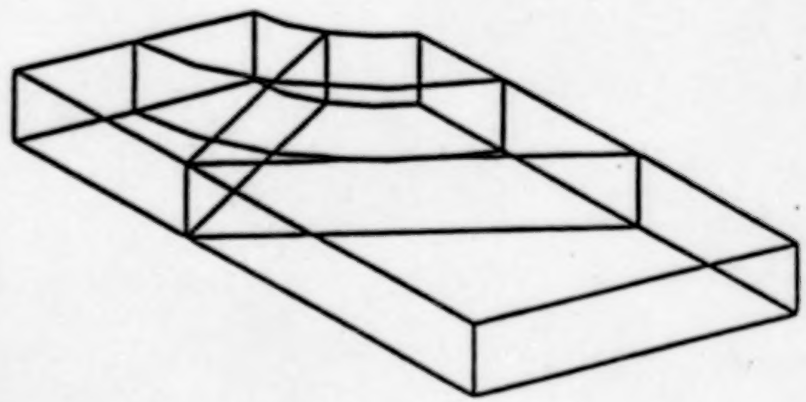

EQUALLY SPACED MESH

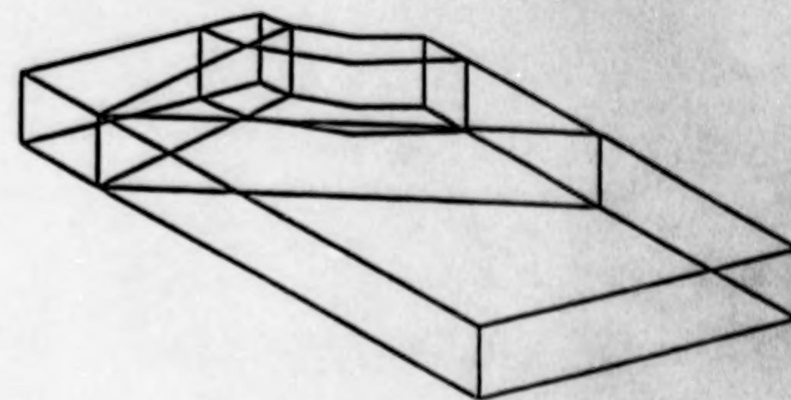

WEIGHTED MESH

Boundary Element Models for Benchmark Notch Analysis

Several BEM models were also used for the analysis of the same geometry. Proper weighting of element sizes in the region of expected stress concentrations is very effective in improving accuracy for a given mesh.

MANUAL MODE

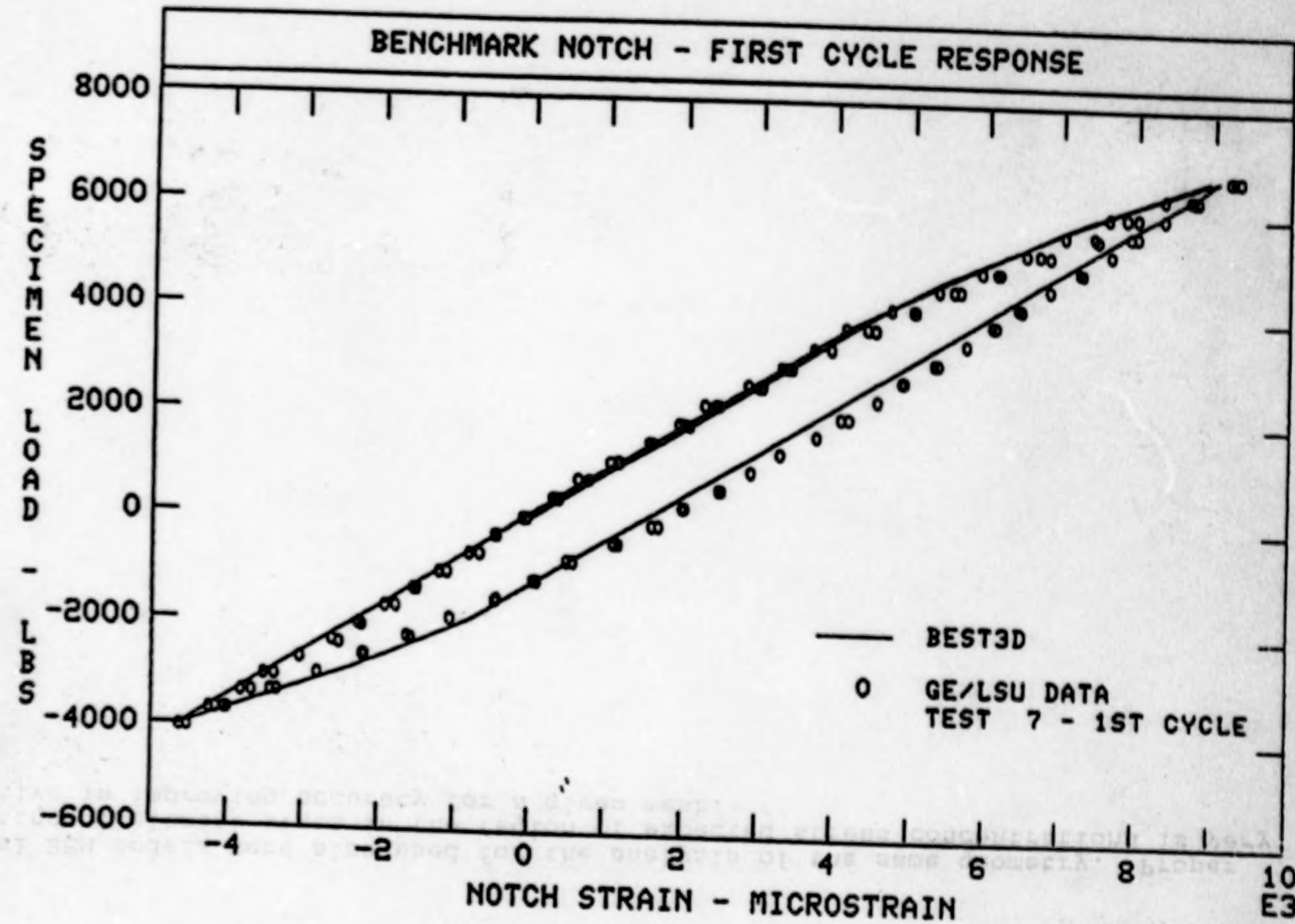
BENCHMARK NOTCH - FIRST CYCLE RESPONSE
SPECIMEN LOAD - LBS
8000
6000
4000
2000
0
-2000
-4000
-6000
-4
-2
0
2
4
6
8
10
E3
NOTCH STRAIN - MICROSTRAIN
BEST3D
O GE/LSU DATA
TEST 7 - 1ST CYCLE

Use of the weighted mesh shown on the previous chart gave good agreement with experimentally measured strains at the notch root, over two and one-quarter load cycles. Use of the finest finite element model gave equivalent results, in about twice the CPU time.

RESIDUAL STRESS IN QUENCHED BAR

- Entire load thermal
- Steep plastic gradients
- Data available
- Axisymmetric analysis
- Volume cells, iteration used

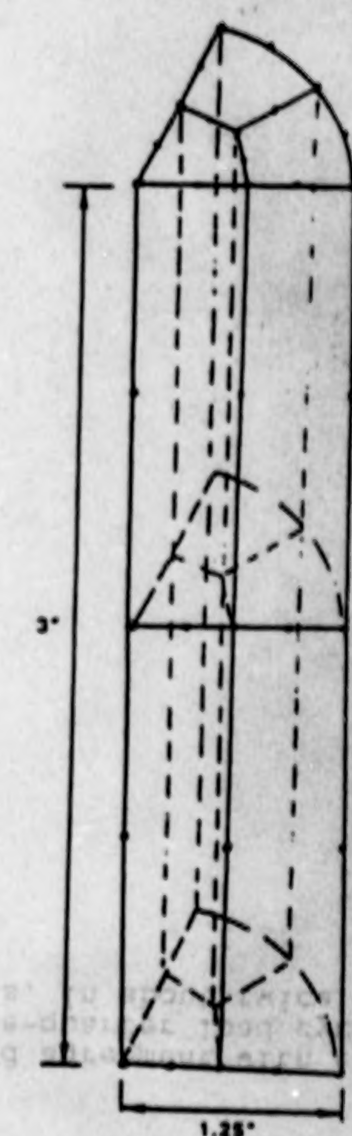

A problem of significant interest in the gas turbine industry is the development of residual stress in large parts during forming and heat treatment. BEST3D was used to analyze a test in which a cylindrical bar was rapidly quenched from 1250° F and the residual stresses subsequently measured. Two nominally identical specimens were used in the experimental work.

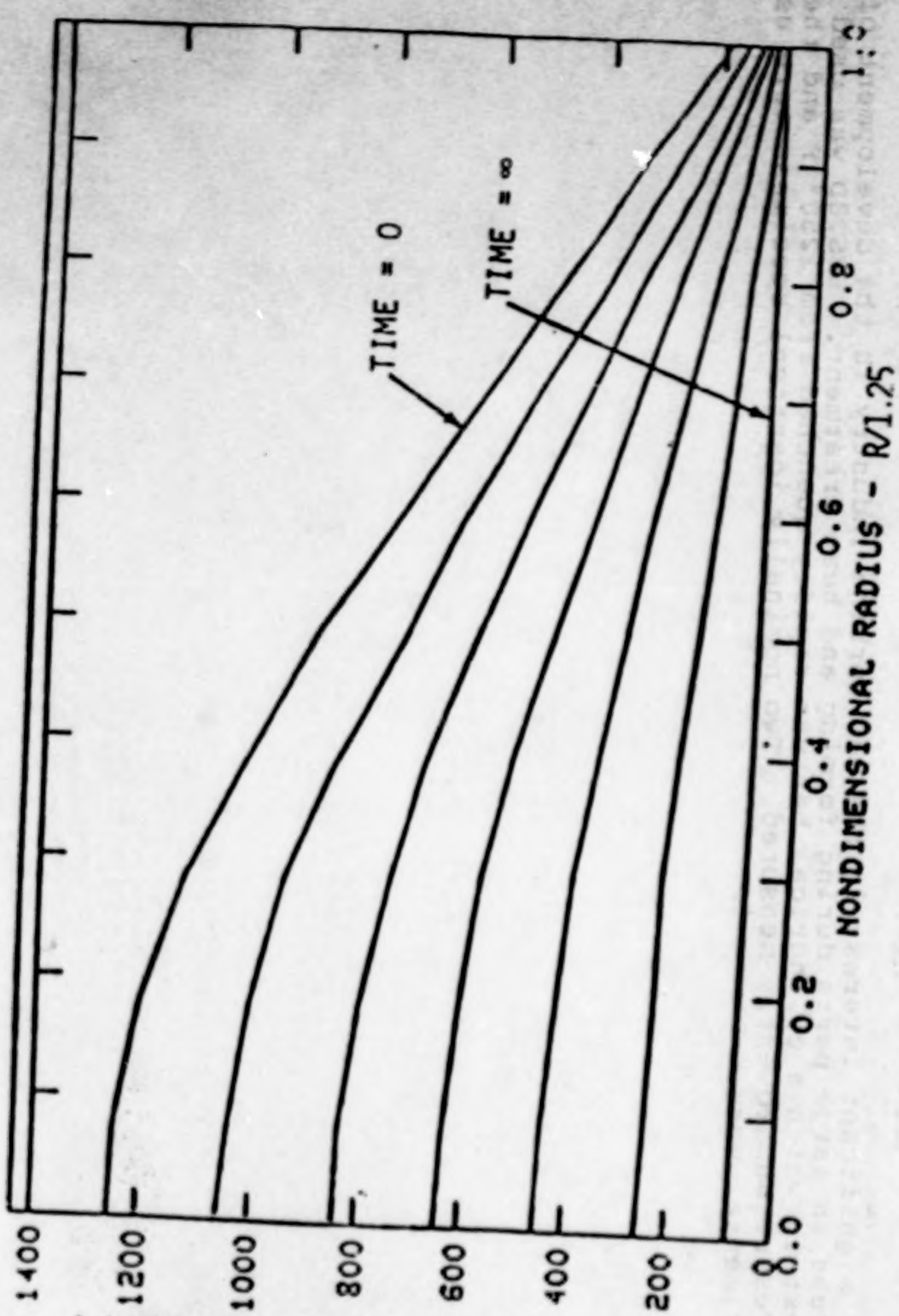
TIME = 0
TIME = ∞
TEMPERATURE - DEG F
1400
1200
1000
800
600
400
200
0
0.0
0.2
0.4
0.6
0.8
1.0
NONDIMENSIONAL RADIUS - R/1.25

The temperature gradient was initially very severe (over 1000° F between the surface and center of the specimen), dropping to essentially zero at large times.

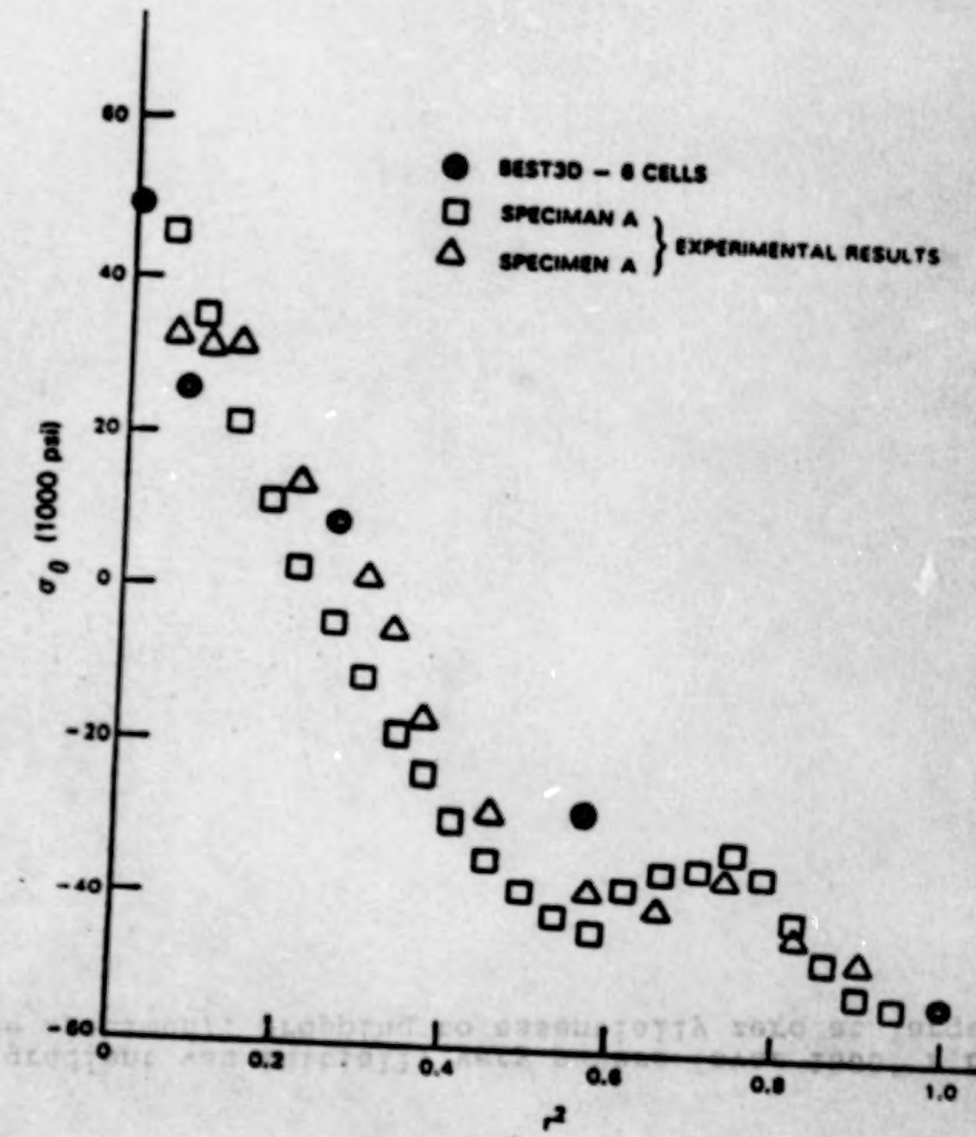

BEST3D – 8 CELLS
SPECIMAN A
SPECIMEN A
EXPERIMENTAL RESULTS
σ_θ (1000 psi)
60
40
20
0
-20
-40
-60
0
0.2
0.4
0.6
0.8
1.0
r^2

The BEST3D analysis shows good agreement with the experimentally measured stresses, even for the relatively coarse model used.

VIBRATI N ISOLATION

- o Goal is to calculate effectiveness of trenches for isolation of sensitive equipment
- o Time harmonic analysis used

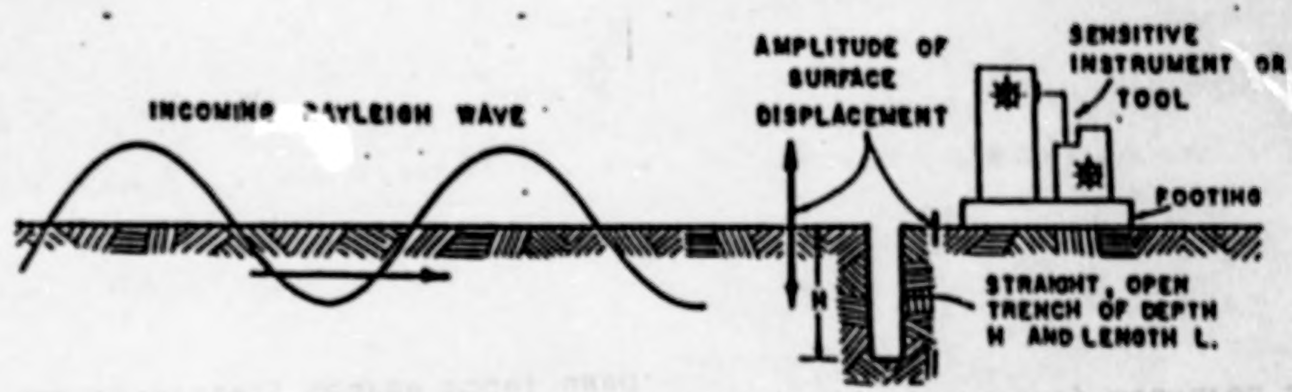

To calibrate the dynamic capabilities of BEST3D a BEM model vas constructed to evaluate the effectiveness of trenches for the vibration isolation of sensitive equipment.

Passive Isolation Testing

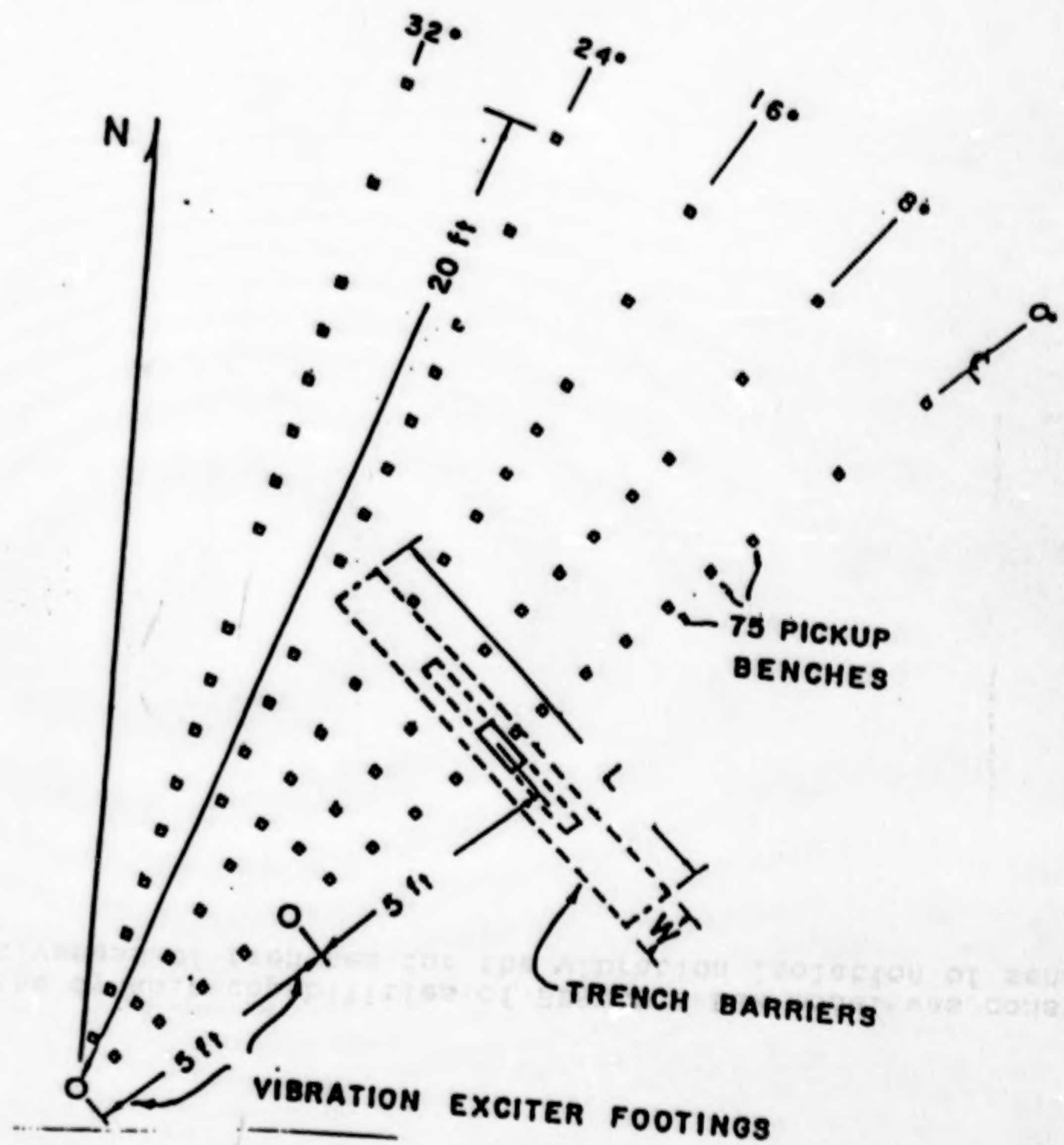

Extensive test data is available for this problem. The relative locations of the exciter, trench and vibration pickups are shown on this chart.

Substructured BEST3D Analysis Required

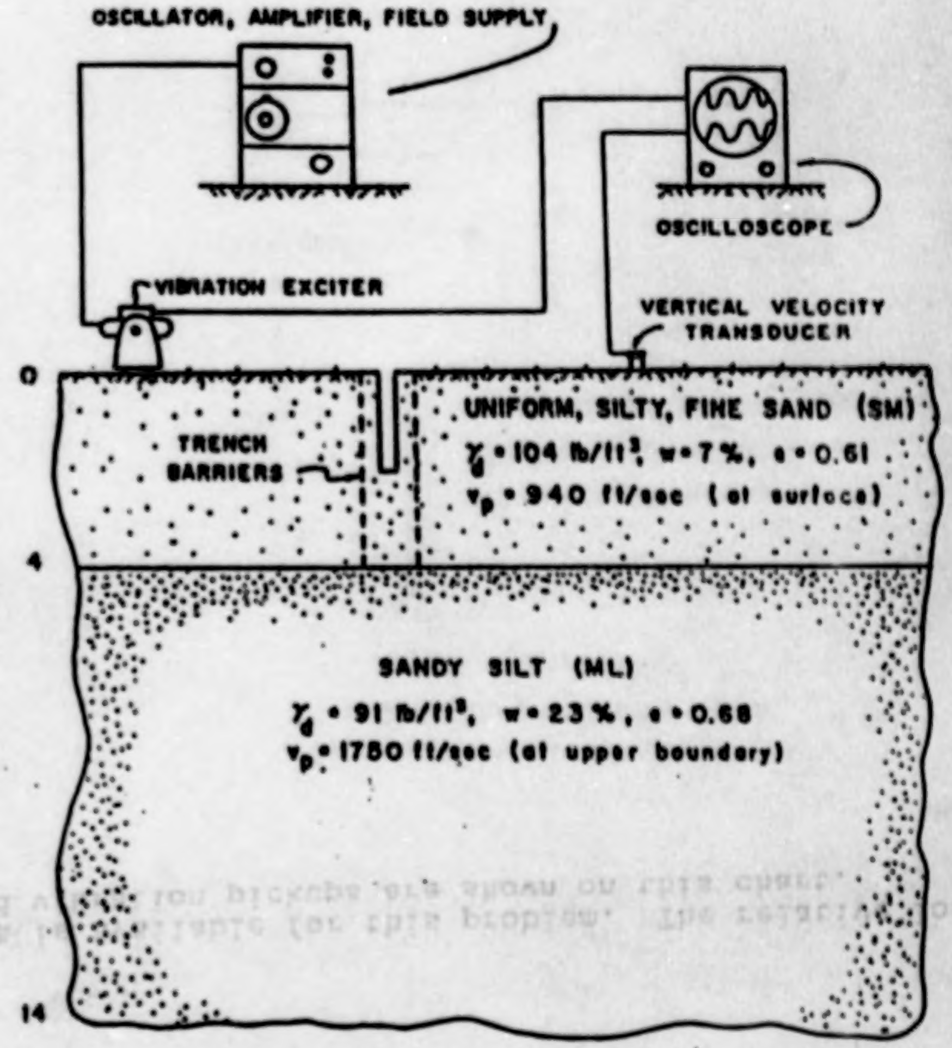

The inhomogeneous nature of the soil required the use of a substructured BEST3D analysis. The use of infinite boundary elements, automatically incorporating the radiation condition at infinity, eliminated the need for any modelling of far field boundaries.

Amplitude Reduction Factor Contours

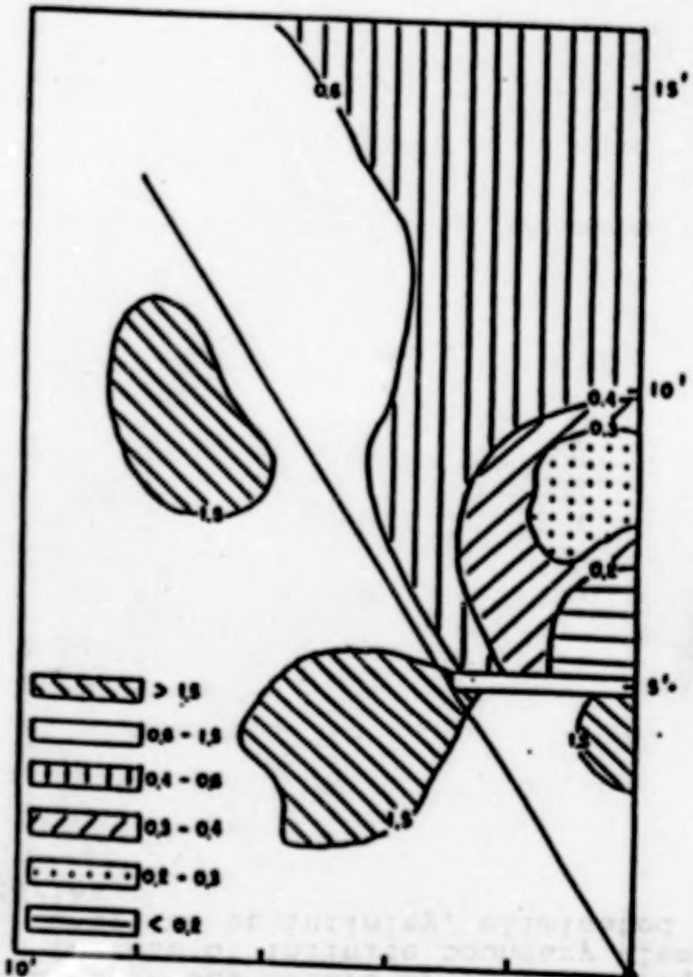

BEST3D

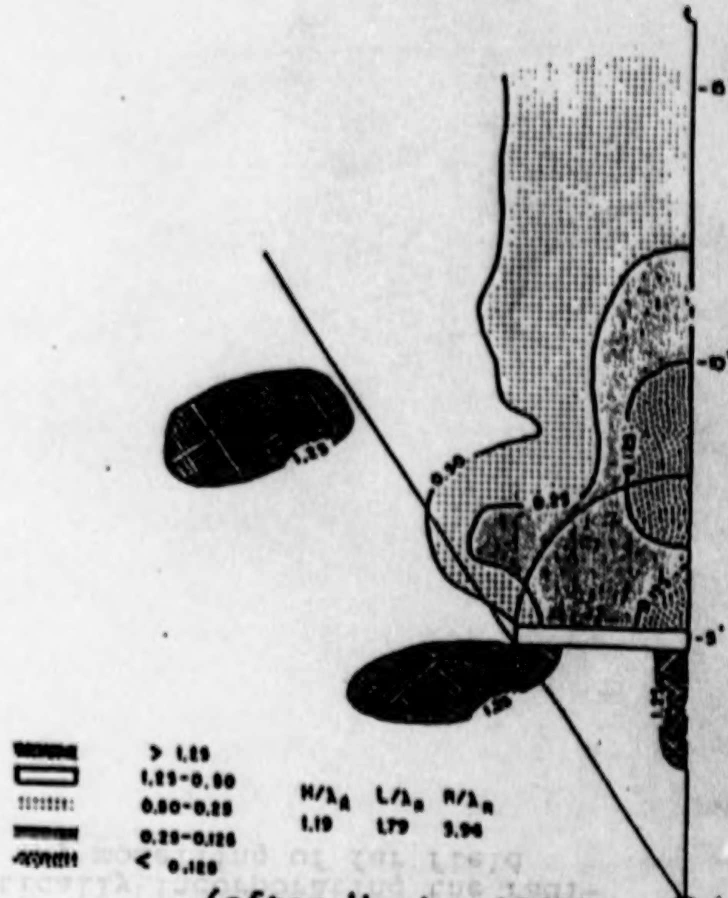

(after Woods, 1968)

experimental

BEST3D predictions of amplitude reductions and amplifications show good agreement with the experimental results.

BEM USE IN DESIGN/ANALYSIS

- Communication with existing geometry and pre-/post-processing codes required
- Rapid job turnaround required – for elastic analyses

  .5 to 2 days for 2D (with iterations)

  2 to 10 days for 3D
- Calibration sufficient for intended use

The fundamental requirement for the incorporation of the BEM in practical design/analysis is the ability to produce credible results fast enough to impact the design or development process. The analysis turnaround time required is highly dependent on the type and complexity of the analysis involved. The degree of calibration required is also dependent on the intended use of the BEM results. Replacing an existing design system requires a much more thorough calibration process than does the use of a new tool simply for the ranking of a number of candidate designs.

COMPRESSOR DOVETAIL ANALYSIS

- o BEM replacing FEM
- o Calibration done
- o Interactive system

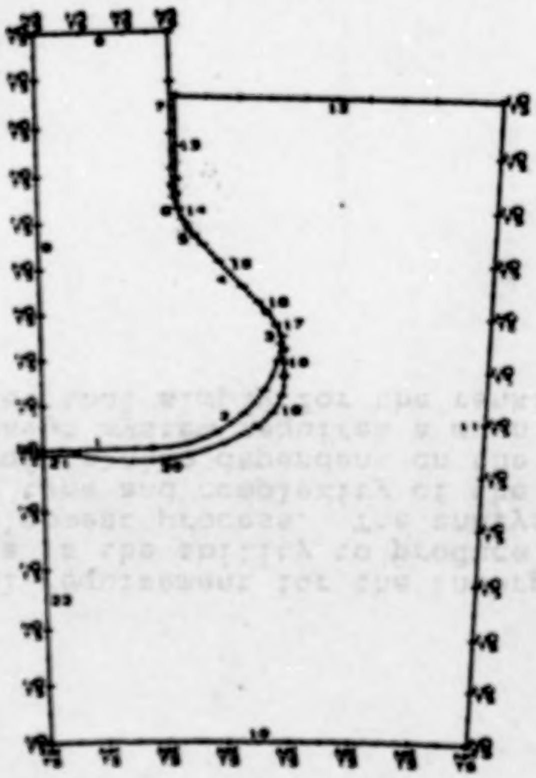

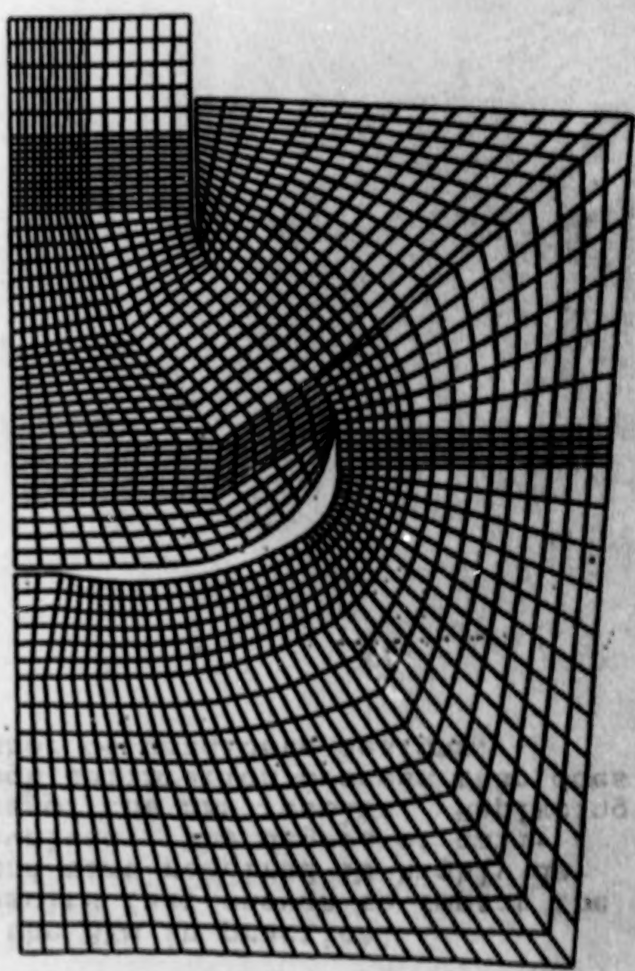

Pratt & Whitney is presently in the process of applying its interactive two-dimensional BEM system to the determination of stress concentrations in compressor dovetails. A typical finite element model previously used for these studies is shown, together with a BEM model of the same geometry. The BEM analysis is interactive, while the finite element analysis requires a batch (usually overnight) run.

Compressor Blade Dovetail Fillet Stress Kt Study
BEST2D vs 2D Finite Element

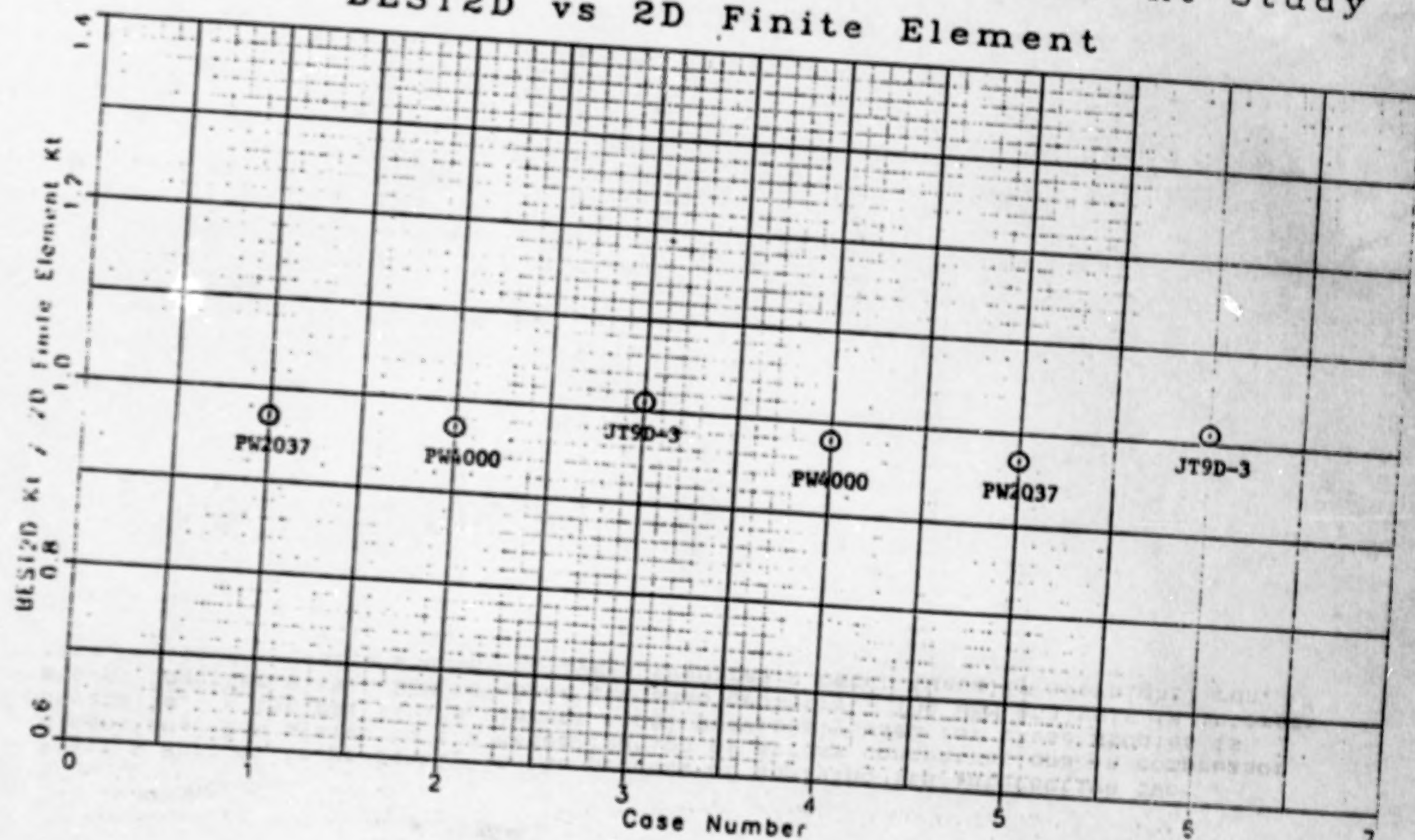

The new BEM system shows excellent agreement with the old system for a variety of actual engine geometries.

PRE/POST PROCESSING FOR BEST3D

- Solid modeller output available as

  IGES files

  (faceted) surface definitions

- These files can be input to existing FE preprocessors

- BEST3D models generated in terms of 6/8 node plate elements

- Local implementation should be a 2-4 week process

TIE BOLT HEAD
(SINGLE CUT BACK)

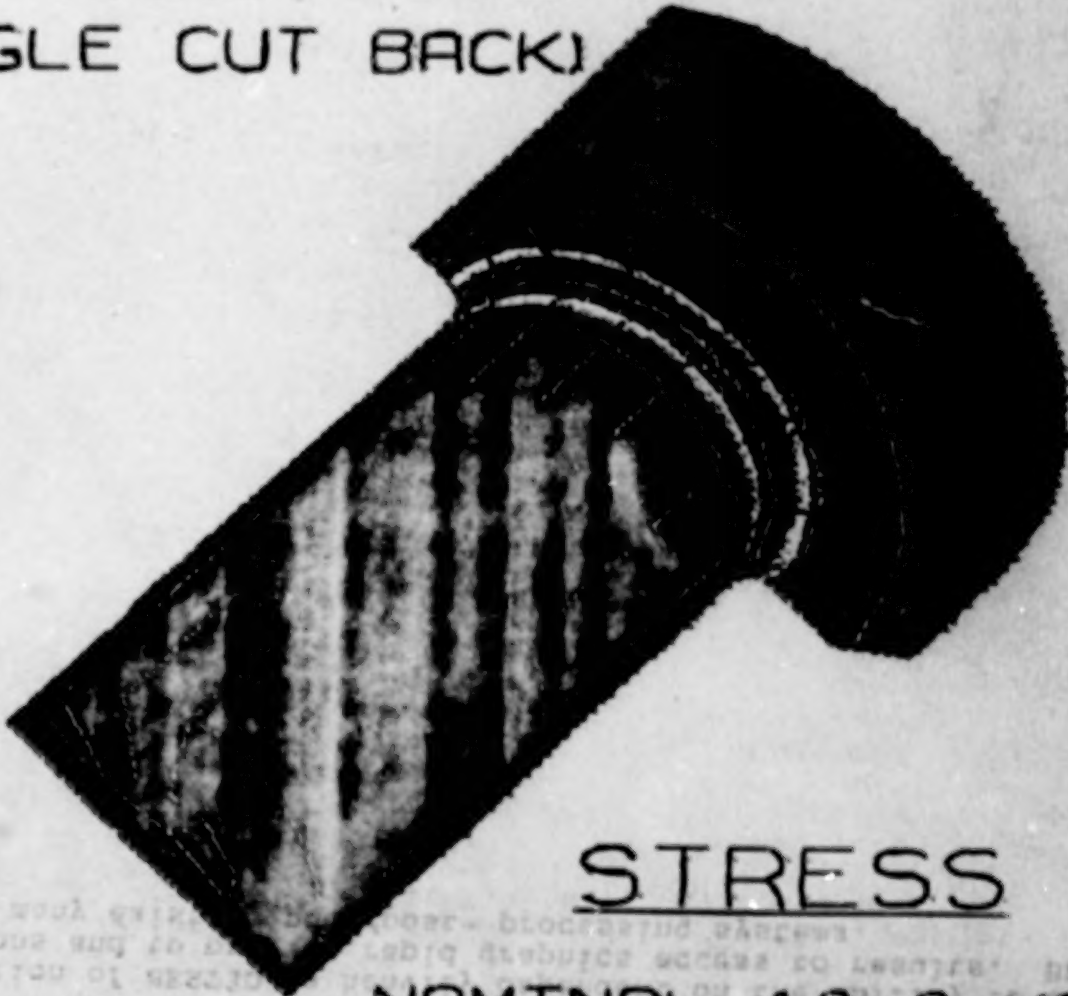

STRESS

NOMINAL 10.0 KSI
MAX 27.9 KSI

Both of the tie bolt geometries shown were input directly from a solid modeller into a P&W pre-processor for generation of BEST3D models. The same system allowed immediate evaluation of the results. It was possible to complete the entire model building process with a part-time effort over three days. Use of a CRAY computer to run the analyses allowed daytime turnaround of iterations on loads and boundary conditions.

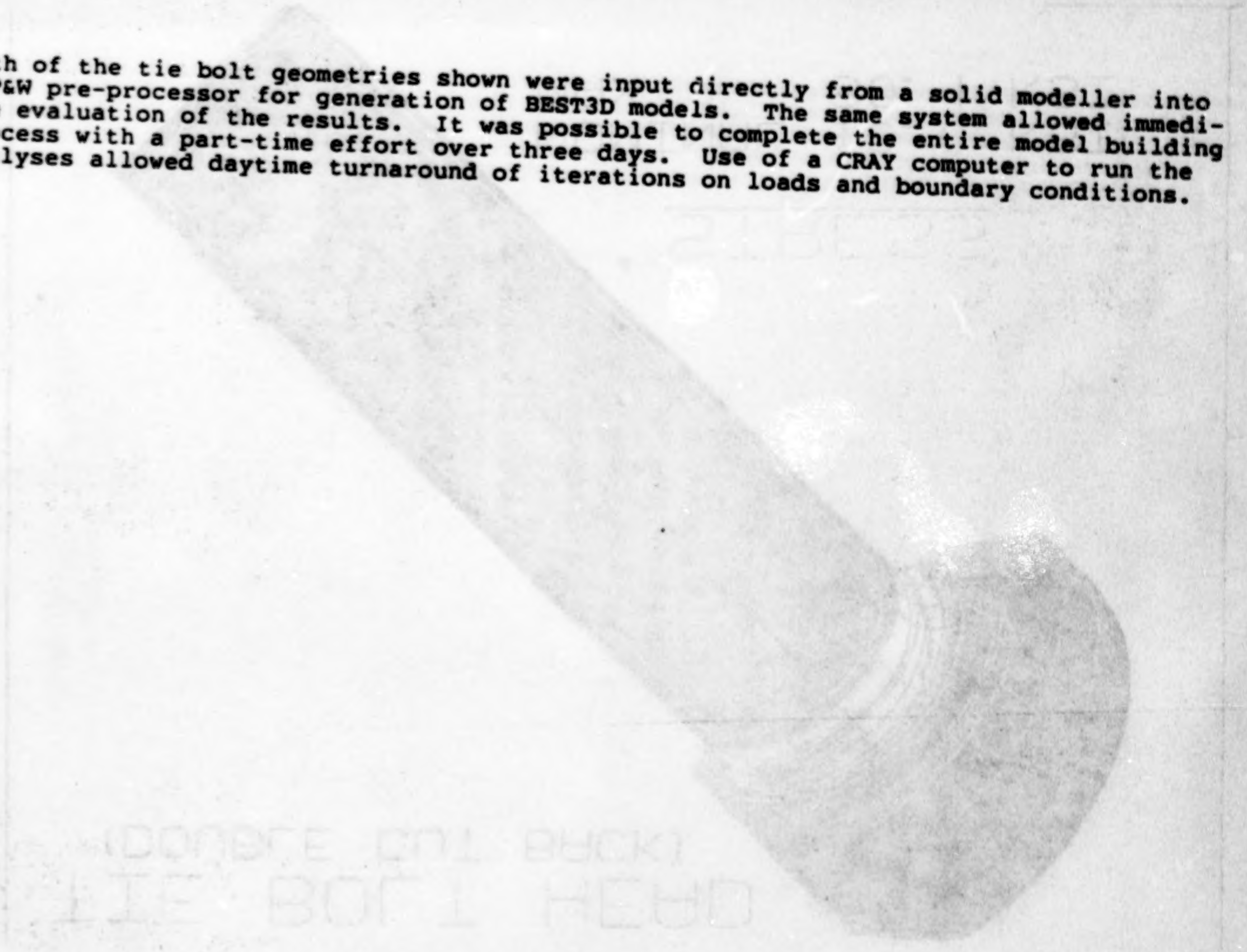

TIE BOLT HEAD
(DOUBLE CUT BACK)

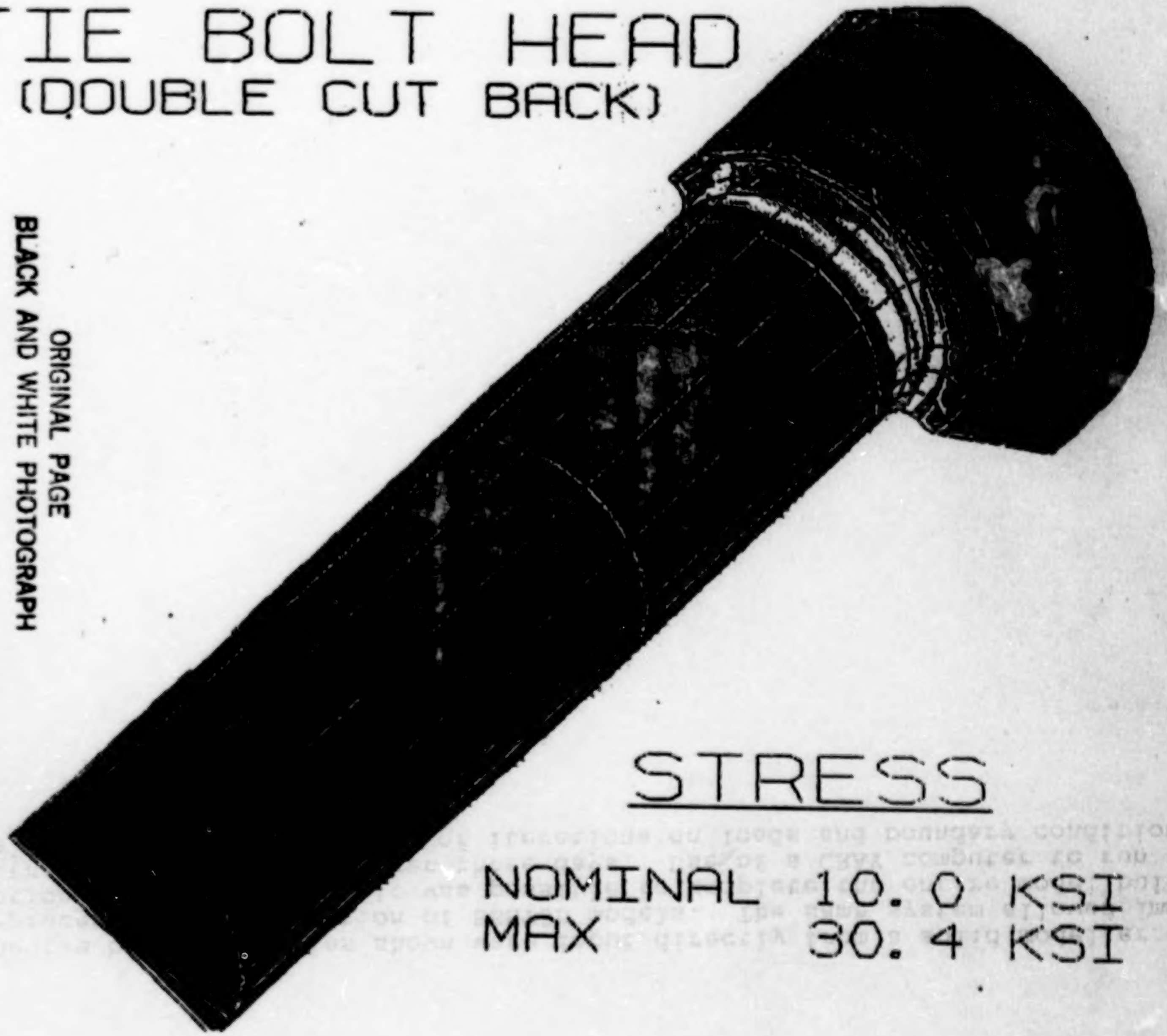

STRESS

NOMINAL 10.0 KSI
MAX 30.4 KSI

ORIGINAL PAGE
BLACK AND WHITE PHOTOGRAPH

It was possible to provide a 3D comparison between the baseline geometry and a proposed modification rapidly enough to guide the design process.

Present supercomputer capabilities will allow fairly routine elastic analysis of 3D geometries, with daytime turnaround easily available for the less complex analyses. With proper attention to effective modelling, nonlinear analysis of structures such as turbine airfoils will also be feasible, using present computing capabilities, although probably on an overnight basis. Routine nonlinear analysis of very complex structures, such as an entire turbine blade (including platform and firtree) will probably require the exploitation of parallel processing capabilities.

N89

29801

UNCLAS

DEVELOPMENT OF AN INTEGRATED BEM FOR HOT FLUID-STRUCTURE INTERACTION

P. K. Banerjee
G. F. Dargush

Department of Civil Engineering
State University of New York at Buffalo

Summary

One very difficult problem in the engine structural component durability analysis is the determination of the temperatures and fluxes in the structural components directly in contact with the hot gas flow path. Currently there exists no rational analytical or numerical technique which can effectively deal with this problem. The analysts involved in the hot fluid dynamics who use the finite difference method very rarely interact with those engaged in the thermal analysis of the structural components where the dominant numerical method is the finite element method. Since the temperature distribution in the structural components is strongly influenced by both the fluid flow and the deformation as well as the cooling system in the structure, the only effective way to deal with this problem is to develop an integrated solid mechanics, fluid mechanics and heat transfer analysis for this problem. The Boundary Element Method (BEM)

~~In the present work~~, BEM is chosen as a basic analysis tool principally because the definition of quantities like fluxes, temperature, displacements, velocities is very precise on a boundary base discretisation scheme. One fundamental difficulty is, of course, that the entire analysis requires a very considerable amount of analytical work which is not present in other numerical methods. During the last 18 months all of this analytical work has been completed and a two-dimensional, general purpose code has been written. Some of the early results are described. It is anticipated that within the next two to three months almost all two-dimensional idealisations will be examined. It should be noted that the analytical work for the three-dimensional case has also been done and numerical implementation will begin next year.

DEVELOPMENT OF AN INTEGRATED BEM FOR HOT FLUID-STRUCTURE INTERACTION

- INTRODUCTION
- REVIEW OF CURRENT PRACTICE
- FUTURE ANALYTICAL REQUIREMENTS
- BEM DEVELOPMENT
  - OBJECTIVES
  - STATE-OF-THE-ART
  - FORMULATION
  - IMPLEMENTATION
  - EXAMPLES
  - FUTURE DIRECTION
- SUMMARY

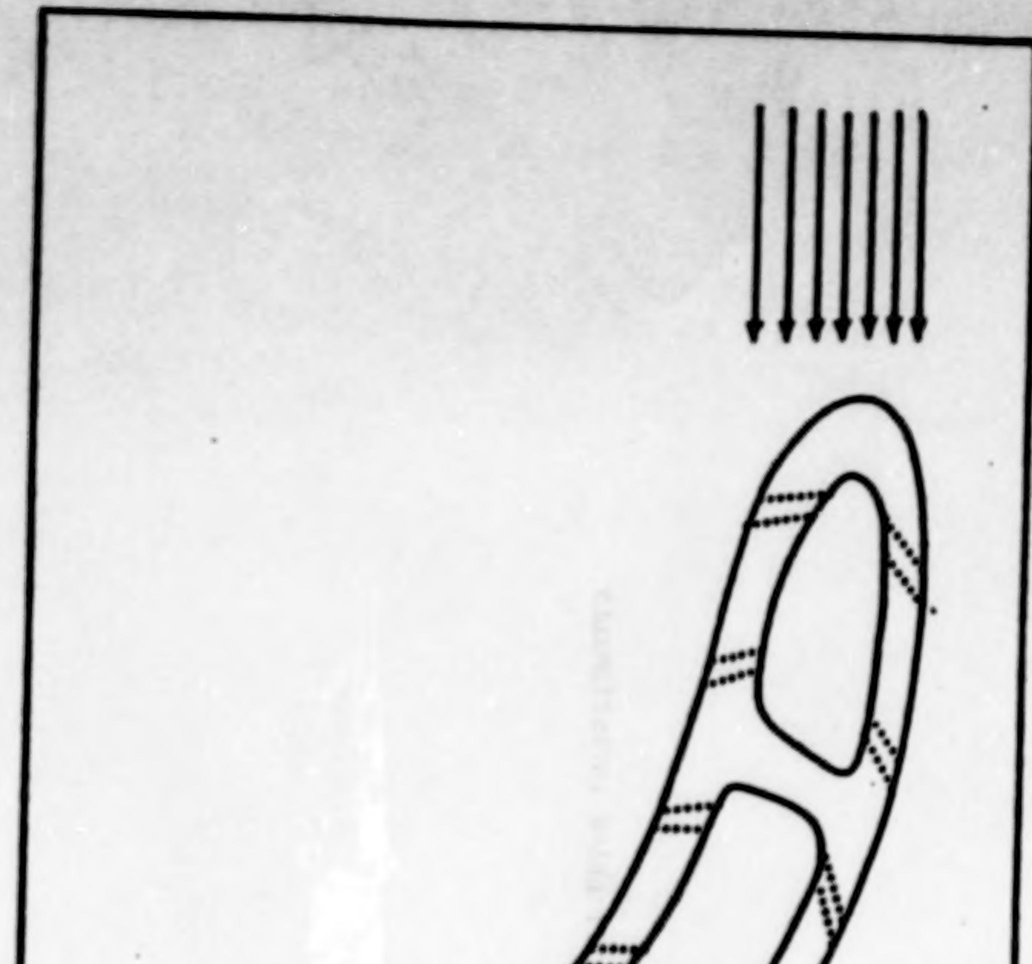

PAGE 833 INTENTIONALLY BLANK

PRECEDING PAGE BLANK NOT FILMED

VIEW GRAPH 3

A typical fluid structure interaction problem relevant to the present discussion is shown. The passage of hot fluid is modified by the structure which itself is being cooled. The temperature distribution in the structure is affected by the hot fluid dynamics, the heat conduction through the structure and convection of fluid inside the structure. Without a rational analysis of these interactions, one needs a very large amount of empirical data of convection coefficients which will have to be varied spatially and in time. On the other hand, in a rational analysis, the behavior is controlled by measurable physical parameters.

FUTURE ANALYTICAL REQUIREMENTS

- CONTINUAL NEED TO ENHANCE CAPABILITIES
- FLUID AND STRUCTURE ARE NOT SEPARATE PROBLEMS
- SIGNIFICANT INTERACTION
  - THERMAL GRADIENTS
  - DISTORTION

VIEW GRAPH 4

The need for an integrated analysis will be even greater in the future because of increased demand for more efficient and powerful engines leading to higher thermal gradients and severe structural deformation. Fluid and structure cannot be independently analyzed.

BEM DEVELOPMENT

OBJECTIVE (1986-1989)

Conduct a pilot study to assess the appropriateness of BEM for the coupled fluid-structure problem

STATE-OF-THE-ART

- SOLID
  - ELASTIC
  - INELASTIC (PLASTICITY,VISCOPLASTICITY)
  - TRANSIENT DYNAMICS
- FLUID
  - INVISCID (POTENTIAL) FLOW
  - VISCOUS FLOW

VIEW GRAPH 5

The BEM has reached a very high level of performance in the solid mechanics where elastic, elastoplastic, viscoplastic, thermoelastic, thermoplastic and large deformation analyses can now be carried for any large two-dimensional, axisymmetric and three-dimensional problems both under steady-state, as well as transient loading. (BEST3D, BEST2D and GPBEST were developed with funding from NASA, Pratt and Whitney and other large industrial corporations, respectively.)

The development in the fluid mechanics applications, however, is many years behind. Almost all of the available work is in the area of inviscid potential flow. Only a few have attempted viscous flow problems.

In the early phases of this work, the fundamental solution necessary for the solid part of the problem was derived from Nowaki's work. This involves the determination of transient displacements due to a set of unit forces and a temperature source in an infinite solid. For fluid, a similar solution has never been attempted. Without this fundamental solution, BEM cannot be developed.

BEM DEVELOPMENT
FORMULATION AND IMPLEMENTATION

- SOLID
  - UNCOUPLED THERMOELASTICITY
    - TRANSIENT HEAT TRANSFER ANALYSIS
    - STRESS ANALYSIS
  - THERMOPLASTICITY
- FLUID
  - THERMALLY-SENSITIVE, COMPRESSIBLE, VISCOUS FLOW
  - VORTICITY-DILATATION-TEMPERATURE FORMULATION
  - VELOCITY-TEMPERATURE FORMULATION

VIEW GRAPH 6

As mentioned earlier, solid mechanics formulations for the present problem are at a very well developed stage. For the fluid mechanics part of the problem, three formulations are feasible. From some preliminary studies, it was apparent that for the entire flow regime (low Reynolds number to high Reynolds number) different formulations are needed. Of these, the velocity-temperature formulation was adopted primarily because it provides precise definitions at boundary points.

COMPRESSIBLE VISCOUS FLOW

GOVERNING EQUATIONS

Momentum Balance

$$(\lambda + \mu)\frac{\partial^2 v_j}{\partial x_i \partial x_j} + \mu \frac{\partial^2 v_i}{\partial x_j \partial x_j} - \frac{\partial p}{\partial x_i} = \rho \frac{\partial v_i}{\partial t} + \rho v_j \frac{\partial v_i}{\partial x_j}$$

Energy Balance

$$k\frac{\partial^2 T}{\partial x_j \partial x_j} - \rho c_v \frac{\partial T}{\partial t} = -\psi$$

Conservation of Mass

$$\frac{\partial \rho}{\partial t} + v_j \frac{\partial \rho}{\partial x_j} + \rho \frac{\partial v_j}{\partial x_j} = 0$$

Equation of State

$$p = \rho R T$$

BOUNDARY INTEGRAL EQUATION

$$c_{\beta\alpha} v_\beta = \int_s (G_{\beta\alpha} \bullet t_\beta - F_{\beta\alpha} \bullet v_\beta)dS + \int_v (G_{\beta\alpha} \bullet f_\beta)dV$$

VIEW GRAPH 7

One of the biggest disadvantages of BEM is that it cannot be developed if the fundamental solution for the set of governing differential equations of the problem does not exist. Unfortunately, this is true for the coupled set of governing equations for the present problem.

Unlike the finite element or the finite difference method where very little mathematical (analytical) work is necessary to derive the shape functions, the fundamental solutions (which play the same role as the shape functions do in FEM) require a great deal of mathematical work.

By separating the density into a reference density and a variable part and adding the variable part times the time derivative of velocity with the convective derivative (second term on the right hand side of the momentum balance equation), a separate right hand side nonlinear body force term can be developed. Similarly the energy balance equation can be modified to include the convective term in a source term on the right hand side. For this coupled set of transient equations, a fundamental solution can now be constructed. For the present work, both two and three-dimensional solutions have been derived. These solutions give the velocity and temperature due to an impulsive body force in the interior of an infinite fluid mass of reference density. It also provides the velocity and temperature due to a unit heat source within an infinite fluid mass of reference density. These fundamental solutions can now be used to develop an exact boundary integral equation in which the changes in the density, as well as convective body force terms appear in the volume integral. This is indeed the basis of all nonlinear analysis by BEM where unknown nonlinear quantitives are taken as a volume integral and they are needed only where nonlinearities exist.

BEM DEVELOPMENT

FORMULATION AND IMPLEMENTATION

FORMULATION

- **INTEGRAL EQUATION FOR MOMENTUM AND ENERGY BALANCE**
- **CONTINUITY VIA GLOBAL SHAPE FUNCTION**

IMPLEMENTATION

- **TWO DIMENSIONAL**
- **GENERALIZED DEGREES-OF-FREEDOM**
- **STATE-OF-THE-ART INFRASTRUCTURE**

VIEW GRAPH 8

In numerical implementation, the integral representation for the momentum and energy balance are taken care of by the discretization of the exact boundary integral equation. The density changes are then corsidered via volume integral with the aid of global shape functions in the continuity equation.

The computer program has been developed in a very general manner to admit solutions of any two-dimensional hot fluid structure interaction problem.

STEADY STATE COUETTE FLOW

Boundary Element Model

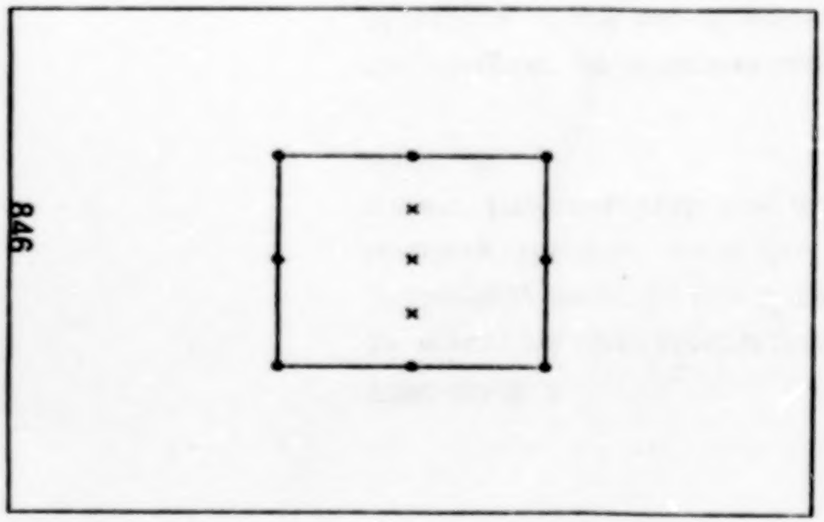

Test Problem - Incompressible Fluid

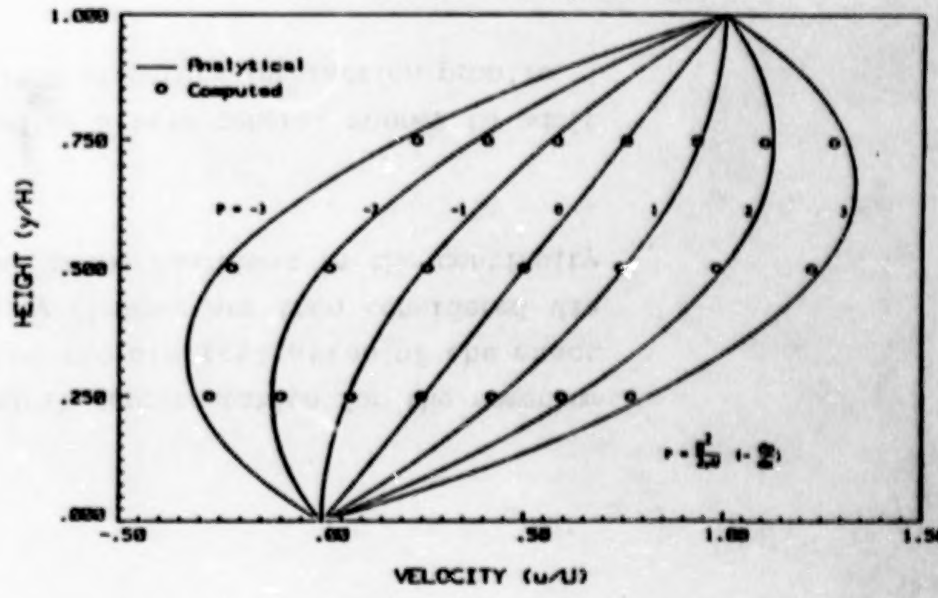

VIEW GRAPH 9

As a test problem, the simplest problem of couette flow is shown. It is possible to get a very accurate solution with just 4 quadratic boundary elements.

FIGURE 1 - Driven Cavity Problem Definition

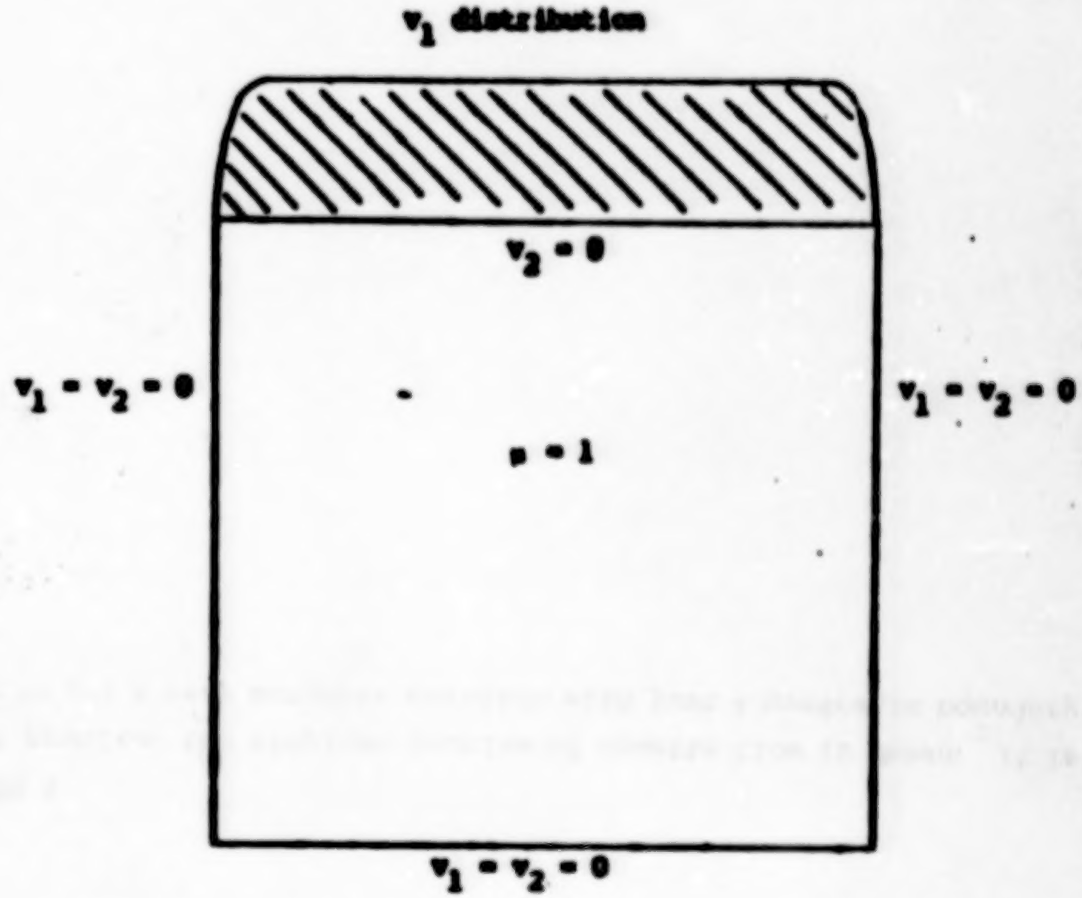

I. ITERATIVE

II. VARIABLE STIFFNESS TYPE

III. SUBSTRUCTURED

VIEW GRAPH 10

As a more challenging nonlinear problem, the driven cavity flow is analyzed. Two of the three nonlinear algorithms (namely iterative and variable stiffness type) have been implemented. The program also allows extensive substructuring or multizoning. Note that the boundary conditions for this problem at both top corners are ambiguous. While the lack of precision at boundaries, both in FEM and FDM, allows one to overlook this problem, in BEM the ambiguity is eliminated by applying a parabolic velocity input near the corners.

DRIVEN CAVITY (INCOMPRESSIBLE VISCOUS FLOW)

Boundary Element Model

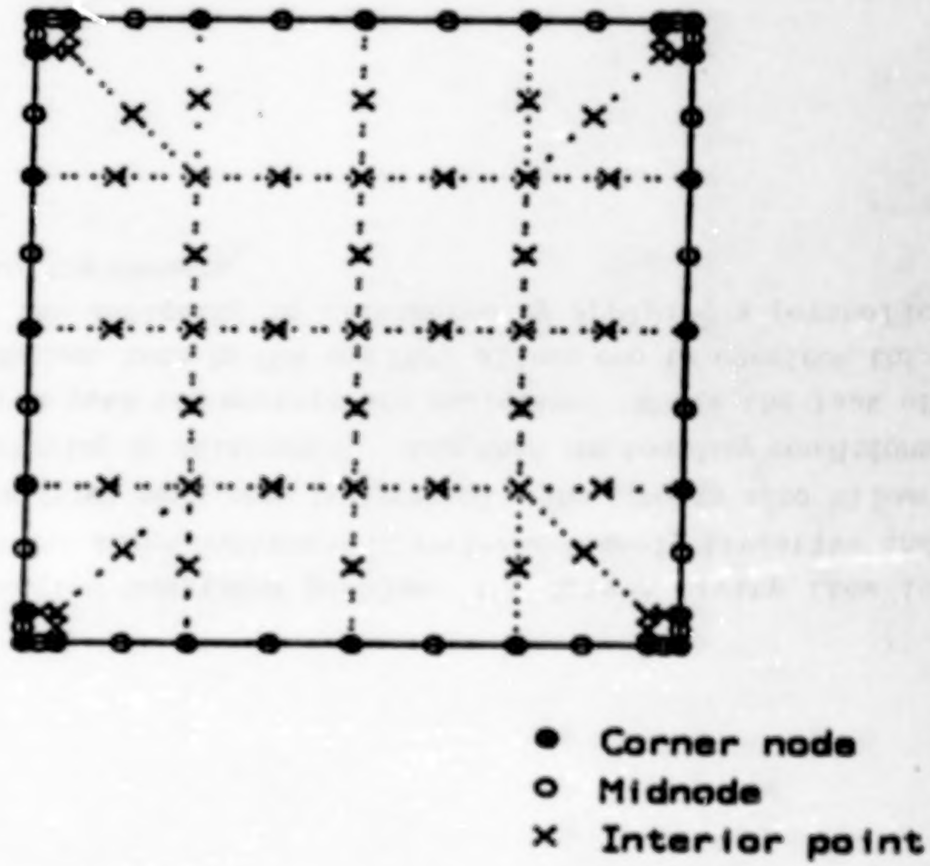

VIEW GRAPH 11

Shows the discretization on boundaries and interior using quadratic boundary elements and cells.

DRIVEN CAVITY (INCOMPRESSIBLE VISCOUS FLOW)

VELOCITY DISTRIBUTION (Re=0)

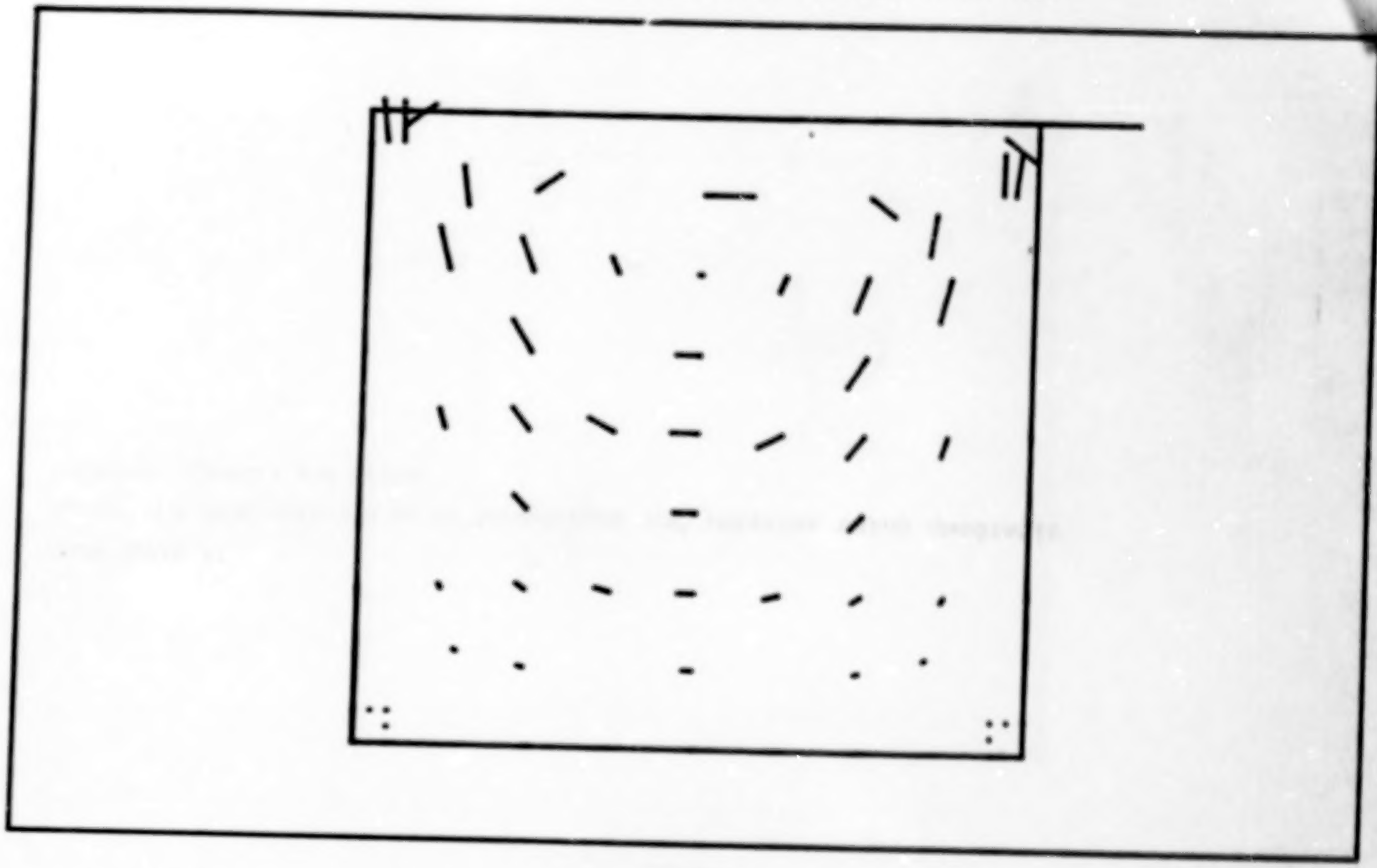

DRIVEN CAVITY (INCOMPRESSIBLE VISCOUS FLOW)

VELOCITY DISTRIBUTION (Re=100)

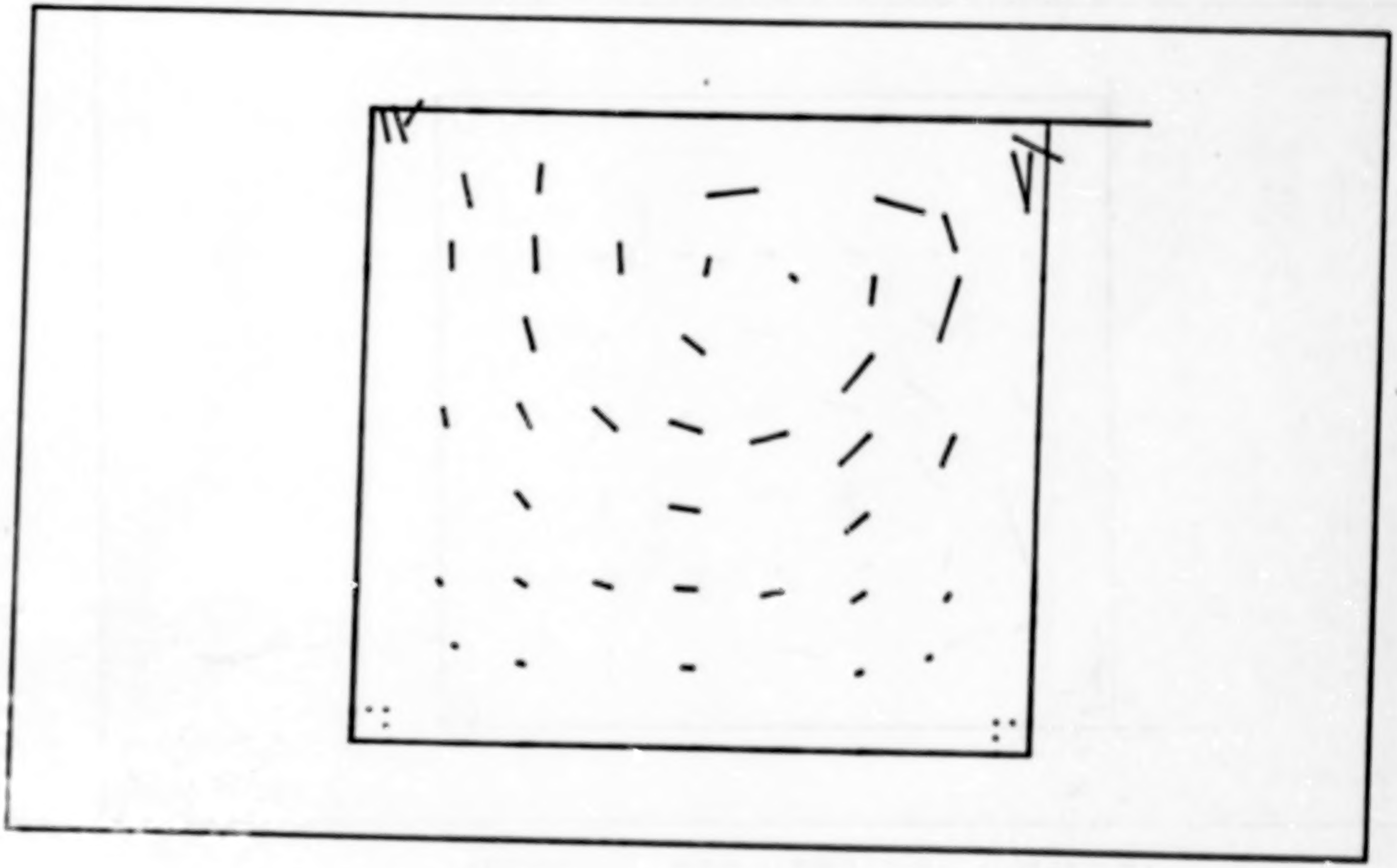

DRIVEN CAVITY (INCOMPRESSIBLE VISCOUS FLOW)

VELOCITY DISTRIBUTION (Re=250)

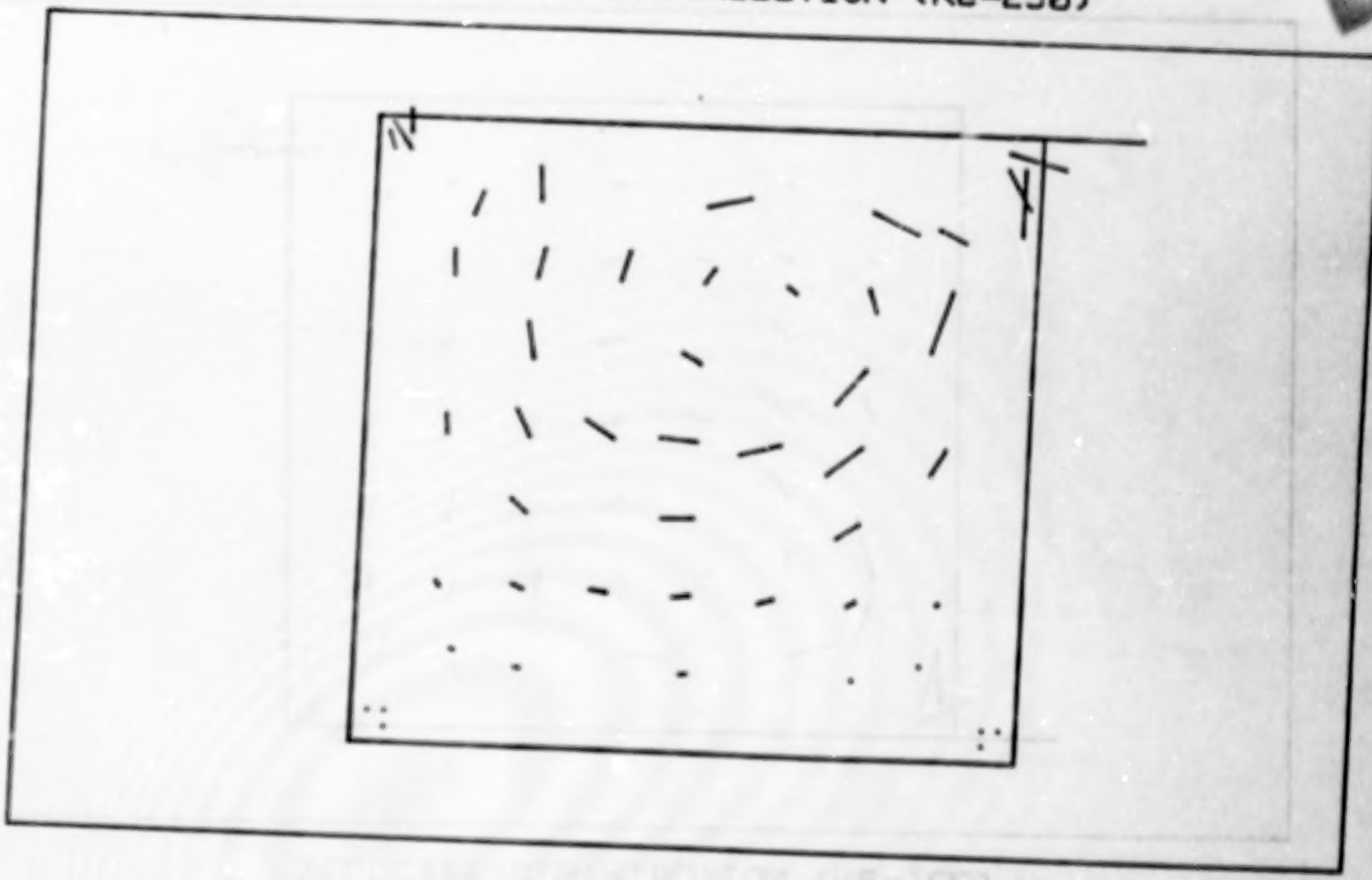

VIEW GRAPHS 12-14

These show the developing flow starting with nearly zero Reynolds number to one about 250. Note that circulation center moves slightly.

FIGURE 5 - Driven Cavity (Three Region, Thirty-six Cell Model)

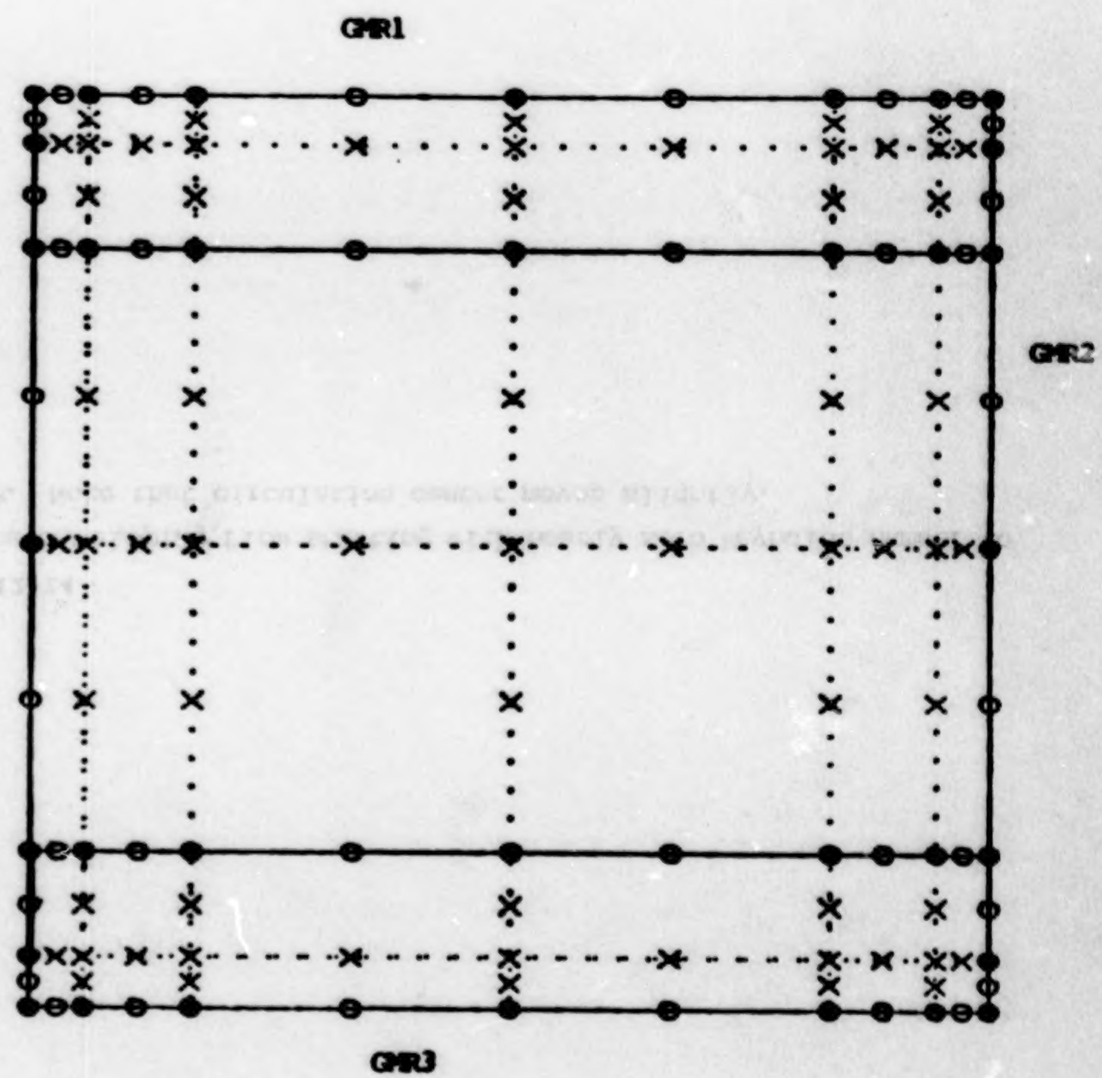

C-2

VIEW GRAPH 15

Same problem was also analyzed using 3 subregions to check out the program.

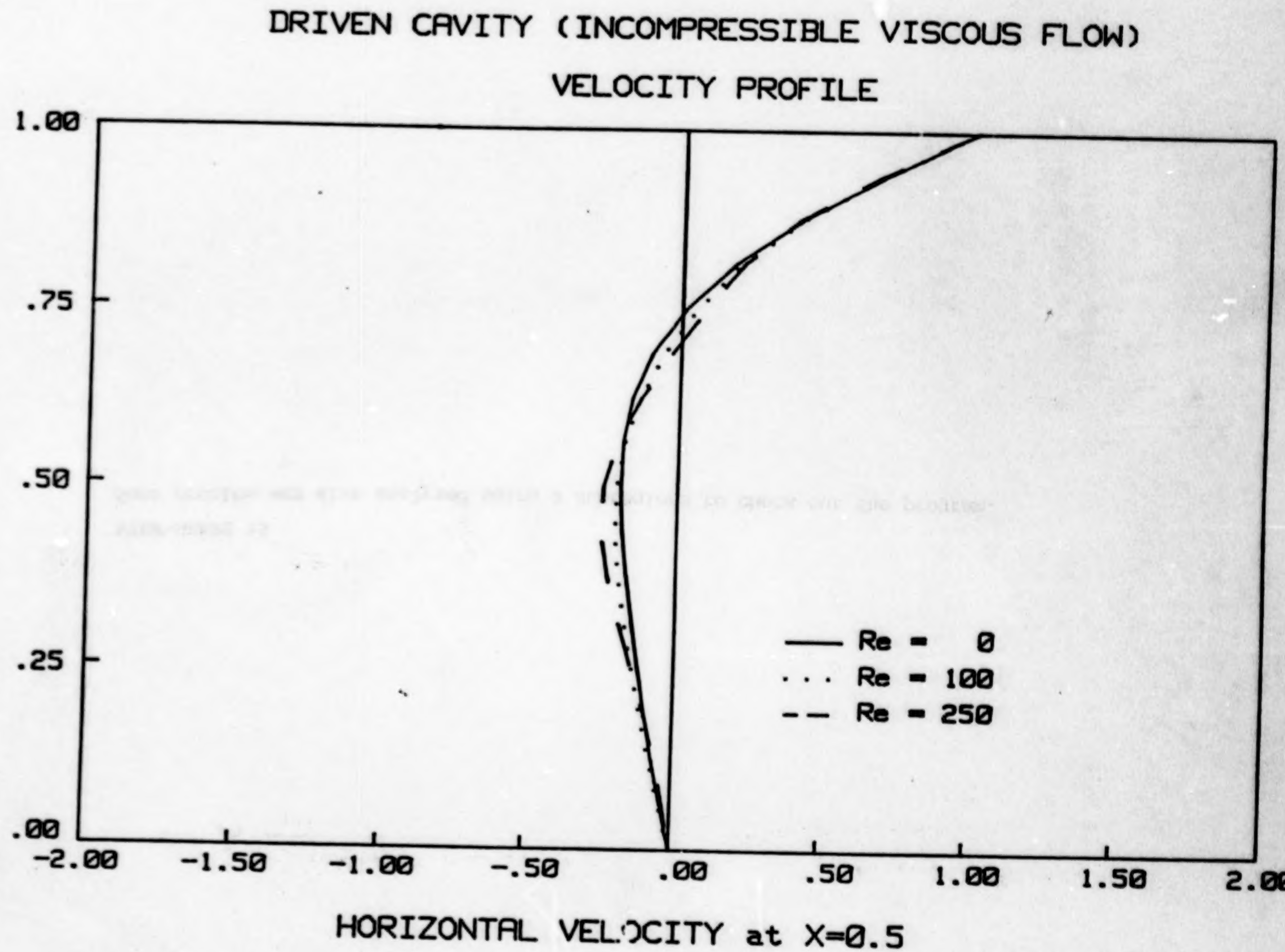
DRIVEN CAVITY (INCOMPRESSIBLE VISCOUS FLOW)
VELOCITY PROFILE
1.00
.75
.50
.25
.00
Y
-2.00
-1.50
-1.00
-.50
.00
.50
1.00
1.50
2.00
Re = 0
Re = 100
Re = 250
HORIZONTAL VELOCITY at X=0.5

VIEW GRAPH 16

Shows the horizontal velocity profile through the depth at different Reynolds numbers.

FIGURE 7
BUOYANCY DRIVEN CAVITY
VELOCITY DISTRIBUTION

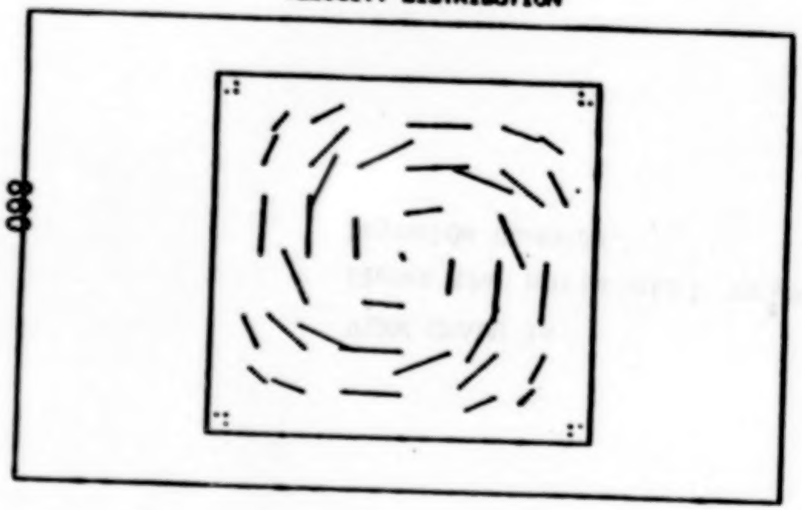

FIGURE 8
BUOYANCY DRIVEN CAVITY
TEMPERATURE PROFILE

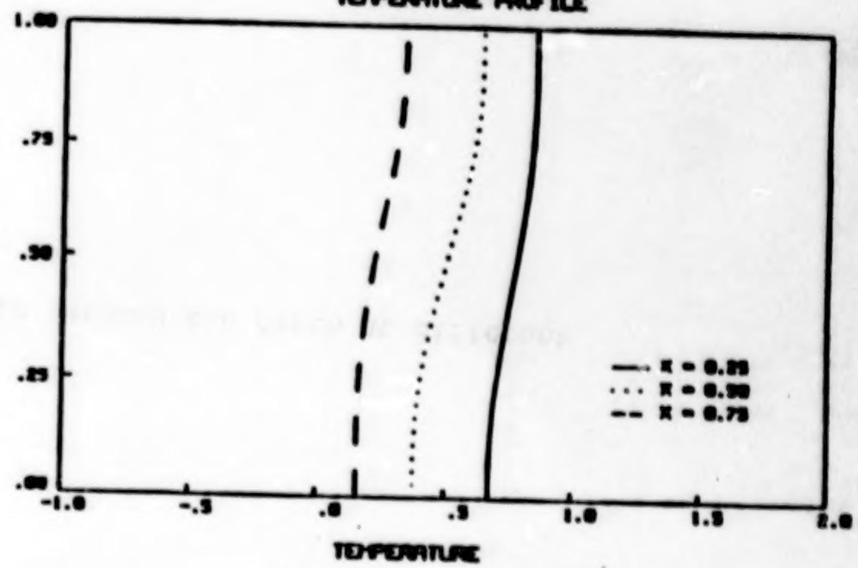

VIEW GRAPH 17

To check the thermal coupling in the fluid flow, the nonlinear problem of buoyancy driven cavity problem is examined. As a result of a steady-state heat flow from left to right, the fluid circulates and the resulting temperature profile is no longer uniform over the height.

BEM DEVELOPMENT
FUTURE DIRECTION

- SUMMER 1987
  - CONTINUE VERIFICATION OF EXISTING FORMULATION
  - DEVELOP FUNDAMENTAL SOLUTION INCLUDING INERTIA TERMS IN MOMENTUM EQUATIONS
- FALL-WINTER 1987
  - IMPLEMENT AND VERIFY NEW KERNELS
  - CONDUCT CONVERGENCE STUDIES
- 1988
  - EXAMINE MORE REALISTIC PROBLEMS
  - DEVELOP AND IMPLEMENT FLUID-STRUCTURE INTERACTION CODING

VIEW GRAPH 18

We have achieved the objective of bringing the BEM development of fluid mechanics to nearly the same level of development which currently exists in solid mechanics. Within the next few months, it will be possible to examine the hot-fluid structure interaction problems which hopefully will establish that empirical convection coefficients are not necessary to determine the temperature and fluxes at solid boundaries.

N89
29802
UNCLAS

PROBABILISTIC STRUCTURAL ANALYSIS METHODS FOR SELECT SPACE PROPULSION SYSTEM STRUCTURAL COMPONENTS*

T. A. CRUSE
P. O. DRAWER 28510
SOUTHWEST RESEARCH INSTITUTE
SAN ANTONIO, TEXAS 78284

is presented.

ABSTRACT

~~The paper presents~~ a summary of the ~~status~~ of this five-year project which is now in its third year of research and development. The goal of the project is the development of several methodologies for probabilistic structural modeling. Probabilistic structural modeling consists of stochastic models of material properties, part geometries, boundary conditions, as well as loading conditions. The current presentation focuses on one methodology — coupling of an advanced finite element structural analysis code with probabilistic modeling strategies. The essential algorithm developments for combining the finite element and probabilistic analysis methods are reported. The validity of the resulting probabilistic structural analysis method is confirmed through a series of test problems with exact results based on Monte Carlo simulations. Additionally, the applicability of the method to a Space Propulsion System (a turbine blade) is demonstrated for static stresses.

* This work is supported by Contract NAS3-24389; Dr. Christos C. Chamis, Program Manager, NASA Lewis Research Center

N89-29805

PROBABILISTIC DESIGN METHODS WILL SIMULATE "REAL WORLD" STRUCTURAL RESPONSES

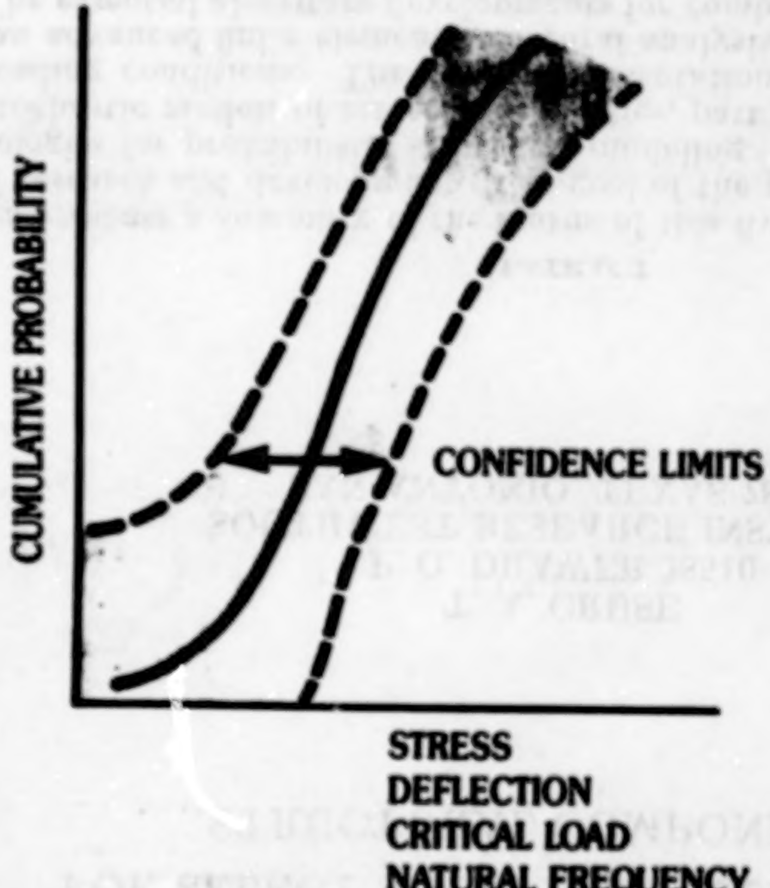

DUE TO DESIGN UNCERTAINTIES:

- LOADING
- MATERIAL BEHAVIOR
- GEOMETRY, TOLERANCES
- BOUNDARY CONDITIONS

THE GOAL OF THE PSAM PROJECT IS TO PROVIDE THE STRUCTURAL ANALYST WITH THE ABILITY TO SIMULATE "REAL WORLD" PROBLEMS WHERE MANY OF THE KEY VARIABLES ARE SUBJECT TO DESIGN VALUE UNCERTAINTIES. SPECIFICALLY, PSAM WILL PROVIDE A COMPLETE CUMULATIVE DISTRIBUTION FUNCTION OF USER DEFINED OUTPUT VARIABLES OVER A SPECIFIED RANGE OF PROBABILITY LEVELS. FOR CASES WHERE THE UNCERTAINTIES ARE BASED ON LIMITED EXPERIMENTAL DATA, PSAM WILL ALSO ESTIMATE CONFIDENCE BANDS ON THE CDF RESULTS.

RELIABILITY ESTIMATION METHODS INTEGRATED WITH FINITE ELEMENT ANALYSIS

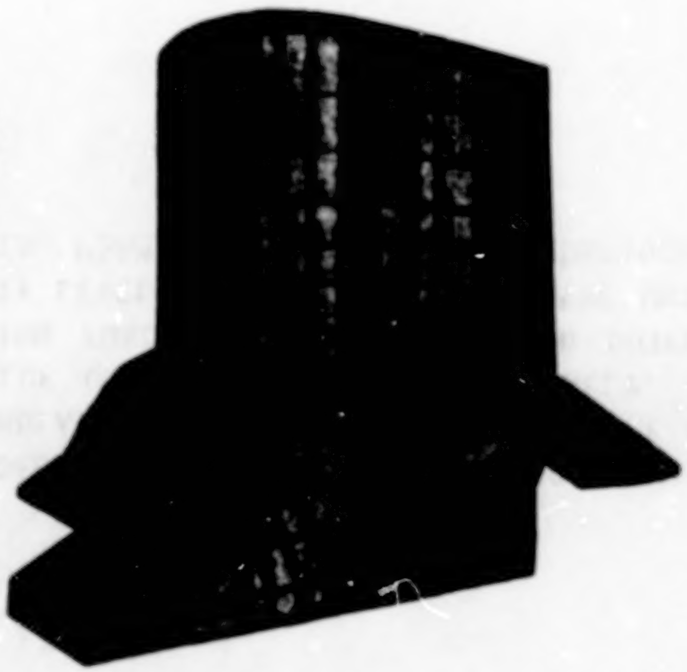

- USER DEFINES UNCERTAIN DATA IN MODEL
- FEM MODELS PREDICT DESIGN SENSITIVITY
- RELIABILITY METHODS COMBINE UNCERTAINTY AND SENSITIVITY DATA
  - FAST PROBABILITY INTEGRATION (FPI)
  - MONTE CARLO SIMULATION (MC)

ORIGINAL PAGE
BLACK AND WHITE PHOTOGRAPH

THE FIRST PROBABILISTIC STRUCTURAL ANALYSIS TOOL IN THE PSAM SYSTEM IS THE FINITE ELEMENT METHOD. A MEANS FOR COMBINING THE FEM WITH PROBABILISTIC METHODS HAS BEEN ESTABLISHED. THE FEM IS USED TO ESTABLISH THE SENSITIVITIES OF THE STRUCTURAL ANALYSIS RESULT TO CHANGES IN USER-DEFINED RANDOM VARIABLES. ADVANCED RELIABILITY METHODS FOR PROBABILISTIC CALCULATIONS COMBINE THE FEM-GENERATED SENSITIVITIES WITH USER-DEFINED STATISTICS FOR THE INPUT RANDOM VARIABLES. TWO PROBABILITY INTEGRATION ALGORITHMS ARE COMBINED WITH THE FEM MODULE: (1) FAST PROBABILITY INTEGRATION (FPI); AND (2) AN ENHANCED MONTE CARLO SIMULATION.

AN OVERVIEW OF THE NESSUS CODE
Five Major Software Modules Working Together

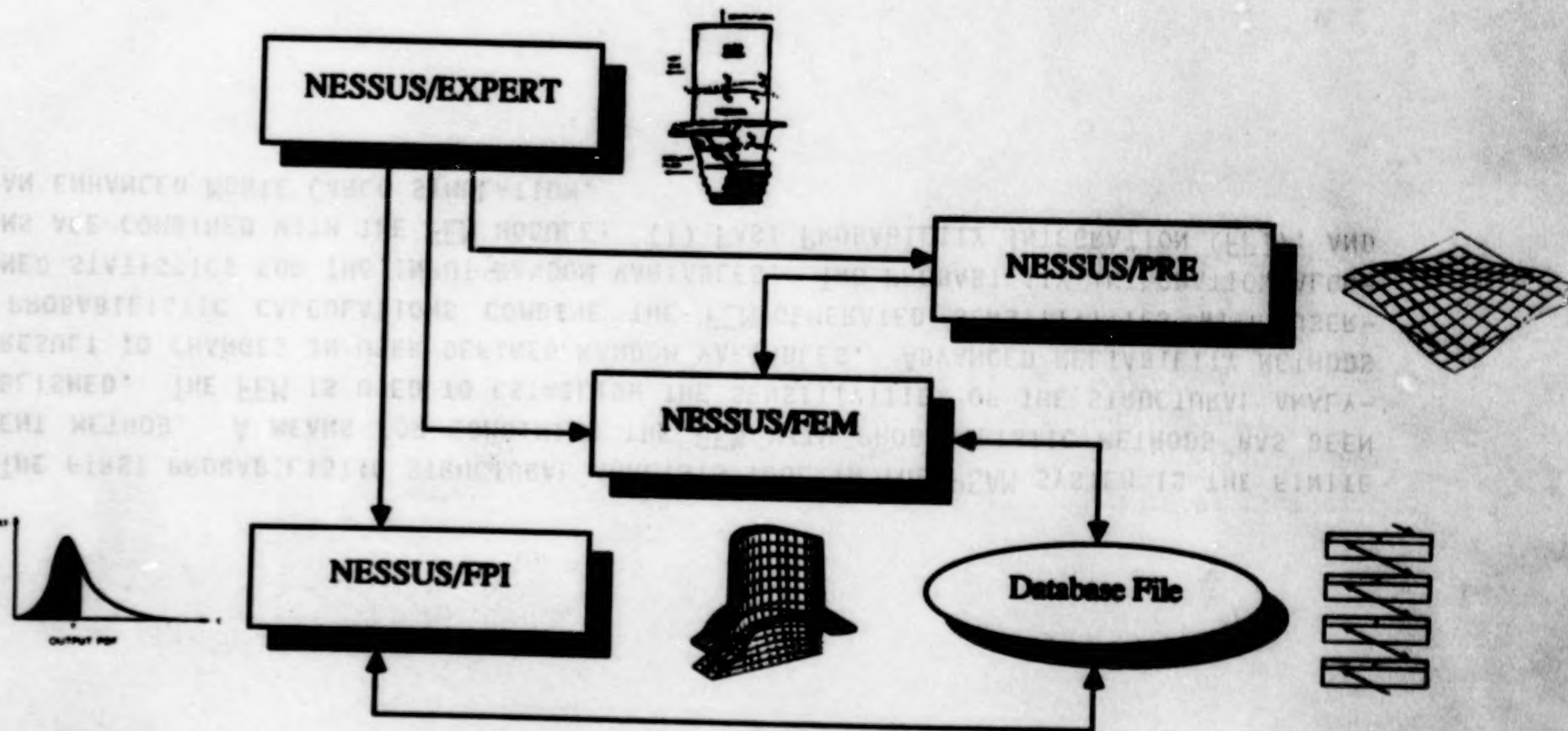

MARC Analysis Research Corporation

THE COMBINATION OF FEM AND FPI ALGORITHMS IS ACCOMPLISHED WITHIN A MODULAR PACKAGE CALLED NESSUS (NONLINEAR EVALUATION OF STOCHASTIC STRUCTURES UNDER STRESS). THE MODULES INCLUDE EXPERT (THE USER INTERFACE), PRE (DEFINES INDEPENDENT RANDOM VARIABLES FOR PARTIALLY CORRELATED RANDOM FIELDS--E.G., PRESSURES AND TEMPERATURES), FEM, FPI, AND A SPECIAL DATA BASE. THE FEM, FPI, AND EXPERT MODULES WILL BE DISCUSSED.

NESSUS/FEM CODE DEVELOPED FOR PROBABILISTIC MODELING

NODAL SOLUTION STRATEGY
- ALL INPUT DATA
- EQUILIBRIUM ITERATION
- ALL OUTPUT DATA

USER INTERFACE STRATEGY
- KEYWORD DATA STRUCTURE
- INTERFACE TO NESSUS/PRE
- DATABASE TRANSLATORS
- EXPERT SYSTEM

GENERAL SOLUTION CAPABILITY
- LINEAR, NONLINEAR
- STATIC, DYNAMIC
- IN-CORE SOLUTION
- MULTIPLE ELEMENT TYPES
- RANDOM LOADS
- RANDOM VARIABLES

ADVANCED ELEMENT FORMULATIONS
- SURFACE NODE BASED
- HYBRID SHELL/PLATE
- ENHANCED SOLID
- SPECIAL THERMAL LOADS

A SPECIAL FEM CODE HAS BEEN DEFINED FOR NESSUS. THE FEM CODE IS BASED ON NODAL VARIABLES AND NODAL EQUILIBRIUM (USING A MIXED VARIATIONAL METHOD). THE FEM ANALYSIS INCLUDES LINEAR, NONLINEAR, STATIC, DYNAMIC, AND TRANSIENT CAPABILITIES. RANDOM VARIABLES INCLUDE THOSE SHOWN. THE USER INTERFACE IS BASED ON A KEYWORD DATA STRUCTURE WITH INTERFACES TO PRE AND EXPERT. THE ELEMENTS IN THE FEM MODULE INCLUDE STANDARD ELEMENTS PLUS AN ASSUMED STRAIN 8-NODE SOLID ELEMENT AND AN ASSUMED STRESS 16-NODE SOLID ELEMENT. BOTH THE ELEMENTS ARE TO HAVE HIGH ASPECT RATIOS AND SEVERE THERMAL LOAD CAPABILITIES.

NESSUS/FEM GENERATES RESPONSE MODEL BY EFFICIENT PERTURBATION ANALYSIS

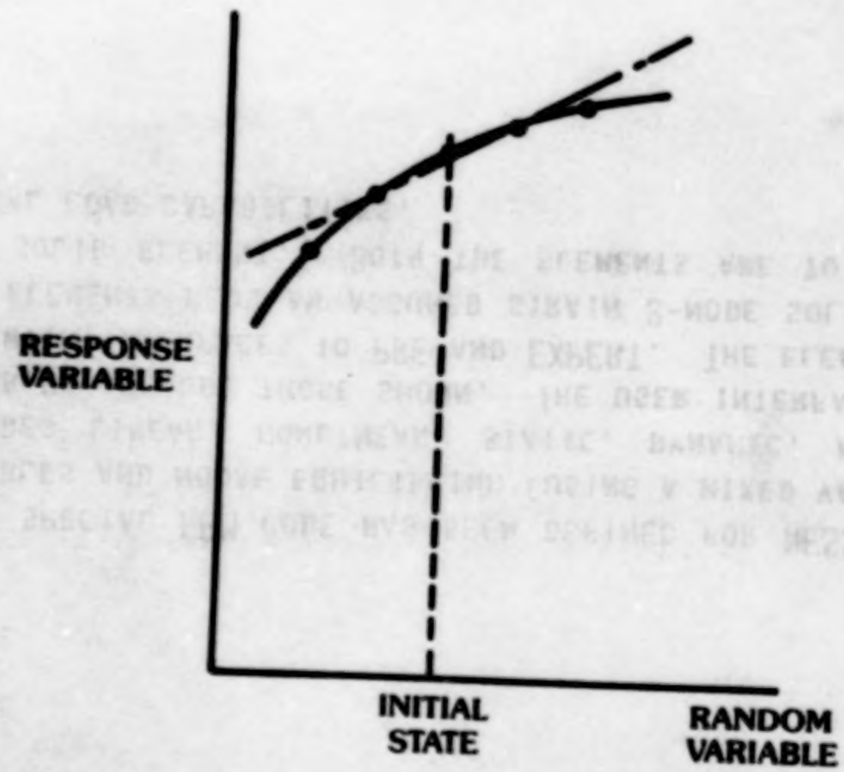

- INDEPENDENT RANDOM VARIABLES
  - GEOMETRY
  - MATERIAL PROPERTIES
  - BOUNDARY CONDITIONS
- ITERATIVE SOLUTION ALGORITHM
  - SMALL PERTURBATIONS
  - RETAIN INITIAL STIFFNESS MATRIX
  - MODIFY RIGHT-HAND SIDE ONLY
- RESPONSE SURFACE FITTING
  - LEAST SQUARES ERROR
  - LINEAR OR QUADRATIC

THE PERTURBATION OF THE FEM ANALYSIS TO DETERMINE SOLUTION SENSITIVITY TO THE RANDOM VARIABLES HAS BEEN TREATED BY A SPECIAL ALGORITHM. FOR SMALL PERTURBATIONS, THE FEM ANALYSIS USES ITERATION WITH THE NON-PERTURBED REDUCED STIFFNESS MATRIX AS A PRE-CONDITIONER MATRIX. THE EFFECTS OF RANDOM VARIABLES CHANGES ARE TRANSFERRED TO THE RIGHT-HAND SIDE OF THE SYSTEM EQUATIONS. THE SOLUTION STATE (RESPONSE SURFACE) IS LEAST-SQUARES FITTED TO THE PERTURBED SOLUTIONS AS A HYPERPLANE OR A QUADRATIC SURFACE.

NESSUS/FPI USES ITERATION TO FIND MOST PROBABLE SET OF RANDOM VARIABLES

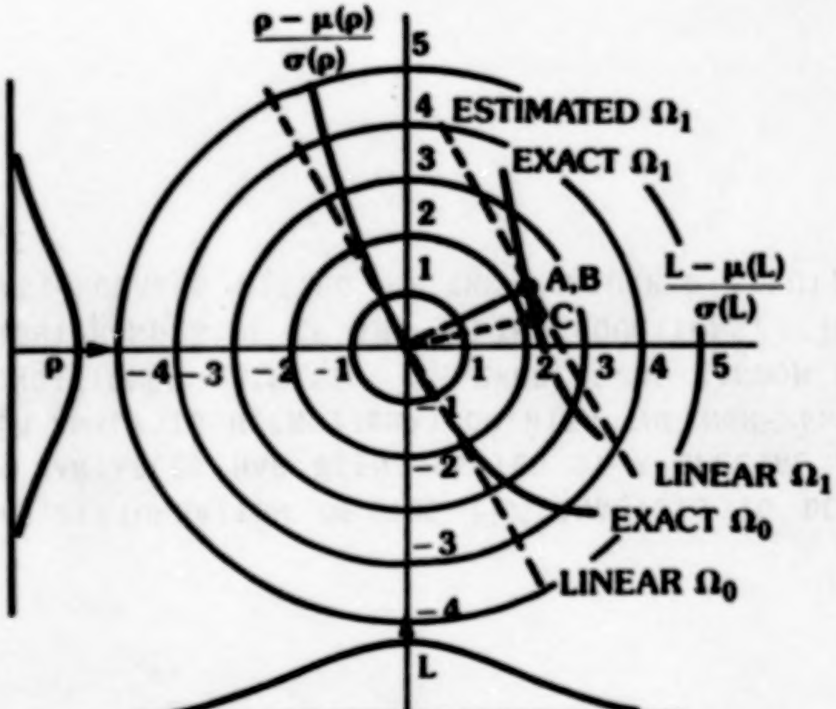

- BEAM VIBRATION EXAMPLE
- ρ, L RANDOM VARIABLES
- JOINT PROBABILITY PLOTTED
- Ω_0 IS DETERMINISTIC SOLUTION
- SHORTEST DISTANCE TO Ω_1 CURVE IS MOST PROBABLE
- A: ESTIMATED MOST PROBABLE VALUES FROM Ω_0 LINEAR
- B: CALCULATED Ω_1 @ ρ_A, L_A
- C: ESTIMATED MOST PROBABLE VALUES ρ_c, L_c

THE FPI ALGORITHM IS DEMONSTRATED IN A SAMPLE PROBLEM OF VIBRATION OF A CANTILEVER BEAM. TWO RANDOM VARIABLES (DENSITY, LENGTH) ARE NORMALIZED TO THEIR MEAN VALUES (μ) AND STANDARD DEVIATION (σ). AN EXACT SOLUTION SURFACE FOR THE VALUE OF NATURAL FREQUENCY FOR THE DETERMINISTIC STATE IS TAKEN TO BE Ω_0, SHOWN AS A CARTOON-CURVE DEPENDING ON ρ,L. A LINEAR APPROXIMATION TO THIS EXACT RESPONSE SURFACE IS SHOWN. IF ρ,L ARE ARBITRARILY TAKEN TO BE GAUSSIAN DISTRIBUTIONS, THE JOINT PROBABILITY LEVELS ARE CIRCLES, AS SHOWN. IF WE DESIRE TO ESTIMATE THE PROBABILITY OF EXCEEDING A NATURAL FREQUENCY $\hat{\Omega}_1$ ($< \Omega_0$), THE PROCESS INVOLVES A SIMPLE ITERACTION ALGORITHM. THE LINEAR FIT AT Ω_0 IS USED TO ESTABLISH THE ρ,L SURFACE FOR $\hat{\Omega}_1$. THE FPI CODE RAPIDLY CALCULATES THE VOLUME UNDER THE JOINT-PDF SURFACE FOR POINTS BEYOND THE SHIFTED LINEAR APPROXIMATION--CORRESPONDING TO POINT A IN FIGURE 8. DUE TO SOLUTION NONLINEAR DEPENDENCE ON ρ,L, THE ACTUAL NATURAL FREQUENCY AT A IS Ω_1, SHOWN AS POINT B IN FIGURE 8. THE VALUE $\hat{\Omega}_1$ IS OBTAINED BY A REFORMULATION SOLUTION STEP ON THE FEM MODEL. A NEW TANGENT PLANE TO THE RESPONSE SURFACE FOR Ω_1 IS OBTAINED BY PERTURBATION OF THE FEM MODEL. FPI THEN CALCULATES A REVISED PROBABILITY ESTIMATE-POINT C IN FIGURE 8. THE RESULT IS SEEN TO HAVE CONVERGED TO THE EXACT SOLUTION IN THESE TWO STEPS.

ITERATION ALGORITHM ACHIEVES ACCURATE PROBABILITY ESTIMATES

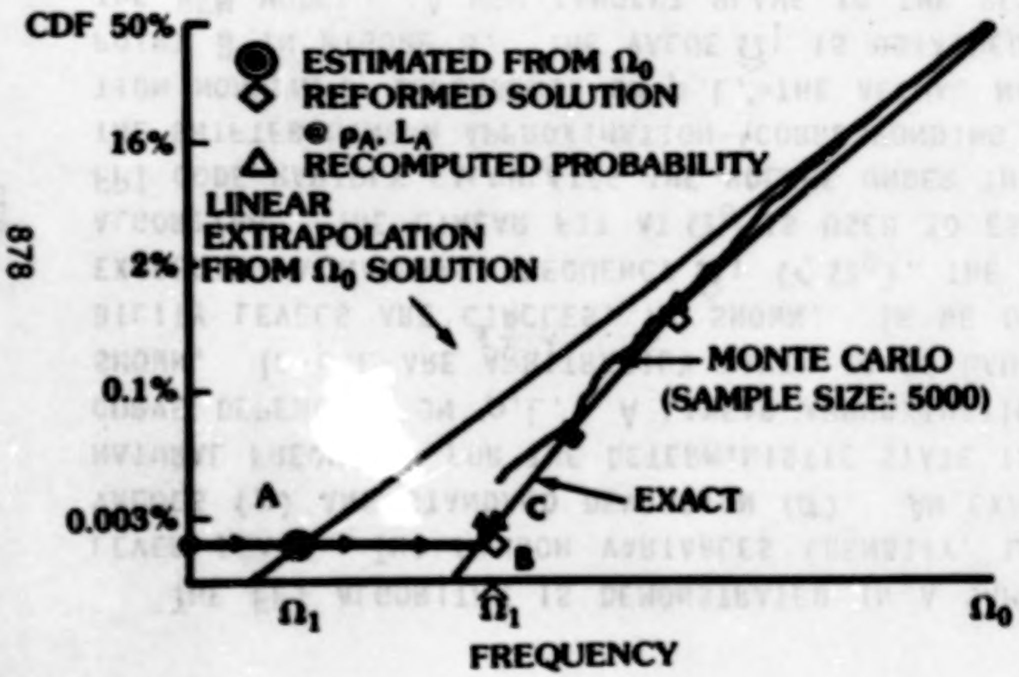

- EXTRAPOLATES RANDOM VARIABLES FROM APPROXIMATE SOLUTIONS
- REFORMS SOLUTION AT NEW RANDOM VARIABLE VALUES
- RECALCULATES PROBABILITY FROM LOCAL APPROXIMATION
- TESTS ON CONVERGENCE

EXPERT KNOWLEDGE WILL GOVERN USER INTERFACE

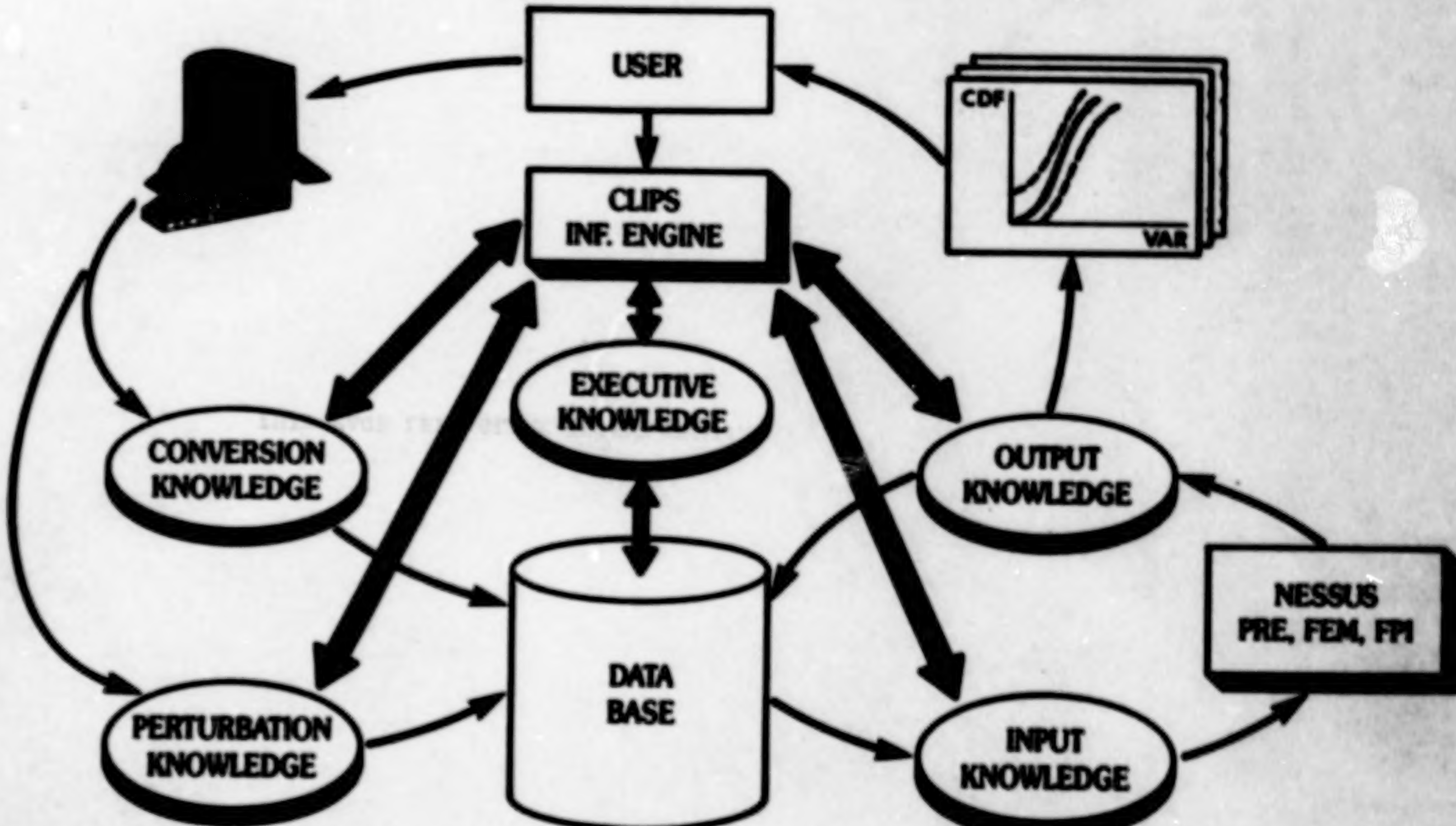

PRECEDING PAGE BLANK NOT FILMED

PAGE 879 INTENTIONALLY BLANK

THE USER INTERFACE IS BEING ESTABLISHED USING AN EXPERT SYSTEM SUPPORTED BY A VARIETY OF FORTRAN SUBROUTINES. THE EXPERT SHELL IS CLIPS, WRITTEN AT NASA/JSC IN C-LANGUAGE. EXPERT KNOWLEDGE IS BEING INCORPORATED IN CLIPS-RULES TO GOVERN EACH OF THE MAJOR ITEMS IN A PROBABILISTIC STRUCTURAL ANALYSIS. AS AN EXAMPLE, THERE ARE RULES REGARDING ELEMENT TYPES AND PERTURBATION SIZES THAT CAN BE USED TO ALLOW CLIPS TO DEFINE PERTURBATION SIZES SUCH THAT A FORTRAN SUBROUTINE AUTOMATICALLY CREATES THE FORTRAN DATA SET CORRESPONDING TO THE PERTURBATION.

NESSUS ASSESSES BUCKLING SENSITIVITY

First Shell Buckling Mode

- Pinned ends
- Infinite length
- Uniform pressure
- 10% error in mean solution
- NESSUS 75 (4-node flat shell)

Probabilistic Analysis

- Thickness uncertainty
- Log normal distribution
- 5% COV

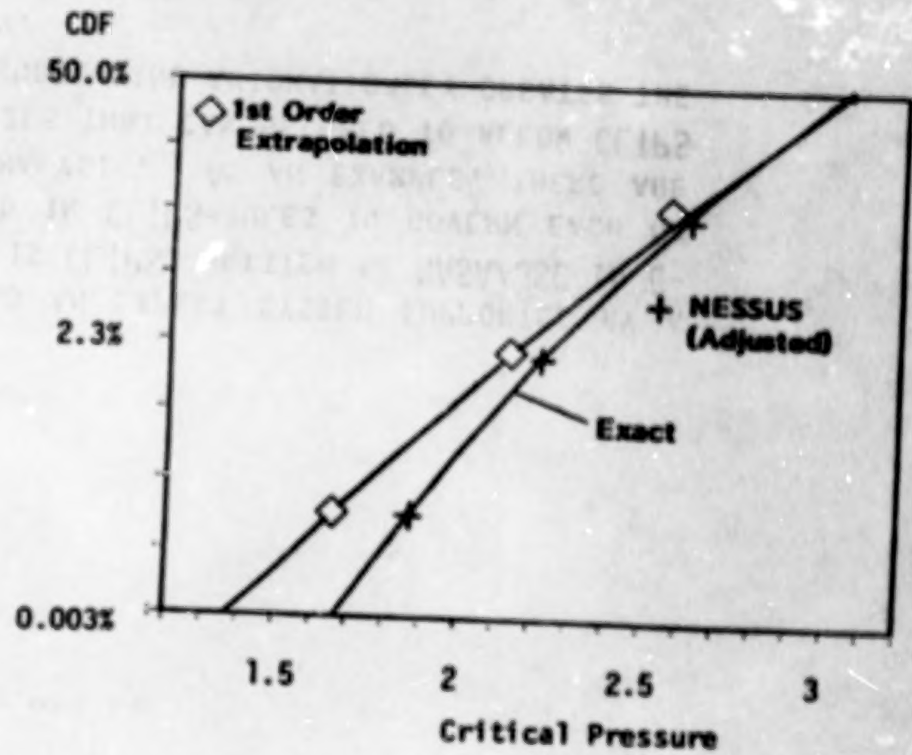

The next NESSUS validation problem concerns prediction of the critical buckling pressure of a cylindrical shell with an uncertain shell thickness, for the indicated buckling mode. The solution parameters are given along with the statistical input data. The solution was established at three probability levels shown by the data points. The MVFO solution corresponds to the A-solutions on Figure 8. The X-data points correspond to the B-solutions (no C-solution iteration required). Correspondence to the exact solution was excellent, based on a calibrated shift of the predicted buckling pressures, based on a 10% error in the mean (deterministic) solution. Thus we see that the NESSUS algorithm is able to accurately predict distributions even though there will always be modeling errors in the deterministic solution.

NESSUS FEM/FPI MODELS TOLERANCE EFFECTS ON K_T

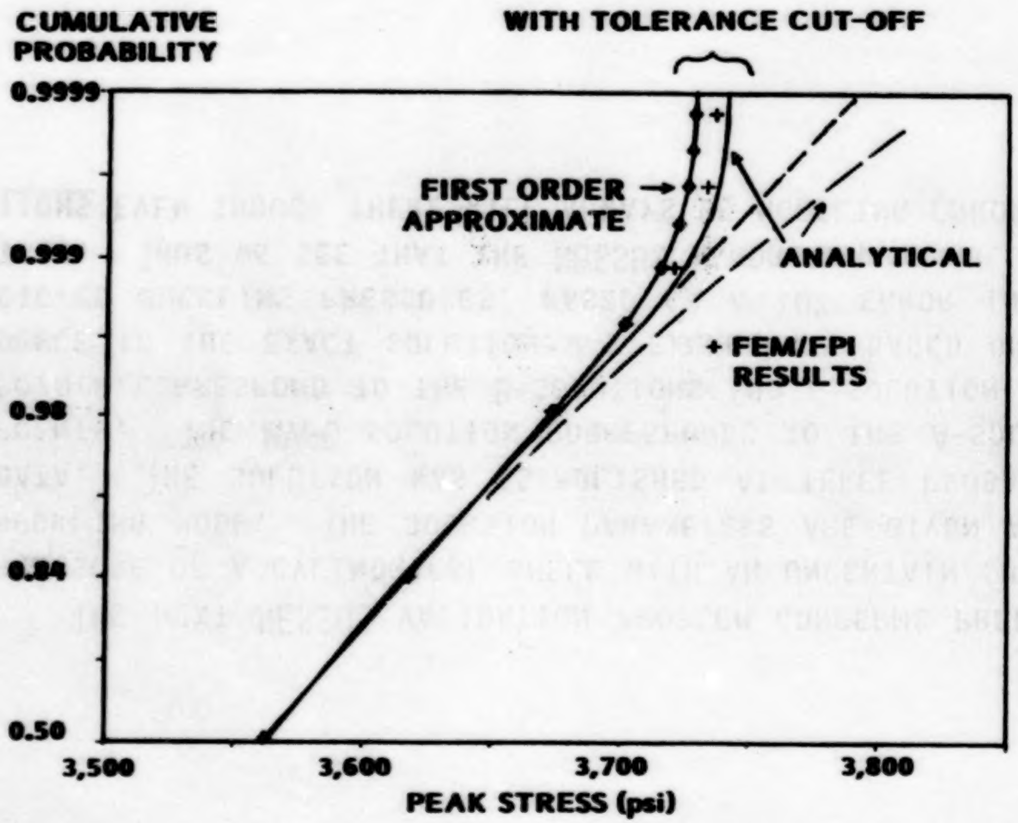

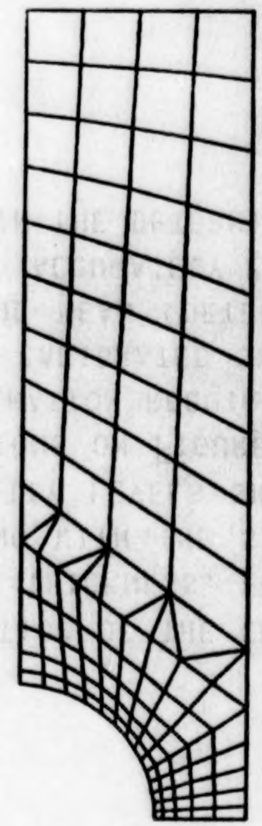

LOCAL STRESSES

- o 2D Plane Stress
- o Uniform Tension
- o Uncertain Radius
  - ±2%
  - ± 6% Cut-off
  - Normal Distribution

This validation problem demonstrates the use of a truncated distribution to describe one of the input variables--the notch radius. The finite element model simulates the effect of geometric uncertainty on the peak stress concentration. The Gaussian distribution of notch size uncertainty was truncated at ±6% variation to simulate tolerance limits. The truncation on the maximum stress is clearly shown.

TURBINE BLADE ANALYSIS

- RANDOM VARIABLES
  - GEOMETRY
  - MATERIAL ORIENTATION
  - MATERIAL PROPERTIES
- STEADY STATE
  - CENTRIFUGAL LOAD
  - TEMPERATURE
  - STATIC PRESSURE AND ΔP
- RESPONSE VARIABLES
  - CENTRIFUGAL STRESS
  - PRESSURE STRESS
  - FREQUENCY

- 3-D SOLID MODEL

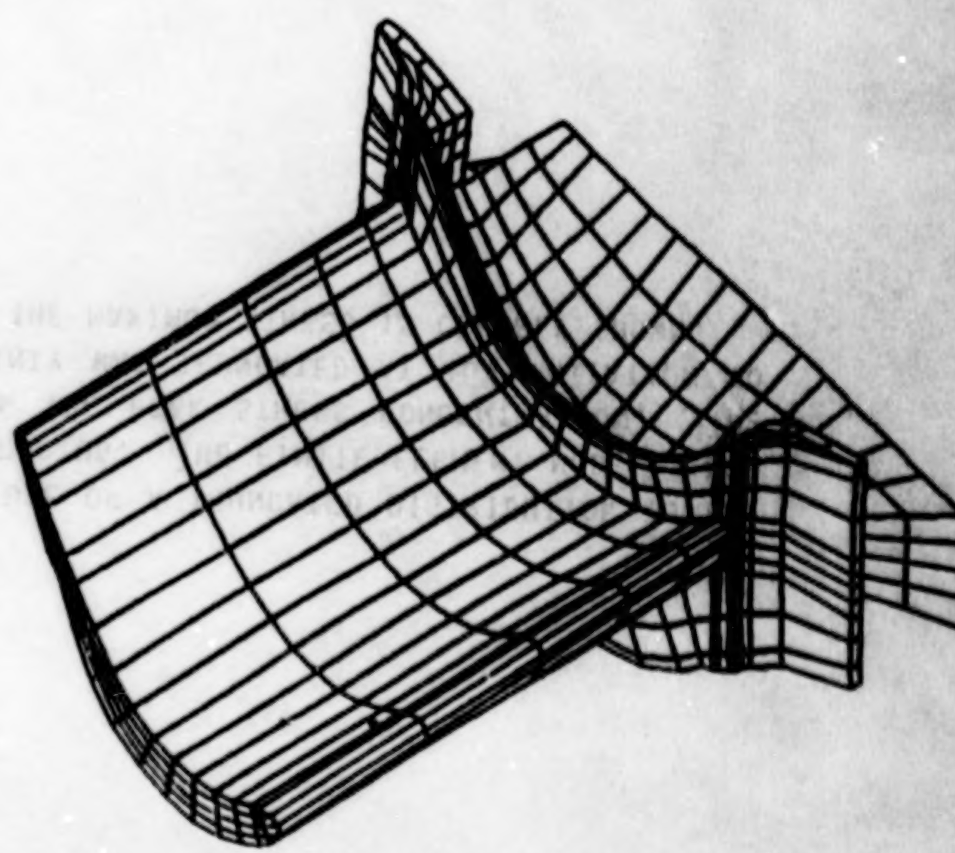

Rockwell International

SOME NUMERICAL RESULTS FOR THE FIRST VERIFICATION PROBLEM FOR PSAM ARE TO BE GIVEN. THE MODEL RESULTS ARE FOR THE SSME TURBOPUMP BLADES. THE FEM MODEL OF THE TURBINE BLADE HAS ABOUT 2,500 NODES (1,456 ELEMENTS) AND 6,000 DEGREES OF FREEDOM USING EIGHT-NODE ISOPARAMETRIC SOLID ELEMENTS. THE STEADY-STATE LOAD RESPONSE IS ANALYZED WITH BLADE GEOMETRY (TWIST, TILT), SINGLE-CRYSTAL AXIS ORIENTATIONS (PRIMARY, SECONDARY), AND ELASTIC PROPERTIES AS THE TEN RANDOM VARIABLES.

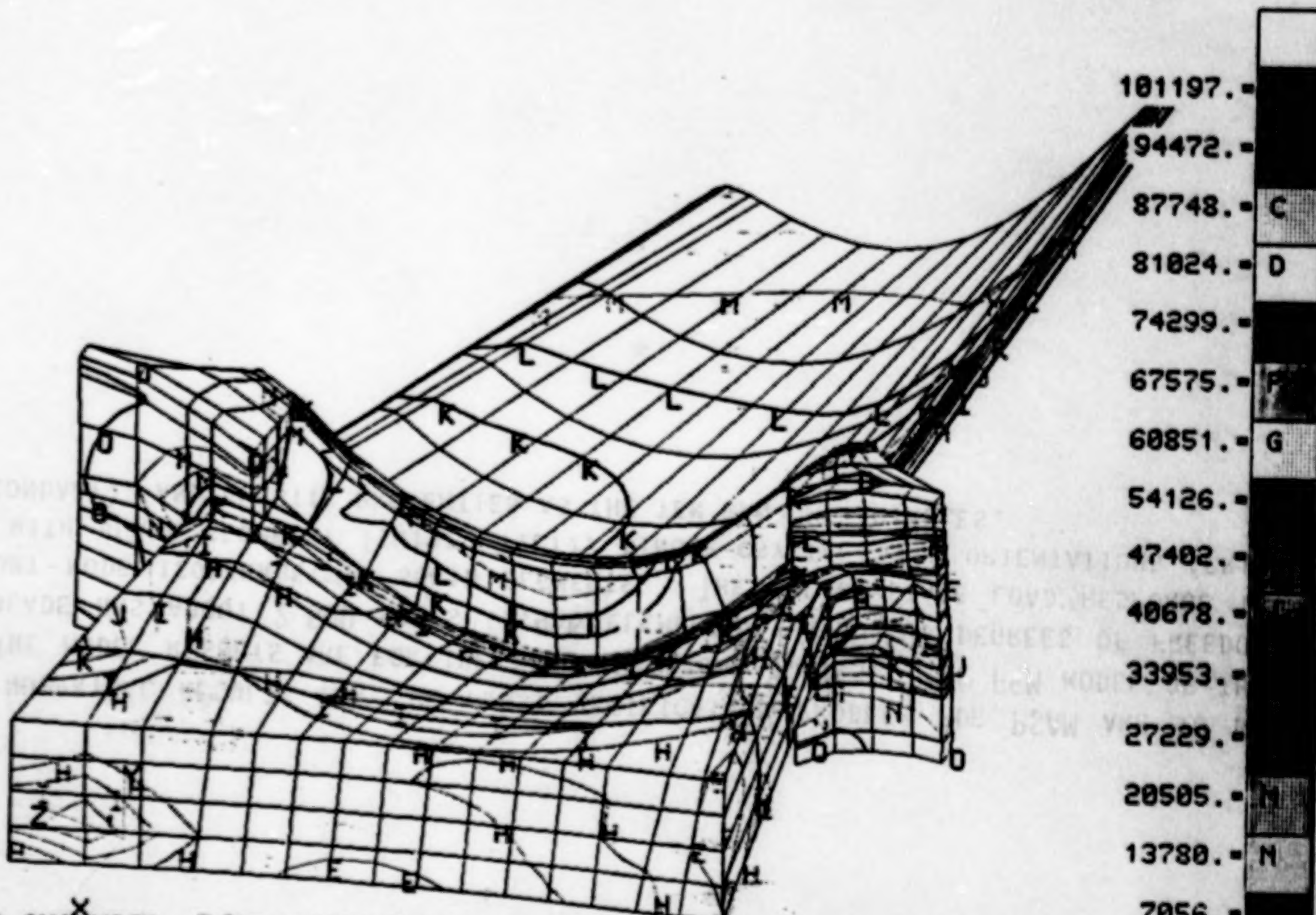

PROB.ANALYSIS - MAT.ORIEN,ELASTIC CONSTANTS AND GEOMETRY AS RANDOM

MEAN VALUE - EFFECTIVE STRESS (PSI)

THE CONTOUR PLOTS SHOW THE MEAN VALUE LEVELS OF THE EFFECTIVE STRESS FOR THE DETERMINISTIC LOAD CASE.

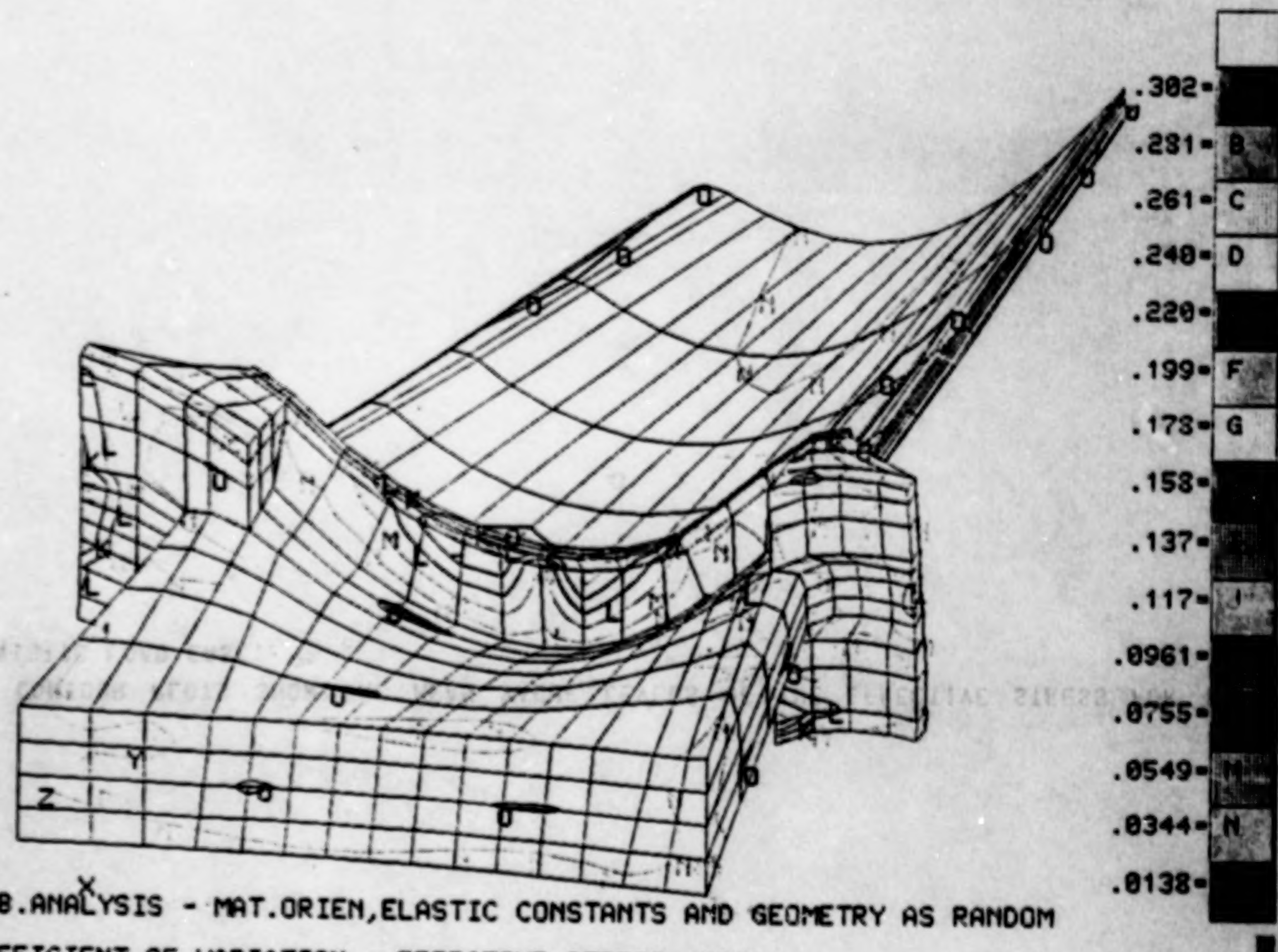

PROB.ANALYSIS - MAT.ORIEN,ELASTIC CONSTANTS AND GEOMETRY AS RANDOM
COEFFICIENT OF VARIATION - EFFECTIVE STRESS (PSI)

THE COEFFICIENT OF VARIATION CONTOURS ARE PLOTTED FOR THE RANDOM CONDITIONS. THE COEFFICIENT OF VARIATION IS DETERMINED BASED ON THE FIRST-ORDER PERTURBATION ABOUT THE MEAN STATE.

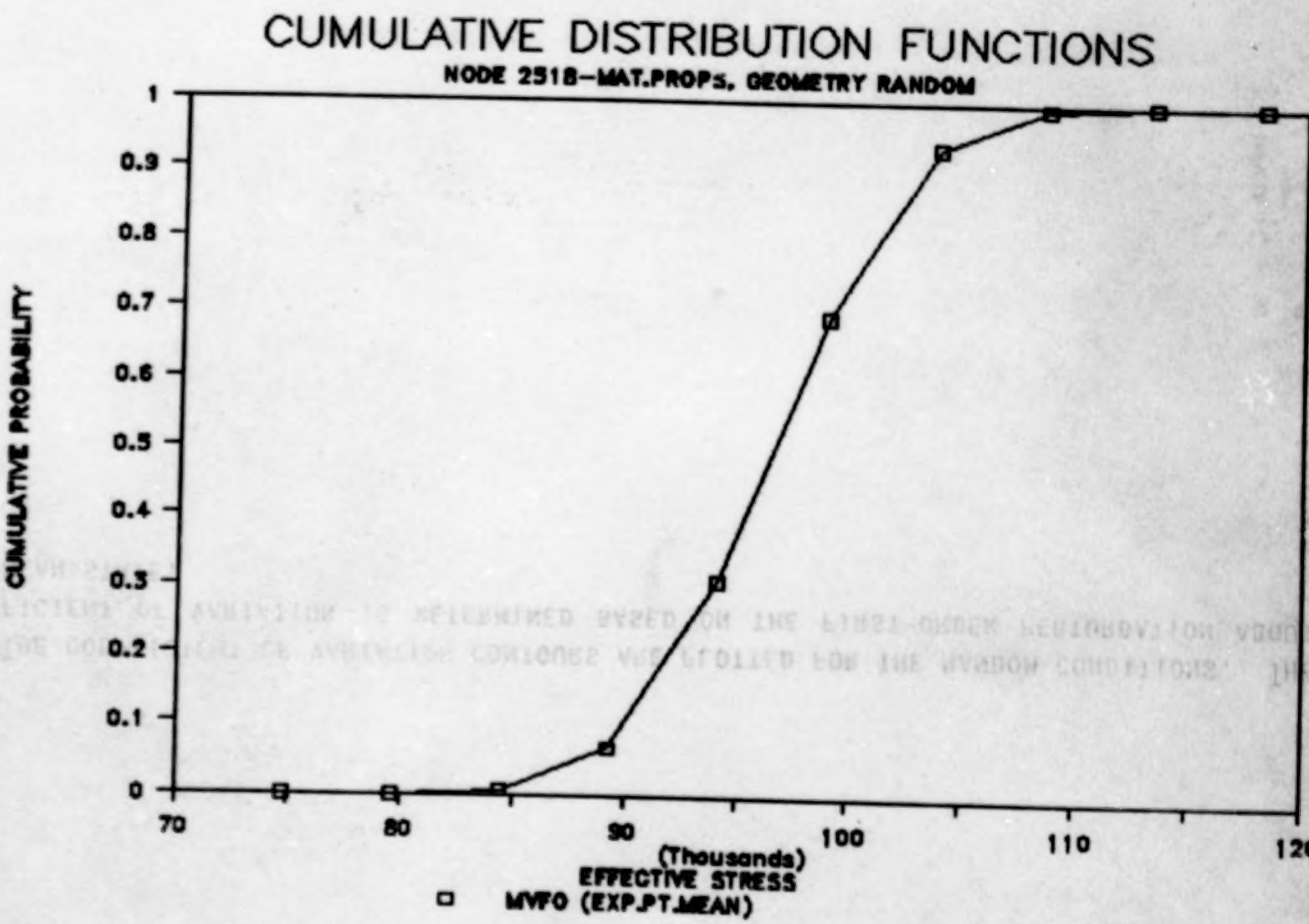
CUMULATIVE DISTRIBUTION FUNCTIONS
NODE 2518—MAT.PROPS. GEOMETRY RANDOM
CUMULATIVE PROBABILITY
1
0.9
0.8
0.7
0.6
0.5
0.4
0.3
0.2
0.1
0
70
80
90
100
110
120
(Thousands)
EFFECTIVE STRESS
MVFO (EXP.PT.MEAN)

THE CUMULATIVE DISTRIBUTION FUNCTION FOR THE EFFECTIVE STRESS AT NODE 2518 IS PLOTTED BASED ON THE FIRST-ORDER PERTURBATION ABOUT THE MEAN STATE.

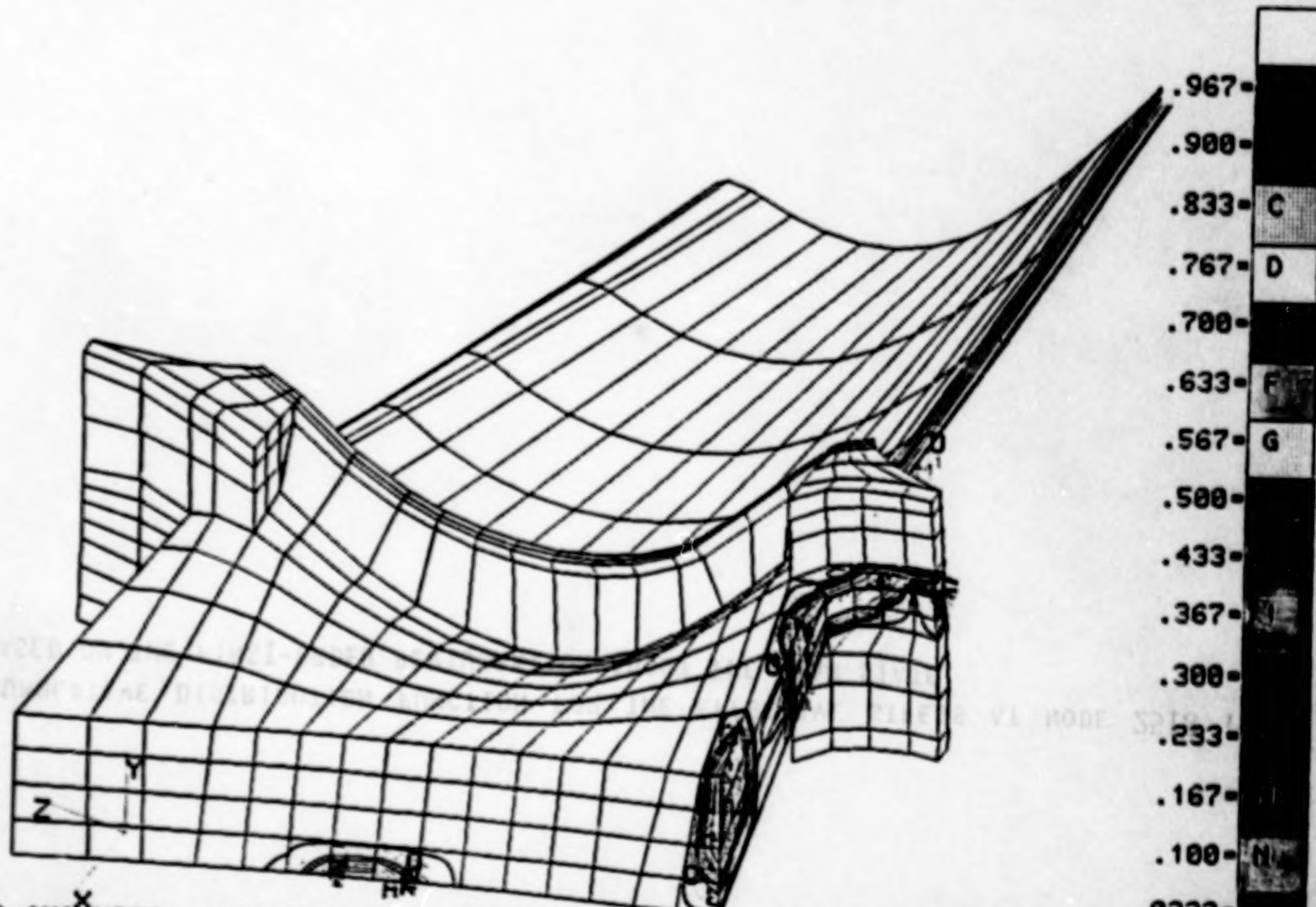

PROB.ANALYSIS - MAT.ORIEN,ELASTIC CONSTANTS AND GEOMETRY AS RANDOM
EFFECTIVE STRESS - PROB.OF EXCEEDING 80000 PSI

CUMULATIVE PROBABILITY LEVEL CONTOURS ARE PLOTTED SHOWING THE PROBABILITY OF EXCEEDING 80,000 PSI DUE TO THE DEFINED RANDOM VARIABLES. THREE "HOT-SPOTS" ARE INDICATED.

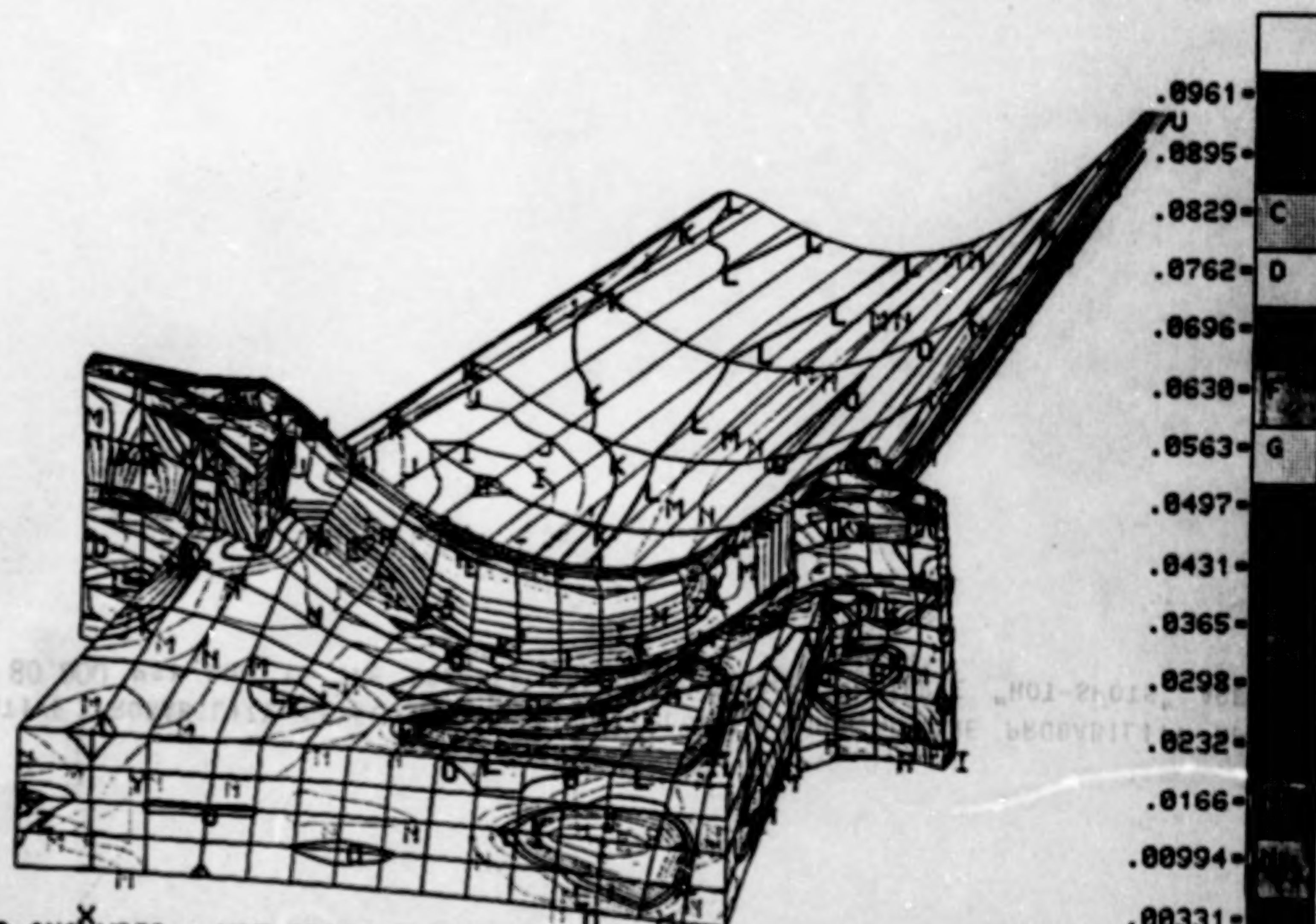

PROB.ANALYSIS - MAT.ORIEN,ELASTIC CONSTANTS AND GEOMETRY AS RANDOM
SENSITIVITY FACTOR FOR THE GEMETRIC TWIST ANGLE

ORIGINAL PAGE IS
OF POOR QUALITY

The contours indicated a relative measure of sensitivity of the effective stress due to the random variable of geometric twist of the model. The sensitivity level measure is nondimensional and includes the effect of the statistical character of the variable and the sensitivity of stress to the variable.

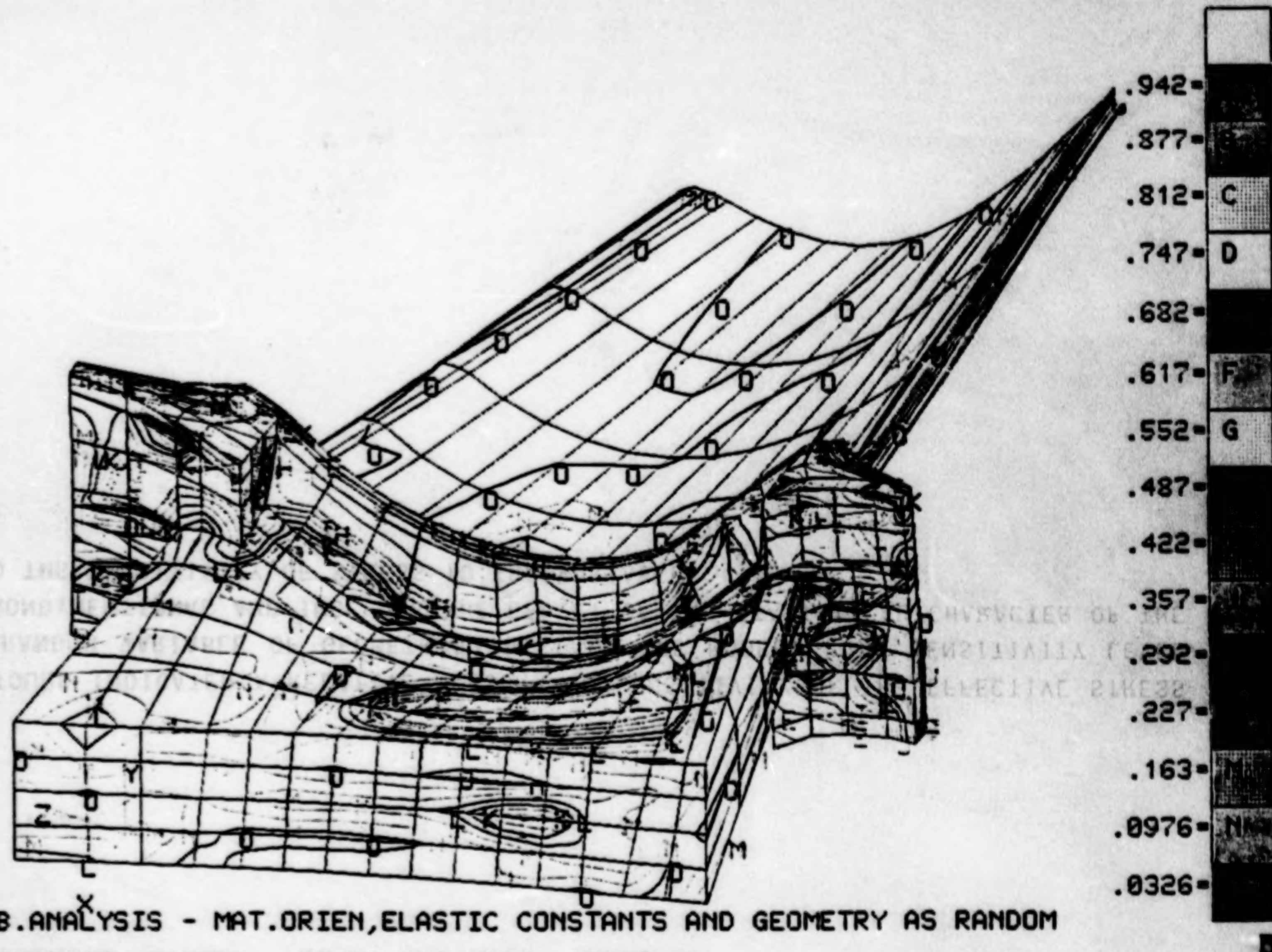

PROB.ANALYSIS - MAT.ORIEN,ELASTIC CONSTANTS AND GEOMETRY AS RANDOM

SENSITIVITY FACTOR - SECON.MAT.ORIEN.(THETAX)

ORIGINAL PAGE IS
OF POOR QUALITY

THE CONTOURS OF SENSITIVITY FACTOR FOR EFFECTIVE STRESS DUE TO THE SPECIFIED UNCERTAINTY IN THE SECONDARY MATERIAL ORIENTATION ARE SHOWN.

WHY DO PROBABILISTIC DESIGN?

- HOW SAFE IS IT?
- HOW WILL IT PERFORM?
- WHAT IS MY CONFIDENCE?
- HOW CAN I MAKE IT MORE RELIABLE?

THE USE OF PROBABILISTIC STRUCTURAL ANALYSIS IS FUNDAMENTAL TO THE ASSESSMENT OF STRUCTURAL PERFORMANCE FOR UNCERTAINTIES IN MATERIAL PROPERTIES, GEOMETRY, BOUNDARY CONDITIONS, AND LOADING. THE NUMERICAL RESULTS CAN BE USED TO DEFINE THE RELATIVE IMPORTANCE OF THE UNCERTAIN VARIABLES, THEREBY PROVIDING DESIGN SUPPORT CAPABILITY FOR MAKING THE STRUCTURE MORE RELIABLE.

N89
29803
UNCLAS

PROBABILISTIC FINITE ELEMENTS (PFEM)
APPLIED TO STRUCTURAL DYNAMICS AND FRACTURE MECHANICS

PRINCIPAL INVESTIGATORS:
Wing-Kam Liu
Ted Belytschko

RESEARCH ASSISTANTS:
A. Mani
G. Besterfield

Northwestern University
Evanston, IL 60208

NASA Grant NAG-3-535
Contract Monitor: Christos Chamis
May 1, 1984 to August 31, 1987

OBJECTIVES OF PFEM PROGRAM:

- o TO PROVIDE INTEGRATED METHODOLOGIES FOR PROBABILISTIC FINITE ELEMENTS BASED ON VARIATIONAL PRINCIPLES WHICH ARE COMPUTATIONALLY EFFICIENT
- o TO INVESTIGATE FUNDAMENTAL ASPECTS OF IMPLEMENTATION OF PROBABILISTIC FINITE ELEMENTS IN TRANSIENT ANALYSIS
- o TO DEVELOP BENCHMARK PROBLEMS AND SOLUTIONS

SLIDE 1

PROBABILISTIC FINITE ELEMENTS (PFEM) APPLIED TO STRUCTURAL DYNAMICS AND FRACTURE MECHANICS

Wing-Kam Liu, Ted Belytschko, A. Mani, and G. Besterfield

SLIDE 1

The purpose of this work is to develop computationally efficient methodologies for assessing the effects of randomness in loads, material properties, and other aspects of a problem by a finite element analysis. The resulting group of methods is called probabilistic finite elements (PFEM). The overall objective of this work is to develop methodologies whereby

1. the lifetime of a component can be predicted, accounting for the variability in the material and geometry of the component, the loads, and other aspects of the environment;
2. the range of response expected in a particular scenario can be presented to the analyst in addition to the response itself.

Emphasis in this work has been placed on methods which are not statistical in character, that is, they do not involve Monte Carlo simulations. The reason for this choice of direction is that Monte Carlo simulations of complex nonlinear response require a tremendous amount of computation.

The focus of our efforts so far has been on nonlinear structural dynamics. However, in the continuation of this project, emphasis will be shifted to probabilistic fracture mechanics so that the effect of randomness in crack geometry and material properties can be studied interactively with the effect of random load and environment. The ultimate goal of this effort will be to predict the behavior of cracks in such environments, which is an essential step towards lifetime prediction of structural components.

In addition, we are investigating how these methods should be implemented and developing benchmark problems.

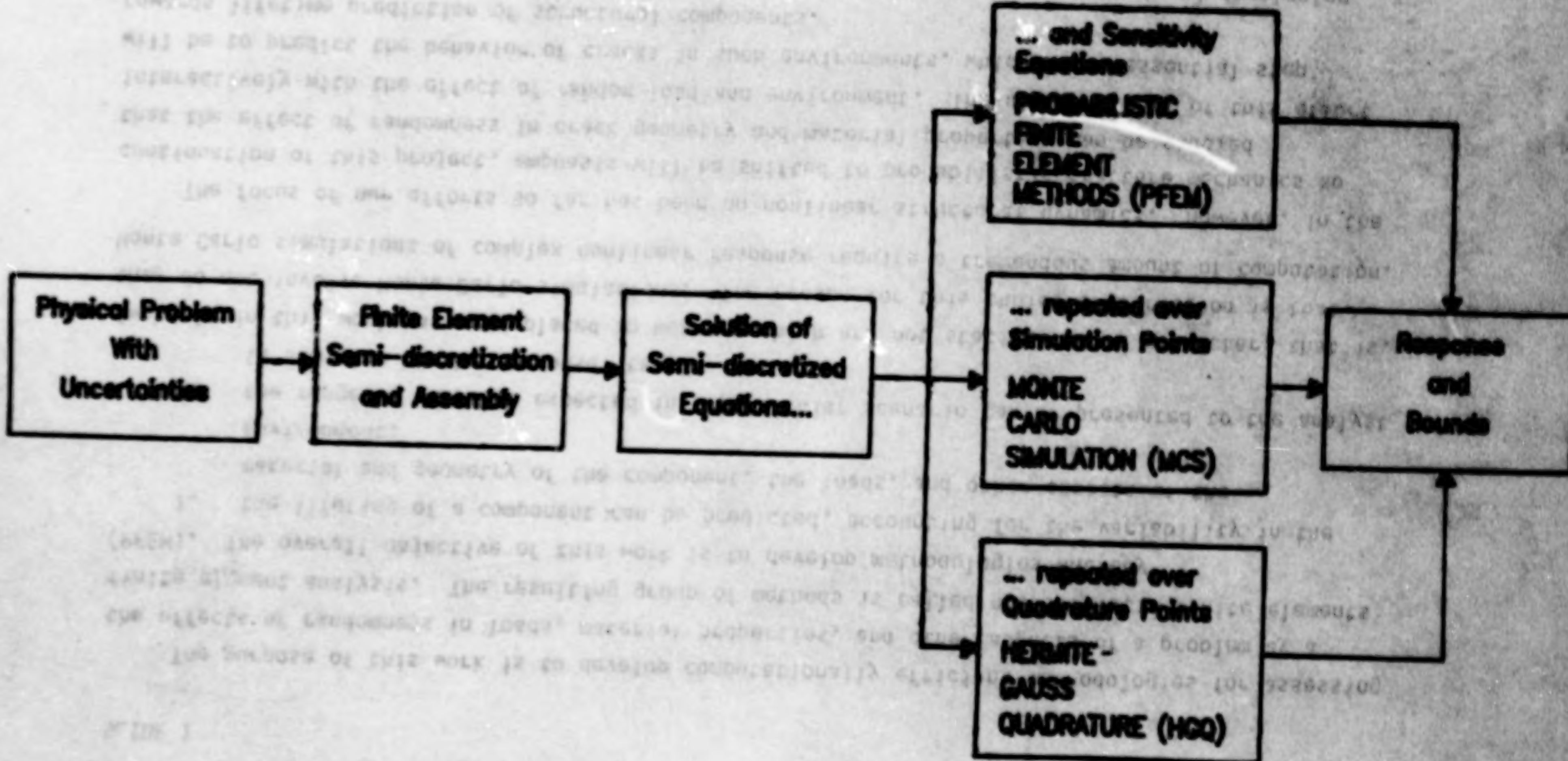
Physical Problem With Uncertainties
Finite Element Semi-discretization and Assembly
Solution of Semi-discretized Equations...
... and Sensitivity Equations
PROBABILISTIC FINITE ELEMENT METHODS (PFEM)
... repeated over Simulation Points
MONTE CARLO SIMULATION (MCS)
... repeated over Quadrature Points
HERMITE - GAUSS QUADRATURE (HGQ)
Response and Bounds

SLIDE 2

SLIDE 2

An outline of the schema in applying probabilistic finite elements is shown on this slide. The starting point is the physical problem which is characterized by uncertainties and the development of a finite element model. The latter involves the development of semidiscretized equations for the elements and their assembly into global equations. In the methods we have developed, the randomness of the problem is also described on an element basis, and the development of the global description of randomness is obtained by the same assembly procedure as for the deterministic variables.

The result of this assembly procedure is a set of semidiscretized equations, which, for a nonlinear structural dynamics system, are nonlinear algebraic equations. This slide shows three methods of approach to the solution of these equations.

1. Hermite-Gauss quadrature, which involves numerical quadrature over the probabilistic space which describes the problem; this method is feasible only for three to ten probabilistic functions.
2. Monte Carlo simulation, in which the semidiscretized equations are solved repeatedly with the values of the probabilistic variables in the model and environment determined by a random-number generator; this approach involves substantial computational effort.
3. Combination of the semidiscretized equation with sensitivity equations and some type of a perturbation method; this is the type of method which has been adopted in probabilistic finite elements, where a second-order moment method has been used.

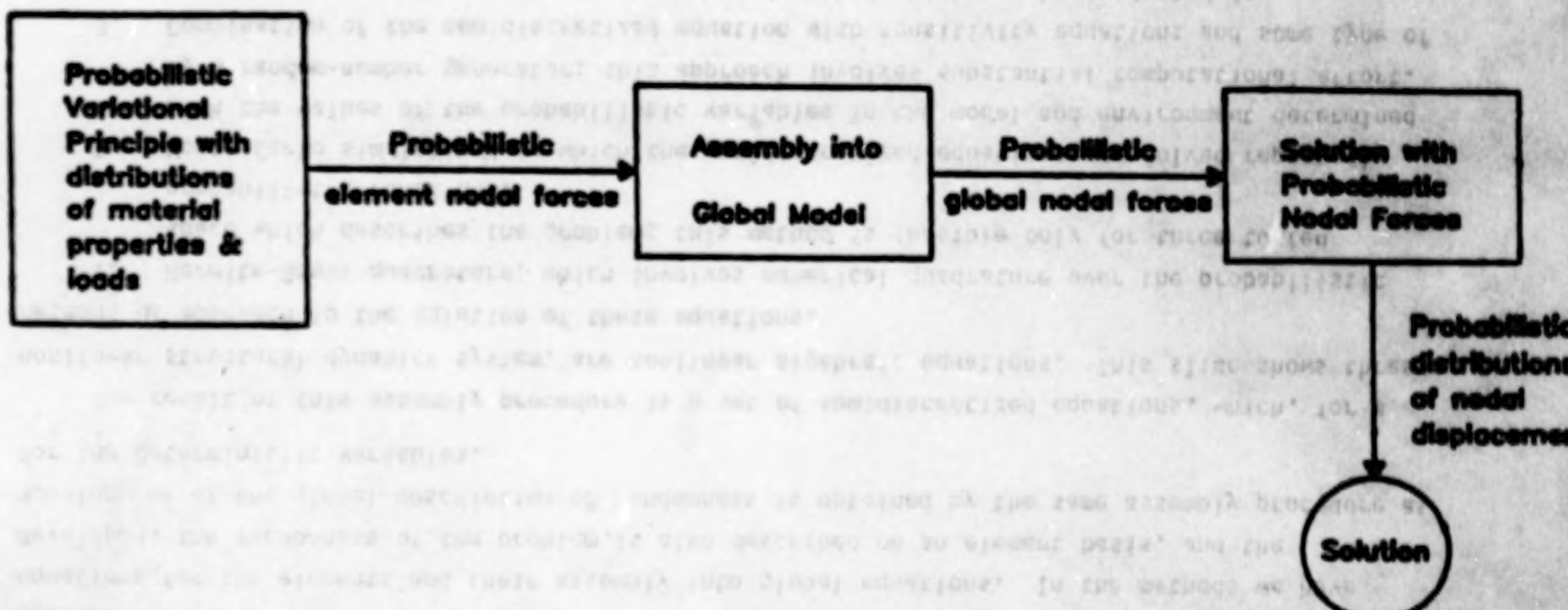
Probabilistic Variational Principle with distributions of material properties & loads
Probabilistic element nodal forces
Assembly into Global Model
Probabilistic global nodal forces
Solution with Probabilistic Nodal Forces
Probabilistic distributions of nodal displacements
Solution

SLIDE 3

SLIDE 3

An essential element in obtaining semidiscretized equations is a variational principle which provides a weak form for the governing equations. At the right, we show the relationship between the variational principle and the solution. The variational principle is used to obtain the weak form, which, in terms of the computer architecture, leads to the probabilistic nodal forces. All of the deterministic and random properties are assembled in the same way from the element level to the global model. The solution of the semidiscretized system yields the probabilistic distributions of nodal displacements, which can then be returned to the element level to yield probabilistic distributions in strain, stress, and other response variables.

HU-WASHIZU VARIATIONAL FORM FOR PROBABILISTIC FINITE ELEMENT

$$\delta u_{iI} f_{iI} - \int_{\Omega_e} \Big[\delta\epsilon_{ij} \underbrace{(C_{ijk\ell}\epsilon_{k\ell} - \sigma_{ij})}_{\text{CONSTITUTIVE}} + \delta u_{i,j} \underbrace{\sigma_{ij} - \delta u_i b_i}_{\text{EQUILIBRIUM}} + \delta\sigma_{ij} \underbrace{(u_{i,j} - \epsilon_{ij})}_{\text{STRAIN-DISPLACEMENT}} \Big] d\Omega$$

b_i . . . RANDOM DESCRIPTION OF MATERIAL, LOAD, BOUNDARY CONDITIONS $i = 1$ TO 9

$$\underset{\sim}{M}\,\underbrace{\underset{\sim}{a}}_{\ddot{d}} + \underset{\sim}{f}(\underset{\sim}{b}, \underset{\sim}{d}, \dot{\underset{\sim}{d}}) = \underset{\sim}{F}(\underset{\sim}{b})$$

CD-87-30816

SLIDE 4

The starting point for the development of the probabilistic finite element method is the Hu-Washizu variational form. This variational form constitutes a weak form for the following equations:

1. the constitutive equations;
2. the equilibrium equations;
3. the strain displacement equations.

The randomness of the material and geometry in the component and in the environment is described by random variables b_i. We do not account for the effect of randomness on changes in inertial properties as reflected in the mass matrix $\underset{\sim}{M}$, so the structure of the semidiscretized probabilistic equations is as shown on the bottom of this slide. These equations are nonlinear ordinary differential equations; the nonlinearity arises from the nonlinear character of the internal forces, $\underset{\sim}{f}$.

SECOND MOMENT METHOD OPERATORS FOR FORMULATING PROBABILISTIC FINITE ELEMENTS

EXPECTED VALUE OPERATOR

$$E\left[\underset{\sim}{\Phi}(\underset{\sim}{b})\right] = \underbrace{\bar{\underset{\sim}{\Phi}}}_{\equiv \text{MEAN}} + \underbrace{\frac{1}{2} \frac{\partial^2 \bar{\Phi}}{\partial b_i \partial b_j} \text{COV}(b_i, b_j)}_{\Delta \bar{\Phi}} \quad \text{SUM ON } i, j$$

OBTAINED BY TAYLOR SERIES

$$E\left[\underset{\sim}{f}\right] = \bar{f}$$

$$+ \frac{1}{2} \frac{\partial^2 \bar{f}}{\partial b_i \partial b_j} \text{COV}(b_i, b_j)$$

$$+ \left(\frac{\partial \bar{\underset{\sim}{C}}}{\partial b_i} \frac{\partial \bar{\underset{\sim}{v}}}{\partial b_j} + \frac{\partial \bar{K}}{\partial b_i} \frac{\partial \bar{d}}{\partial b_j} \right) \text{COV}(b_i, b_j)$$

$$+ \frac{1}{2} \left(\bar{\underset{\sim}{C}} \frac{\partial^2 \bar{\underset{\sim}{v}}}{\partial b_i \partial b_j} + \bar{\underset{\sim}{K}} \frac{\partial^2 \underset{\sim}{d}}{\partial b_i \partial b_j} \right) \text{COV}(b_i, b_j)$$

SLIDE 5

SLIDE 5

The development of the probabilistic finite element method is based on a second-order moment method. A fundamental aspect of this method is the representation of the probabilistic distribution by the mean value, which is denoted by superposed bars, and the covariance of the random variables. The expectation of any function of the probabilistic variables is given in the first expression on this slide.

The expectation of the internal nodal forces is obtained by a Taylor series and a linearization of the nonlinear equations of motion as indicated in the second equation. Here, $\bar{\underset{\sim}{K}}$ is a tangent stiffness matrix about the mean nonlinear path, $\bar{\underset{\sim}{C}}$ is a damping matrix, and $\bar{v}$ indicates the mean velocity history.

PROBABILISTIC FINITE ELEMENT GOVERNING EQUATIONS

<u>MEAN VALUE EQUATION</u>

$$\underset{\sim}{M}\underset{\sim}{\bar{a}} + \underset{\sim}{\bar{f}} = \underset{\sim}{F}$$

OR

$$\underset{\sim}{M}\underset{\sim}{\bar{a}} + \underset{\sim}{\bar{C}}\underset{\sim}{\bar{v}} + \underset{\sim}{\bar{K}}\underset{\sim}{\bar{d}} = \underset{\sim}{F}$$

<u>SENSITIVITY EQUATIONS</u>

$$\underset{\sim}{M}\frac{\partial \bar{a}}{\partial b_j} + \underset{\sim}{\bar{C}}\frac{\partial \bar{v}}{\partial b_j} + \underset{\sim}{\bar{K}}\frac{\partial \bar{d}}{\partial b_j} = \partial \underset{\sim}{f}/\partial b_j$$

<u>VARIANCE EQUATION</u>

$$\underset{\sim}{M}\,\Delta\underset{\sim}{\bar{d}} + \underset{\sim}{\bar{C}}\,\Delta\underset{\sim}{\bar{v}} + \underset{\sim}{K}\,\Delta\underset{\sim}{\bar{d}} = \Delta\bar{f}$$

$$\Delta\bar{\Phi} = \frac{1}{2}\sum_{j=1}^{9}\frac{\partial^2\bar{\Phi}}{\partial b_i^2}\,\mathrm{VAR}(b_i)$$

SLIDE 6

The governing equations for the system can then be written as follows. The mean value equation is a nonlinear equation which reflects the nonlinearities of the system. In addition, we have a system of sensitivity equations; the number of these equations is equal to the number of discrete random variables which define the probabilistic aspects of the component and its environment. Finally, we have the variance equation which gives the variance of the response variables in terms of the variance of the probabilistic variables.

ITEM	CALCULATED QUANTITIES	EQUATION NUMBERS	NUMBERS OF INTEGRATIONS in time
1	The mean values i.e. $\bar{\underline{d}}$, $\bar{\underline{v}}$ and $\bar{\underline{a}}$	(3.1a)	1
2	The sensitivity derivatives for each random variable b_j, $j = 1, \ldots, q$ i.e., $\frac{\partial \bar{\underline{d}}}{\partial b_j}$, $\frac{\partial \bar{\underline{v}}}{\partial b_j}$ and $\frac{\partial \bar{\underline{a}}}{\partial b_j}$	(3.2a)	q
3	The second order variations i.e., $\Delta\bar{\underline{d}}$, $\Delta\bar{\underline{v}}$ and $\Delta\bar{\underline{a}}$	(3.1b)	1
			Total = q + 2

SLIDE 7

SLIDE 7

The number of equations to be solved is summarized in this slide. The mean values are computed by a nonlinear equation in time, whereas the first-order variations are obtained by the q linearized sensitivity equations about the mean path. Finally, the second-order variations are obtained by a single equation in time. The total number of equations is then given by q+2, where q is the number of discrete random variables.

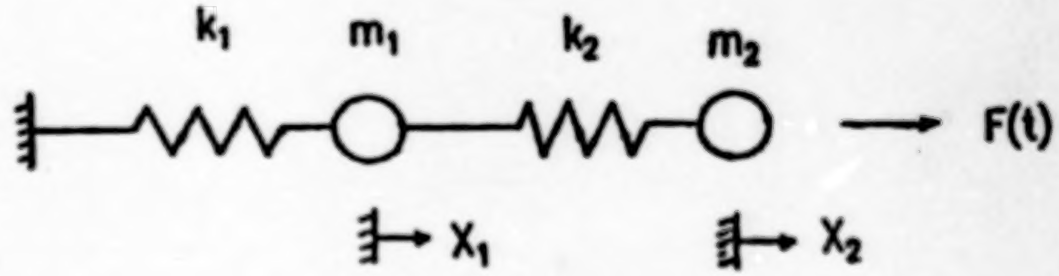

$F(t)=25.0 \times 10^6 \, \mathrm{Sin}(2000t)$

$$\left.\begin{array}{ll} m_1=0.372 & k_1=24.0 \times 10^6 \\ m_2=0.248 & k_2=12.0 \times 10^6 \end{array}\right] \text{Coefficient of Variation} = 0.05$$

SLIDE 8

SLIDE 8

We will now consider several sample problems which have been solved in order to illustrate the type of output which is provided by the method and the capabilities of the method. The first example is a simple two-degree-of-freedom problem with the loading, mass, and stiffness given in the slide. The loading and the masses were considered to be deterministic, while the stiffness was assumed to be random with a coefficient of variation of 5%.

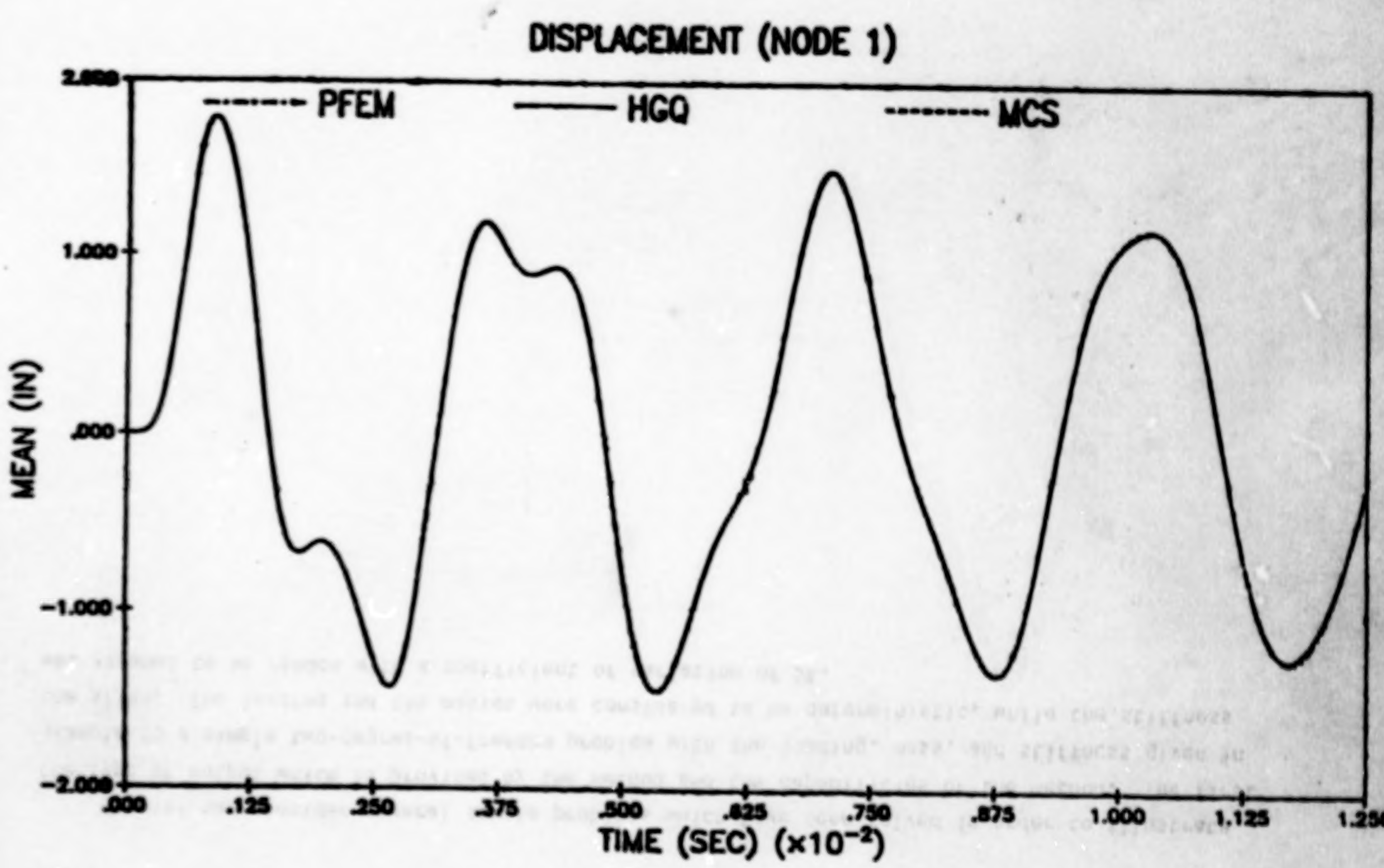
DISPLACEMENT (NODE 1)
PFEM
HGQ
MCS
MEAN (IN)
2.000
1.000
.000
-1.000
-2.000
.000
.125
.250
.375
.500
.625
.750
.875
1.000
1.125
1.250
TIME (SEC) (×10⁻²)

SLIDE 9

SLIDE 9

The two-degree-of-freedom problem was solved by three methods:

1. the probabilistic finite element method (PFEM);
2. Hermite-Gauss quadrature (HGQ);
3. Monte Carlo simulation (MCS).

The reason for choosing the three methods was to evaluate the accuracy of the PFEM method. The PFEM method is much faster than the other two methods for large-scale problems, but it involves certain assumptions about the effects of probabilistic distributions in parameters which govern the component and its environment and their effect on the response. As can be seen from results given here, a mean displacement for node 1 as predicted by the probabilistic finite element method agrees exactly with the other two methods.

DISPLACEMENT (NODE 1)

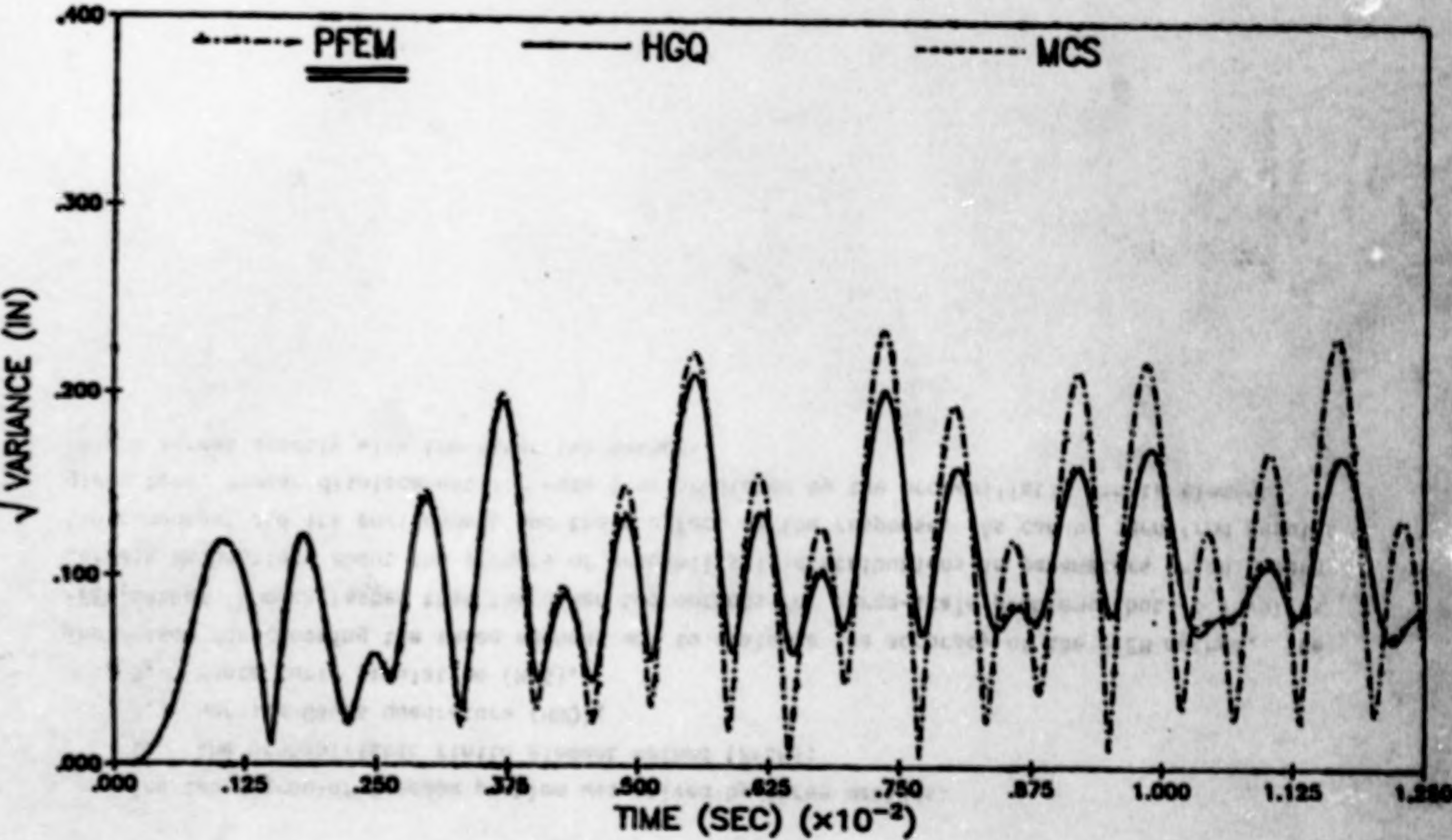

SLIDE 10

SLIDE 10

This slide shows the variance in the displacement at node 1 as predicted by the three methods. In the variance, we see somewhat larger deviation in the three methods. The major reason for this is the effect of the canonical terms on the higher order equations. We have recently developed methods to ameliorate this effect, and these methods have been published in the forthcoming paper, "Probabilistic Transient Systems" (W. K. Liu, G. Besterfield, and T. Belytschko, Computer Methods in Applied Mechanics and Engineering, to appear).

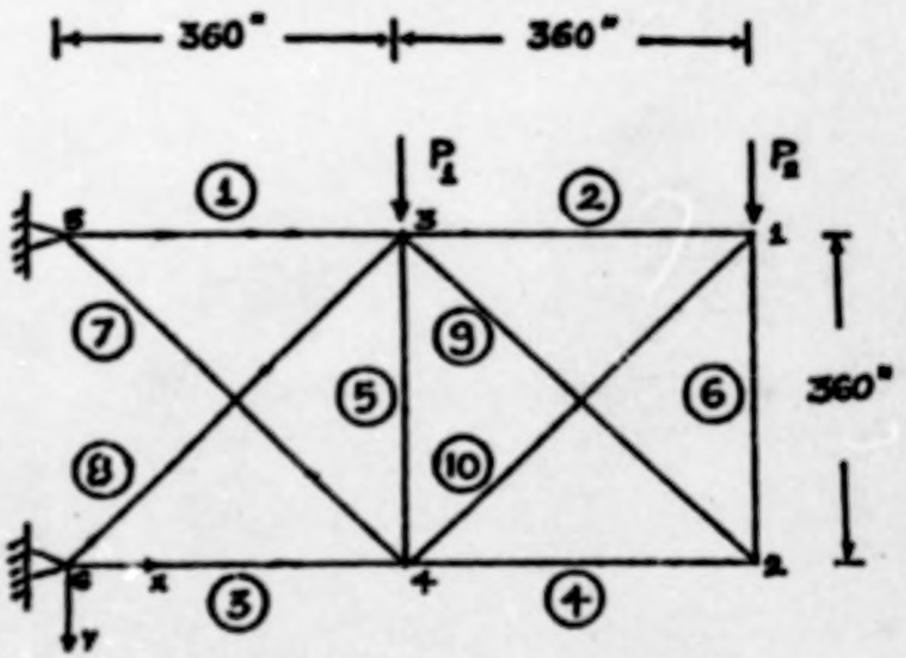

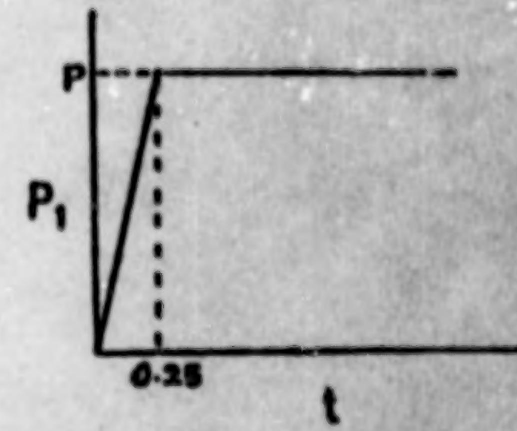

$E = 30.0 \times 10^6$

$E_T = 30.0 \times 10^4$

$A = 6.0$

$\rho = 0.30$

$\sigma_Y = 15000.0$

$P = 175.0 \times 10^3$

$P_2 = 0.0$

5% coef of
variation in
yield stress

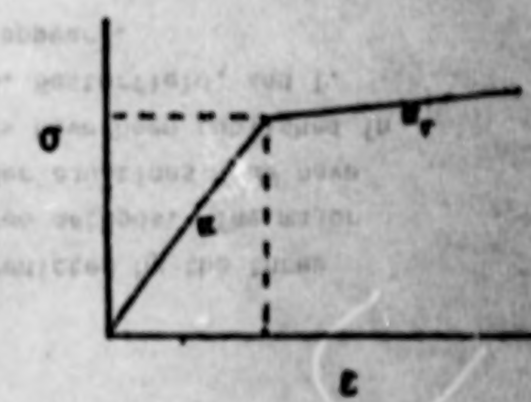

SLIDE 11

SLIDE 11

This example is far more complex and involves strong nonlinearities because the yield stress of the bars is assumed to be random and to have a coefficient of variation of 5%. The parameters of the problem are summarized on the figure.

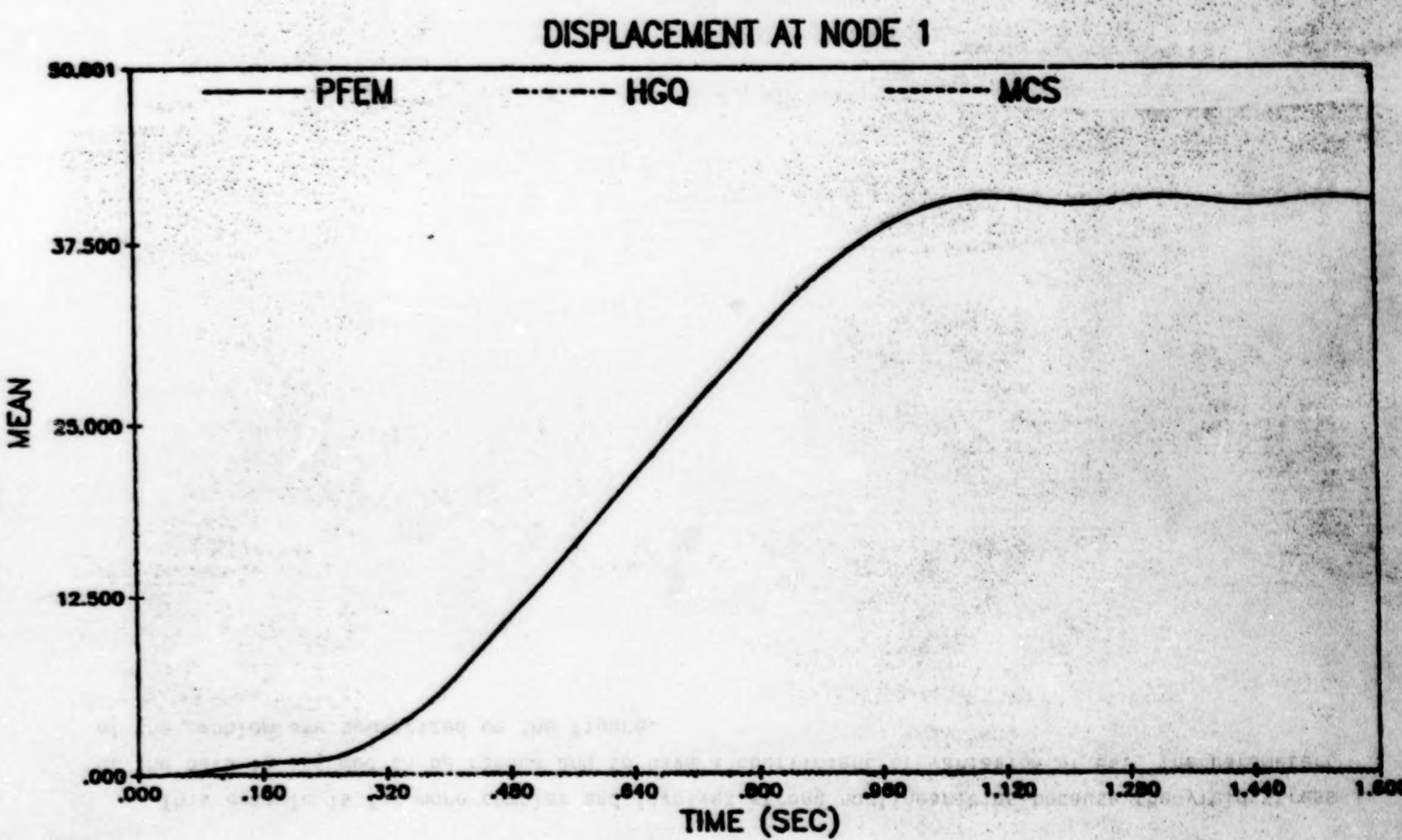
DISPLACEMENT AT NODE 1
PFEM
HGQ
MCS
MEAN
50.001
37.500
25.000
12.500
.000
.000
.160
.320
.480
.640
.800
.960
1.120
1.280
1.440
1.600
TIME (SEC)

SLIDE 12

SLIDE 12

This shows the mean displacement at node 1, which again has been calculated by the probabilistic finite element method, Hermite-Gauss quadrature, and Monte Carlo simulation. As can be seen from the slide, even in this highly nonlinear problem, the three methods agree quite well.

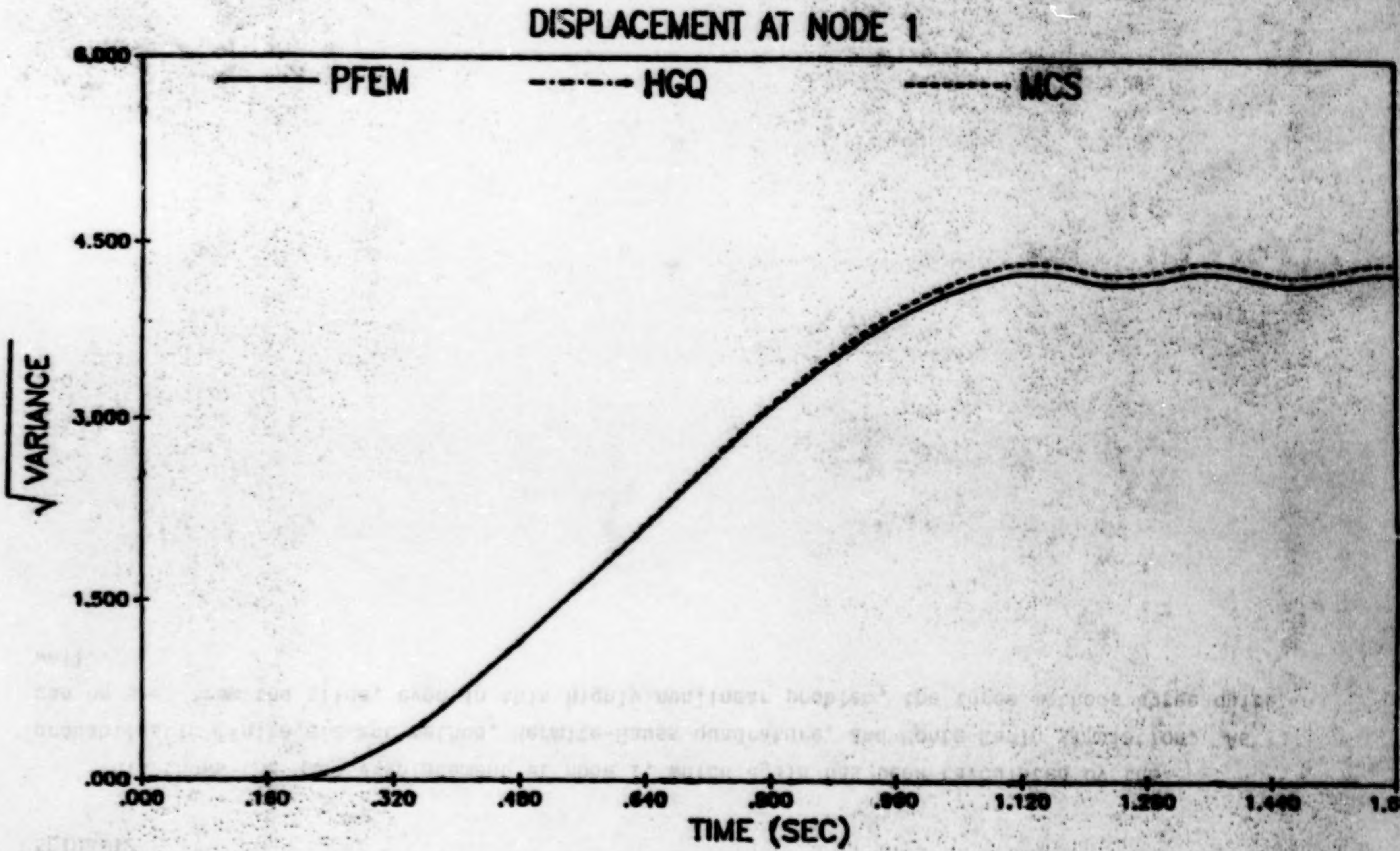

DISPLACEMENT AT NODE 1
PFEM
HGQ
MCS
√VARIANCE
6.000
4.500
3.000
1.500
.000
.000
.160
.320
.480
.640
.800
.960
1.120
1.280
1.440
1.600
TIME (SEC)

SLIDE 13

SLIDE 13

This shows the variance in the displacement at node 1 for this nonlinear example. In contrast to the linear problem, the agreement of the three methods is much better because the canonical terms have little effect in nonlinear response.

DISPLACEMENT BOUNDS AT NODE 1(PFEM)

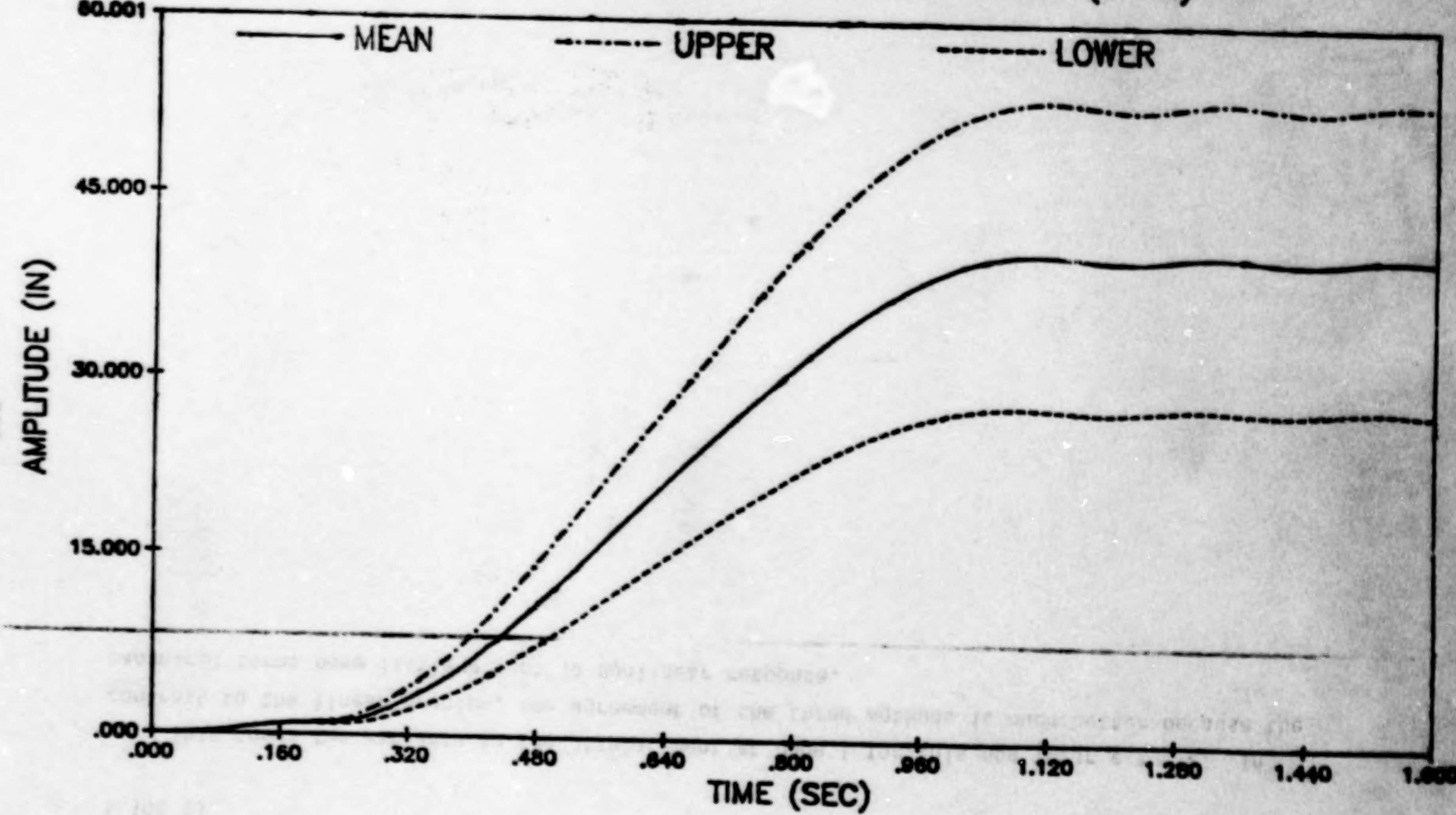

SLIDE 14

This shows the way displacement output would be presented to a typical user of a probabilistic finite element method computer program. The upper and lower bounds here are the displacements which are three standard deviations from the mean. As can be seen from these results, in nonlinear problems of this type, the effects of small variations in the yield stress on displacement results can be very severe.

STRESS BOUNDS IN ELEMENT 1(PFEM)

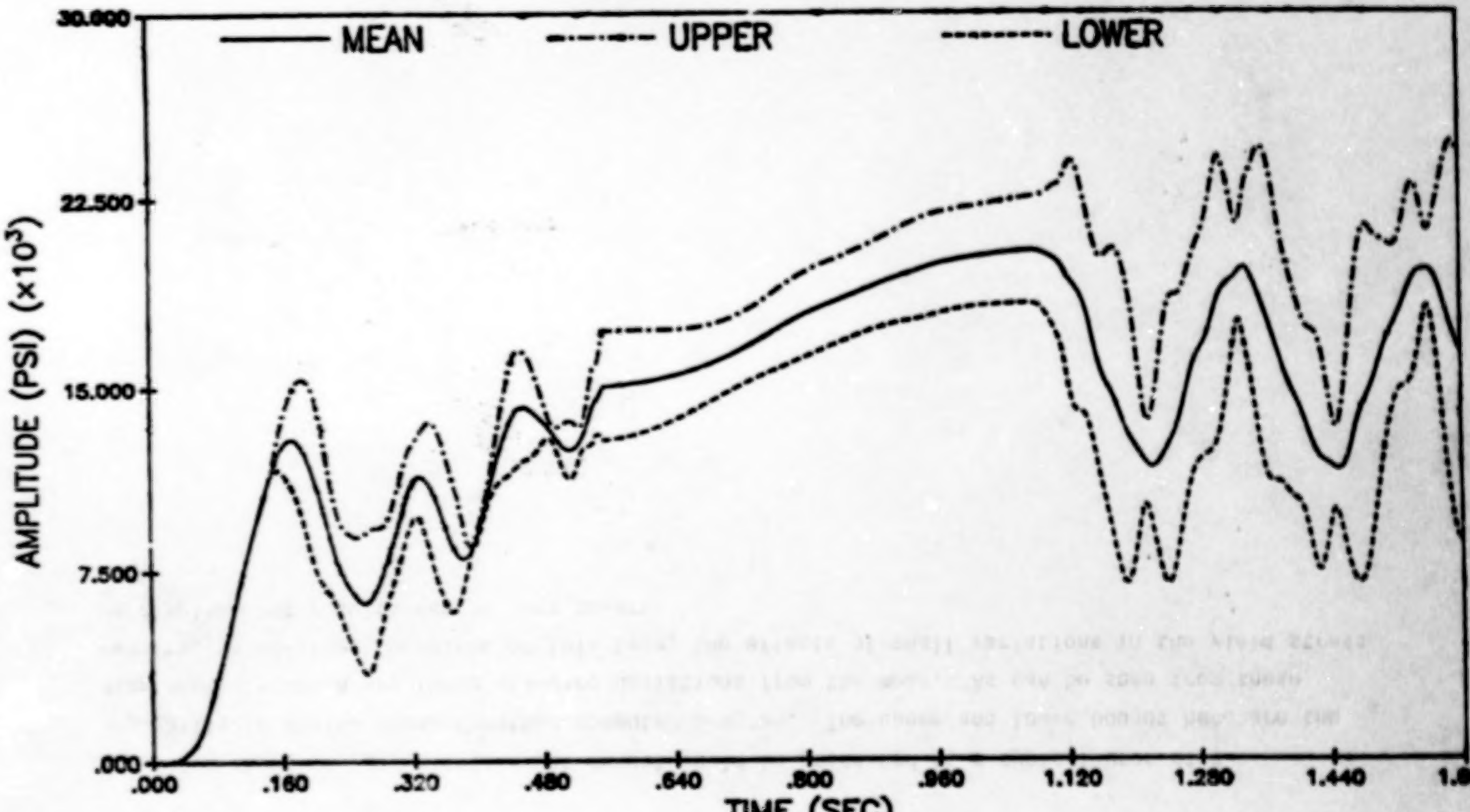

SLIDE 15

This slide shows a similar representation for the stress in element no. 1. This can be seen from the time history of the response; until plasticity is initiated at about .15 seconds, all of the responses are the same, because the only randomness is in the yield stress. Subsequently, the method predicts a reasonably large range in the stresses.

CANTILEVERED SHELL: "TURBINE BLADE SIMULATION"

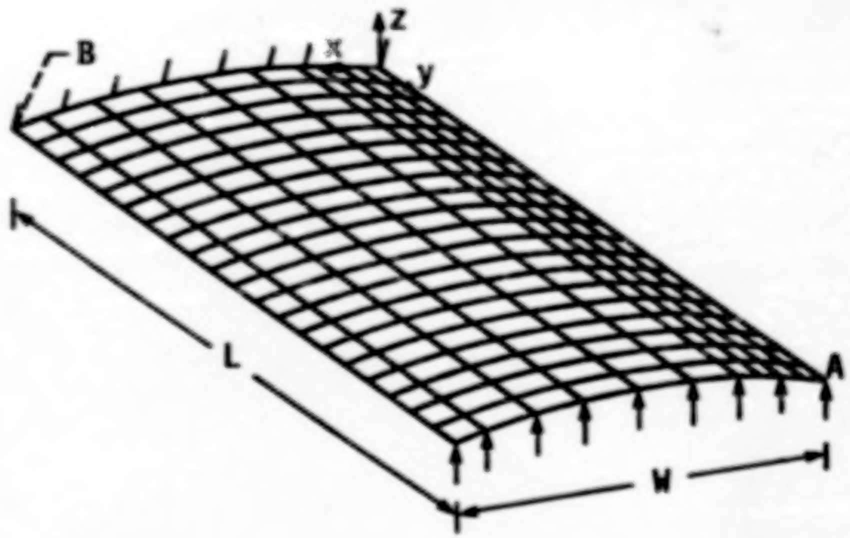

$E = 30.0 \times 10^6$
$E_t = 30.0 \times 10^4$
$\sigma_y = 25000.0$
(ISOTROPIC HARDENING)
$\nu = 0.3$ IN.
$L = 6.3$ IN.
$R = 2.29$ IN.

4 NODE SHELL ELEMENT
WITH SRI
462 NODES, 200 ELEMENTS
DISP. POINT A
STRESS POINT B
MAXIMUM THICKNESS
= 0.3 IN.

<u>RANDOM LOAD CHARACTERISTICS</u>

SIZE OF RANDOM LOAD VECTOR (q) = 10
COEFFICIENT OF VARIATION = 0.10
CORRELATION LENGTH (λ) = 4W
MAXIMUM MEAN LOAD = 13.25 LB

<u>RANDOM MATERIAL CHARACTERISTICS</u>

SIZE OF RANDOM MATERIAL VECTOR (q) = 20
COEFFICIENT OF VARIATION = 0.10
CORRELATION LENGTH (λ) = 4L
MEAN YIELD STRESS = 25000.0

<u>SPATIAL CORRELATION OF RANDOM LOAD AND YIELD STRESS</u>

$R(x_i, x_j) = \text{EXP}(-\text{ABS}(x_i - x_j)/\lambda)$

<u>RANDOM LENGTH</u>

1 VARIABLE, COV = 0.02

CD-87-30817

SLIDE 16

This figure shows a simplified model of a turbine blade which has randomness both in the geometry, as reflected in the length of the blade, and in the material properties, where the yield stress is random. In addition, the load, which is applied at the tip, is a random function.

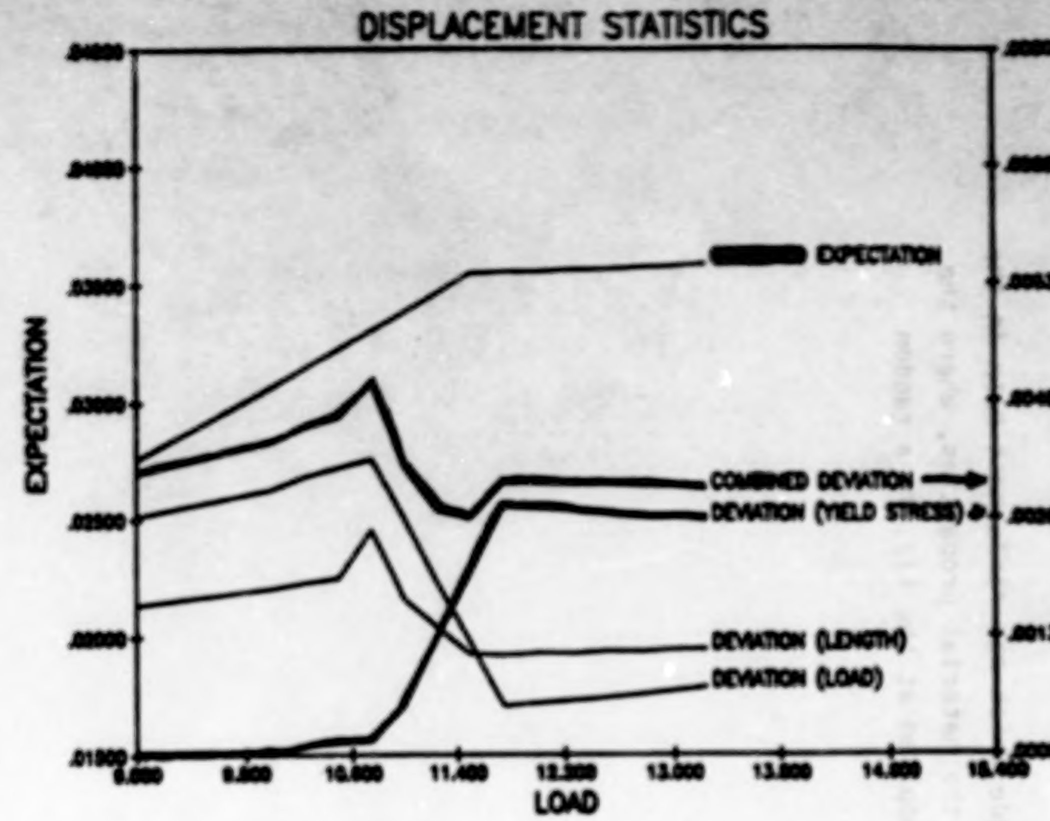
DISPLACEMENT STATISTICS
EXPECTATION
COMBINED DEVIATION
DEVIATION (YIELD STRESS)
DEVIATION (LENGTH)
DEVIATION (LOAD)
EXPECTATION
DEVIATION
LOAD

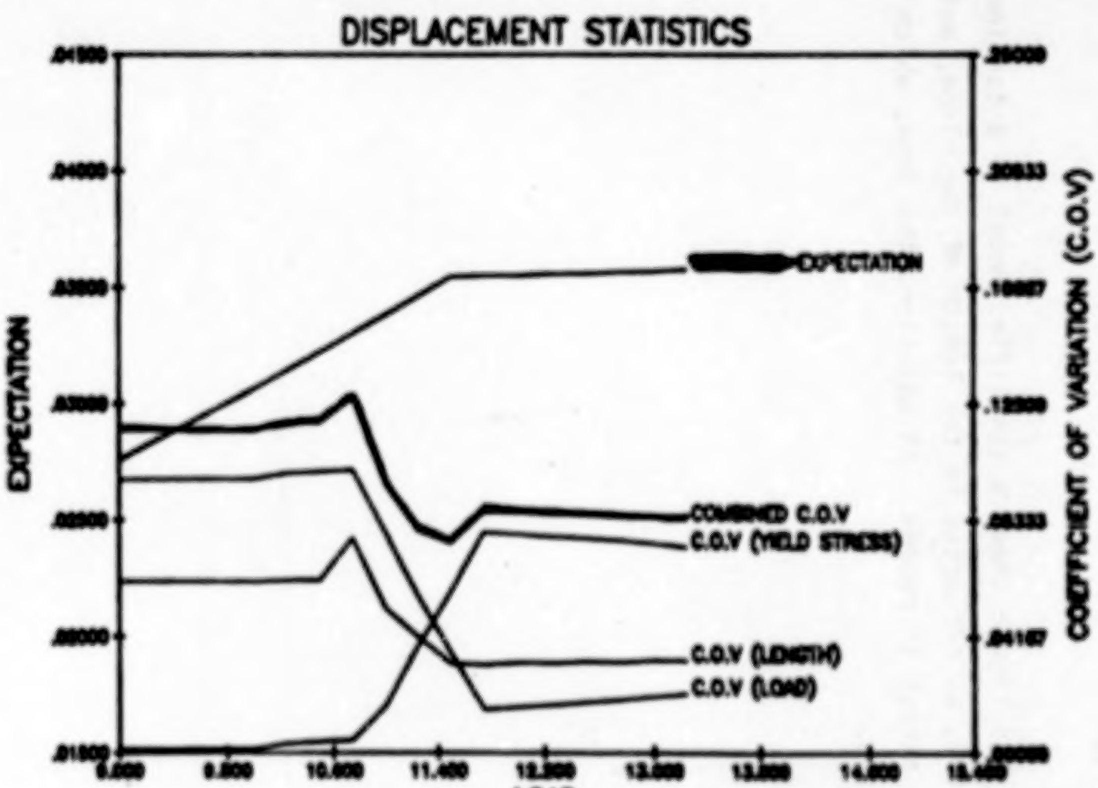
DISPLACEMENT STATISTICS
EXPECTATION
COMBINED C.O.V
C.O.V (YIELD STRESS)
C.O.V (LENGTH)
C.O.V (LOAD)
EXPECTATION
COEFFICIENT OF VARIATION (C.O.V)
LOAD

SLIDE 17

SLIDE 17

This slide shows the expected value of the displacement at node a, labeled "expectation", and the variation of the displacement at that point. In addition to the variation which results from combined effects of randomness in load, length, and yield stress, the effects of the randomness in these three parameters are considered separately. It can be seen that randomness in the load has a major effect during the initial portion of the response, which is elastic, but its effect diminishes later. By contrast, the yield randomness in the yield stress becomes the dominant factor later in the response when the behavior of the turbine blade is elastic-plastic.

COMPUTATION TIME (Hu-Washizu V.P.)

- Plane Strain Beam Under Large Deflection
- 205 Nodes/160 4-Node Elements, 12 Load Steps
- Random Load, Material and Height

PHWVP Approach to PFEM

81 Corr. R.V.'s to 9 Uncorr. R.V.'s

1.5 cpu hrs. Total

Monte Carlo Simulation (MCS)

100 Samples: 60 cpu hrs.

400 Samples: 240 cpu hrs. (Projected)

Savings

PHWVP + MCS 100, 400: 97.5%, 99.4%

Note: Zeroth Order Eqn. is Nonlinear Whereas the First and Second Orders are Linear

SLIDE 18

To provide some guidelines as to why Monte Carlo simulation cannot be used for problems of this type, we have given the computation times for the PFEM method and Monte Carlo simulation for a 205-node, 160-element problem. The PFEM approach on a Harris H800 required about 1.5 cpu hours. By contrast, a 100-sample simulation requires 60 cpu hours. One hundred samples would probably not be sufficient to obtain reliable bounds on ±3 standard deviations, but increasing the number of samples to 400 would require 240 cpu hours.

PROPOSED WORK

- APPLY PFEM TO A STRAIGHT CRACK IN A "STRUCTURE" (BEAM. TURBINE BLADE) TO OBTAIN STATISTICS ON CRACK GROWTH
- ADD FIRST ORDER RELIABILITY ANALYSIS
- DEVELOP METHODOLOGIES FOR CRACKS THAT DO NOT GROW RECTILINEARLY AND FOR ELASTO-PLASTIC FRACTURE MECHANICS

SLIDE 19

This slide summarizes the work which is proposed in the continuation of this grant. The major objective of the work in the next year will be to incorporate a crack element into the probabilistic finite element program, so that the effects of randomness in the crack and load can be studied for a low-cycle fatigue-type problem. For this purpose, a straight crack will be incorporated in the program, and its growth will be predicted for a given random load.

A key feature of this development will be to incorporate the effect of the feedback between the actual structural configuration and the stress intensity at the crack into the growth model for the crack. Most current work for crack growth under random load or in random materials assumes the crack to be in an infinite medium, so that the effects of the structural configuration on the growth of the crack are not properly represented.

In these developments, in addition to the second-order moment methods which we have used for nonlinear structural dynamics, we will incorporate a first-order reliability analysis so that the probability of the crack's exceeding a certain threshold will be computable.

In subsequent years, we will extend these methods so that we can deal with cracks which do not grow in a straight line and to incorporate elasto-plastic fracture mechanics.

N89
29804
UNCLAS

N89-29804 , 55-39
338.
311972
ND315753

STRUCTURES DIVISION

STRUCTURAL MECHANICS BRANCH

NASA
Lewis Research Center

3-D INELASTIC ANALYSES FOR COMPUTATIONAL STRUCTURAL MECHANICS

D. A. HOPKINS/C. C. CHAMIS

NASA LEWIS RESEARCH CENTER

NASA WORKSHOP ON COMPUTATIONAL STRUCTURAL MECHANICS

NASA LANGLEY RESEARCH CENTER, HAMPTON, VIRGINIA

NOVEMBER 18-20, 1987

See P 945

PRECEDING PAGE BLANK NOT FILMED

PAGE 942 INTENTIONALLY BLANK

N89-29804

STRUCTURES DIVISION

STRUCTURAL MECHANICS BRANCH

NASA Lewis Research Center

3-D NONLINEAR HIGH TEMPERATURE STRUCTURAL ANALYSIS

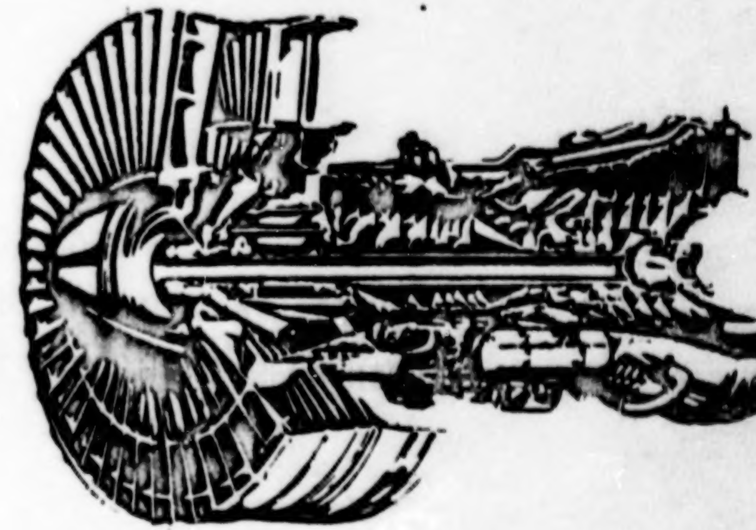

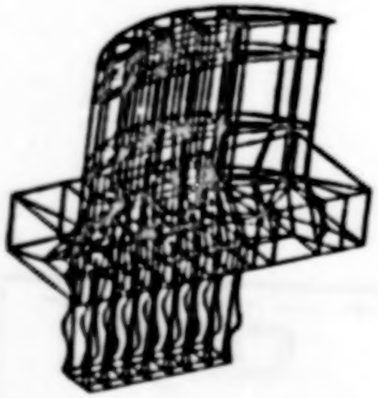

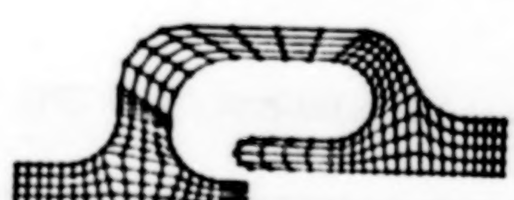

- MATERIAL NONLINEARITIES
- GEOMETRIC NONLINEARITIES
- TEMPERATURE DEPENDENCE
- TIME DEPENDENCE

ORIGINAL PAGE
BLACK AND WHITE PHOTOGRAPH

THE 3-D INELASTIC ANALYSIS METHOD IS A FOCUSSED PROGRAM WITH THE OBJECTIVE TO DEVELOP COMPUTATIONALLY EFFECTIVE ANALYSIS METHODS AND ATTENDANT COMPUTER CODES FOR THREE DIMENSIONAL, NONLINEAR TIME AND TEMPERATURE DEPENDENT PROBLEMS PRESENT IN THE HOT SECTION OF TURBOJET ENGINE STRUCTURES. DEVELOPMENT OF THESE METHODS WAS A MAJOR PART OF THE HOT SECTION TECHNOLOGY (HOST) PROGRAM OVER THE PAST FIVE YEARS AT LEWIS RESEARCH CENTER.

OBJECTIVE:

DESCRIBE ADVANCED METHODS DEVELOPED FOR 3-D INELASTIC ANALYSIS, COMPUTER CODES, AND REPRESENTATIVE RESULTS FOR ENGINE STRUCTURES CRITICAL HOT SECTION COMPONENTS

CD-87-25451

PRESENTATION OUTLINE

- o DESCRIPTION OF METHODS
  - APPROXIMATE METHODS (MOMM)
  - SPECIALTY FINITE ELEMENTS (SFINES)
  - MIXED FINITE ELEMENTS (MHOST)
- o CONCLUSIONS

THREE DIFFERENT FORMULATION APPROACHES WERE USED IN THE DEVELOPMENT OF THE 3-D INELASTIC ANALYSES METHODS. THESE INCLUDE: (1) APPROXIMATE METHODS BASED ON MECHANICS OF MATERIALS METHODS (MOMM), (2) SPECIALTY FINITE ELEMENTS (SFINES) AND (3) MIXED FINITE ELEMENTS INCORPORATED IN A MODIFIED AND SCALED DOWN MARC CODE (MHOST). EACH OF THESE WILL BE DESCRIBED IN SUMMARY FORM WITH RESPECT TO CAPABILITY, FEATURES AND REPRESENTIVE RESULTS.

MECHANICS OF MATERIALS METHODS

MOMM COMPUTER CODES

FRAMEWORK REPRESENTATION OF PLATE

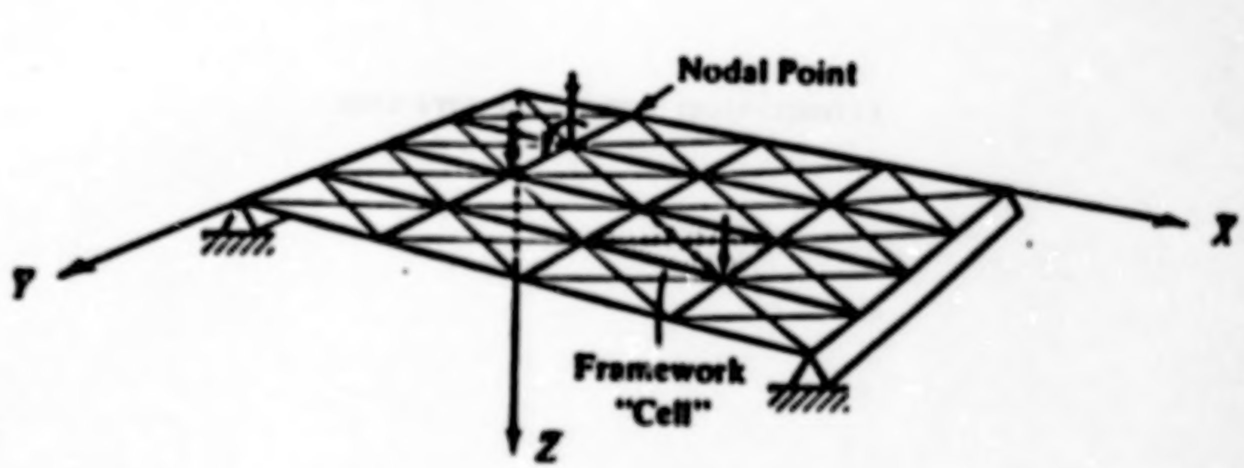

PRECEDING PAGE BLANK NOT FILMED

MOMM IS BASED ON A FRAMEWORK OF BEAM ELEMENTS WHERE EACH BEAM IS REPRESENTED BY A CUBIC ISOPARAMETRIC DISPLACEMENT INTERPOLATION FUNCTION. THE FRAMEWORK IS TRANSPARENT TO THE USER. THE USER SPECIFIES ONLY THE COMPONENT GEOMETRY AND THE DESIRED ANALYSIS-MODEL MESH.

CONSTITUTIVE MODELS

- SIMPLIFIED MODEL
  - USES BILINEAR STRESS-STRAIN CURVE BASED UPON ELASTIC MODULUS AND HARDENING SLOPE
- STATE OF THE ART MATERIAL MODEL
  - ELASTIC-PLASTIC-CREEP STRAIN DECOMPOSITION
  - STEADY STATE POWER LAW CREEP MODEL
  - PLASTICITY MODEL CONTAINS ISOTROPIC AND KINEMATIC HARDENING
- MODIFIED WALKER'S MODEL
  - UNIFIED VISCOPLASTIC MODEL
  - ACCOUNTS FOR INTERACTION OF CREEP AND PLASTICITY UNDER CYCLIC LOADING

THREE DIFFERENT NONLINEAR CONSTITUTIVE RELATIONSHIPS, WITH PROGRESSIVE LEVEL OF SOPHISTICATION, ARE INCORPORATED IN MOMM. THE LAST ONE IS CONSIDERED TO BE THE MOST ADVANCED AVAILABLE AT THIS TIME. NONLINEAR 3-D INELASTIC PROBLEMS CAN BE ANALYZED USING EACH OF THESE CONSTITUTIVE RELATIONSHIPS IN ORDER TO OBTAIN RELATIVE ACCURACY WITH RESPECT TO LOCAL STRESS STATES AND RESPECTIVE MATERIAL NONLINEARITIES.

MOMM CPU TIME COMPARISONS

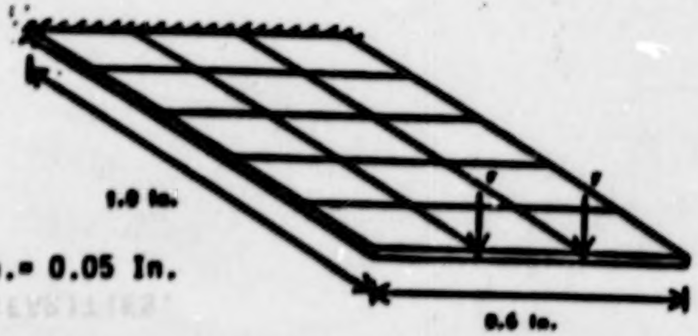

th.= 0.05 In.

Cantilevered Plate with Edge Load

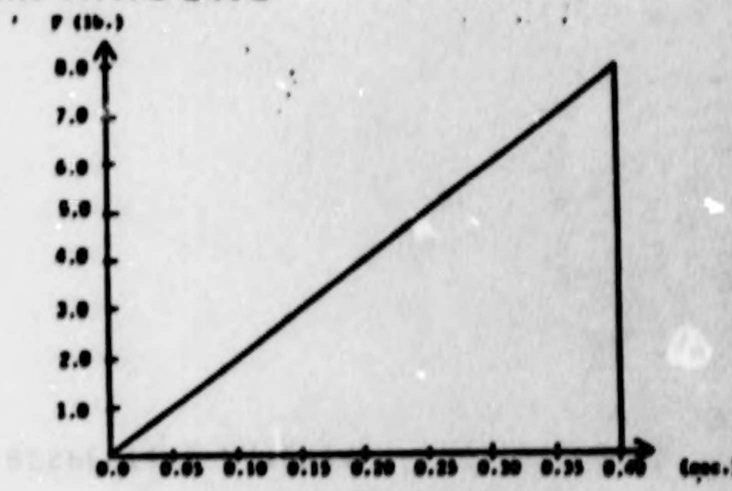

(8 Load Increments)

LOAD HISTORY

	CPU Time	Max. Displ.(In.)
MOMM – Simplified Material Model	29 sec.	0.0309
MOMM – Elastic–Plastic–Creep Model	35 sec.	0.0351
MOMM – Modified Walkers Model	73 sec.	0.0361
MARC – Modified Walkers Model (4 node plate element #50)	47 sec.	0.0376

C-3

REPRESENTATIVE RESULTS OBTAINED WITH EACH OF THESE NONLINEAR CONSTITUTIVE RELATIONSHIPS, USING THE MOMM CODE, ARE SUMMARIZED IN THE ACCOMPANYING CHART TOGETHER WITH COMPUTER CPU TIMES.

SPECIALTY FINITE ELEMENTS FOR

3-D INELASTIC ANALYSIS (SFINES)

(9 - DIFFERENT CODES)

INPUT FEATURES

FEATURE		SIMPLE MODEL			CLASSICAL MODEL			UNIFIED MODEL		
		8-NODE	9-NODE	20-NODE	8-NODE	9-NODE	20-NODE	8-NODE	9-NODE	20-NODE
Free Format Data Input		X	X	X	X	X	X	X	X	X
Global Coordinate System:	Cartesian	X	X	X	X	X	X	X	X	X
	Cylindrical									
	Spherical									
Local Coordinate System:	Cartesian	X	X	X	X	X	X	X	X	X
	Cylindrical									
	Spherical									
Automatic Generation of Nodal Coordinates			N/A			N/A			N/A	
Automatic Generation of Element Connectivities		X	X	N/A	X	X	N/A	X	X	N/A
Skewed Coordinate System		X	X	X	X	X	X	X	X	X
Orthotropic Orientation Definition		X	X	X	X	X	X	X	X	X

SIGNIFICANT FEATURES OF THE SPECIALTY FINITE ELEMENTS (SFINES) CODES INCLUDE THOSE ASSOCIATED WITH USER FRIENDLY ASPECTS.

ANALYSIS TECHNIQUES

FEATURE	SIMPLE MODEL			CLASSICAL MODEL			UNIFIED MODEL		
	8-NODE	9-NODE	20-NODE	8-NODE	9-NODE	20-NODE	8-NODE	9-NODE	20-NODE
Dynamic Allocation	X	X	X	X	X	X	X	X	X
Blocked Column Skyline Equation Solver	X	X	X	X	X	X	X	X	X
Initial Stress Iterative Scheme			X			X			X
Aitken's Acceleration Scheme			X			X			X
Dynamic Time Incrementing			X			X			X
Convergence Criteria: Effective Plastic Strain			X			X			X
Convergence Criteria: Effective Stress			X			X			X
Dynamic Analysis: Eigenvalue	X	N/A	N/A	X	N/A	N/A	X	N/A	N/A
Dynamic Analysis: Eigenvector	X	N/A	N/A	X	N/A	N/A	X	N/A	N/A

CAPABILITIES IN THE SFINES CODES INCLUDE THREE DIFFERENT FINITE ELEMENTS, EACH WITH ONE DEDICATED NONLINEAR CONSTITUTIVE RELATIONSHIP. THIS PROVIDES NINE DIFFERENT AND STAND ALONE COMPUTER CODES. THE FINITE ELEMENT FORMULATIONS ARE BASED ON ISOPARAMETRIC DISPLACEMENT SHAPE FUNCTIONS. EACH CODE CONTAINS A LIBRARY OF NONLINEAR SOLUTION FEATURES.

CYLINDRICAL SHELL ROOF

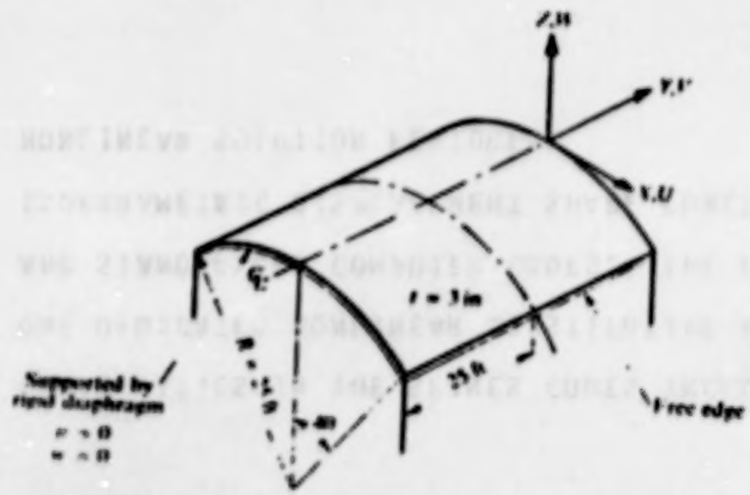

Shell Thickness = 3 in.

E = $432(10)^6$ psf

Specific Weight = 360 pcf

Poisson's Ratio = 0.0

Sverdrup

REPRESENTATIVE RESULTS OBTAINED FOR THE CYLINDRICAL SHELL ROOF "CLASSICAL EXAMPLE" IN THE ACCOMPANYING CHART ARE PRESENTED GRAPHICALLY VERSUS ELEMENT ASPECT (EDGE/THICKNESS) RATIO IN THE NEXT CHART WHERE RESULTS FROM COMMERCIAL CODES AND INDEPENDENT ANALYSIS ARE ALSO SHOWN.

VERTICAL DISPLACEMENT AT POINT A OF
THE CYLINDRICAL SHELL ROOF

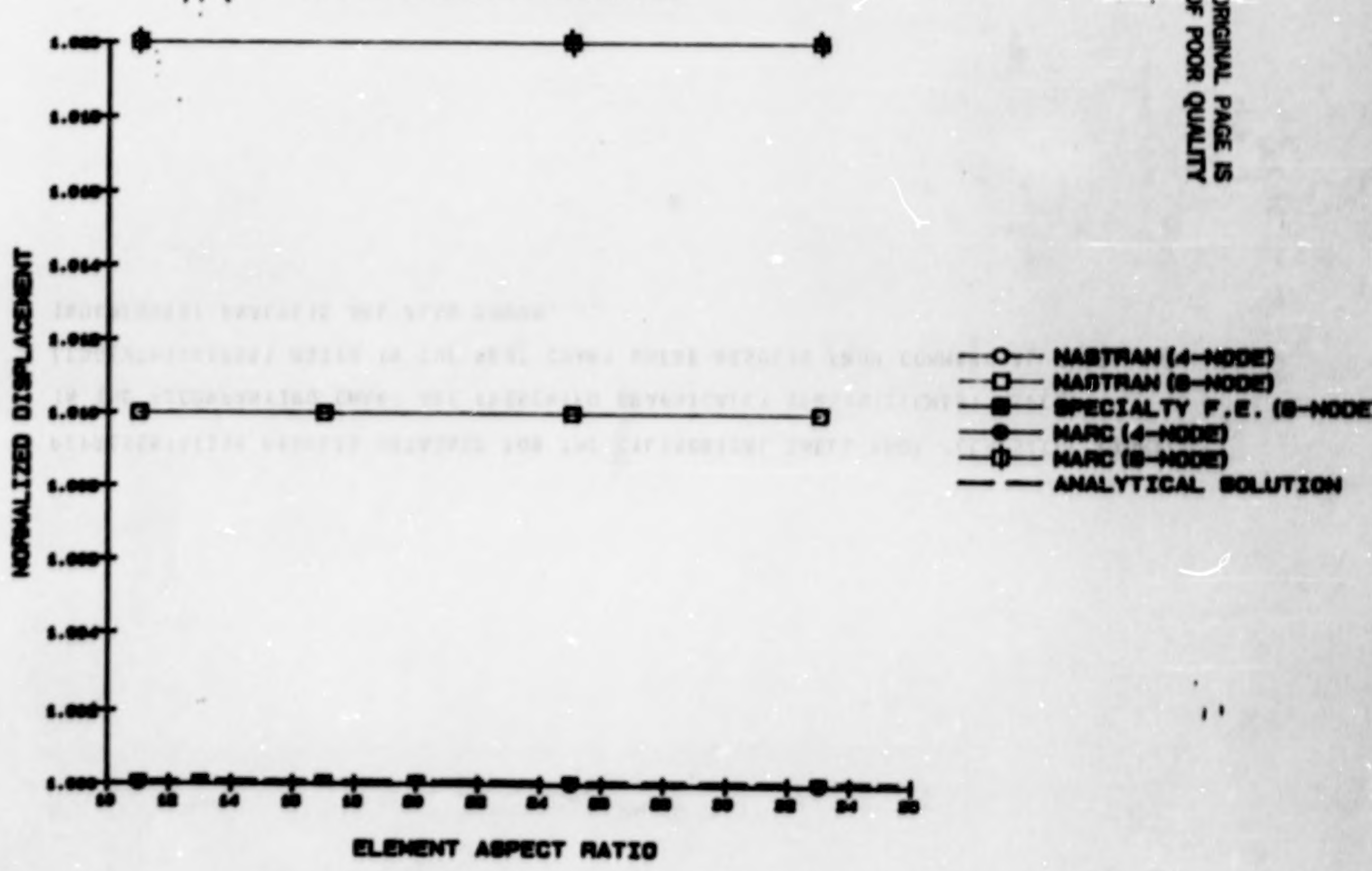

MIXED FINITE ELEMENTS FOR

3-D INELASTIC ANALYSIS

(MHOST CODE)

HNOST SOLUTION CAPABILITY

ELEMENT DEFINITION OPTIONS	BEAM	PLANE STRESS	PLANE STRAIN	AXI-SYMMETRIC SOLID	THREE-DIMENSIONAL SOLID	THREE-DIMENSIONAL SHELL
LINEAR ISOTROPIC ELASTICITY	X O	X	X	X	X O	X O
ANISOTROPIC[1] ELASTICITY		X	X	X	X O	
COMPOSITE[1] LAMINATE						X O
SIMPLIFIED PLASTICITY		X	X	X	X O	X O
ELASTO-PLASTICITY		X	X	X	X O	X O
UNIFIED CREEP-PLASTICITY		X O	X	X	X O	X O
STRESS STIFFENING	X	X	X	X	X O	X O
CENTRIFUGAL MASS	X	X	X	X	X O	X O
THERMAL[2] STRAIN	X	X	X	X	X O	X O
CREEP[2] STRAIN	X	X	X	X	X O	X O

NOTES: [1]APPLICABLE ONLY TO LINEAR ELASTICITY.
[2]NOT APPLICABLE TO THE UNIFIED CREEP-PLASTICITY IN WHICH THE QUANTITIES ARE INTEGRATED AS PART OF THE MODEL.

ORIGINAL PAGE IS
OF POOR QUALITY

THE MHOST COMPUTER CODE HAS SIX DIFFERENT FINITE ELEMENTS, EACH BASED ON MIXED-ELEMENT FORMULATION. THESE ELEMENTS CONTAIN THE ISOPARAMETRIC DISPLACEMENT FORMULATION AS A SPECIAL CASE. THE SOLUTION CAPABILITIES ARE SUMMARIZED IN THE ACCOMPANYING CHART. MHOST: (1) CONISISTS OF ABOUT 50,000 FORTRAN 77 STATEMENTS; (2) IS HIGHLY PORTABLE (PRIME, VAX, IBM, CRAY); (3) IS MODULAR WITH MULTIPLE-DRIVER PROGRAMMING FOR MAINTAINABILITY; (4) IS PROGRAMMED TO BE USED IN EITHER BATCH OR INTERACTIVE MODES; AND (5) IS SELF DOCUMENTED USING EXTENSIVE COMMENTS IN THE SOURCE CODE.

MHOST SOLUTION ALGORITHM LIBRARY

ANALYSIS MODULE OPTION	BEAM	PLANE STRESS	PLANE STRAIN	AXI-SYMMETRIC SOLID	THREE-DIMENSIONAL SOLID	THREE-DIMENSIONAL SHELL
QUASI-STATIC ANALYSIS	X	X	X	X	X O	X O
BUCKLING ANALYSIS	X	X	X	X	X O	X O
MODAL ANALYSIS	X	X	X	X	X O	X O
MODAL SUPERPOSITION	X	X	X	X	X O	X O
TRANSIENT DYNAMICS	X	X O	X	X	X O	X O

CD-87-25446

MHOST INCLUDES A LIBRARY OF SOLUTION ALGORITHMS. THESE ALGORITHMS ENHANCE ITS COMPUTATIONAL EFFECTIVENESS FOR 3-D INELASTIC PROBLEMS. A UNIQUE FEATURE OF MHOST IS THAT THE STRUCTURAL RESPONSE VARIABLES (DISPLACMENTS, FORCES, STRAINS, STRESSES) ARE DEFINED AT THE NODES. ANOTHER FEATURE IS THAT NONLINEAR/LARGE DISPLACEMENT SOLUTION IS BASE ON THE UP-DATED LAGRANGEAN WHICH SIMPLIFIES THE DESCRIPTION OF THE NONLINEAR CONSTITUTIVE RELATIONSHIPS (LOCAL DEFORMED GEOMETRY VERSUS INITIAL UNDEFORMED GEOMETRY).

BURNER BLISTER MHOST ANALYSIS

FINITE ELEMENT MODEL

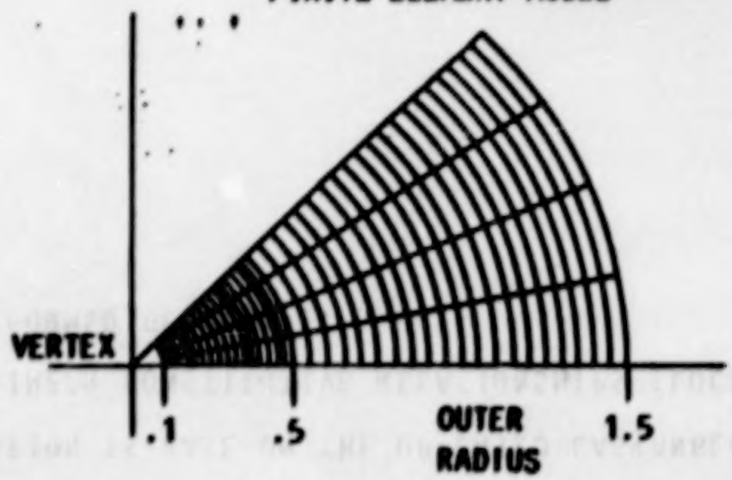

BLISTER REGION MODEL

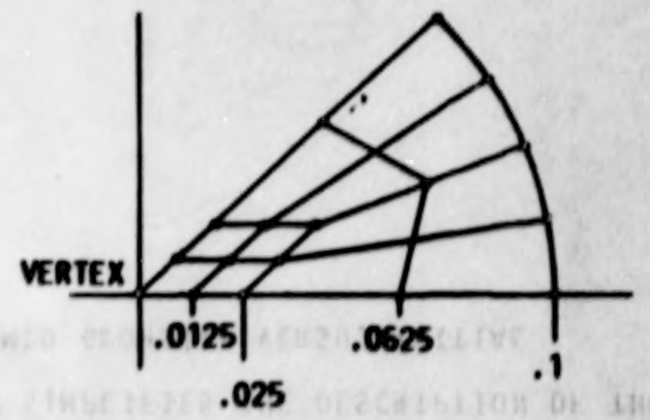

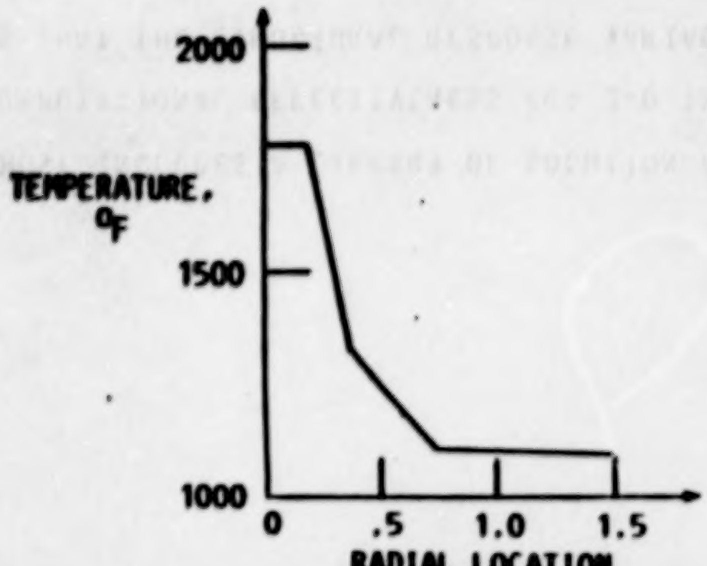

HOT SPOT TEMPERATURE DISTRIBUTION (MID-PLANE)

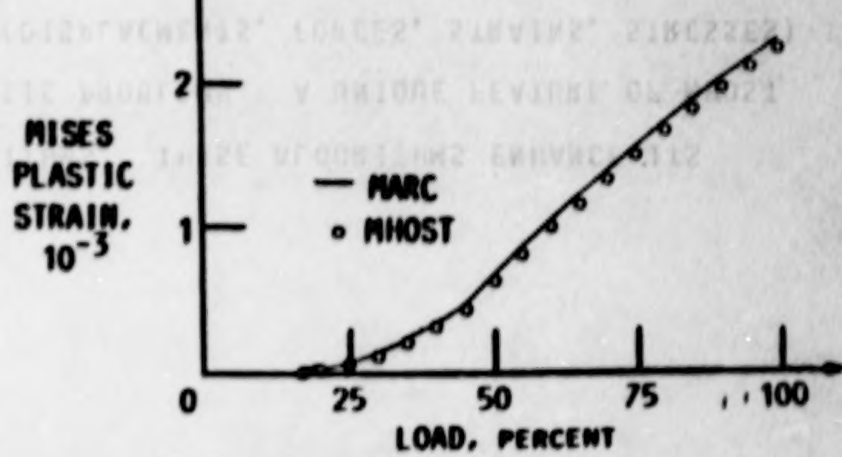

MISES PLASTIC STRAIN AT MID-PLANE
VERTEX MODE

CD-87-25495

MHOST RESULTS FOR A HOT SPOT PROBLEM ARE PRESENTED IN THE ACCOMPANYING CHART AND COMPARED WITH THOSE OBTAINED BY USING THE THE MARC CODE.

TIME-STEP SENSITIVITY ON TRANSIENT RESPONSE

(TIME HISTORY OF DISPLACEMENT AT POINT A IN X DIRECTION
FOR A 3-D BEAM SUBJECTED TO COUPLES)

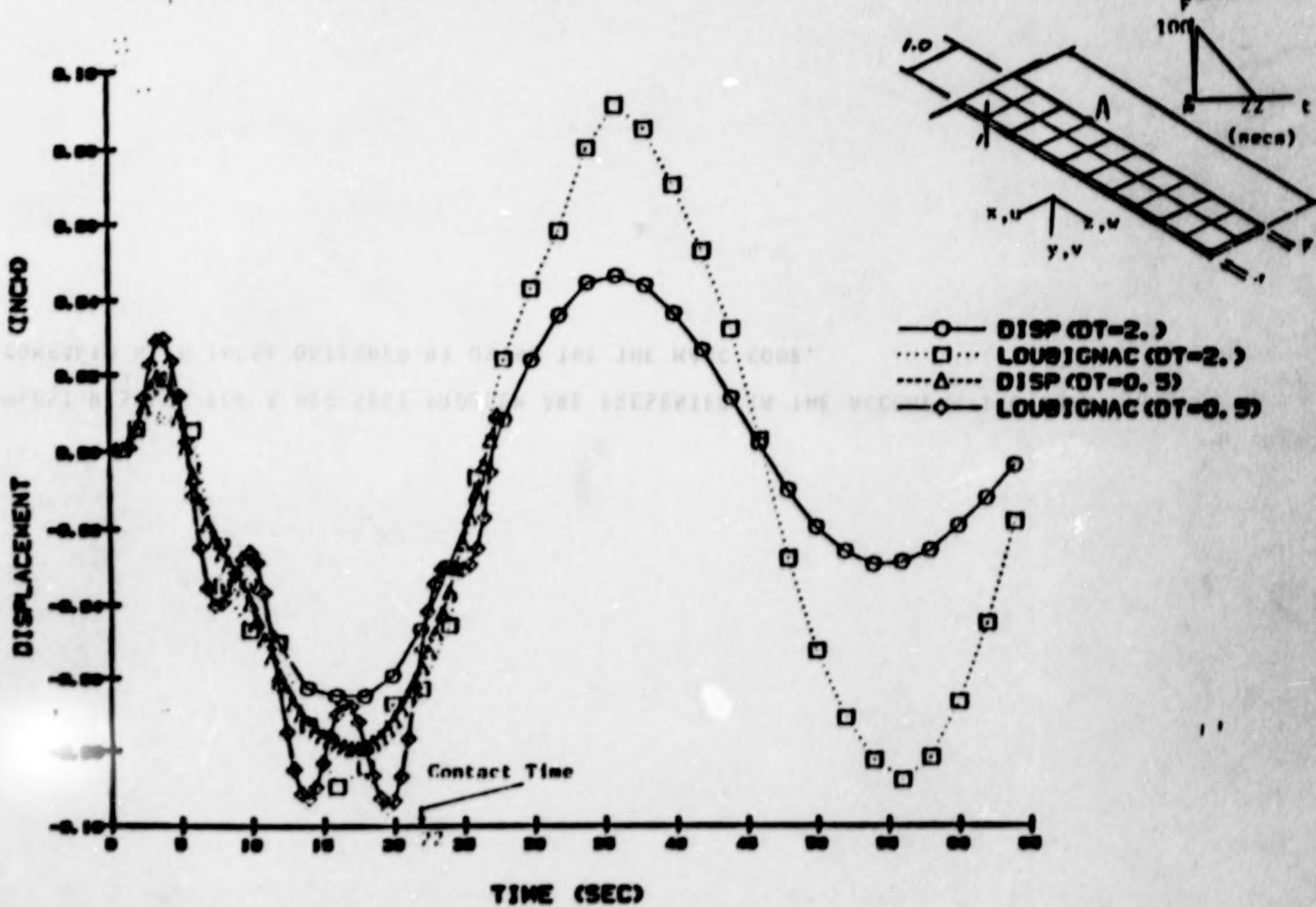

ORIGINAL PAGE IS
OF POOR QUALITY

MHOST TRANSIENT RESULTS COMPARING THE TIME-STEP SENSITIVITY ARE SHOWING IN THE ACCOMPANYING CHART. AS IS WELL KNOWN, THE TIME-STEP CANNOT BE SELECTED ARBITRARILY. THE VARIOUS SOLUTIONS ALGORITHMS IN MHOST PROVIDE AN ADAPTIVE STRATEGY FOR SELECTING TIME-STEP/SOLUTION-ALGORITHM TO OBTAIN A CONVERGENT SOLUTION - ACCOMPANYING AND NEXT CHARTS.

SOLUTION ALGORITHM INFLUENCE ON TRANSIENT RESPONSE

(TIME HISTORY OF DISPLACEMENT AT POINT A IN X DIRECTION FOR A 3-D BEAM SUBJECTED TO COUPLES)

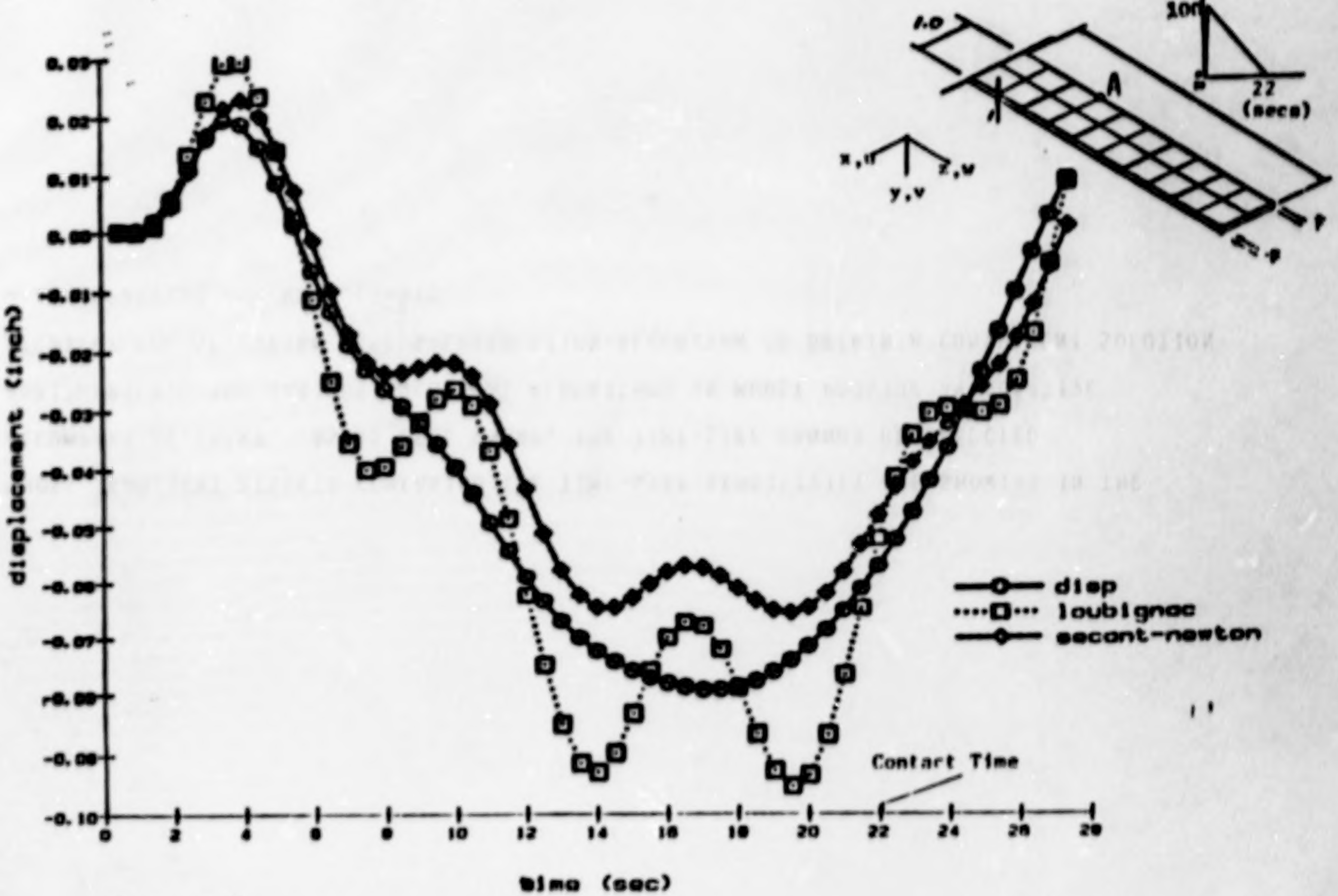

MHOST ILLUSTRATIVE EXAMPLE OF VERSATILE GLOBAL/LOCAL ANALYSIS CAPABILITIES FOR INELASTIC STRESS CONCENTRATION PROBLEMS

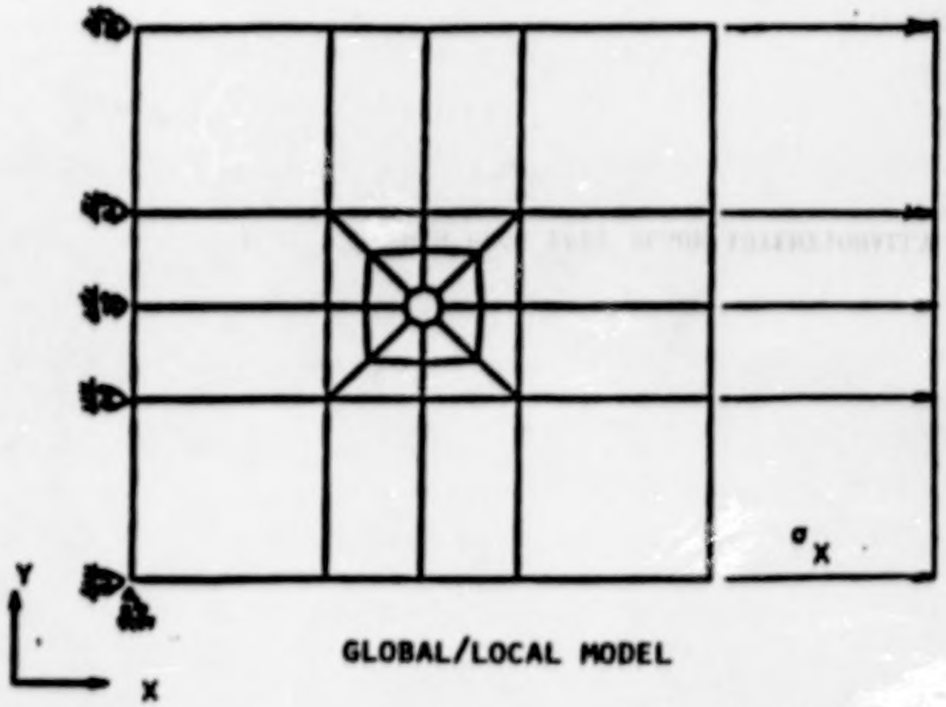

GLOBAL/LOCAL MODEL

LOCAL (ϵ)/GLOBAL (ϵ_X) STRAIN CONTOURS

NOTES:

- O GLOBAL MODEL - LINEAR ELEMENTS
- O LOCAL MODEL - QUADRATIC ELEMENTS

PAGE 977 INTENTIONALLY BLANK

PRECEDING PAGE BLANK NOT FILMED

MHOST IS THE ONLY CODE WITH EMBEDDED SUB-ELEMENT CAPABILITY FOR SIMULTANEOUS LOCAL/GLOBAL ANALYSIS NEAR DISCONTINUITIES. RESULTS OBTAINED BY USING THIS CAPABILITY ARE ILLUSTRATED IN THE LAST CHART.

THE LONG RANGE OBJECTIVE OF THESE 3-D INELASTIC ANALYSIS METHODS IS TO DEVELOP THE METHODOLOGY READINESS TO RELIABLY PREDICT THE INTEGRITY, DURABILITY AND LIFE OF HOT SECTION ENGINE STRUCTURES. THESE CODES CONSTITUTE ANALYSIS MODULES IN THE ENGINE STRUCTURES COMPUTATIONAL SIMULATOR, CURRENTLY UNDER DEVELOPMENT AS A PART OF THE LEWIS RESEARCH CENTER COMPUTATIONAL STRUCTURAL MECHANICS PROGRAM, DESCRIBED ELSEWHERE IN THESE PROCEEDINGS.

N89
29805
UNCLAS

N89-29805

56-39
32P.
211973
ØM 593208

SPECIALTY FUNCTIONS FOR SINGULARITY MECHANICS PROBLEMS[1]

by
Nesrin Sarigul
Department of Aeronautical and Astronautical Engineering
The Ohio State University
Columbus, OH 43210

With the increasing use of new materials and elevated temperature applications studies involving more accurate predictions on the values of the field variables and more efficient computational methods are receiving considerable attention.

The focus of this research is in the development of more accurate and efficient advanced methods for solution of singular problems encountered in mechanics. At present, finite element methods in conjunction with special functions, boolean sum and blending interpolations are being considered. In dealing with systems which contain a singularity, special finite elements are being formulated to be used in singular regions. Further, special transition elements are being formulated to couple the special element to the mesh that model the rest of the system, and to be used in conjunction with 1-D, 2-D and 3-D elements within the same mesh. Computational simulation with a least squares fit is being utilized to construct special elements, if there is an unknown singularity in the system.

A novel approach is taken in formulation of the elements in that; i)the material properties are modified to include time, temperature, coordinate and stress dependant behavior within the element, ii) material properties vary at nodal points of the elements, iii) a hidden-symbolic computation scheme is developed and utilized in formulating the elements, and iv)special functions and boolean sum are utilized in order to interpolate the field variables and their derivatives along the boundary of the elements.

It may be noted that the proposed methods are also applicable to fluids and coupled problems.

1 Research is being performed under the support of NASA Lewis Research Center under grant number NAG3-790.

PRECEDING PAGE BLANK NOT FILMED

PAGE 980 INTENTIONALLY BLANK

OUTLINE

- MOTIVATION
- OBJECTIVE
- APPROACH
- NUMERICAL CONSIDERATIONS
- CONCLUDING REMARKS

O B J E C T I V E

DEVELOPMENT OF ADVANCED METHODS TO SOLVE SINGULARITY PROBLEMS ENCOUNTERED IN MECHANICS

SPECIAL FUNCTIONS _ SINGULAR PROBLEMS

KNOWN SINGULARITY

δ DIRAC

.
.
.

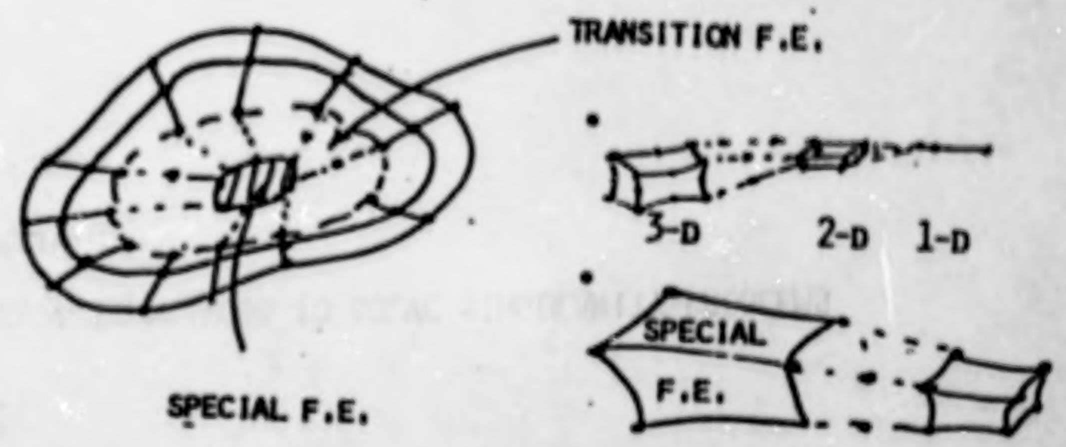

SOLID	FLUID	
GEOMETRY (IRREGULAR)	FLOW SEP.	
NONLINEARITIES , MATERIAL LOADING	SHOCK FORMATION	HEAT SOURCE
.	:	:
UNKNOWN SINGULARITY		
COMPUTATIONAL SIMULATION		

. . . .

SPECIAL FUNCTIONS - SINGULAR PROBLEMS

Special finite elements are being formulated for solution of singular problems encountered in mechanics such as due to sudden change in geometry or loading, shock formation, and heat source. In cases where the singularity is known prior to the analysis, known singularity, the analytical solution available is incorporated in the element formulation. If the singularity is an unknown type, then a computational simulation together with a least squares fit is being utilized with special functions to formulate the special elements. In order to blend the special elements to the mesh with traditional finite elements, the transition finite elements are being formulated.

ELEMENT FORMULATION

- BOOLEAN SUM $P[F(R,S)] = (P_R \oplus P_S)\, F$
- BLENDING INTERPOLANTS

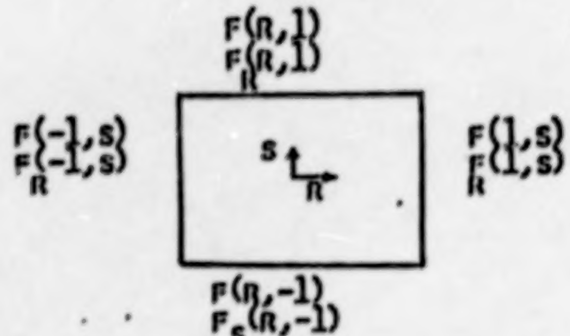

$[-1,1] \times [-1,1]$

$\bar{F} \simeq F$

$F(R,S)\big\rvert_{R=1} = F(1,S)$	$F_R(R,S)\big\rvert_{R=1} = F_R(1,S)$	F "INTERPOLATION FUNCTION"
$F(R,S)\big\rvert_{R=-1} = F(-1,S)$	$F_R(R,S)\big\rvert_{R=-1} = F_R(-1,S)$	C "BLENDING FUNCTION"
$F(R,S)\big\rvert_{S=1} = F(R,1)$	$F_S(R,S)\big\rvert_{S=1} = F_S(R,1)$	P "PROJECTOR OPERATOR"
$F(R,S)\big\rvert_{S=-1} = F(R,-1)$	$F_S(R,S)\big\rvert_{S=-1} = F_S(R,-1)$	

FOR R DIRECTION $P_R[F(R,S)] = F(-1,S)\, C_1(R) + F(1,S)\, C_2(R) + F_R(-1,S)\, C_{1R}(R) + F_R(1,S)\, C_{2R}(R)$

S DIRECTION $P_S[F(R,S)] = F(R,-1)\, C_1(S) + F(R,1)\, C_2(S) + F_S(R,-1)\, C_{1S}(S) + F_S(R,1)\, C_{2R}(S)$

ELEMENT FORMULATION

The boolean sum is utilized to construct the finite elements. As it is illustrated in figure the field variable F is approximated as $\overline{F}$. It may be noted that along the boundary of the element the approximation function and its normal derivatives are identical to the field variable and its normal derivatives respectively. The projector operators are given in terms of the interpolation functions and the blending functions.

FINITE ELEMENT FORMULATION 3-D

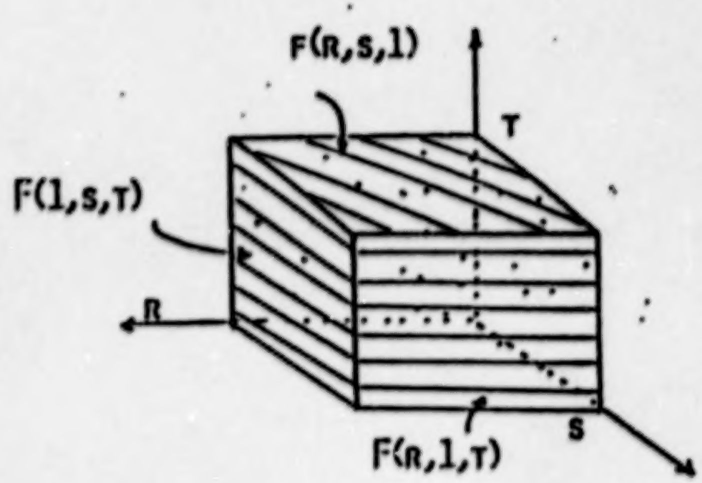

$$\omega \equiv [0,1] \times [0,1] \times [0,1]$$

$$\bar{\omega} \equiv \omega \cup \partial\omega$$

THE BOOLEAN SUM

$$P\,[F(R,S,T)] \equiv P_R \oplus (P_S \oplus P_T)\,[F]$$

OR

$$P[F] \equiv (P_R + P_S + P_T - P_R P_S - P_S P_T - P_R P_T + P_R P_S P_T)[F]$$

$\bar{F}(R,S,T) \equiv F(R,S,T)$.
FOR ALL (R,S,T) ON $\partial\omega$

SURFACES

$$P_R[F] = RF(1,S,T) + (1-R)F(0,S,T)$$
$$P_S[F] = SF(R,1,T) + (1-S)F(R,0,T)$$
$$P_T[F] = TF(R,S,1) + (1-T)F(R,S,0)$$

FINITE ELEMENT FORMULATION 3-D

The boolean sum is expressed in terms of the three projector operators along R,S and T directions. The continuity requirement for this example is for the field variable itself only. The approximation function exactly matches the values of the field variable on the boundary surface. Therefore, it is anticipated that the results obtained from the analysis will give better approximations on the field variable.

TRANSFORMATION OF THE DOMAIN

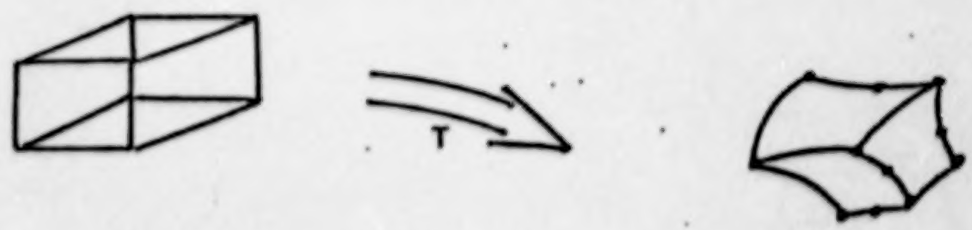

$$T[XYZ] \equiv (P_R \oplus P_S \oplus P_T)[XYZ]$$

$$XYZ = (X, Y, Z)^T$$

TRANSFORMATION OF THE DOMAIN

Transfinite interpolation formula is being utilized in order to account for arbitrary geometry. The unit cube is mapped onto the curved domain by utilizing the projectors along r,s, and t directions.

FORMULATION OF A TRANSITION ELEMENT

TRANSITION F.E.

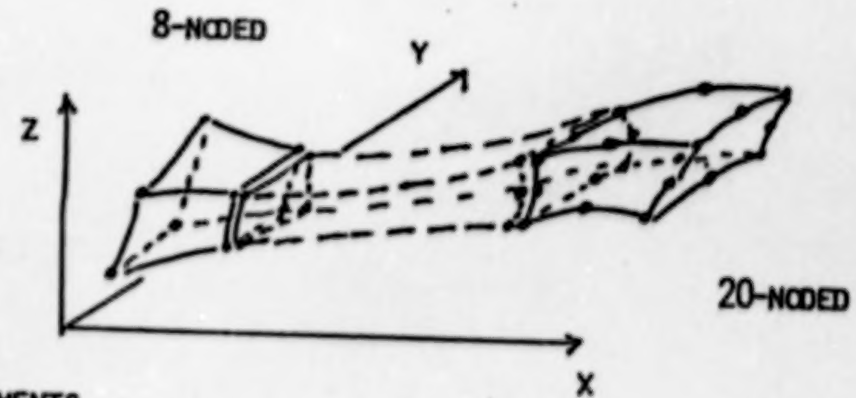

REQUIREMENTS

- CONNECTS TWO VARIABLY DEGREES OF FREEDOM 3-D ELEMENTS
- ANISOTROPIC MATERIAL
  (ELEVATED TEMPERATURES)
- NONLINEAR MATERIAL BEHAVIOR
- LARGE DEFORMATIONS
- MATERIAL PROPERTIES KNOWN AT THE NODES

FORMULATION OF A TRANSITION ELEMENT

In order to connect three dimensional meshes obtained from different traditional finite elements, various 3-D finite elements are being formulated. For the elements formulated anisotropic material behavior and large deformation effects are also being included in the formulation.

A 12-NODE TRANSITION FINITE ELEMENT

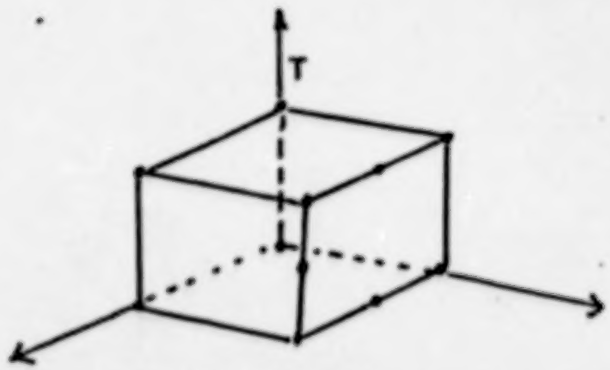

$$\omega \equiv [0,1]\times[0,1]\times[0,1]$$

$$P_R[U] \equiv RU(1,S,T) + (1-R)U(0,S,T)$$

$$P_S[U] \equiv SU(R,1,T) + (1-S)U(R,0,T)$$

$$P_T[U] \equiv TU(R,S,1) + (1-T)U(R,S,0)$$

$$\bar{U}(R,S,T) \equiv P_R \oplus (P_S \oplus P_T)[U]$$

$$\bar{U}(R,S,T) \equiv U(R,S,T) \quad \text{ON} \quad \partial\omega$$

A 12-NODE TRANSITION ELEMENT

A 12-node three dimensional transition element is formulated and is being tested. The formulation is based on the boolean sum, and the integrations involved in element matrices are performed exactly by utilizing a hidden-symbolic computation approach.

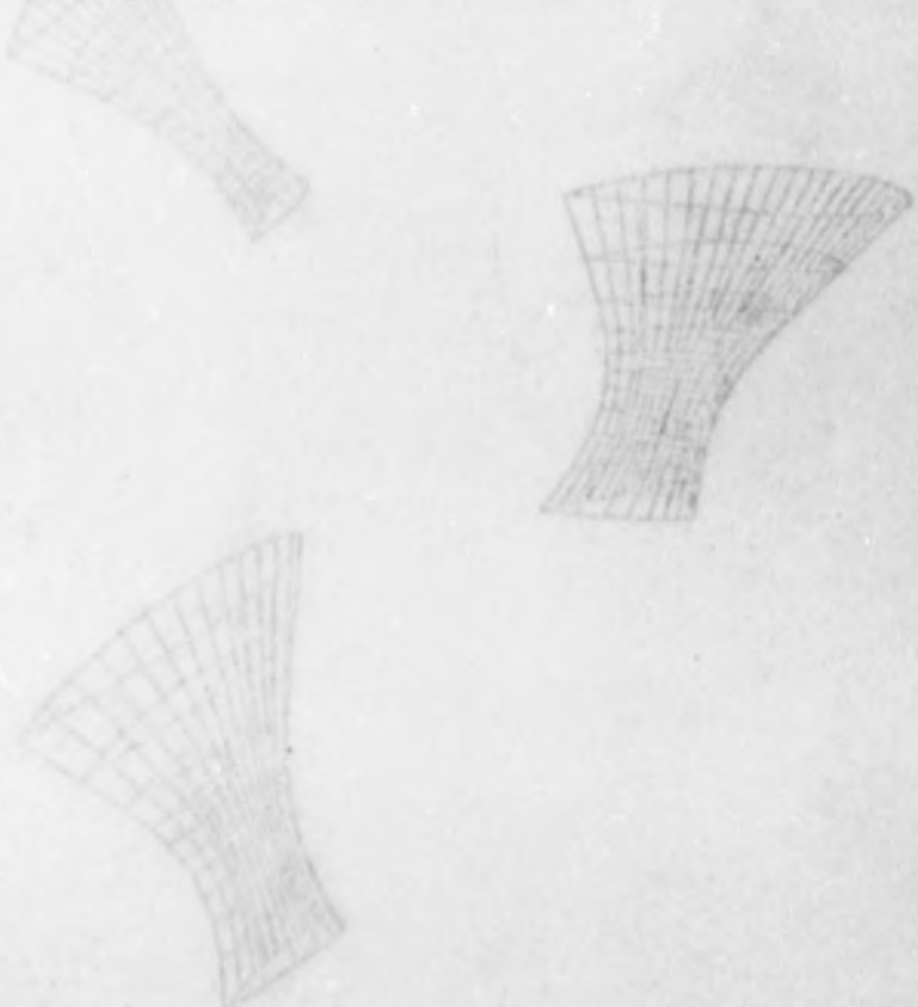

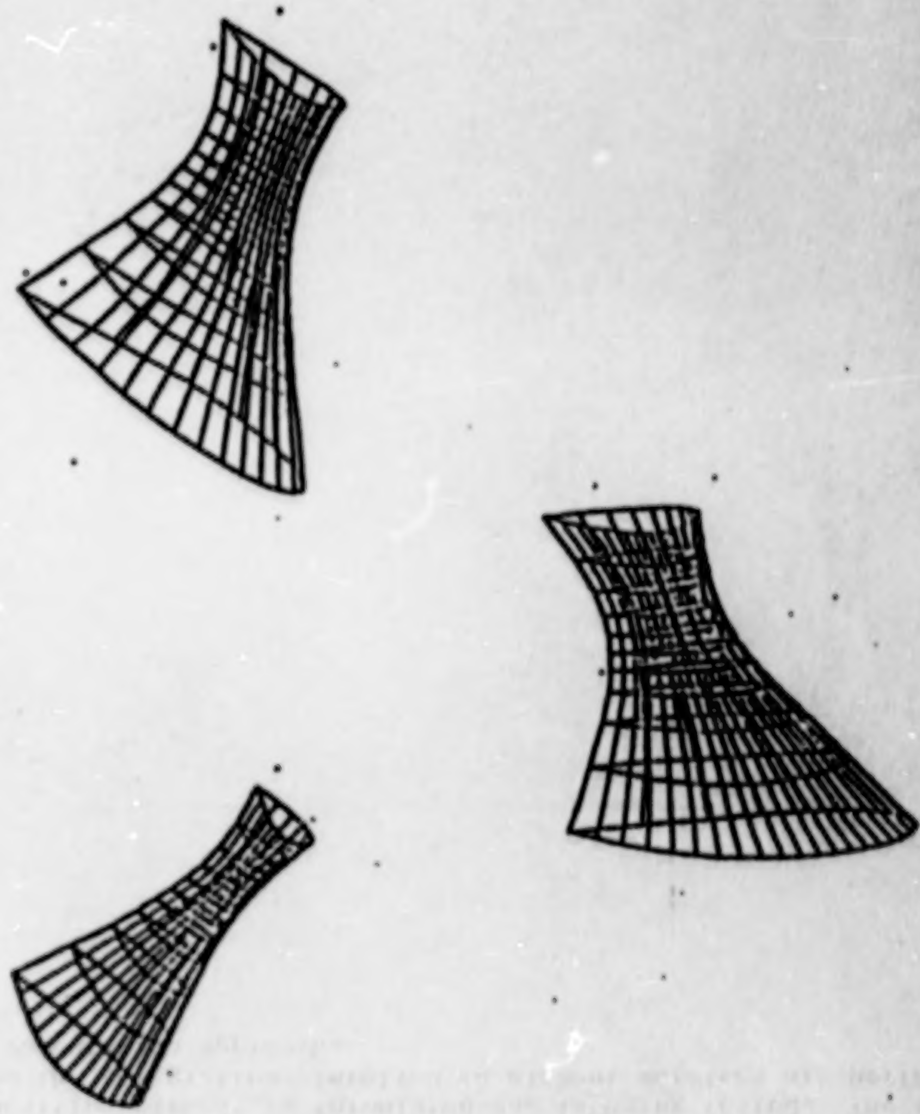

Modeling of a closed shell

Modeling of a closed shell

By utilizing similar interpolation and blending functions various size finite element meshes are obtained from a closed shell structure.

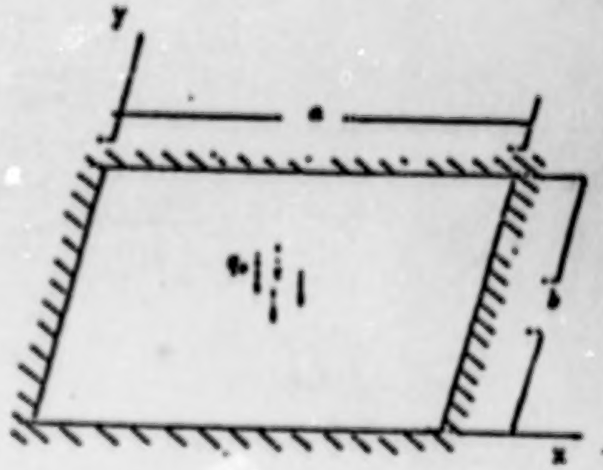

Figure 5.4: Uniformly loaded rectangular plate with built-in edges.

For this example the results are compared with the solutions given by reference[1]. The comparison is made in the form of plot of the plate center deflection $\bar{w}$, versus the number of elements used in the discretization. The results are tabulated in table 5.3, and the plot is shown in Fig. 5.5.

The theoretical value for the maximum deflection provided by reference[1], for a length-to-width ratio equal to 3/2 is : $w = 0.1053$ mm

Table 5.3: Center deflection of a uniformly loaded clamped plate.

Number of elements	center deflection (in.)
4	0.1390
8	0.1113
16	0.1100
24	0.1080

Center Deflection of a Uniformly Loaded Clamped Plate

Two dimensional bending finite elements based on the boolean sum are utilized for solution of a rectangular plate under uniformly distributed loads. The results obtained are in excellent agreement with the theoretical values even with a coarse mesh size.

TEST CASE NUMBER 5

This test case consists of a rectangular pin - pin plate that has no rotation speed. This case will yield the free vibrations of the plate with no external loads being present. The mesh size is four elements square. Table 1 shows the numerical data obtained from D.A.R.T. and theoretical results.

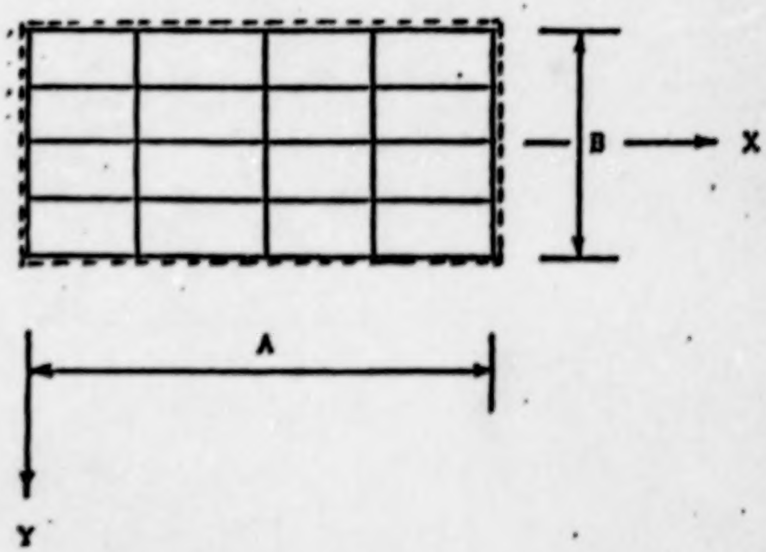

Setup Test 1
4x4 case
16 B.C.
A= 10.0 in,
B= 10.0 in.
Thk=.2879 in.
Angle= 90
Speed= 0 rps
Radius= 0 in.

Frequency (cps)

MODE	D.A.R.T. RESULTS	EXACT SOLN.	% ERROR
1	59.673	59.758	-.142
2	148.910	149.394	-.324
3	148.910	149.394	-.324
4	234.190	239.031	-2.03
5	299.050	298.788	+.088,

Natural Frequencies of a Square Plate

A simply-supported plate is analyzed for its natural frequency response. A mesh size of 4X4 was utilized for this purpose. The results obtained show very good agreement with the theoretical values.

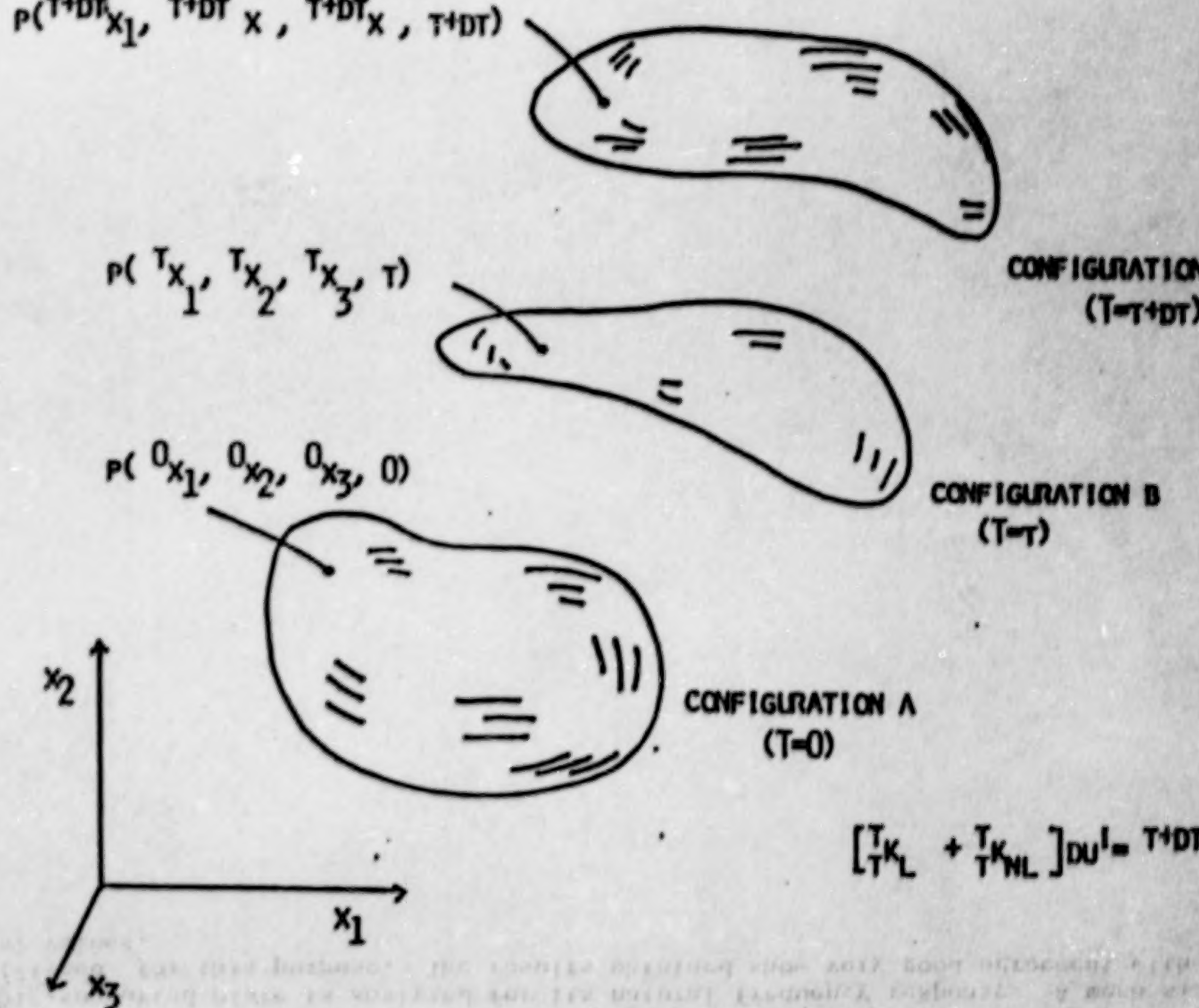

$$\left[{}^{T}_{T}K_L + {}^{T}_{T}K_{NL}\right] DU^{I} = {}^{T+DT}R - {}^{T+DT}_{T+DT}F^{I-1}$$

DESCRIPTION OF A BODY IN MOTION

DESCRIPTION OF A BODY IN MOTION

An Updated Lagrangian formulation is being utilized to account for large displacements and large rotations.

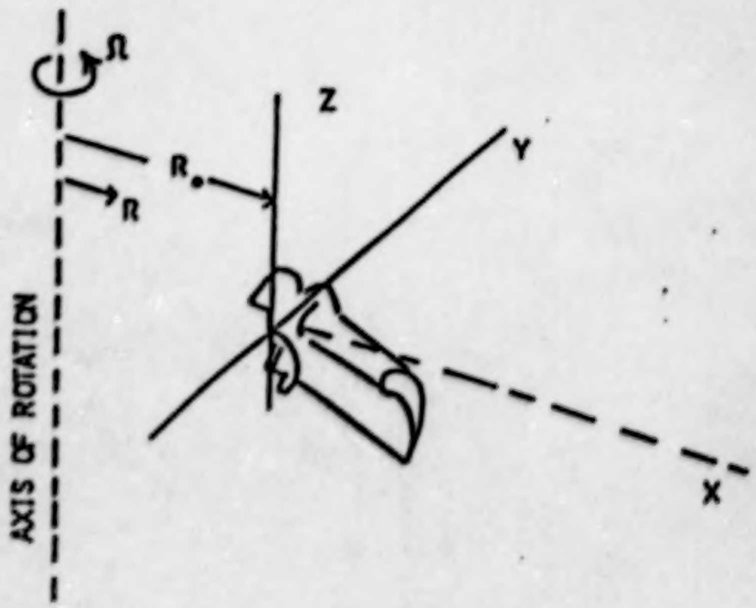

CENTRIFUGAL FORCES

$$\{F_C\} = \int_V [N]^T \{F\} \, DV$$

$$\{F\} = \begin{Bmatrix} F_X \\ F_Y \\ F_Z \end{Bmatrix} = \begin{Bmatrix} \rho \Omega_X^2 R_X \\ \rho \Omega_Y^2 R_Y \\ \rho \Omega_Z^2 R_Z \end{Bmatrix}$$

$$[M]\{\ddot{U}\} + [\dot{M}(T) + C]\{\dot{U}\} + [K]\{U\} = \{F(T)\}$$

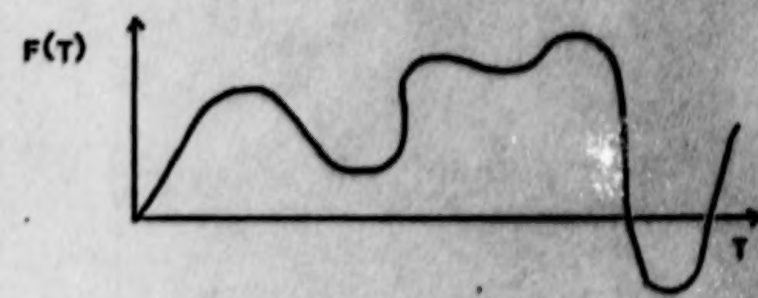

ELEVATED TEMPERATURES

ANISOTROPIC MATERIAL

LOADING

Elevated temperature effects, centrifugal forces and time dependent mass effects will be incorporated in the solution.

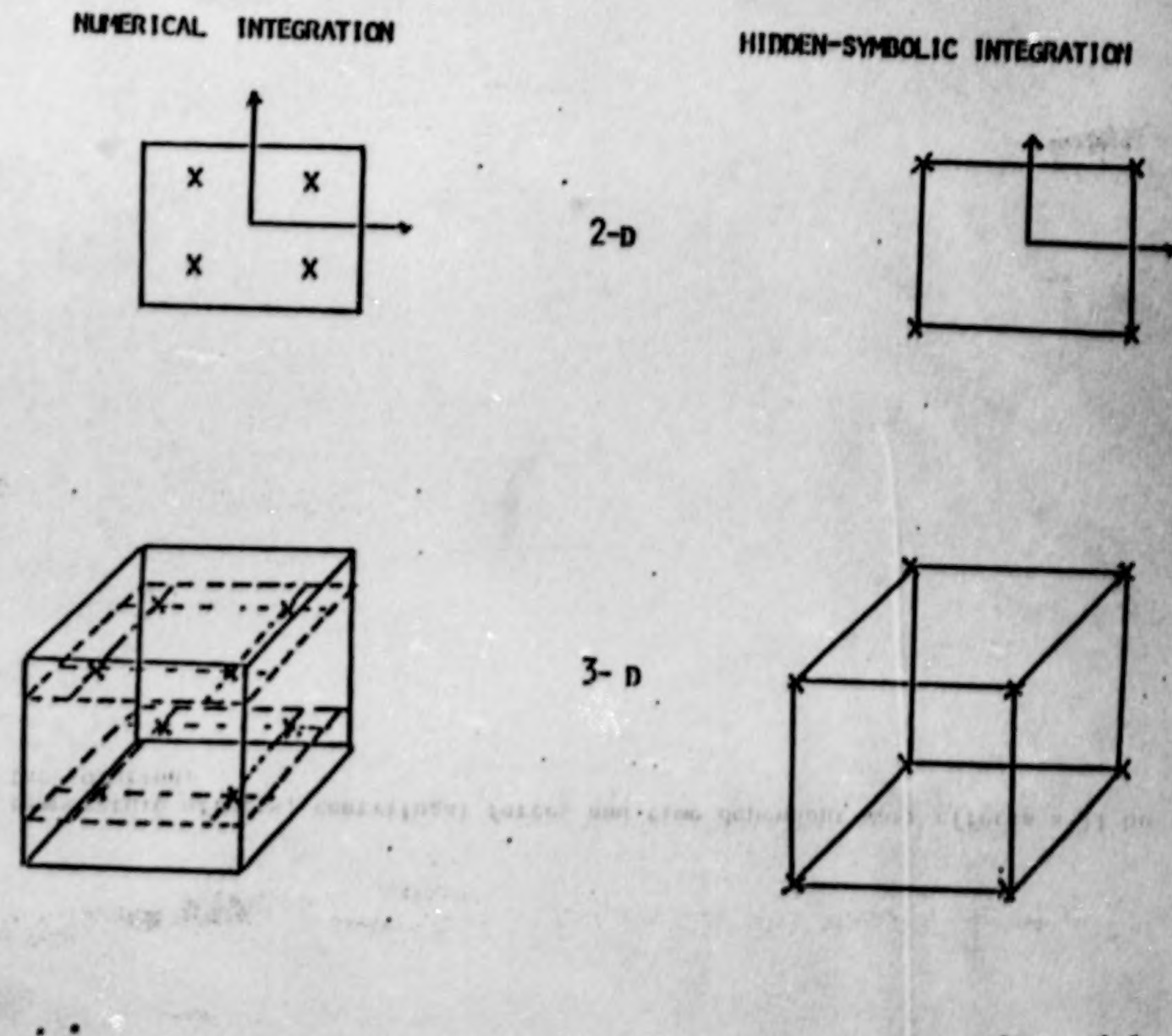
NUMERICAL INTEGRATION
HIDDEN-SYMBOLIC INTEGRATION
2-D
3- D

NUMERICAL INTEGRATION - HIDDEN SYMBOLIC INTEGRATION

The integrations involved in the element matrices are obtained exactly by utilizing a hidden-symbolic integration scheme that is developed here. As it is seen in the figure, the accuracy of the results will be improved since one can calculate the required nodal values at the nodes instead of at the numerical integration points.

ELEMENT

POLYNOMIAL

[K] — $\int, \iint, \iiint$

[M] — $\frac{\partial}{\partial R}$

{F} — $\frac{\partial^2}{\partial R^2}$

⋮

HIDDEN-SYMBOLIC COMPUTATIONS
POLDIF (P, IX, PX, NTERM, NDIMC)
POLMLT (. . .)
POLADD (...)
POLINT (. . .)
POLIEV (. . .)
⋮

EXACT

[K]

[M]

{F}

. . .

BENEFITS

TIME

ACCURACY

(P, H, "E" VERSION F.E.)

. . . .

. . . .

HIDDEN-SYMBOLIC COMPUTATIONS

A computer module is developed to operate on polynomials. These operations include differentiation, addition, multiplication, integration and integral evaluation. These modules are being utilized to formulate the finite element stiffness and mass coefficeents exactly,""E"-version finite elements."

MATERIAL CONSIDERATIONS

- MATERIAL PROPERTIES VARY AT ELEMENT NODAL POINTS
- $P(T, \dot{T}, \sigma, x)$

$$[A]_I = \sum_{J=1}^{8} N_J [A]_J$$

$$\frac{P_M}{P_{M_0}} = \left[\frac{T_M - T}{T_M - T_0}\right]^N \left[\frac{S_F - \sigma}{S_F - \sigma_0}\right]^M \left[\frac{\dot{S}_F - \dot{\sigma}_0}{\dot{S}_F - \dot{\sigma}}\right]^L$$

C.C.CHAMIS, (1985)

MATERIAL CONSIDERATIONS

Unlike the traditional formulations, the material properties vary at the nodal points of the elements. The material properties are considered as functions of time, temperature, stress and the coordinates. The interpolation functions are for the geometry, for the material, and for the field variables. It may be noted that different interpolation functions are selected for interpolating the geometry, material and the field variables.

CONCLUDING REMARKS

- NOVEL METHODS ARE UNDER INVESTIGATION FOR SOLUTION OF SINGULARITY PROBLEMS ENCOUNTERED IN MECHANICS. AT PRESENT, ONLY THE STRUCTURAL APPLICATIONS ARE BEING CONSIDERED. RELAIBILITY ON THE RESULTS (THE STRUCTURAL RESPONSE) IS THE PRIMARY CONCERN. EFFICIENCY AND CAPACITY OF THE METHODS ARE BEING INVESTIGATED.

- MATERIAL PROPERTIES ARE MODIFIED TO INCLUDE T, $\dot{T}$, X, σ EFFECTS. MATERIAL PROPERTIES VARY AT NODAL POINTS OF THE FINITE ELEMENTS FORMULATED. DIFFERENT CLASS OF INTERPOLATION AND BLENDING FUNCTIONS ARE UTILIZED IN ORDER TO REPRESENT MATERIAL BEHAVIOR UNDER ELEVATED TEMPERATURES WITHIN THE ELEMENT.

- TWO TRANSITION FINITE ELEMENTS ARE FORMULATED AND ARE BEING TESTED.

- A HIDDEN-SYMBOLIC COMPUTATION SCHEME IS DEVELOPED. FINITE ELEMENTS ARE BEING FORMULATED BY UTILIZING THIS SCHEME. INTEGRATIONS ARE PERFORMED EXACTLY IMPROVING ACCURACY AND EFFICIENCY.

- THE METHODS ARE ALSO APPLICABLE TO FLUIDS AND COUPLED PROBLEMS.

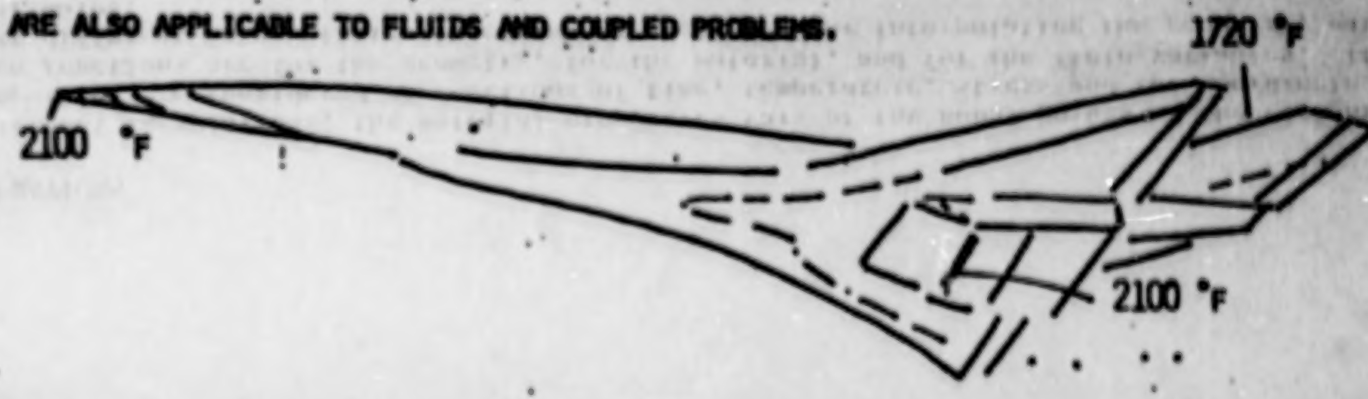

N89
29806
UNCLAS

LaRC Computational STRUCTURAL DYNAMICS OVERVIEW

PRESENTED AT

CSM 1987 WORKSHOP

J. M. Housner

November 20, 1987

See p 1015

LaRC Computational Structural Dynamics Overview

OBJECTIVES

Develop Advanced Computational Methods For Transient And Simulation Analyses of Aircraft, Launch Vehicles and Space Structure Components

ACTIVITIES:

In-House

- Development of Multibody Simulation Tool
- Procedures for Articulating Structures

Out-of-House

- Subcycling in Parallel Computing Environment
- Large Deformation/Motion Beam Formulation
- Constraint Stabilization
- Direct Integration Transient Algorithms in Parallel Computing Environment

LANGLEY RESEARCH CENTER COMPUTATIONAL STRUCTURAL DYNAMICS OVERVIEW

Present research centers on the development of advanced computational methods for transient simulation analyses. Aircraft, launch vehicles and space structure components are potential applications, but primary focus is presently on large space structures.

There are both in-house and out-of-house activities. The in-house activity centers around the development of a multibody simulation tool for truss-like structures called LATDYN for Large Angle Transient DYNamics. Multibody analysis involves articulation of structural components as well as robotic maneuvers. These items are necessary for construction (erection or deployment) of large space structures in orbit and the carrying out of certain operations on board the space station. Thus part of the in-house activity involves the development of methods which treat the changing mass, stiffness and constraints associated with articulating systems.

The out-of-house activity involves subcycling, development of large deformation/motion beam formulation, constraint stabilization and direct time integration transient algorithms in parallel computing.

RECENT PROGRESS - Out-of-House Research

- Subcycling Explored With Vectorization and Concurrency
  - Preliminary Tests Indicate Speed Increases on the Order of 10 +
- Multi-body Dynamics Developments
  - Hierachical Flexible Beam Elements
  - Staggered Constraint Stabilization Procedure
  - Integration of Large Rotation Equations
  - Automated Partitioning Procedure
- A Non-Conventional Partitioning Procedure Developed
  - PANTA (Partitioned Algorithm for Nonlinear Transient Analysis)
  - Speed Increases Due To Both Partitioning and Concurrency

RECENT PROGRESS - Out-of-House Research

Subcycling or spatially non-uniform time step procedures for explicit temporal integration has particular emphasis on the trade-off between long vectors for vectorization efficiency and blocking of operations for use of many computational processors in parallel. This work is being accomplished at Northwestern University. Preliminary trade-off studies involving vectorization and concurrent processing indicate speed increases on the order of 10+ are possible.

At the University of Colorado, a large deformation/motion beam formulation has been developed which treats translational and rotational motions in two separate ways and allows for transverse shearing members or components. The university has also developed a constraint stabilization technique which uses a penalty function approach and has exhibited much potential on sample problems.

Finally, a direct integration transient algorithm has been established for use in a parallel computing environment. The method exhibits considerable efficiency even on a sequential machine and in a parallel environment the method appears to be a significant breakthrough.

LATDYN

Large Angle Transient DYNamics

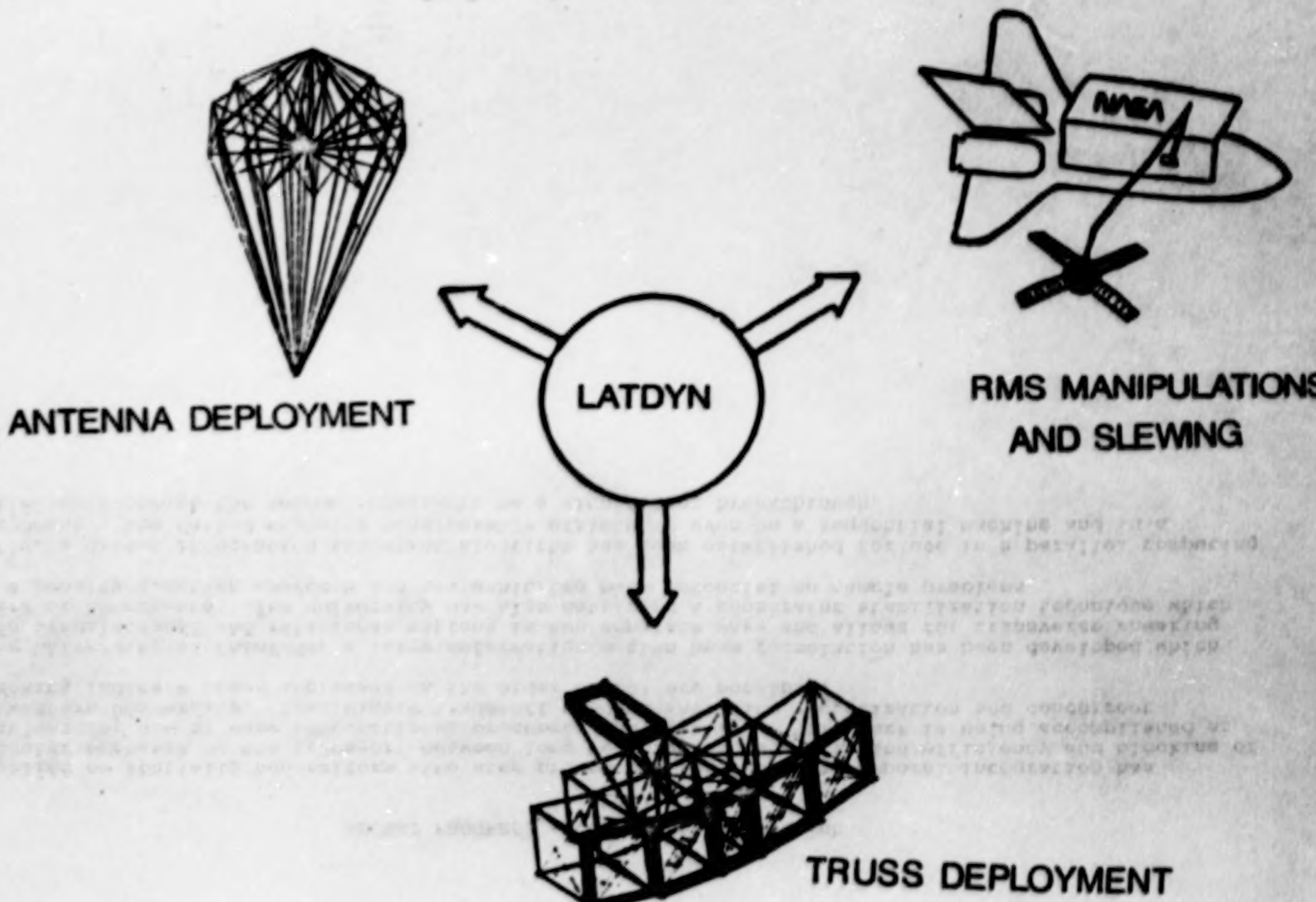

1018

LATDYN

The LATDYN (Large Angle Transient DYNamics) computer program is an analytical simulation tool for multi-body structural dynamics behavior involving large angle rotation between structural components. The tool finds application in large space structure deployment, robotic arm manipulation and modeling of deformable mechanisms. It has been developed at the Langley Research Center through a team effort composed of NASA and contractor (the COMTEK Company) personnel. The program has not been developed as a commercial production code, but rather as a research code which provides a testbed for studying computational aspects of this class of problems. Presently, only a two-dimensional working version exists. The program is written in FORTRAN 77 and is operational on the VAX/VMS and CDC/NOS. Extensive graphics output capability is provided including line drawings, and deformed and undeformed geometry. A three dimensional version is under development.

LATDYN CAPABILITIES

Finite Element Based

- General geometry including closed loop topologies

Rigid or Flexible Beams

Applied Forces,Displacements,Velocities or Accelerations

Fortran Based Command Language

- Permits external user access to internal fortran code
- User written logic commands provide added control over program flow

Nonlinear Springs and Dampers

Control Forces

- Functions of system variables
- Time delay

Lock-up, Docking, Impact

LATDYN CAPABILITIES

LATDYN is a finite element structural program. It is intended for use in classes of problems where the multi-body system undergoes some deformation; that is, there is some strain energy associated with the motion. The structure is modeled with a mesh of finite elements as in any finite element program. The program does not depend upon mode shapes to characterize motion of the component bodies, rather, component bodies are discretized into finite elements. As in most finite element codes, generalized coordinates map the motion of the element end points and shape interpolation functions characterize motion internal to the element. However, provision is made for global shapes on the component level. One significant advantage of a finite element approach is its allowance for general geometry, including closed loop topologies, as attested to by its wide popularity in the structures community.

Presently, the library of elements is limited to rigid or flexible beams, springs, dampers and lumped masses. Use of a convected coordinate system, described on a subsequent chart, permits the beam members to undergo unlimited rotations and large deformations. The user may specify either applied forces, displacements, velocities or accelerations.

A FORTRAN based language allows the input of user defined relationships thereby permitting the definition of nonlinear springs, dampers, control forces which are functions of system variables, time delay and a host of other capabilities. Furthermore, user written true or false logic commands make use of all FORTRAN logic statements, (such as, .AND., .OR., IF, etc.), to permit the user an added degree of control over which commands are executed and their order of execution.

In addition, time varying constraints are permitted, and an algorithm known as ACCIDS (Algorithm for Constraint Changes In Dynamic Systems), as discussed in reference 2 and on a subsequent chart, is used to perform lock-up, docking, impact or any other situation where system constraints change suddenly.

LATDYN FRAMEWORK

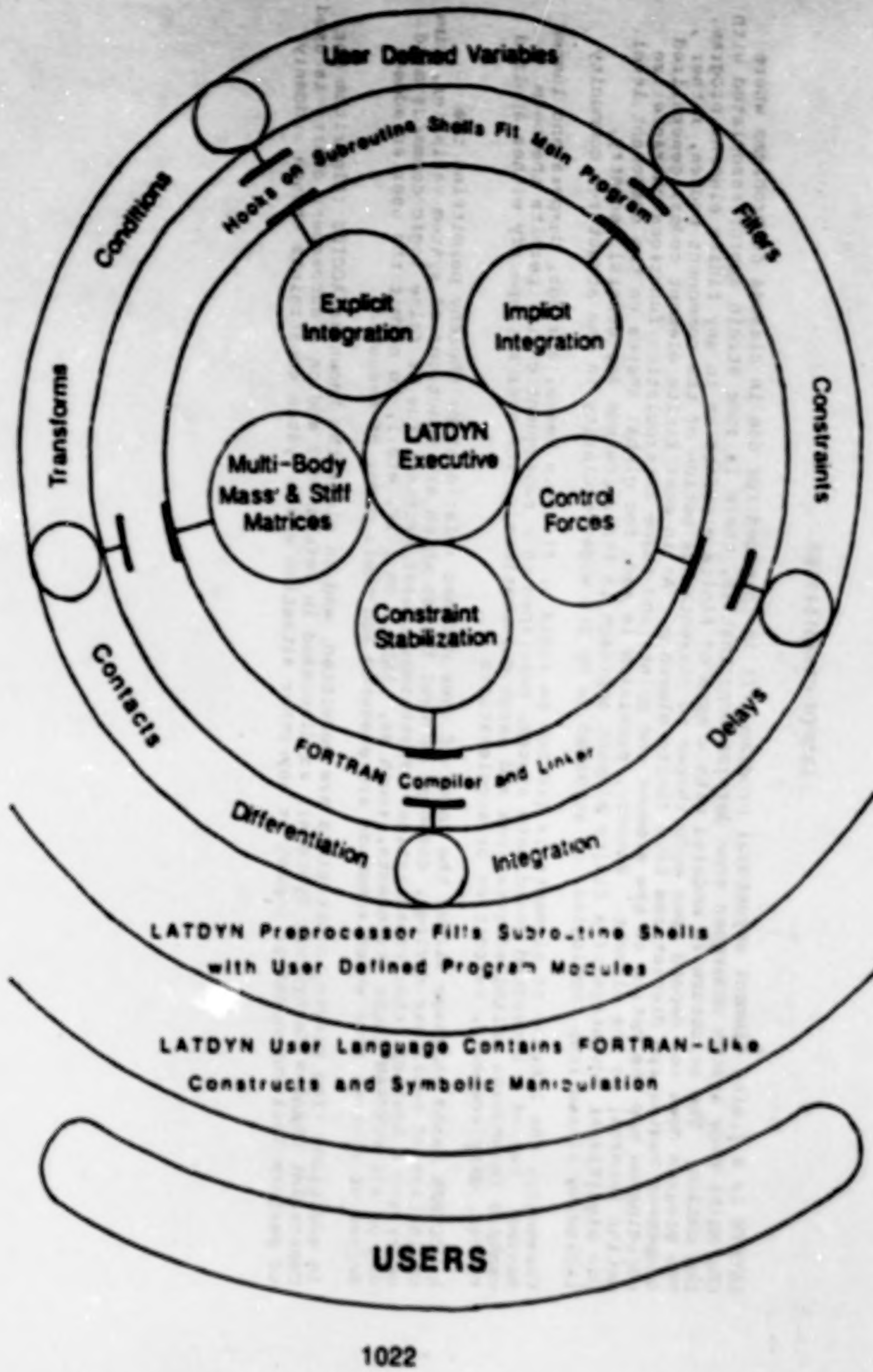

LATDYN FRAMEWORK

The figure schematically illustrates the framework of the LATDYN program. The user communicates with the program through a FORTRAN-like command language. A preprocessor interprets the commands and generates FORTRAN code which fills a shell of potential program capabilities. Hooks and scars on the core of the LATDYN program permit the shell to become part of the program via the computer system's FORTRAN compiler and linker. This provides the user easy access to the internal code without having to compose user written subroutines which invariably are very cumbersome for the average user.

GENERIC HINGE BODY WITH MEMBER CONNECTIONS

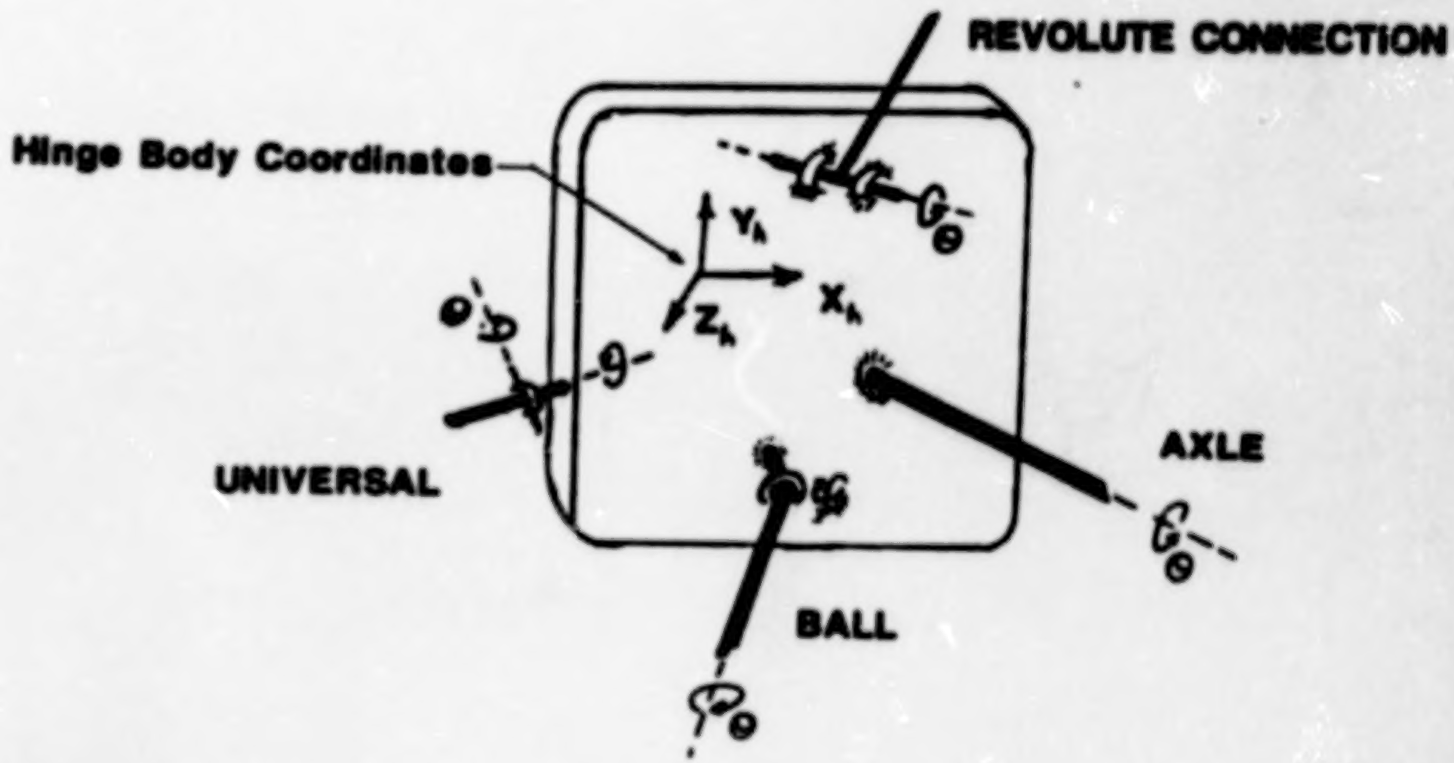

Define:

$[\Gamma]$, Fixed Orientation of Hinge Connection Relative to Hinge Body

θ, Time Varying Rotation About a Hinge Line

GENERIC HINGE BODY WITH MEMBER CONNECTIONS

The class of structures to be treated by this program are joint dominated. That is, the mass of the interconnecting joints between the bodies represents a significant portion of the total mass and the orientation of the joint's hinge lines plays an important role in determining structural behavior and whether or not a mechanism exists. It is thus reasonable to construct the finite element program with the joints, herein denoted as hinge bodies as a part of the element connectivity. This avoids numerical problems which can arise due to what might be called "the tail wagging the dog" phenomenon. Furthermore, since large angular rotations are not vectors, connectivity relationships could be time varying and quite complex. The use of hinge bodies circumvents these connectivity complications. Thus, the hinge bodies are introduced into the formulation from the outset.

A generic hinge body with several members connected to it through various types of joints is depicted in the figure. Accommodations for hinge connections to various members connected to the hinge body are built into the formulation. Again, this avoids the cumbersome and often difficult task of composing the time varying constraint relations to represent member connections. If there is no hinge, but rather a rigid connection, the constraint is set to zero. It is easier to set a constraint to zero than to create a complex time varying one.

A cartesian coordinate system is used to measure three translations of a designated point on a hinge body and a transformation matrix, T_h, provides the orientation of three orthogonal axes embedded into the hinge body. Members are assumed to be hinge-connected to a hinge body. The connecting hinge line is embedded into the hinge body and is related to the hinge body axes through a fixed transformation matrix Γ. The rotation, θ, about the hinge line is time varying.

Generalized Coordinates

For Each Hinge Body

- 3 Translational Displacements of Hinge Body
- 3 Angular Rotational Rates of Hinge Body
- 1 Relative Angle Between Hinge Body and Finite Element

GENERALIZED COORDINATES

For each hinge body, there exist three translational generalized coordinates, three angular rotational generalized coordinates and one relative angle generalized coordinate for each hinge located on the hinge body.

DEFORMED FINITE ELEMENT

Element Coordinates Move

With Cross-Section

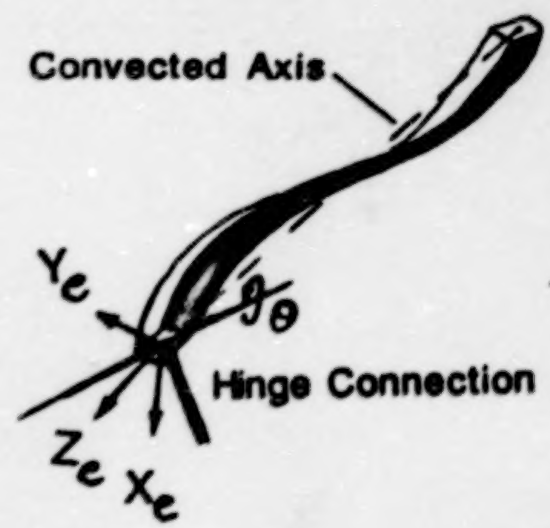

Deformations Are Measured From Convected Axes

Define:

[Γ], Fixed Orientation of Hinge Connection on Finite Element

θ, Time Varying Rotation About Hinge Line

DEFORMED FINITE ELEMENT

Each structural member is divided into finite elements. A typical deformed element is shown in the figure. The orientation of the element at its ends is monitored by means of two element coordinate systems, one at each end, though only one is shown in the figure. These coordinates move with the element. The x-axis of the element system is tangent to the element at its end and the other two orthogonal axes are parallel to the principal axes of the element cross-section. The orientation along the length is found from an assumed polynomial shape function as in any finite element analysis. As with the hinge body, a hinge line is embedded into the end of the element with associated fixed transformation Γ. The rotation, θ, about the hinge line is time varying.

A convected coordinate system is used to define a reference for measuring element flexural deformations. This separates rigid body and deformable motions. As shown in the figure, the convected x-axis connects the end points of the element. Its other two orthogonal axes roll with the element.

Connectivity of Finite Element/Hinge Body

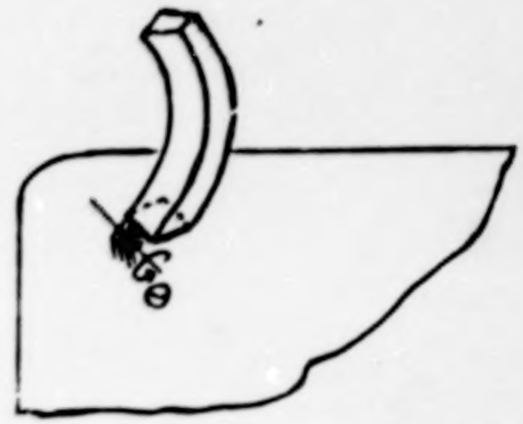

Hinge lines on finite element and on hinge body coincide

On Hinge Body		On Finite Element
$T_h \, \Gamma \, \Gamma_\theta$	$=$	$T_e \, \overline{\Gamma}$

Transform to global system

Transform to hinge body system

Rotate hinge connection

Orientation of embedded hinge line in finite element

Transform to Global System

CONNECTIVITY OF FINITE ELEMENT/HINGE BODY

Since the hinge lines on the hinge body and on the finite element must coincide, and since axes orthogonal to the hinge lines must also coincide when rotated through an angle θ, the transformation from a global system to the element system, T_e, may be related to the transformation from the global system to the hinge body system, T_h,

$$T_e = T_h \Gamma \, \Gamma_\theta \Gamma^T$$

Thus in the analysis, T_h for the hinge body is monitored and θ for the hinge connection.

Element Deformations

<u>Deformation matrix is product of transformation matrices</u>

$$\text{Deformation Matrix} = T_c^{\mathrm{T}}\, T_h\, \Gamma\, \Gamma_\theta\, \overline{\Gamma}^{\mathrm{T}}$$

Rotation θ about common hinge line

Convected System

Hinge Body System

Embedded Hinge Line On Element End

Embedded Hinge Line On Hinge Body

For small deformations:

$$\text{Deformation Matrix} = \begin{bmatrix} 1 & -\phi_z & \phi_y \\ \phi_z & 1 & -\phi_x \\ -\phi_y & \phi_x & 1 \end{bmatrix}$$

. . . .

ELEMENT DEFORMATIONS

Element deformations are measured from the convected axes. The convected x axis joins the two element end points, so it is fully determined by the translations of the element end points. It is assumed that the finite element grid is sufficiently refined so that element deformations are small, however, the overall member deformations may be large. In fact, the convected analysis was first utilized to treat large deformation rather than large rigid body motion problems. (See for example references 3-7).

Under the small element deformation assumption, the element and convected axes are related by,

$$T_e = T_c D$$

$$D = \begin{vmatrix} 1 & -\phi_z & \phi_y \\ \phi_z & 1 & -\phi_x \\ -\phi_y & \phi_x & 1 \end{vmatrix}$$

Since T_e is related to T_h, the deformation matrix D is given by,

$$D = T_c^T T_h \Gamma \, \Gamma_\theta \Gamma^T$$

and the flexural deformation angles are given by,

$$\phi_y = (1,0,0) T_c^T T_h \Gamma \, \Gamma_\theta \Gamma^T (0,0,1)^T \; ; \; \phi_z = -\,(1,0,0) T_c^T T_h \Gamma \, \Gamma_\theta \Gamma^T (0,1,0)^T$$

The twist over the member or change in roll rotation is given by,

$$\Delta\phi_x = (0,0,1) [\Gamma \, \Gamma_\theta^T \Gamma^T T_h^T]_1 \; [T_h \Gamma \, \Gamma_\theta \Gamma^T]_2 (0,1,0)^T$$

where subscripts 1 and 2 refer to the two ends of the element.

It is important to note that extraction of element deformations only requires defining the convected axis joining the two element ends and not any axes orthogonal to it.

Equations of Motion and Their Numerical Integration

At n^{th} time step,

$$M^n a^n + f^n = F^n$$

Newmark-Beta Integrator at k^{th} iteration:

$$a_k^n = a_{k-1}^n + \left[M_{k-1}^n + \frac{h}{2} G_{k-1}^n + \beta h^2 K_{k-1}^n\right]^{-1} R_k^n \qquad \text{:Update Accelerations}$$

$$R_k^n = \text{iterative residual} = F^n - f_{k-1}^n - M_{k-1}^n a_{k-1}^n$$

$$V_k^n = V^{n-1} + \left(\frac{h}{2}\right)\left(a^{n-1} + a_k^n\right) \qquad \text{:Update Velocities}$$

Split into translational and rotational d.o.f.

Translational displacements are

$$d_k^n = d^{n-1} + h v^{n-1} + \left(\tfrac{1}{2} - \beta\right) h^2 a^{n-1} + h^2 a_k^n \qquad \text{:Update Translational d.o.f.}$$

Rotational motions are given by transformation matrix:

$$T_k^n = \left[1 + h\overline{\omega}_k^n + \tfrac{1}{2} h \left(\overline{\omega}_k^n\right)^2\right] T^{n-1} \qquad \text{:Update hinge body transformation}$$

. . . .

EQUATIONS OF MOTION AND THEIR NUMERICAL INTEGRATION

In the figure, h is the time step; M, K and G are the mass stiffness and gyroscopic matrices respectively; a, v and d are acceleration, velocity and translational displacement respectively; f is the nonlinear internal force vector whose linearized terms come from K and G; F is the external force vector; R is the iterative residual; ω is the antisymmetric matrix of angular velocity components and T is the hinge body transformation matrix.

Use of Newmark-Beta yields unconditional numerical stability for linear problems and thus can be expected to permit large time steps. The recursion formulas are second order accurate and it can be shown that the predicted transformation matrix retains orthogonality to third order.

COMPARISON OF SOLUTIONS FOR DEPLOYMENT OF FLEXIBLE BOOM

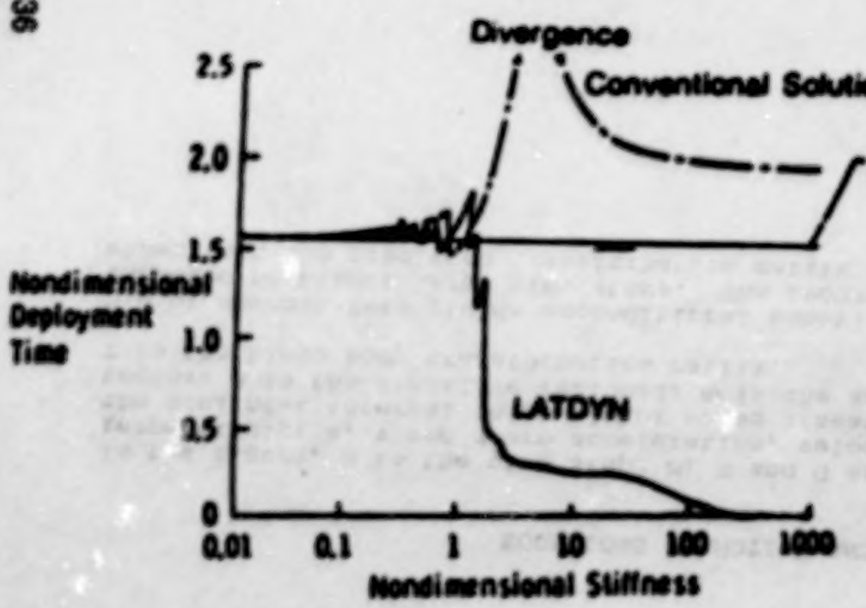

CONVENTIONAL SOLUTION
CAN DIVERGE
-NONLINEAR KINEMATICS
-LINEAR STRUCTURE

NEED TO USE
NONLINEAR STRUCTURE
WITH
NONLINEAR KINEMATICS

COMPARISON OF SOLUTIONS FOR DEPLOYMENT OF FLEXIBLE BOOM

The common use of a linear structural representation can lead to serious difficulaties when the linear structure is combined with the nonlinear kinematics of large angular motion. For example, the use of mode shapes with nonlinear kinematics can produce erroneous results. This is demonstrated in the accompanying figure which is taken from reference 1 with minor changes.

The curve labeled conventional solution was generated using a linear structural and nonlinear kinematic representation. Deployment time is taken as the time it takes the root to rotate ninety degrees, which is assumed to be the boom's final position. The results indicate divergence and are physically unacceptable as the nondimensional stiffness increases. The increase of this parameter implies either increasing deployment rate or boom softening. As shown in reference 1, such erroneous results occur due to the neglect of nonlinear stuctural terms; that is a linear structural representation with a nonlinear kinematics is unacceptable. On the other hand, a consistent nonlinear approach yields reasonable results.

ERRONEOUS DESTABILIZING CORIOLIS FORCE ON ROTATING BOOM DUE TO COUPLING OF LINEAR STRUCTURAL AND NONLINEAR KINEMATICS MODELING

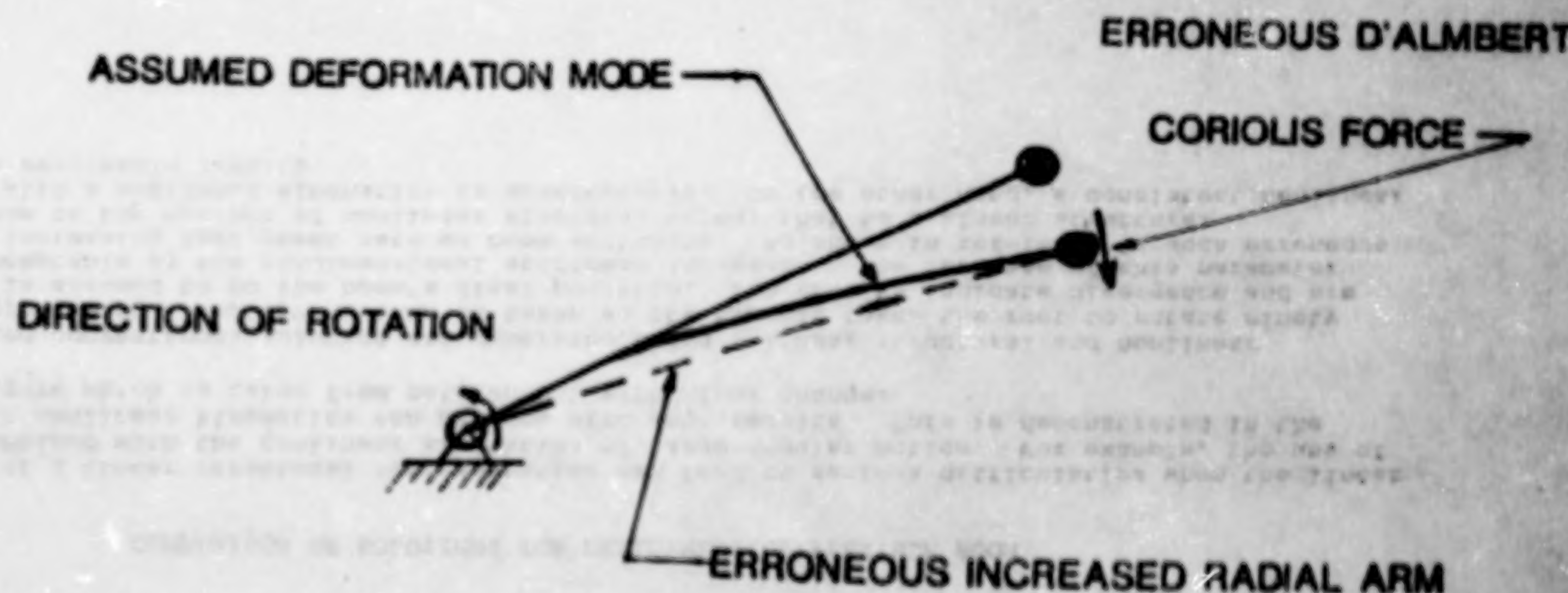

ERRONEOUS DESTABILIZING CORIOLIS FORCE ON ROTATING BOOM DUE TO COUPLING OF LINEAR STRUCTURAL AND NONLINEAR KINEMATICS MODELING

The divergence demonstrated in the previous figure can be understood physically by considering the sketch of figure 3. Though admittedly considerably simplified, the sketch depicts the erroneous occurrence of a Coriolis force when the flexural deformation is not properly coupled nonlinearly to the radial motion so that axial strain in the member is accurately predicted. The assumed transverse motion in the sketch creates an apparent increase in the radial arm length from the center of rotation. In turn this means an apparent outward radial motion on a rotating boom. Consequently, an erroneous destabilizing Coriolis force arises which acts to increase the deformation, thus causing an even greater destabilizing Coriolis force to appear. If the boom lacks the stiffness to return itself to its straight position, it will become destabilized.

FUTURE WORK

- Three dimensional version now being coded and tested
- Implementation of time integration procedures for parallel processing developed by Brown University
- Assessment of University of Colorado Constraint Stabilization Technique
- Experimentation on a class of fundamental benchmark problems to assess code validity

FUTURE WORK

The three dimensional version of the LATDYN program is now being coded. The program's formulation and sample results will be presented at the 29th Structures, Structural Dynamics and Materials Conference in Williamsburg VA, April 1988. Implementation of the time integration method developed at Brown University is being examined on the Alliant FX-8 and Cray 2 computers and the assessment of the University of Colorado constraint stabilization technique is presently taking place. Lastly, a class of fundamental benchmark cases is to be established which will permit method validation.

N89

29807

UNCLAS

ALGORITHMS AND SOFTWARE FOR NONLINEAR STRUCTURAL DYNAMICS

PRINCIPAL INVESTIGATOR:
Ted Belytschko

RESEARCH ASSISTANTS:
Noreen D. Gilbertsen
Mark O. Neal

Northwestern University
Evanston, IL 60208

NASA Grant NAG-1-650
Contract Monitor: Jerry Housner
March 1, 1986 to May 1, 1988

OUTLINE

OBJECTIVE

EFFICIENT IMPLEMENTATION OF

MIXED Δt EXPLICIT NONL. STRUCT.

DYN. CODE ON VECTORIZED,

(II) CONCURRENT COMPUTER

TOPICS

MIXED Δt INTEGRATION

CONFLICT IN (II) + VECTORIZATION

ALGORITHM

EXAMPLES

SLIDE 1

ALGORITHMS AND SOFTWARE FOR NONLINEAR STRUCTURAL DYNAMICS

Ted Belytschko, Noreen D. Gilbertsen, and Mark O. Neal

SLIDE 1

The objective of this research is to develop efficient methods for explicit time integration in nonlinear structural dynamics for computers which utilize both concurrency and vectorization. As a framework for these studies, the program WHAMS, which is described in "Explicit Algorithms for the Nonlinear Dynamics of Shells" (T. Belytschko, J. I. Lin, and C.-S. Tsay, Computer Methods in Applied Mechanics and Engineering, Vol. 42, 1984, pp. 225-251), is used.

There are two factors which make the development of efficient concurrent explicit time integration programs a challenge in a structural dynamics program:

1. the need for a variety of element types, which complicates the scheduling-allocation problem;
2. the need for different time steps in different parts of the mesh, which is here called mixed at integration, so that a few stiff elements do not reduce the time steps throughout the mesh.

delta

interface requires very small Δt

$\Delta t \sim 0.2\,\Delta t_{crit}$

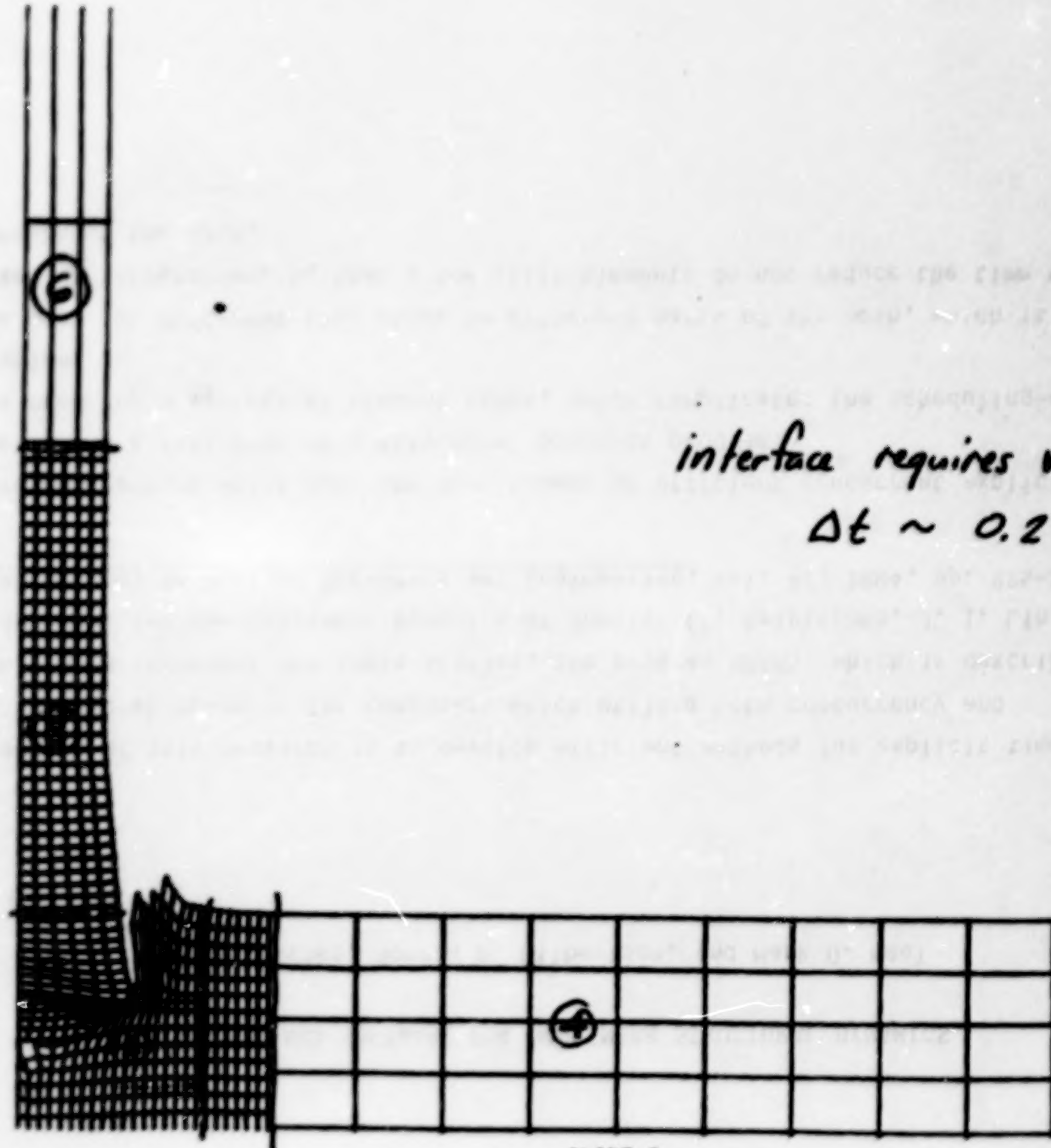

SLIDE 2

SLIDE 2

This mesh illustrates why mixed time integration is crucial in the application of explicit methods to structural dynamics. In this mesh, if a single time step were used thoughout the mesh, it would be set by the very smallest elements in the mesh and the requirement of the interface. If different time steps are used in different parts of the mesh, a time step in each sub-domain depends on the size of the elements and the requirements of that sub-domain. Thus, much larger time steps can be used in sub-domains 3, 4, 5, and 6.

1rst order semidiscretization

$$\underset{\sim}{M}\,\dot{\underset{\sim}{u}} + \underset{\sim}{f}^{int} = \underset{\sim}{f}^{ext}$$

for linear $\underset{\sim}{f}^{int} = \underset{\sim}{K}\,\underset{\sim}{u}$

$$\dot{\underset{\sim}{u}} = \underset{\sim}{M}^{-1}\big(\underbrace{\underset{\sim}{f}^{ext} - \underset{\sim}{f}^{int}}_{\underset{\sim}{f}}\big)$$

explicit (Euler forward)

$$\underset{\sim}{u}^{n+1} = \underset{\sim}{u}^{n} + \Delta t\,\dot{\underset{\sim}{u}}^{n}$$

$$= \underset{\sim}{u}^{n} + \Delta t\,\underset{\sim}{M}^{-1}\underset{\sim}{f}^{n}$$

SLIDE 3

SLIDE 3

This slide shows the fundamental equations involved in an explicit time integration of a first-order system such as the heat conduction equations. The procedures for second-order equations are a little more complicated but fundamentally similar in principle.

In this slide, $\underset{\sim}{M}$ designates the capacitance (mass) matrices, matrix $\underset{\sim}{f}^{int}$ the matrix of internal fluxes, and $\underset{\sim}{f}^{ext}$ the matrix of external fluxes. As can be seen from the last equation, if the capacitance matrix is diagonal, updating the system from state n to state n+1 involves no solution of any equations.

Flow of information

$$u^{n+1} = u^{n} + M^{1}\,(f^{ext} - K\,u)$$

in 1D: row of K . . . 0 -1 2 -1 0 . . . .

-1 +1

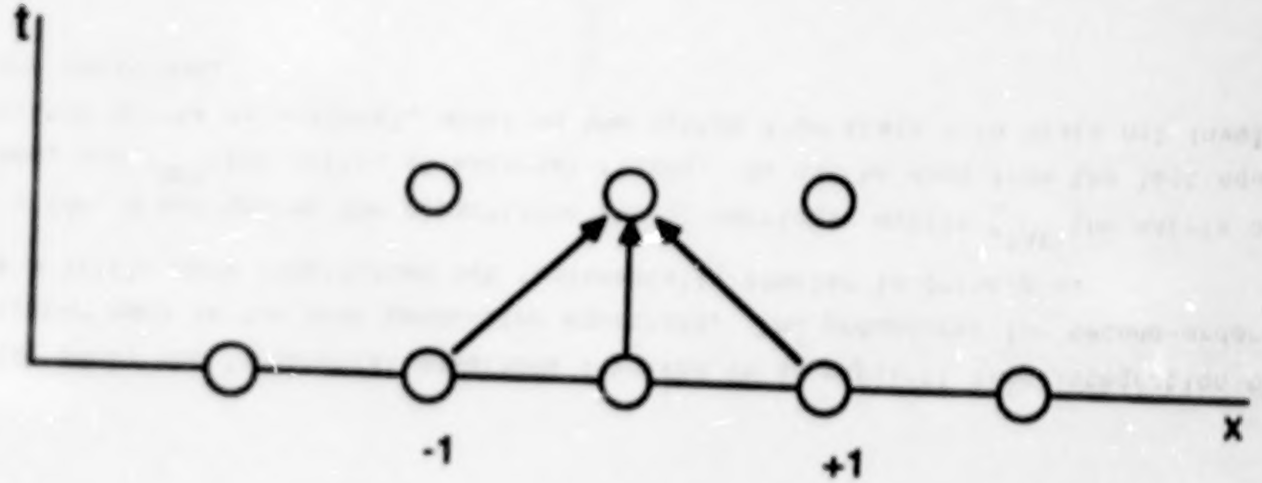

SLIDE 1

SLIDE 4

In order to examine how a multi-time partition is constructed, it is worthwhile to consider the flow of information in a one-dimensional problem with a single time step for explicit time integration. As can be seen from this figure, the state at time step n+1 at any point only depends on the states of the adjacent points at a previous time step. This is represented by the arrows in the figure.

Explicit - explicit nodal partition

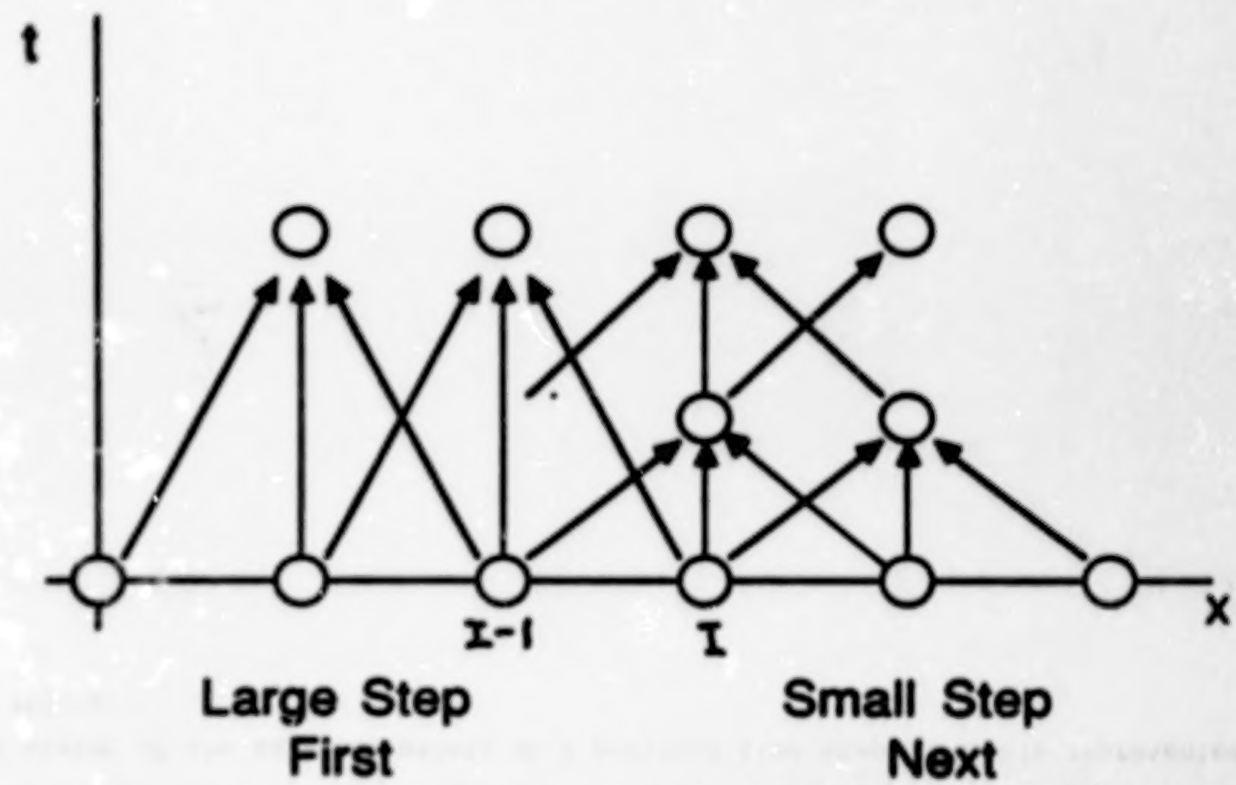

SLIDE 5

SLIDE 5

When we consider this flow of information in a one-dimensional problem with a time-step ratio of 2 to 1, then we can see that the standard procedure can be used at all time steps, except at node I which is the small node time step immediately adjacent to the large node time step. In order to update this node, one needs an interpolated value at node I-1, which is indicated by an x in the figure.

The flow of information for the second-order systems which appear in structural dynamics is identical. In both cases, we have used linear interpolations for u at node I-1 in order to get the intermediate values.

These procedures have been used with ratios of time steps as large as 10 to 1 between adjacent elements. The use of these multi-time step partitions does not seem to diminish the stability. For example, if element-type stability criteria are satisfied in both sub-domains for the first-order equations, stability is maintained in the entire system. This has been proven for a slightly different partition for a linear first-order system in "Stability of Multi-Time Step Partitioned Integrators for First-Order Finite Element Systems" (T. Belytschko, P. Smolinski, and W. K. Liu, Computer Methods in Applied Mechanics and Engineering, Vol. 49, 1985, pp. 281-297).

For second-order systems, no proofs of such stability criteria are yet available. However, numerical experiments indicated that the schemes we have used are stable whenever the elements in each sub-domain satisfy a local Courant condition.

ALLIANT FX/8

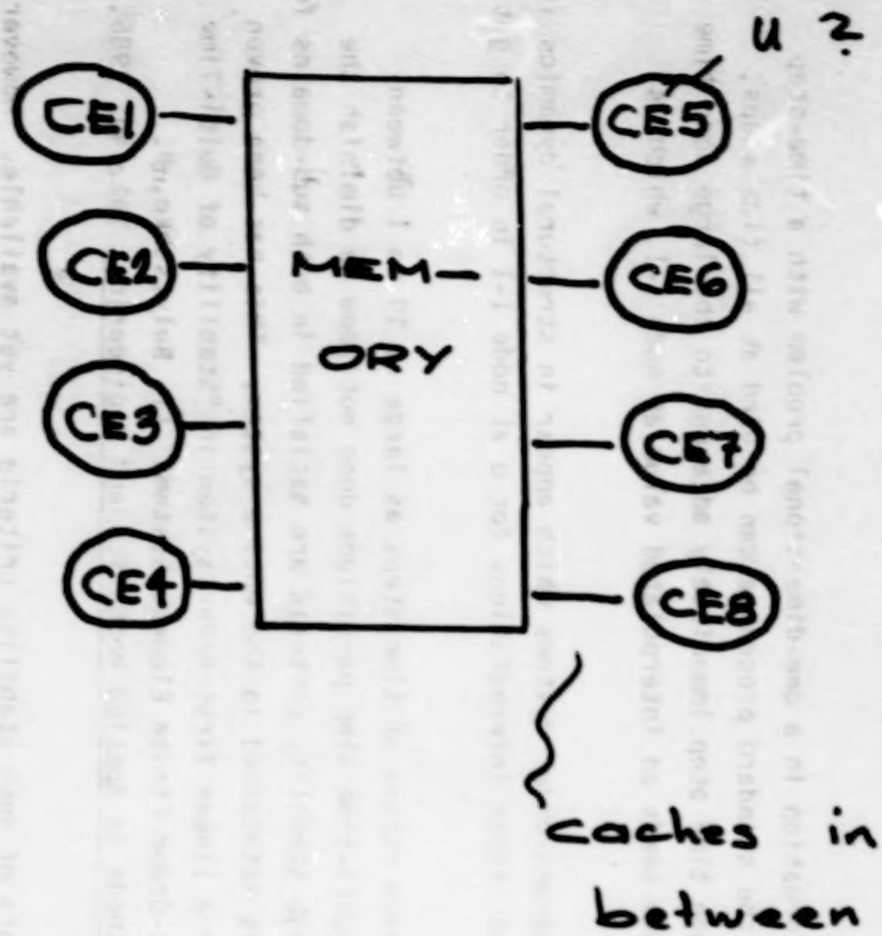

MIMD (multipl instr. multipl data)
shared-memory computer

– memory contention

cu's are vectorized

SLIDE 6

SLIDE 6

The computer program has been implemented on an Alliant FX/8, which is an MIMD (multiple instruction multiple data) shared-memory computer. A schematic of the computer architecture is shown. As can be seen, this is a shared memory computer, so it suffers from the problems of memory contention.

A second difficulty is presented by the fact that the computational units on this computer are vectorized. In vectorized computers, finite element computations have to be done on blocks of elements so that vectorization can be exploited. However, in a concurrent machine, the addition of vectorization presents a major dilemma: how long should the blocks be?

If rather long blocks are used, for example, 64 to 128 elements, then a large number of the processors will often be idle. Furthermore, in a concurrent machine, vectorization with long blocks requires considerable additional storage. On the other hand, short element blocks don't take full advantage of vectorization.

One advantage of blocking is that it has provided us with a natural scheme for assigning time steps to groups of elements. In previous implementations of multi-time step integration, the user has had to select the sub-domains. Since, in a vectorized computer, the blocking of elements is already a required task, we have combined this task with the assignment of time steps so that each sub-domain is assigned a time step automatically.

MIXED TIME INTEGRATION ALGRM

1. set initial cond's. : $\underset{\sim}{u}^0$, $\dot{\underset{\sim}{u}}^{-1/2}$, $n=0$, $n_{cyc}=0$

2. initialize clocks

   $t_{MAST} = 0$ master time

   $t_B = 0$ $B = 1, NB$ element block times

   $t_N = 0$ $N = 1, N_{node}$ nodal times

3. element block loop

   zero $\underset{\sim}{f}^{int}$; for $B = 1$ to NB

   if $t_B \leq t_{MAST}$

   update stress, $\underset{\sim}{T}^{n+1}$ for $e \in B$

   update $\underset{\sim}{f}_e^{int} = \int_{\Omega_e} \underset{\sim}{B}^T \underset{\sim}{T}^{n+1} d\Omega$

   gather $\underset{\sim}{f}^{int} \leftarrow \underset{\sim}{f}_e^{int}$

   if $n_{cyc} = 0$, compute Δt_G

   $t_G \leftarrow t_G + \Delta t_G$

4. nodal integration loop, $N = 1, N_{node}$

   if $n_{cyc} = 0$, set Δt_N

   if $t_N \leq t_{MAST}$

   update $\underset{\sim}{v}_N$, $\underset{\sim}{u}_N$, $t_N \leftarrow t_N + \Delta t_N$

5. $n_{cyc} \leftarrow n_{cyc} + 1$, $n \leftarrow n+1$; if $n_{cyc} = n_{cyc}^{max}$ then $n_{cyc} = 0$

SLIDE 7

SLIDE 7

This slide shows the flow of computations for a structural dynamics program with mixed time explicit integration. The major difference from the standard flow is that it is necessary to set up a number of clocks:

1. the master time, which governs the evolution of the problem;
2. the element block times, which indicate the time to which each of the element blocks has been updated;
3. nodal times (for each node), which indicate to what time the node has been updated.

The structure of the algorithm is almost identical to a standard nonlinear structural dynamics program, except for the fact that element groups and nodes are only updated when their clocks are behind the master time.

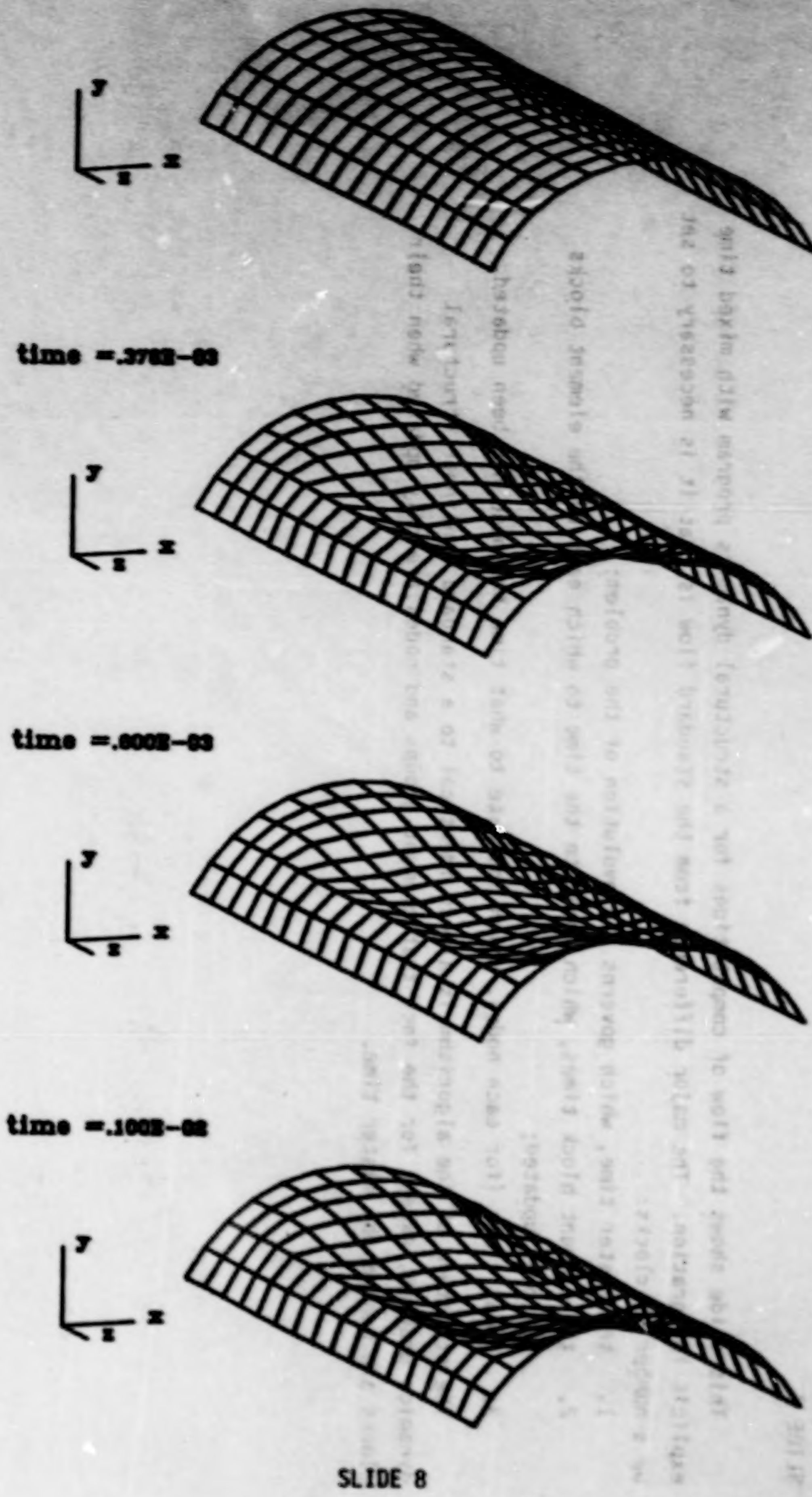

SLIDE 8

SLIDE 8

This is the first example we studied. It is an impulsively loaded cylindrical shell. The problem involves very large displacements and elastic-plastic response. It is solved with several meshes of quadrilateral shell elements. The shell elements are four-node elements with one-point quadrature and stabilization as described in "Explicit Algorithms for the Nonlinear Dynamics of Shells" (T. Belytschko, J. I. Lin, and C.-S. Tsay, Computer Methods in Applied Mechanics and Engineering, Vol. 42, 1984, pp. 225-251).

Table

Cylindrical Panel Timing Study (Seconds of CPU)

Program Version	Number of Processors	Mesh 1 96 elements	Mesh 2 384 elements			Mesh 3 1536 elements	
		12 ele/blk	24 ele/blk	32 ele/blk	48 ele/blk	32 ele/blk	192 ele/blk
Original WHAMS	1	347	2658			20860	
Original WHAMS with Compiler Optimization	8	141	1072			8484	
WHAMS-VECPAR	1	110	669	638	626	4891	4700
	2	66 (83%)	394 (85%)		380 (82%)	2937 (83%)	
	3	55	330		321		
	4	45	270	270	266	1994	2001
	5	44	268		265	1792	
	6	44	242		264	1709	1961
	7	45	240		265	1615	
	8	36 (38%)	231 (36%)	232	230 (34%)	1590 (38%)	1722

SLIDE 9

SLIDE 9

This gives various timings for the previously described problems. The rows labeled "Original WHAMS" pertain to timings on a version of this program which was not designed for concurrency or vectorization. This version of the program was run both with and without the compiler optimization on the Alliant FX/8. Note that in going from one to eight processors and compiler optimization, a speed-up of a factor only slightly greater than 2 was obtained. In the reprogrammed version, which is labeled "VECPAR", an improvement of 3 in running time is obtained in going from the original version of WHAMS. This speed-up is almost entirely due to taking advantage of <u>vectorization</u>. The increases in speed in going from one to eight processors are shown below that. Note that the speed-up in going to two processors is usually about 1.7, which is about 85% efficiency, whereas the speed-up in going to eight processors is only about a factor of 3, which indicates an efficiency of about 35%. Note that as the size of the blocks is increased, computer running time decreases, which indicates the speed-up due to vectorization.

Table

Timings for Containment Vessel Problem
with and without Mixed Time Integration (in sec CPU)

Program Version	Number of Processors	Single Δt	Mixed Time Integration			
		43 ele/blk	8 ele/blk	11 ele/blk	22 ele/blk	43 ele/blk
Original WHAMS	1	1325				
Original WHAMS with Compiler Optimization	8	538				
WHAMS-VECPAR	1	275			168	183
	2	171			101	115
	3	145			83	97
	4	122			71	79
	5	122			64	78
	6	122			61	78
	7	123			61	72
	8	108	63	52	59	67

SLIDE 10

SLIDE 10

This problem, which is labeled a containment problem, contains elements of various sizes, so it can be used to exmaine the effects of mixed time integration. The table contains timings for runs with both a single time step and mixed time integration. As in the previous problem, there is a significant improvement in the vectorized version of the program: running time on a single processor diminishes from 1325 seconds to 275 seconds. As the number of processors is increased in the VECPAR version, the incremental efficiency of additional processors diminishes somewhat. Again, speed-up of about 1.7 is obtained in going to two processors, and a factor of about 2.7 is obtained in going to eight processors. The speed-up in mixed time integration depends on the size of the element block and is actually somewhat better for small element blocks. There are two reasons for the increase in time with increasing element block size.

1. With increasing element blocks, idle time increases.
2. Since the time steps are automatically allocated to each block, the average time step for the blocks decreases when they are larger.

In comparing the single time step version of the original WHAMS with the single time step version of WHAMS-VECPAR, we see an improvement of a factor of 5 in running time. Adding mixed time integration provides another factor of 2, so the current work has been able to yield a twentyfold improvement in running time in this problem.

CONCLUSIONS

- REPROGRAMMING IS NECESSARY TO TAKE ADVANTAGE OF VECTORIZATION AND CONCURRENCY -- IT HAS YIELDED 10-FOLD SPEED INCREASE IN ALLIANT FX/8
- MIXED TIME INTEGRATION HAS SPEEDED UP EXECUTION BY 2
- VECTORIZATION AND CONCURRENCY ARE DIFFICULT TO EXPLOIT SIMULTANEOUSLY

SUGGESTED WORK

- IMPLEMENTATION OF NEW MIXED TIME INTEGRATION WITH NONINTEGER RATIOS
- ITERATIVE IMPLICIT METHODS
- INCORPORATION IN TEST BED

SLIDE 11

SLIDE 11

We list our conclusions and suggestions for future work.

A major new development would be to extend the method for mixed time integration so that the ratios of adjacent time steps need not be integer values. This would yield further speed-ups in the technique. We are also interested in implementing iterative methods on vectorized, concurrent machines because they pose similar scheduling-allocation problems, but the payoffs are substantial.

PUBLICATIONS SUPPORTED BY GRANT

P. Smolinski, T. Belytschko and M. Neal, "Multi-Time Step Integration Using Nodal Partitioning," to appear, International Journal for Numerical Methods in Engineering.

T. Belytschko and N. Gilbertsen, "Concurrent and Vectorized Mixed Time, Explicit Nonlinear Structural Dynamics Algorithms," to appear, Proceedings of Symposium on Parallel Computations and Their Impact on Mechanics, ed. A. K. Noor, ASME, New York, 1987; also submitted to Computer Methods in Applied Mechanics and Engineering.

T. Belytschko and M. Neal, "A New Mixed Time Integration Method for Structural Dynamics," in preparation.

PRESENTATIONS

T. Belytschko, N. Gilbertsen and J. M. Kennedy, "Explicit Time Integration Finite Element Codes Adapted to Parallel Computers"

- - Invited paper presented at Session on Computer Codes and Methods, 9th International Conference on Structural Mechanics in Reactor Technology, Lausanne, Switzerland, August 17-21, 1987.

T. Belytschko and N. Gilbertsen, "Concurrent and Vectorized Mixed Time, Explicit Nonlinear Structural Dynamics Algorithms"

- - Paper to be presented at Symposium on Parallel Computations and Their Impact on Mechanics, 1987 ASME Winter Annual Meeting, Boston, Massachusetts, December 13-18, 1987.

N89
29808
UNCLAS

CONCURRENT ALGORITHMS FOR TRANSIENT FE ANALYSIS

by

M. Ortiz

Brown University
Division of Engineering
Providence, RI 02912

and

B. Nour-Omid

Mechanics and Materials Lab.
Lockheed Palo Alto Research Lab.
Palo Alto, CA 94304

'CUT AND PASTE' ALGORITHMS

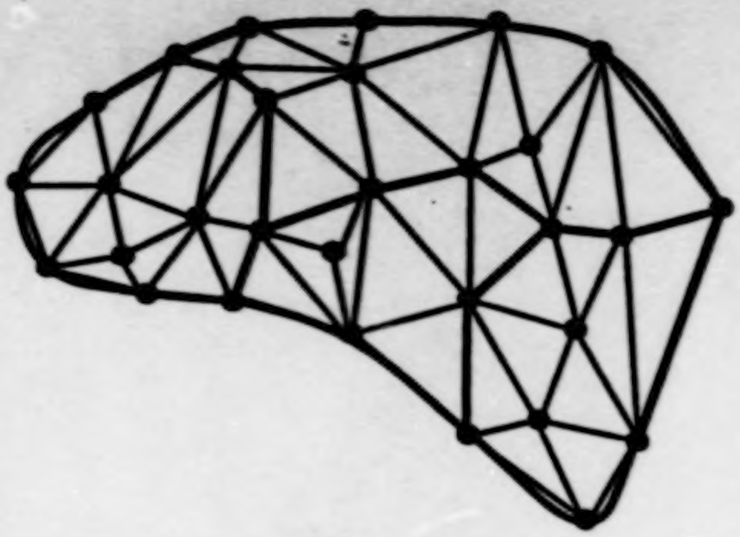

MODEL STRUCTURE

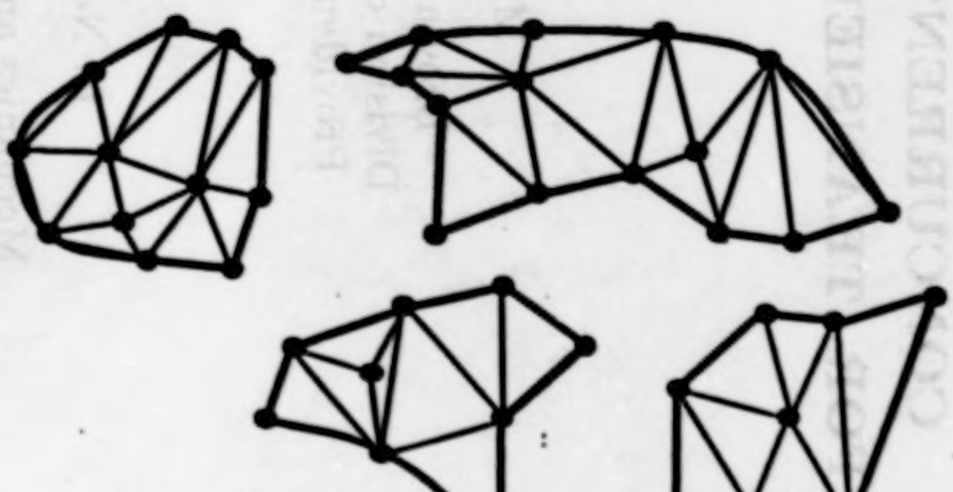

THE STRUCTURE VIEWED AS A COLLECTION OF
DISCONNECTED SUBSTRUCTURES

A 'CUT AND PASTE' ALGORITHM

- Predictor phase:

$$\tilde{\mathbf{d}}_{n+1} = \mathbf{d}_n + \Delta t \mathbf{v}_n + (1/2 - \beta)\Delta t^2 \mathbf{a}_n$$
$$\tilde{\mathbf{v}}_{n+1} = \mathbf{v}_n + (1 - \gamma)\Delta t \mathbf{a}_n$$

- Equation solving phase:

$$\mathbf{a}_{n+1} = \mathbf{0}$$
$$\textit{for } s = 1, NS \textit{ do}$$
$$\tilde{\mathbf{a}}^s_{n+1} = -(\mathbf{M}^s + \beta\Delta t^2 \mathbf{K}^s)^{-1}\mathbf{K}^s \tilde{\mathbf{d}}^s_{n+1}$$
$$\mathbf{a}_{n+1} = \mathbf{a}_{n+1} + \mathbf{M}^s \tilde{\mathbf{a}}^s_{n+1}$$
$$\mathbf{a}_{n+1} = \mathbf{M}^{-1}\mathbf{a}_{n+1}$$

- Corrector phase:

$$\mathbf{d}_{n+1} = \tilde{\mathbf{d}}_{n+1} + \beta\Delta t^2 \mathbf{a}_{n+1}$$
$$\mathbf{v}_{n+1} = \tilde{\mathbf{v}}_{n+1} + \gamma\Delta t \mathbf{a}_{n+1}$$

Definition of concurrent dynamic algorithms. Note three-phase structure similar to that of Newmark's method. Equation solving phase involves subdomain factorizations only. Local accelerations are mass-averaged at the subdomain boundaries.

INTERPROCESSOR COMMUNICATIONS

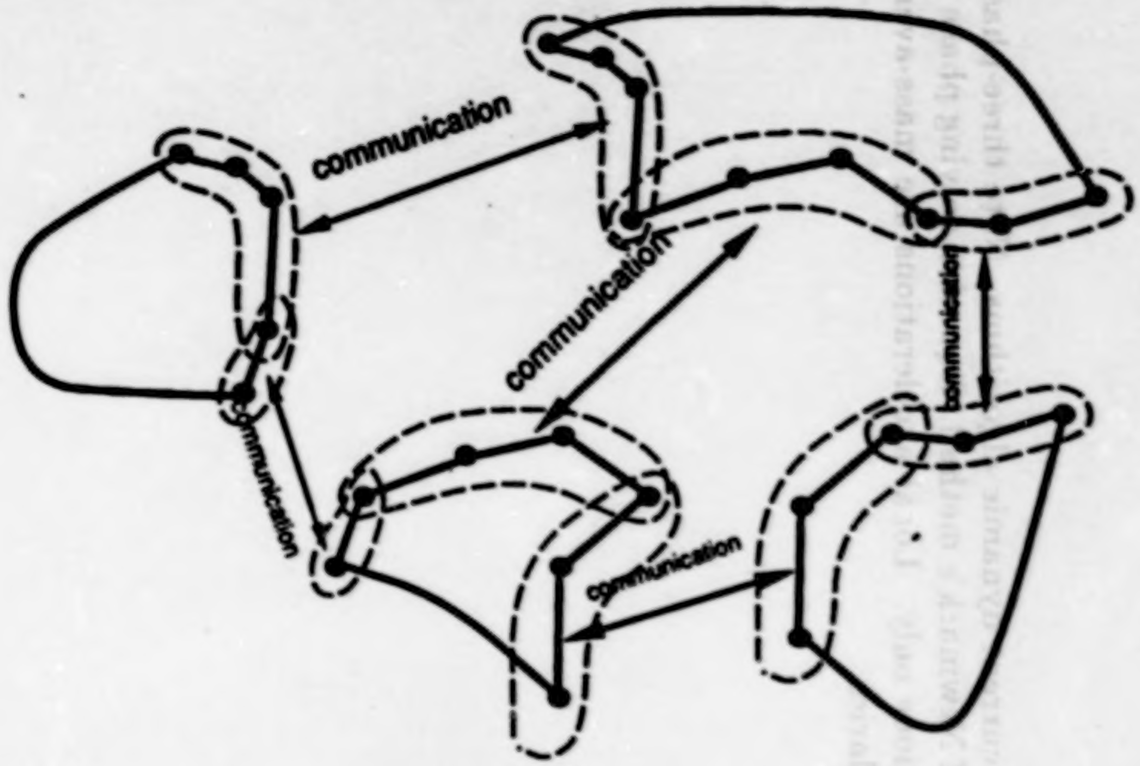

REDUCED SUBSTRUCTURES SHOWING THE COMMUNICATION DUE TO SHARED DEGREES OF FREEDOM.

OVERVIEW OF GENERAL PROPERTIES

- Parameters:

n = Number of dof in structure.
s = Number of element groups.
p = Number of processors.
i = Number of interface dof.

- General properties:

i) Newmark's method is obtained for $s = 1$.

ii) Unconditional stability for all s and $\gamma \geq 1/2$, $\beta \geq \gamma/2$.

iii) Full concurrency on a p-processor machine ($p \leq n$) except for $O(i)$ operation (mass-averaging).

iv) For given accuracy and $n/s \to \infty$,

$$SPEED-UP = \begin{cases} O(p\sqrt{s}), & (2D) \\ O(ps), & (3D) \end{cases}$$

PRECEDING PAGE BLANK NOT FILMED

PAGE 1073 INTENTIONALLY BLANK

General properties. Note two-parameter dependence of speed-up estimates on both the number of processors and the number of subdomains.

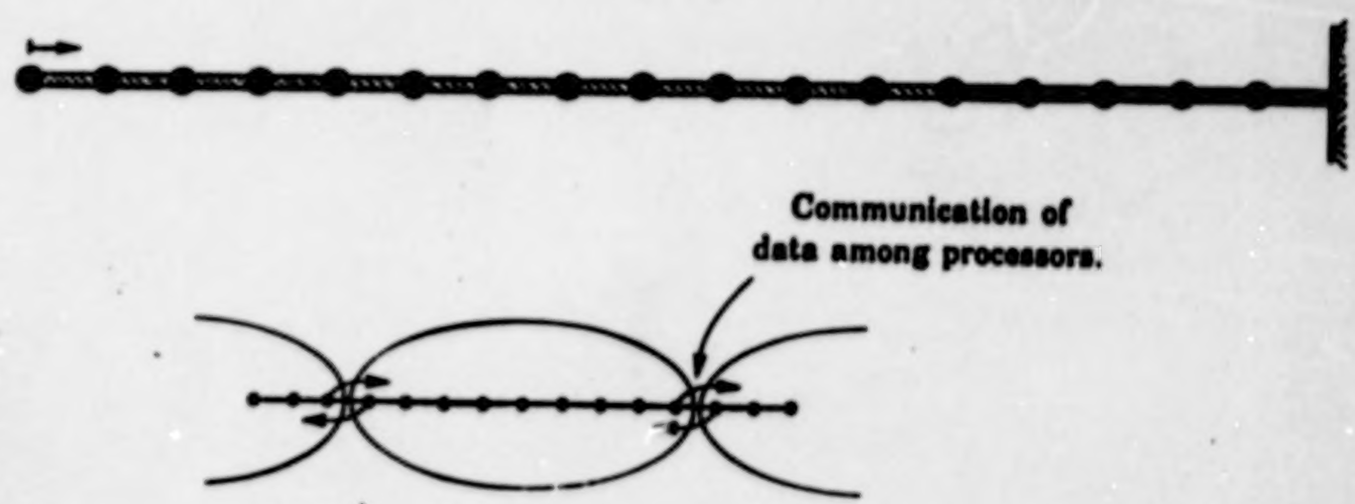

Figure 3. Discretization and partition of the bar problem.

One-dimensional test for assessing communication efficiencies.

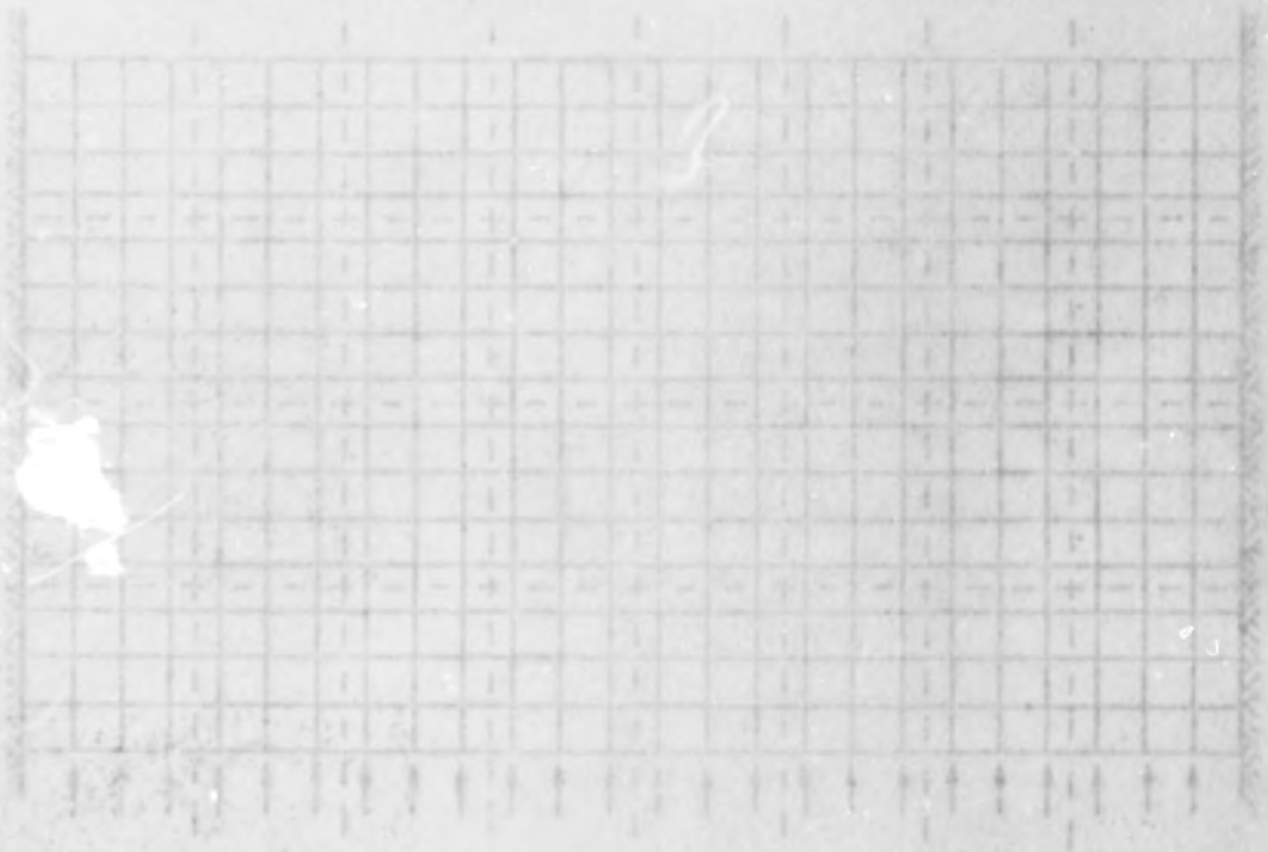

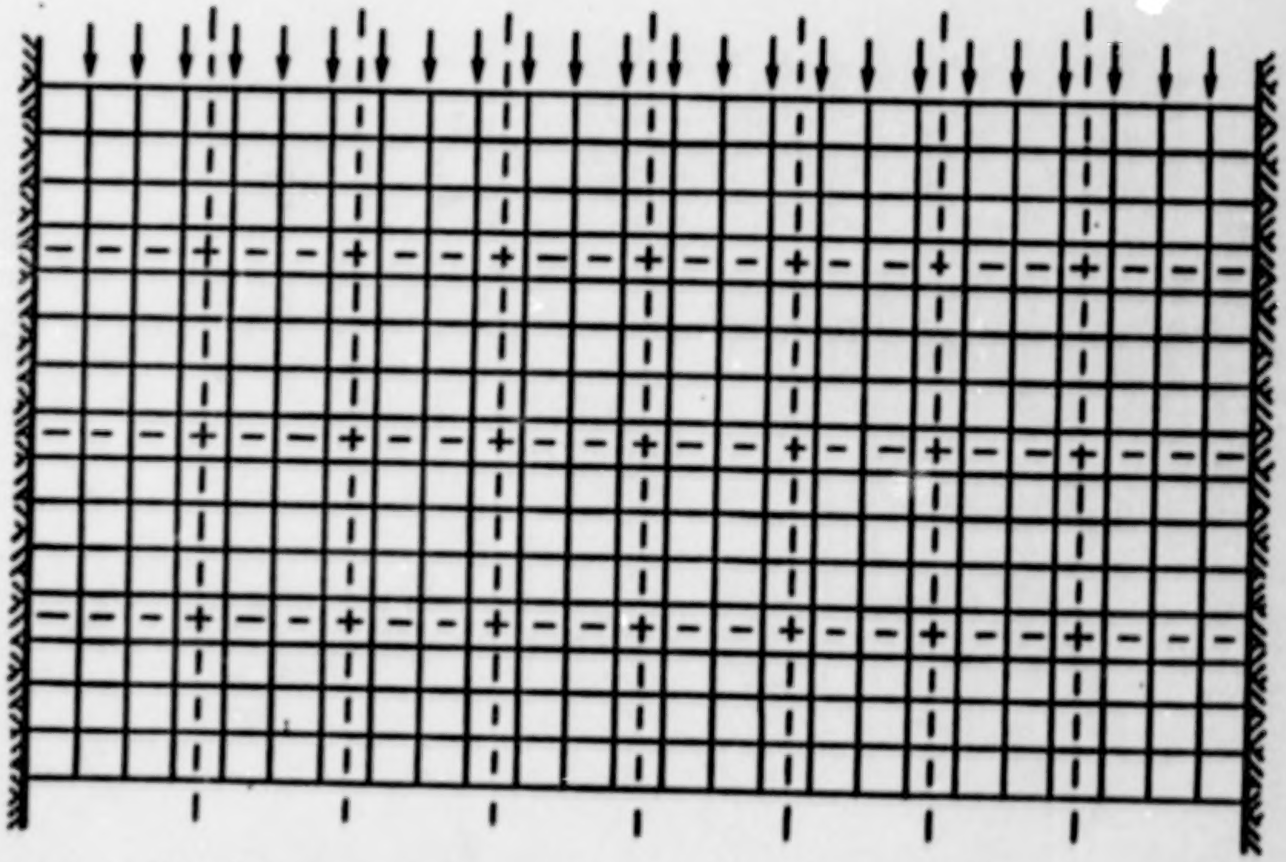

Figure 4. Discretization and partition of the plane stress problem on a 32-processor computer.

Two-dimensional test for assessing communication efficiencies.

N	Computation time (milisec.)	Communication time (milisec.)	efficiency %	Rate Mflop
64	1.47	0.46	76.32	0.233
96	2.20	0.46	82.86	0.253
160	3.67	0.46	88.96	0.271
288	6.61	0.46	93.55	0.285
544	12.49	0.46	96.48	0.294

Table 5. Performance of the Bar problem on the 32 Processor Hypercube.

No. of Elements	Computation time (milisec.)	Communication time (milisec.)	efficiency %	Rate Mflop
128	25.2	7.8	76.3	0.232
288	57.1	8.6	87.0	0.265
800	161.3	10.6	93.9	0.286
2592	530.9	14.6	97.3	0.297
9248	1915.2	22.6	98.8	0.301

Communication efficiencies for 1-D and 2-D test cases. Note efficiencies approaching 99.

COMPUTATIONAL EFFICIENCY

- $COST \approx \frac{1}{2}nb^2 + 2nb$, (b = semi-bandwidth)
- Square mesh, l^2 elements:

$$GLOBAL \approx \frac{1}{2}(l+2)^2(l+1)^2 + 2(l+2)(l+1)^2$$

- Partitioned mesh, $s = m^2$ subdomains:

$$PARTITIONED \approx$$

$$s\left[\frac{1}{2}\left(\frac{l}{m}+2\right)^2\left(\frac{l}{m}+1\right)^2 + 2\left(\frac{l}{m}+2\right)\left(\frac{l}{m}+1\right)^2\right]$$

- Equation solving speed-up ($n/s \to \infty$):

$$SPEED-UP(2D) = \frac{GLOBAL}{PARTITIONED} \approx O(s)$$

$$SPEED-UP(3D) = \frac{GLOBAL}{PARTITIONED} \approx O(s^{4/3})$$

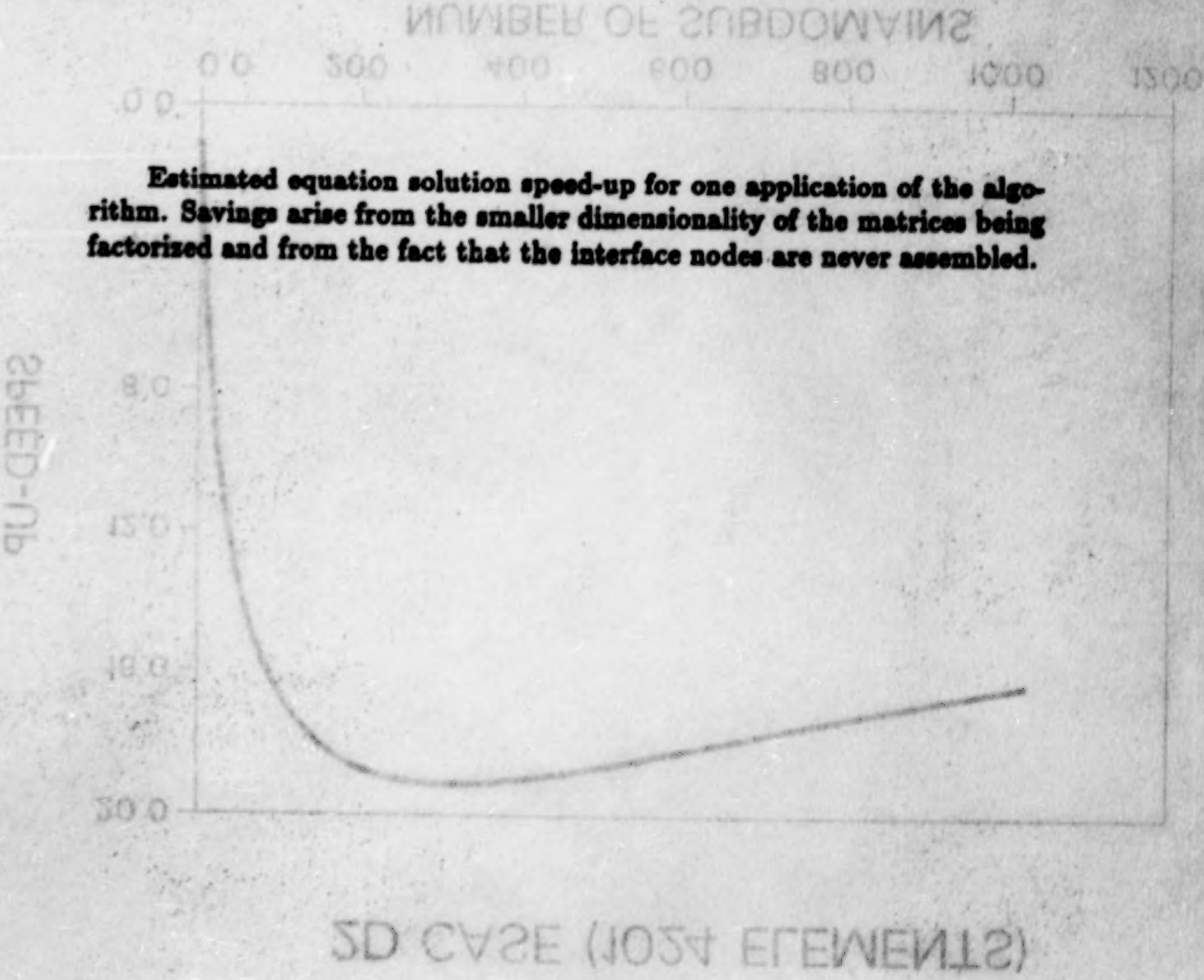

Estimated equation solution speed-up for one application of the algorithm. Savings arise from the smaller dimensionality of the matrices being factorized and from the fact that the interface nodes are never assembled.

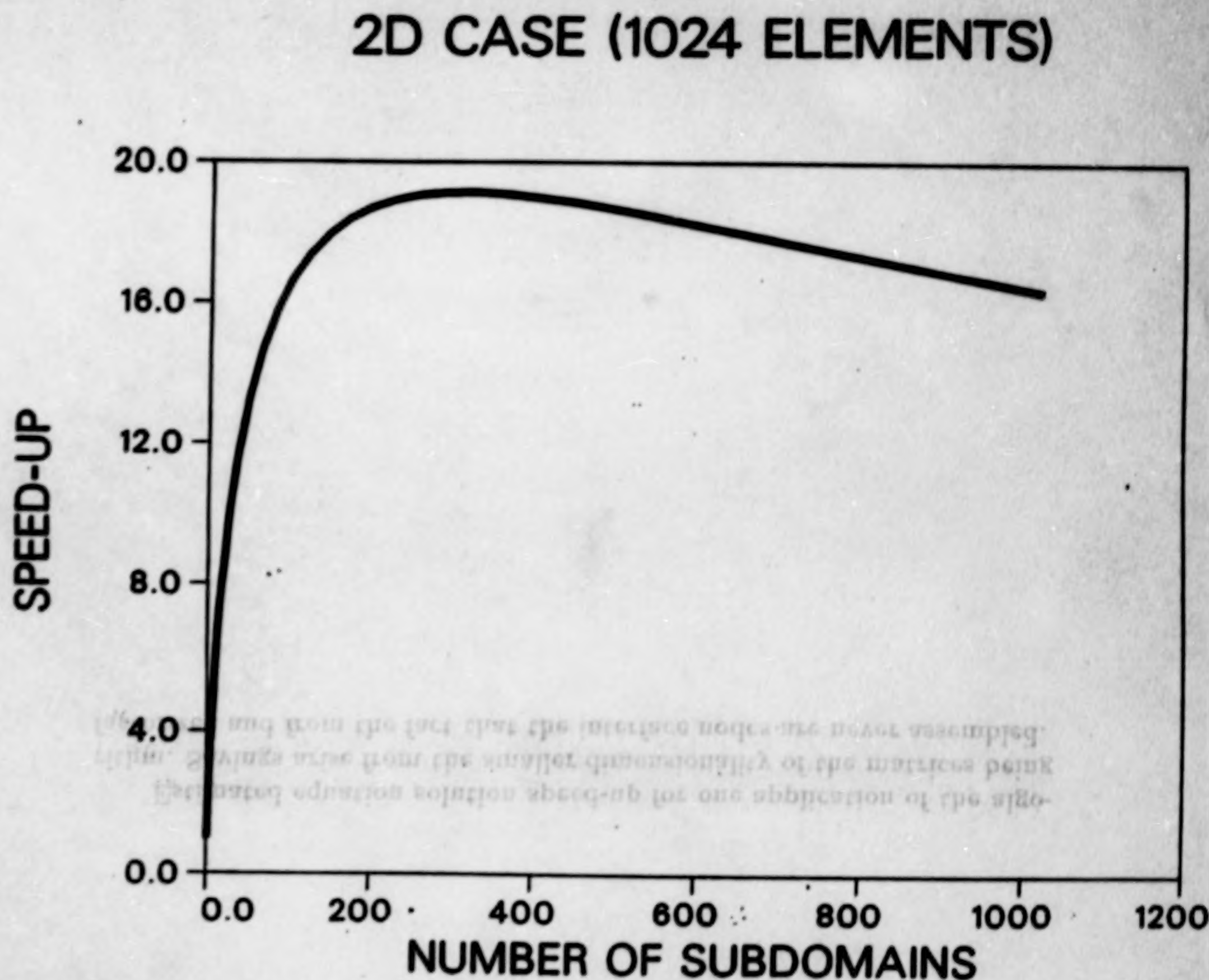
2D CASE (1024 ELEMENTS)
SPEED-UP
20.0
16.0
12.0
8.0
4.0
0.0
0.0
200
400
600
800
1000
1200
NUMBER OF SUBDOMAINS

Estimated equation solution speed-up for one application of the algorithm vs. number of subdomains, 2-D case.

3D CASE (4096 ELEMENTS)

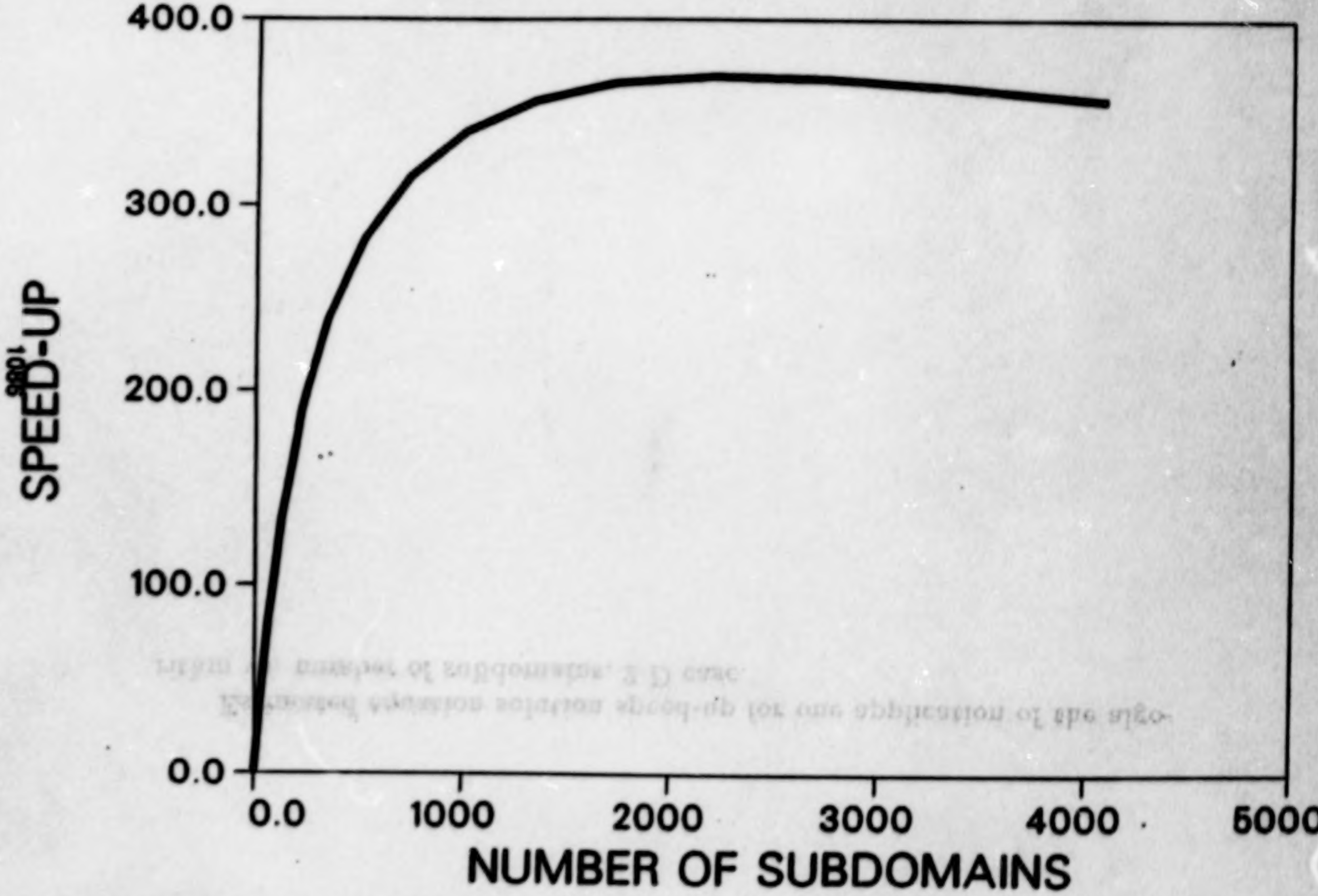

Estimated equation solution speed-up for one application of the algorithm vs. number of subdomains, 3-D case.

ACCURACY ANALYSIS

- Algorithmic phase errors, 1D case:

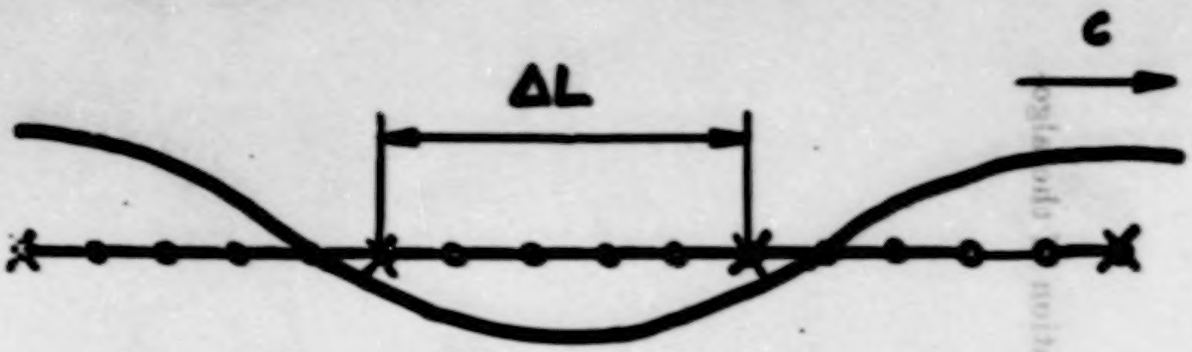

- Maximum celerity of computed waves

$$c_{max} = \Delta L/\Delta t$$

$\Delta L \equiv$ subdomain size

- For accurate results, need to take

$$c_{max} \geq c, \qquad OR \quad \Delta t \leq \Delta L/c$$

$c \equiv$ wave celerity

Accuracy requirements derived from an analysis of phase errors in one dimension. Note the Courant-type condition on the time step to preserve the level of accuracy as the size of the subdomains is increased.

ACCURACY REQUIREMENTS

- Square mesh, $s = m^2$ subdomains:

$$\Delta L = L/m \approx O(1/\sqrt{s})$$
$$\Delta t \leq \Delta L/c = L/mc \approx O(1/\sqrt{s})$$

- Net speed-up ($p = 1$):

$$SPEED - UP(2D) \approx O(s) \times O(1/\sqrt{s}) = O(\sqrt{s})$$

- Cubic mesh, $s = m^3$ subdomains:

$$\Delta L = L/m \approx O(1/s^{1/3})$$
$$\Delta t \leq \Delta L/c = L/mc \approx O(1/s^{1/3})$$

- Net speed-up ($p = 1$):

$$SPEED - UP(3D) \approx O(s^{4/3}) \times O(1/s^{1/3}) = O(s)$$

Estimated equation solution speed-ups for a square mesh in large scale nonlinear computations, for a prescribed level of accuracy. The net speed-up is computed by taking into account both the savings in equation solving afforded by the method as well as the reduction in time step necessary to keep the level of accuracy unchanged as the number of subdomains is increased.

NUMERICAL TESTS

- Square membrane, simply supported, subjected to uniform initial velocity.
- Finite deflection FE formulation. Triangular elements:

$$W = \frac{T}{2}\frac{A^2}{A_0}$$

T = tension
A_0 = initial area of triangle
A = deformed area.

- Quadrilateral elements:

- Parameters: $L = 2$, $T = 1$, $\rho = 1$.
- Error measure:

$$ERROR = \left[\int_0^T \mid w(t) - w_{exact}(t) \mid^2 \frac{dt}{t^2}\right]^{1/2}$$

UNIFORM IMPACT ($\beta = 0.25$, $\gamma = 0.5$)

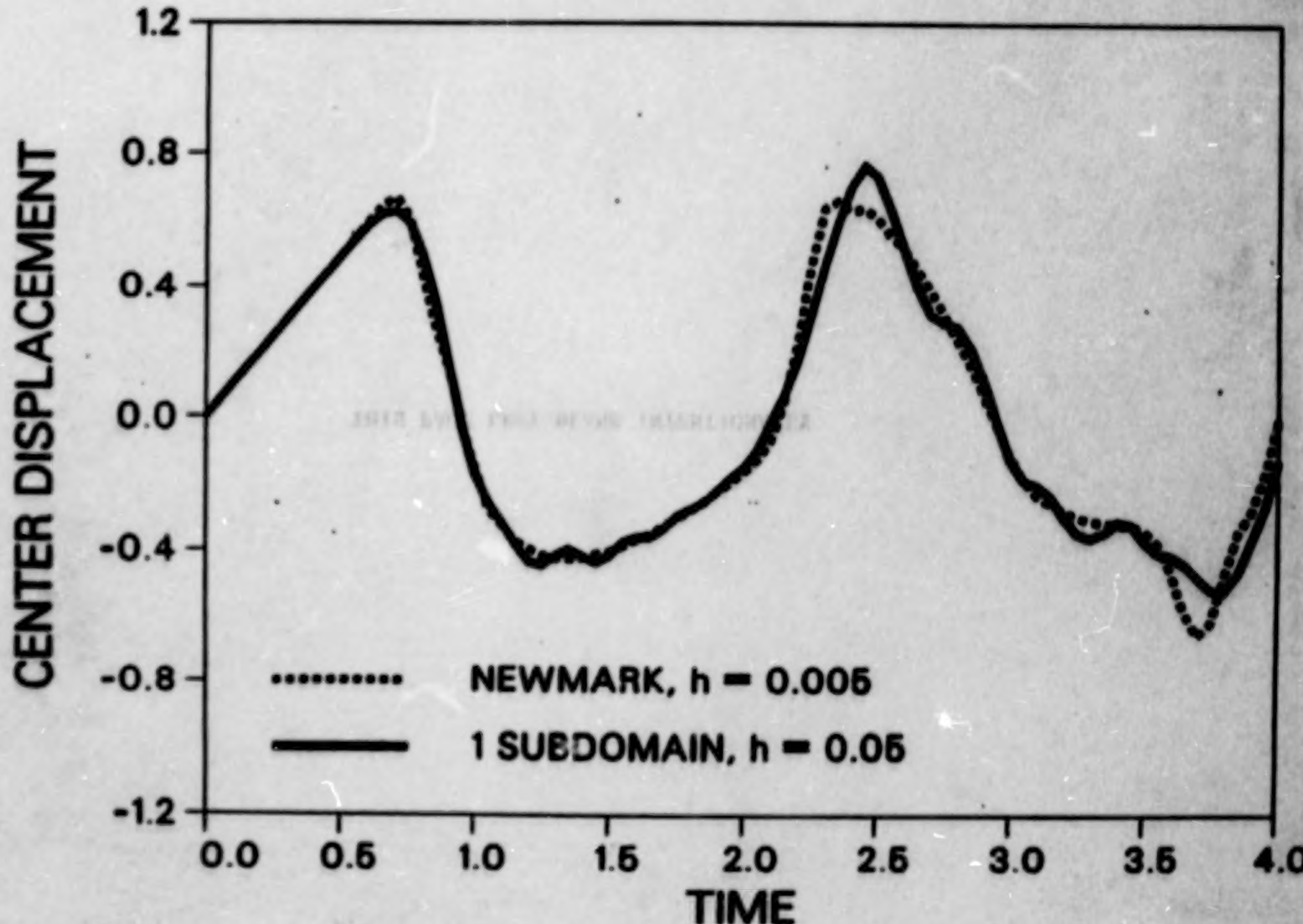

PAGE 1093 INTENTIONALLY BLANK

PRECEDING PAGE BLANK NOT FILMED

UNIFORM IMPACT ($\beta = 0.25$, $\gamma = 0.5$)

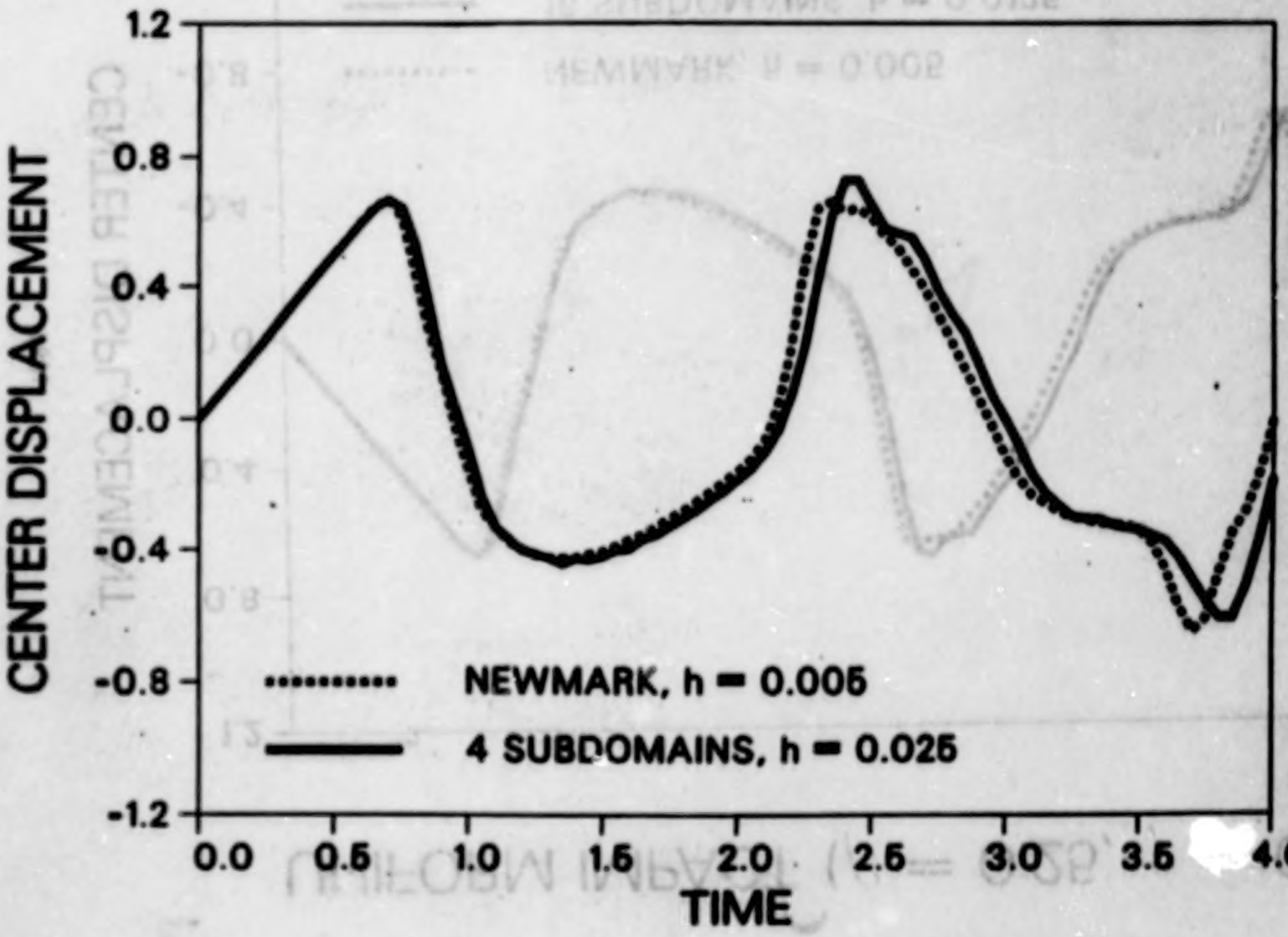

UNIFORM IMPACT ($\beta = 0.25, \gamma = 0.5$)

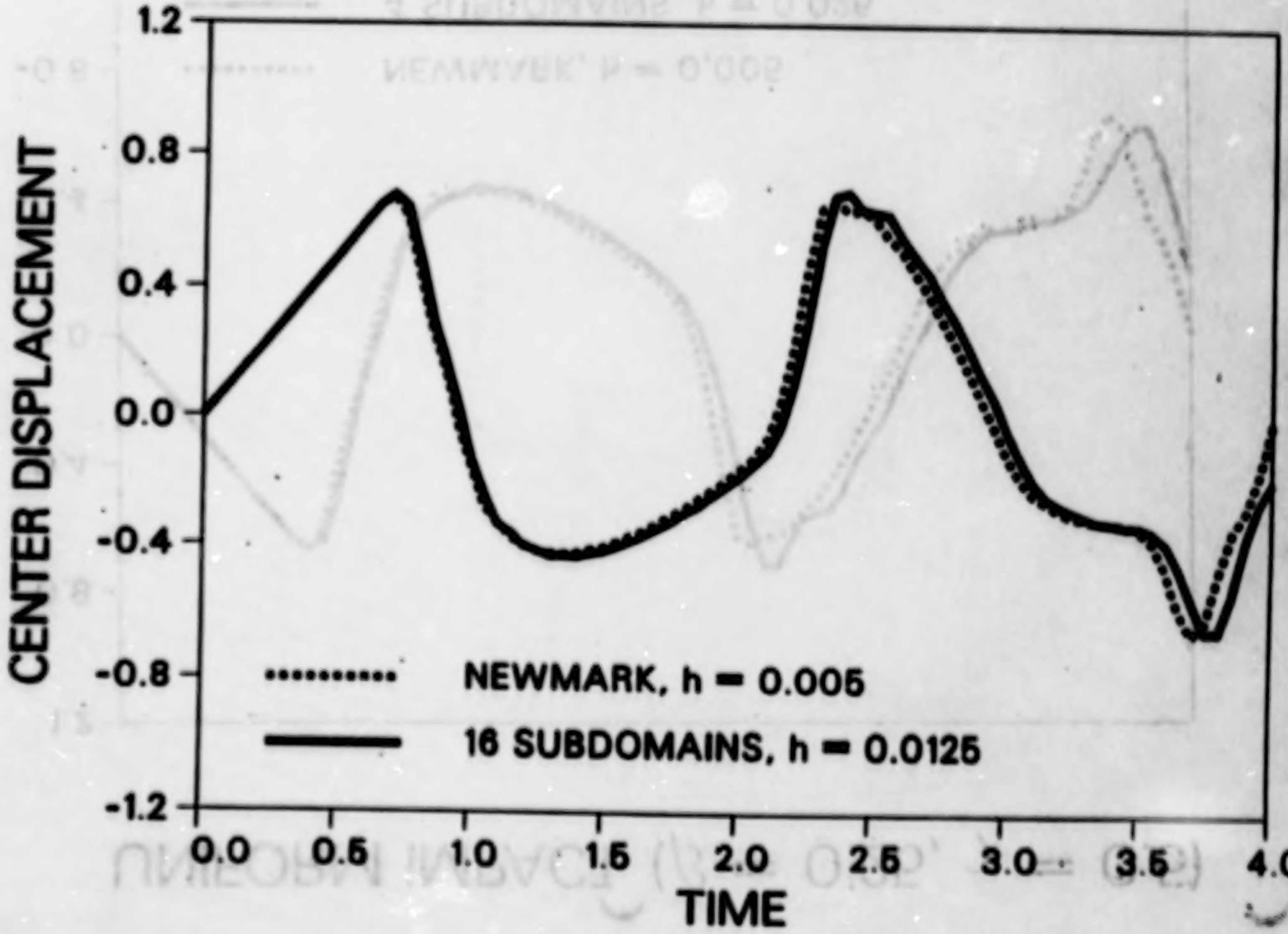

UNIFORM IMPACT ($\beta = 0.25$, $\gamma = 0.5$)

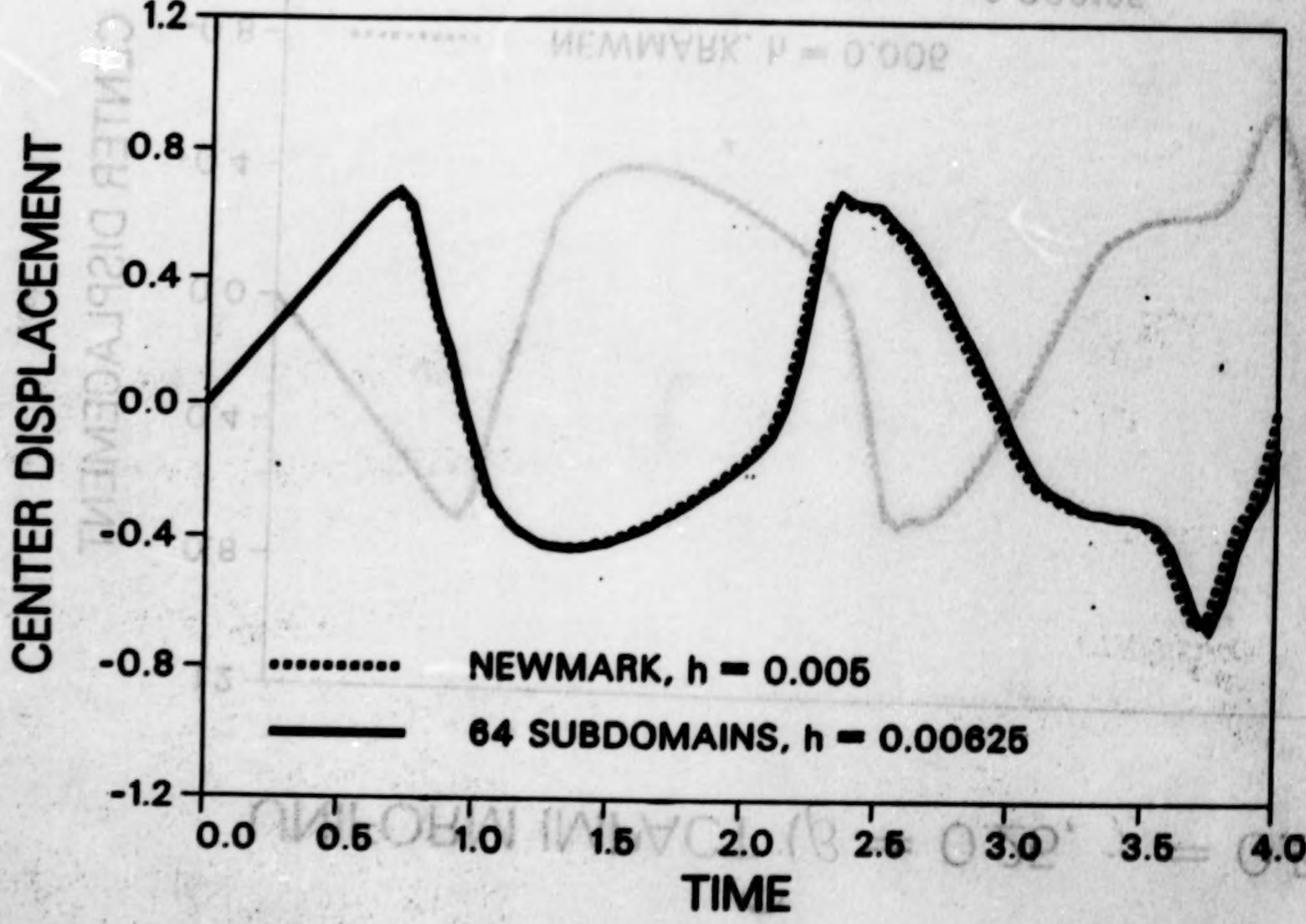

UNIFORM IMPACT ($\beta = 0.25$, $\gamma = 0.5$)

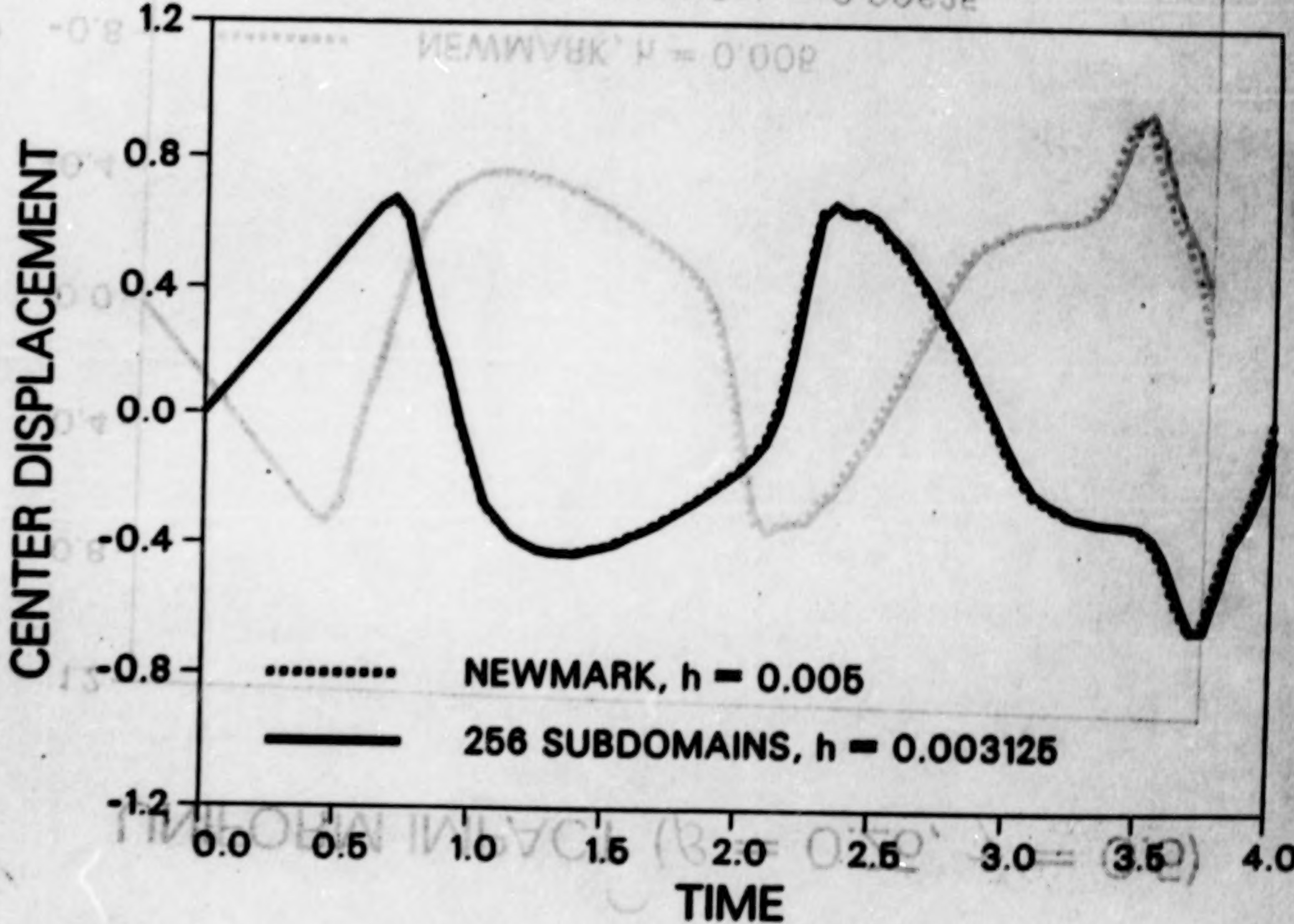

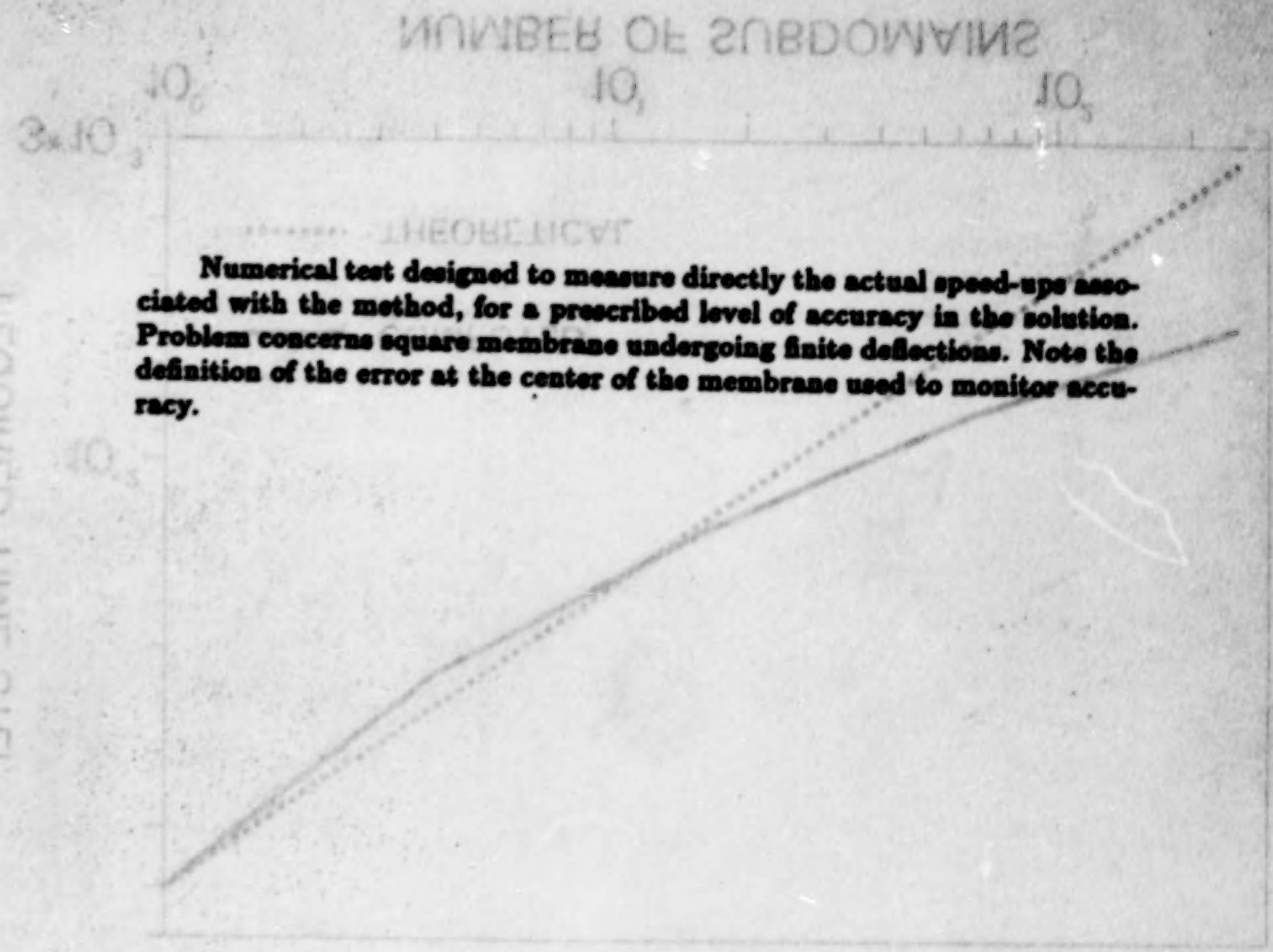

Numerical test designed to measure directly the actual speed-ups associated with the method, for a prescribed level of accuracy in the solution. Problem concerns square membrane undergoing finite deflections. Note the definition of the error at the center of the membrane used to monitor accuracy.

ACCURACY REQUIREMENTS

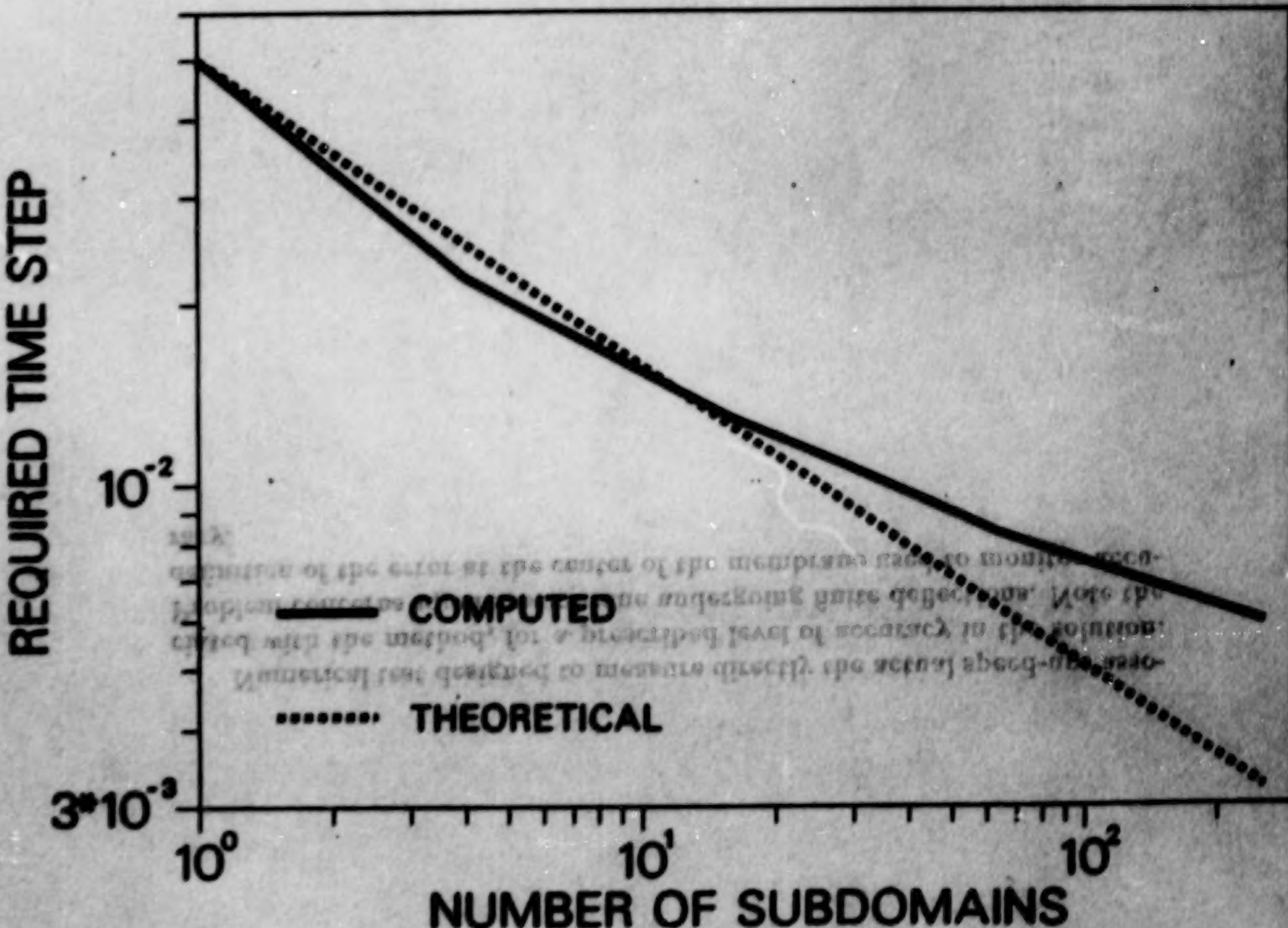

Actual vs. estimated time step requirements as a function of number of subdomains. Theoretical time steps follow from the Courant-type accuracy condition. Actual requirements are determined by monitoring accuracy directly in square membrane test.

SINGLE-PROCESSOR SPEED-UPS

1024 ELEMENT CASE			
NSUB	Secs.	Speed-up	Theory
1	1143	1	1
4	776	1.47	2
16	521	2.19	4
64	326	3.51	8
256	156	7.31	16

Actual vs. estimated speed-ups for square membrane problem on a single processor. Timings correspond to the equation-solving phase only. Time steps were chosen so as to obtain the same level of accuracy from all runs.

N89
29809
UNCLAS

N89-29809

S10-39
26P.
211977
CU 508845

COMPUTATIONAL METHODS AND SOFTWARE SYSTEMS FOR DYNAMICS AND CONTROL OF LARGE SPACE STRUCTURES

K. C. Park, C. A. Felippa, Charbel Farhat
J. D. Downer, J. C. Chiou and W. K. Belvin†
Center for Space Structures and Controls, Campus Box 429
College of Engineering and Applied Science
University of Colorado, Boulder, CO 80309

ABTRACT

The deployment, assembly and mission-oriented maneuvering of space structures in orbit will trigger large motions of flexible, truss-type structures. In addition, the presence of on-board controls both for attitude stabilization and specified vibration tolerance requirements may further complicate the dynamic behavior of the orbiting structures. Because of safety and cost considerations, the dynamic response of the combined structural and control systems must be predicted reliably. This need can only be met through the development of reliable and efficient simulation capabilities, since there is general agreement that on-orbit experiments should be limited because of cost, time and facility constraints.

The long-term objective of this research effort is to develop *a next-generation computer simulator* for the dynamics and control of large space structures. The simulator will be based on integrating four research thrusts: a new multibody dynamics formulation methodology, modeling capabilities in long/slender truss-beam components with realistic joints, efficient computational procedures that can be implemented either in sequential or concurrent computers, and prototype simulation modules that can be easily processed into a modern large-scale engineering software system such as the NASA/CSM testbed.

Computational Structural Mechanics (CSM)

†On academic leave from Structures and Dynamics Division, NASA/Langley Research Center.

RESEARCH THRUST

Logn-Term Research Thrust:

- **Develop a Next-Generation Computational Capability for Dynamics and Control of Large Space Structures.**

Current Research Thrusts:

- **Dynamics of Flexible Beams for Large Motions**
- **Computational Methods for Large Rotational Motions and Constraints**
- **Design of a *CONCURRENT* NICE (C-NICE) Architecture.**
- **Concurrent Computations via FORCE on CRAY-II and Alliant**

Center for Structures and Controls, University of Colorado, Boulder, CO

CURRENT RESEARCH THRUSTS

In order to accomplish the research objectives set forth, we have carefully defined the scope of the present research effort as follows.

1. A multibody dynamics formulation that can represent combined large rigid and flexible motions, and that incorporates an objective way of modeling beams in hierarchical order from Euler-Bernoulli elements to bending-transverse shear and bending-torsion coupling.

2. A set of computational procedures that can treat large rotational motions, kinematic and dynamic constraints, contact-impact phenomena and computational stabilization for momentum and energy conservation, when necessary; these procedures must be able to perform well under both sequential and parallel computing environments.

3. A prototype *concurrent* NICE that preserves the program modularity between the processors and data management tasks and that allows the adoption of loosely coupled multiprocessors so as to achieve a smooth adaptation to parallel computing of processors developed under the sequential computing environment.

4. Implementation of the above three capabilities into a research-mode processor and validation of the module by the use of FORCE on Alliant and CRAY-II.

OVERALL RESEARCH APPROACH

- Emerging Computer Hardware and Software Transportability Should Dictate Software Architecture Design and Implementation.
- Software Architecture Advances Should Influence New Formulations and New Methods Development.
- Needs for New Capability and its Implementability Should Guide New Formulations *From the Outset.*
- Software Modularity Should Be a Key Aspect of Methods Development.

Center for Structures and Controls, University of Colorado, Boulder, CO

PRECEDING PAGE BLANK NOT FILMED

PAGE 1108 INTENTIONALLY BLANK

Overall Approach

(An Experiment in A University Setting)

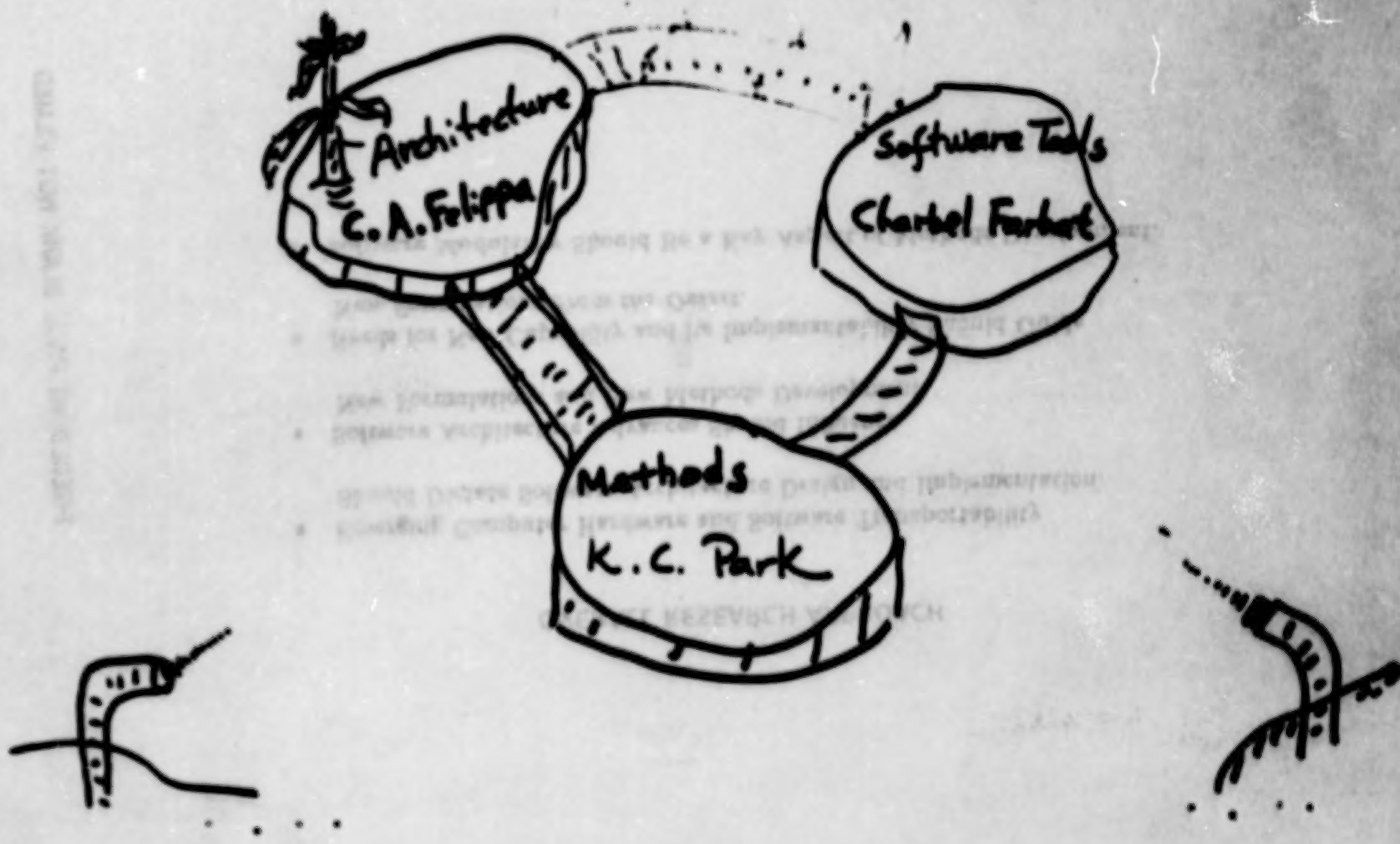

OVERALL RESEARCH APPROACH

In traditional structural mechanics research, the needs for new/improved analysis capabilities are first identified. Next, the necessary formulations are carried out. The methods development is then undertaken to implement the formulations. Finally, the implemented programs are made available to the analyst for testing and applications.

In our approach to computational structural mechanics, we establish the needs for new/improved analysis capabilities. In our case, it is a general multibody dynamics and control simulation capability for parallel computers. First, we survey available analysis modules –i.e., direct time integration module. We then identify new software modules to be constructed. Only after decisions are made as to what new modules need to be developed, we will begin the necessary formulations and methods development.

Upon completion of new software modules, we then rely on a *command language* to integrate both the available and new software modules into a high-level analysis procedure. It is important that this procedure developments require both non-numerical and numerical algorithms. For example, many aspects of partitioned analysis procedures can be implemented during the procedure construction stage rather than in the analysis module development stage.

Center for Structures and Controls, University of Colorado, Boulder, CO

C-NICE: BACKGROUND

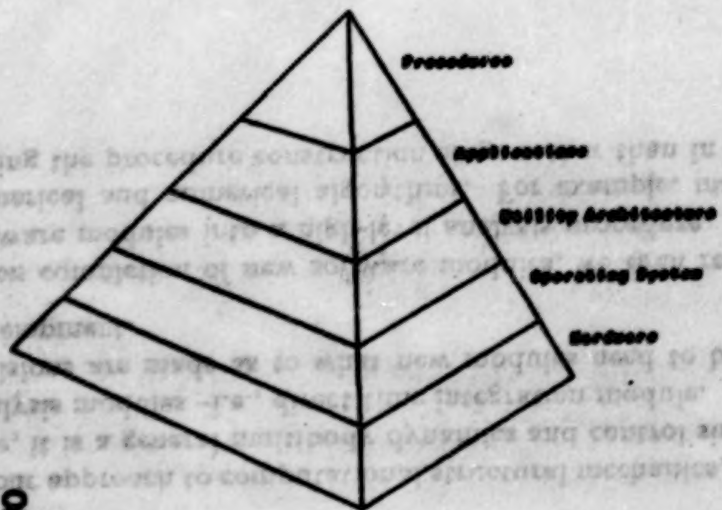

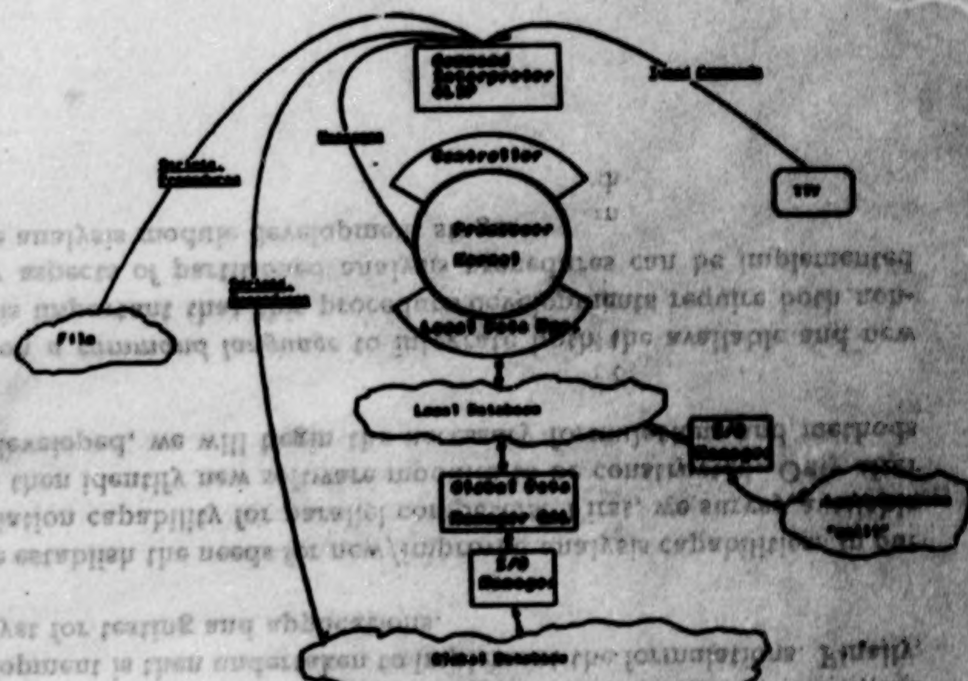

ORIGINAL PAGE IS
OF POOR QUALITY

Center for Space Structures and Controls, Univ. of Colorado, Boulder CO

C-NICE: BACKGROUND

An applications-software architecture may be visualized as a layer of software that helps the development of applications by "cushioning" the interface of the programs with the operating system (see Figure).

A utility architecture is supplied in the form of tools or products that may be used selectively. Utilities architectures are most effective when the tools are in the public domain and subject to scrutiny.

NICE is an utility architecture developed to support computational mechanics applications and in particular finite element computations. This architecture allows the development of individual program modules called processors, and the database coupling of processors to form program networks.

Motivation. The original development of NICE was prompted by the idea of combining the power of logically related but separate programs. The envisioned applications were product design, loosely-coupled research, and the analysis of coupled problems. Additional motivation now arising from concurrent computation is the need to carry out time-critical simulations.

Components of the NICE architecture that enforce network operational compatibility are the command language interpreter CLIP and the global database manager GAL (see Figure). On sequential machines this form of architecture is stable, well developed and gaining acceptance.

Concurrent NICE. The question arises as to the architectural support of large-scale finite element computations on the newer concurrent processing machines. The development of C-NICE addresses that question.

C-NICE: OBJECTIVE

- *General objective:* to develop generic tools for the implementation of application program networks on the next generation of concurrent supercomputers.

- *Specific objective:* to support the development of structural dynamics and controls programs for simulation of large space structures on existing multiprocessors.

C-NICE: APPROACH

- Implement finite element programs on new concurrent machine architectures that span a broad spectrum.

- Keep in mind a wide range of needs, including structural dynamics, controls, and other coupled field problems.

- Develop processor mapping and assignment methods, new data structures, programming language requirements.

- Assess performance, programming difficulties, project future developments.

- Define generic support tools, and make such tools part of the new utility architecture.

Center for Space Structures and Controls, Univ. of Colorado, Boulder CO

C-NICE: OBJECTIVE AND APPROACH

The objective of the architecture is to facilitate the development of applications in computational mechanics. Within this broad field we emphasize the simulation of finite-element-based dynamics and control of space structures on concurrent multiprocessors.

NICE-type architectures for finite element machines on sequential machines are well developed and gaining acceptance. The support of finite element computations on the new concurrent multiprocessors raises two questions: (1) Can the sequential machine architecture be suitably extended to encompass concurrent machines, and (2) Do we need a totally separate architecture for each machine type?

The approach taken is to try to extend selective components of the seqntial NICE architecture. A rewritten segment should (a) try to aniticipate "winners" in the concurrent machince race; (b) emcompass sequential computers naturally, and (c) be a significant improvement over the previous version even on sequential computers. Two components that would benefit substantially from a rewrite are the source code distribution utility MAX, and the input-output manager DMGASP. Therefore they were selected as the first two candidates for rewrite.

The expanded and revised MAX and DMGASP are called TIM and CPIO, respectively. TIM is a true source code preprocessor with knowledge about concurrent machine hardware and operating systems. CPIO is a concurrent paged I/O manager that can handle parallel I/O. Progress in these two components is summarised on the last slide.

Center for Space Structures and Controls, Univ. of Colorado, Boulder CO

C-NICE: PROGRESS

- *Source Code Preprocessor.* A generalized source code preprocessor, TIM, has been coded as a replacement to the NICE tool MAX. The input to TIM is a blocked file. TIM recognizes code blocks in Fortran 77, Force, CWEB and Assembly, TeX documentation blocks, data blocks and database records. It knows about 56 computer (8 concurrent ones) and several operating systems. It generates output file by interpreting very high level expressions (for example: the target system is Alliant) and macro substitution. Handles arbitrary logical expressions and macro substitution.

- *Concurrent Paged I/O Manager.* CPIO has been designed as a successor to the I/O Manager DMGASP of the NICE system. Accepts C and C++ data structures, and allows simultaneous access to logical devices. Logical devices may use parallel disk I/O. Implementation will be based on paged buffer pool serving concurrent processes. It should be also more efficient than the old IOM on sequential machines.

C-NICE: FUTURE PLANS

- *Finite Element Applications.* We shall continue experimentation on the Cray 2 multitasking computer at NASA Ames, helped by a Cray version of Harry Jordan's The Force preprocessor. We plan eventually to experiment with finite element calculations on the ETA10 (under CDC sponsorship) and the Connection machine (under NRL sponsorship).

- *Architecture Tools.* Document and release the TIM programming tool. Implement CPIO on Sun, Alliant, Cray 2/XMP MT, and the Connection Machine.

CONCURRENT FE COMPUTATIONS - PROGRESS

- **Development of a Practical Automatic FE Domain Decomposer.**
- **Development of a Coloring Scheme for Explicit Element-by-Element Computations.**
- **Procedures for Dynamic Re-Mapping of Processors.**
- **Design, implementation and testing of a complete prototype Concurrent Static FE Analyser using FORCE.**
- **Test versions available for:**
  Cray2 with UNICOS Multitasking
  Cray X-MP with UNICOS Multitasking
  Alliant FX/8
  Encore Multimax
  Sequent-Balance

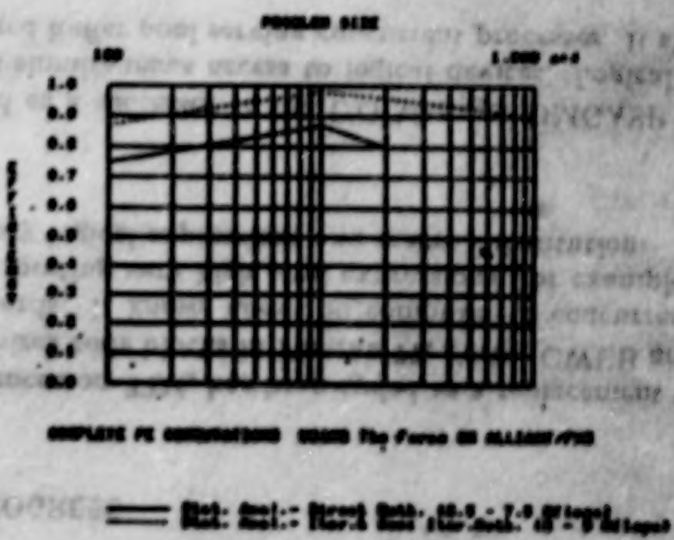

Center for Structures and Controls, University of Colorado, Boulder, CO

CONCURRENT COMPUTATIONS VIA 'FORCE' - PROGRESS

A software architecture that parallelises finite element computations in their totality has been designed and tailored to several different multicomputing environments. Based on the *divide* and *conquer* paradigm, the selected approach has shown the potential of handling various parallel numerical schemes for different purposes.

An automatic domain decomposer was designed and implemented on several multiprocessors. It meets three basic requirements: (1) it handles irregular geometry and arbitrary discretization pattern in order to be general-purpose; (2) it delivers a set of balanced subdomains in order to ensure that the overall computational load will be as evenly distributed as possible among the processors; (3) it minimises the amount of interface mesh nodes because these can become burdensome in communication and/or synchronisation requirements.

On a shared memory multiprocessor, internal boundary elements constitute a source of potential memory conflict during parallel computations that are carried out on the element level. To eliminate the need for serialising computations in these critical regions, a graph coloring type of algorithm was devised and applied to the interface of the subdomains. A general framework for parallel Element-by-Element explicit computations was also devised. Based on the coloring scheme mentioned above, it minimises the amount of *Critical Sections* and requires only one fork/join procedure per global iterative and/or time step.

In order to achieve load balance in fully nonlinear computations, two different processor mappings are combined and dynamically activated: (1) for the element level explicit computations and (2) for the global level implicit computations.

A prototype FE static code for shared memory super multiprocessors is now available. Several numerical algorithms were parallelised and revised to connect the software architecture with the finite element solution algorithms. These include an Active Column equation solver, a Block SOR Iteration, a Block Asymmetric Factorization, and a Preconditioned Conjugate Gradient algorithms. Vectorization is achieved within each concurrent process.

Portability of the code is guaranteed through "The Force"

Center for Structures and Controls, University of Colorado, Boulder, CO

RESEARCH APPROACH: Multibody Dynamics

- **Formulate Equations of Motion for System Components – Flexible Elements, Joints, Rigid Elements, Constraints, Control Systems.**

- **Develop Computational Algorithms for Large-Scale Computations of Each of the System Components.**

- **Develop Concurrent Partitioned Analysis Procedures for Overall Multibody Dynamics Analysis.**

- **Implement the Formulations, Solution Algorithms and Partitioned Analysis Procedures and Perform Large-Scale Simulation of System-Level Dynamics Problems.**

RESEARCH APPROACH: Multibody Dynamics

In the existing multibody formulations, the minimal achievable number of equations has been the driving factor in the derivation of the equtions of motion. For example, the *Order-N* formulation is a special form suited for open-loop connectivity. Such formulations necessarily require to integrate the constraints, joints, rigid elements *in their entirety* into the equations of motion. Such approach, while compact in the equations of motion and efficient for open-end manipulator dynamics, become unwieldy for deployment of lattice truss structures.

In the present approach, we formulate each of the multibody dynamics elements – flexible beams, joints, constraints, rigid bodies, and control forces– as a seperate entity. We separately solve the equations motion for beams, rigid elements, constraint forces and control forces. The system-level dynamic response is obtained by applying the partitioned analysis procedures. When found advantageous, we can reduce part of the system equations through system topology to a set of *Order-N* equations.

We believe that our approach is well suited not only for sequential computations while preserving software modularity but particularly appeals to parallel computations as each of the component solutions can be carried out in parallel.

Center for Structures and Controls. University of Colorado. Boulder. CO

Equations of Motion for MBD

$$\delta \mathcal{F}^I + \delta \mathcal{F}^S + \delta \underline{\Phi}^J \cdot \lambda_J + \delta \underline{\Phi}^c \cdot \lambda_c = \delta F^E$$

Inertia: $\delta \mathcal{F}^I = \delta \underline{u}^T \cdot \underline{M} \cdot \ddot{u} + \delta \underline{\alpha}^T \cdot \underline{J} \times \dot{\underline{\omega}} + \delta \underline{\alpha}^T \cdot \underline{J}\,\underline{\omega} \cdot \underline{\omega}$

Stiffness: $\delta \mathcal{F}^S = \delta u^T \cdot \underline{N}_I + \delta \alpha^T \cdot \underline{M}_I$

Joints: $\delta \underline{\Phi}^J = 0$

Constraints: $\delta \underline{\Phi}^c = 0$

External: $\delta F^E = 0$

17

Implementation of MBD

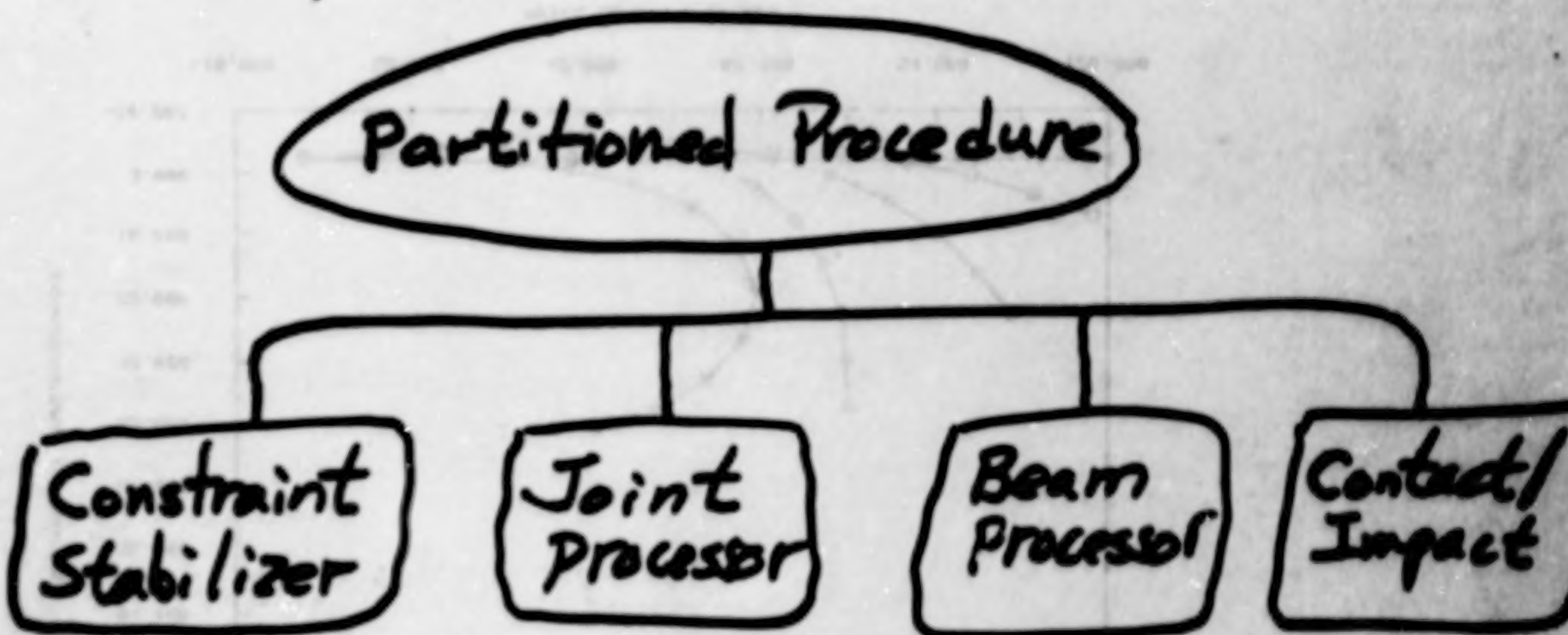

RESEARCH PROGRESS: Multibody Dynamics
(Flexible Beams Undergoing Large Motions)

Cantilever Beam with Tip Follower Force

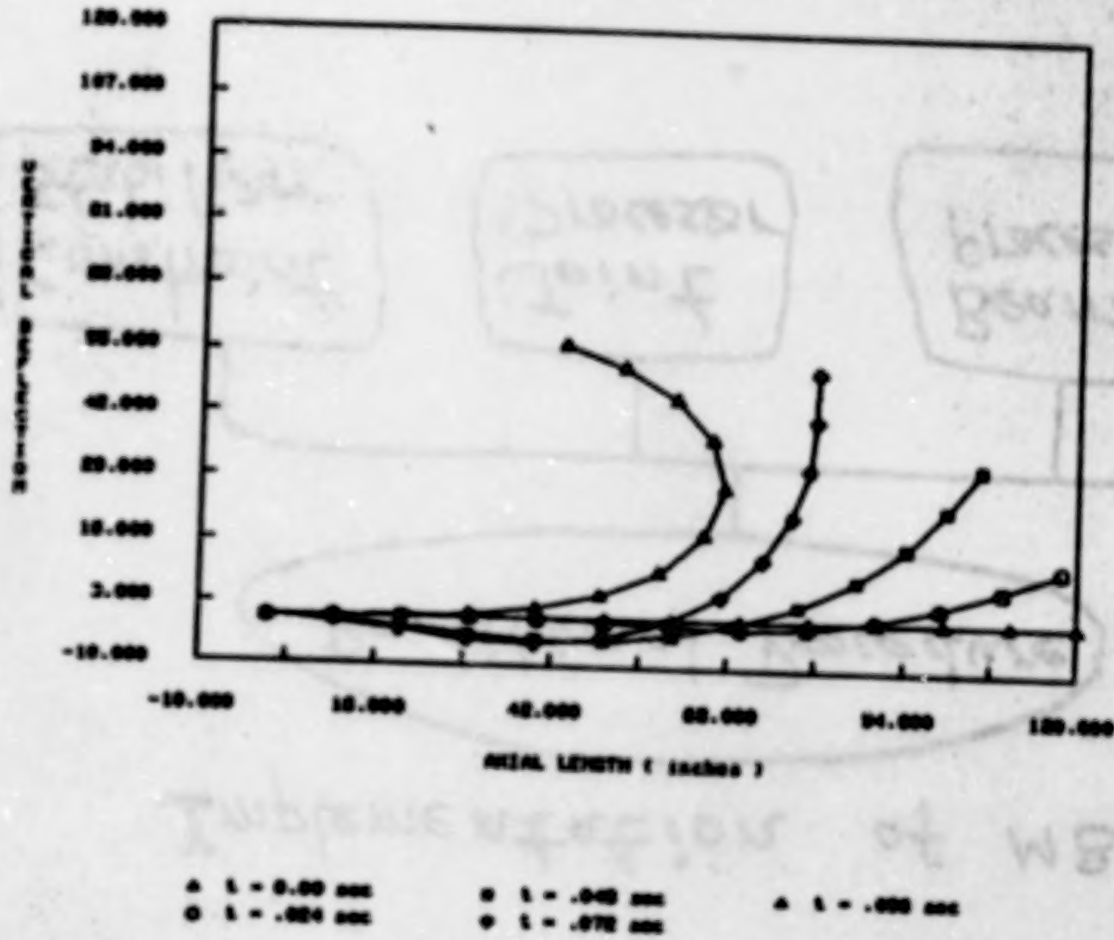

Center for Structures and Controls, University of Colorado, Boulder, CO

19

RESEARCH PROGRESS: Multibody Dynamics
(Flexible Beams Undergoing Large Motions)

A beam formulation that admits large rotational and translational motions has been developed. The beam formulation can be implemented with and/or without transverse shear strains.

Its Specific Features Are:

- When flexibility is negligible, classical rigid-body equations are recovered.
- Translational and angular motions are measured from the inertial and corotational frames, respectively; that is, no coupling between the translational inertia and rotational inertia results.
- Strains are computed directly from total displacements and finite rotation variables; no limitation on the relative magnitudes between rigid and flexible motions is required.

Center for Structures and Controls, University of Colorado, Boulder, CO

RESEARCH PROGRESS: Multibody Dynamics
(Constraint Stabilization and Large Rotation Algorithm)

Sinusoidal Ball Track Mapped on the Sphere

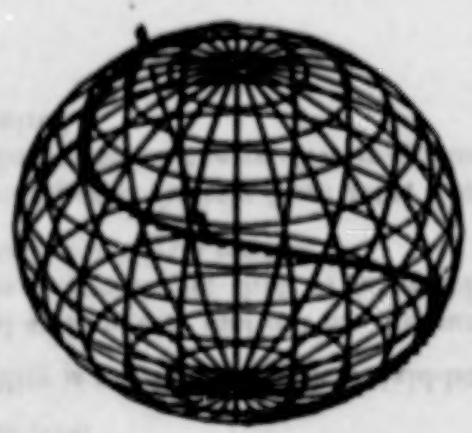

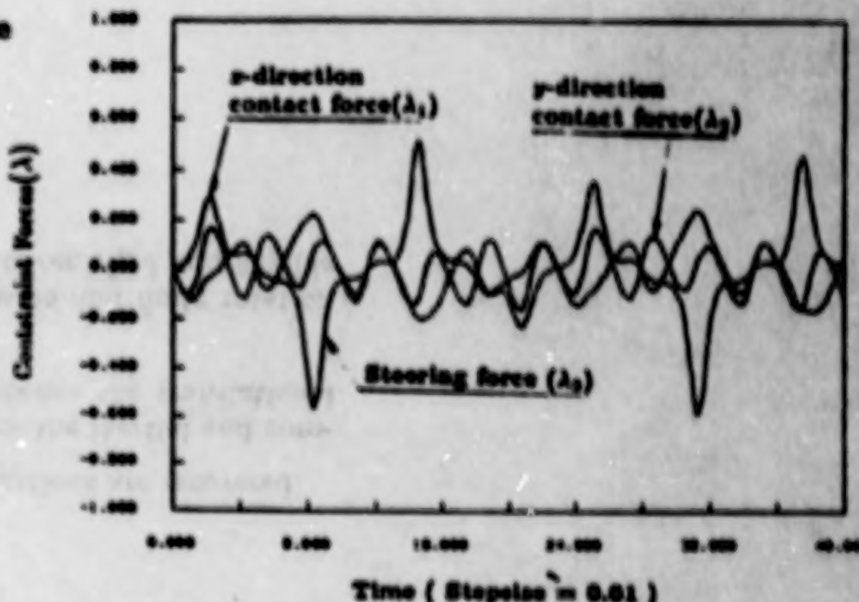

Sphere with Off-Set Center Rolling on a Sinusoidal Curve

Center for Structures and Controls, University of Colorad), Boulder, CO

21

RESEARCH PROGRESS: Multibody Dynamics
(Constraint Stabilization and Large Rotation Algorithm)

A stabilization technique for accurately incorporating both the configuration and motion constraints into the multibody dynamics formalism has been developed. In addition, a computational procedure for updating large rotational motions has been developed.

Specific Features Are:

- **It overcomes singularity difficulty when constraints become linearly dependent within computational precision.**
- **It facilitates a modular solution package for the constraints independent of the solver of the equtions of motion.**
- **It consistently yields more accurate solutions than the Baumgarte technique for problems tested so far.**
- **The large rotational update algorithm computes the translational motions by an explicit integration technique whereas the rotational motions are treated by an implicit integration via the Euler parameters.**

Center for Structures and Controls, University of Colorado, Boulder, CO

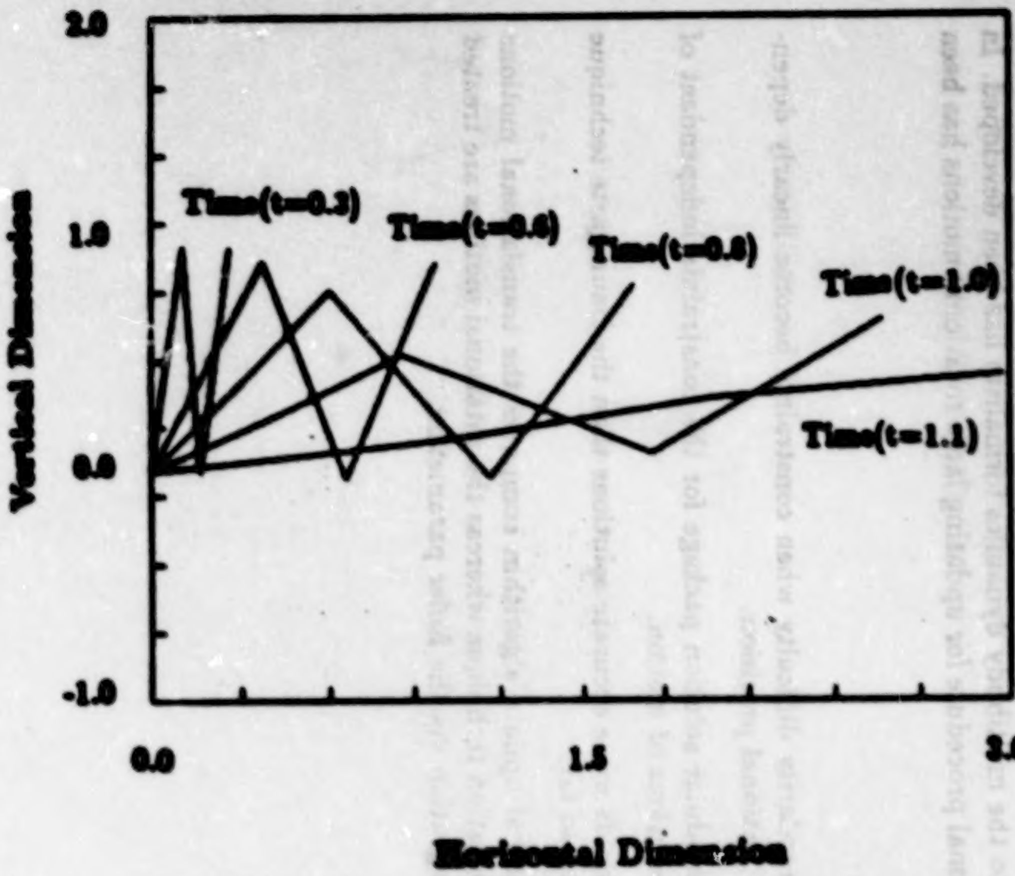

Fig. 6 Deployment of Three-Link Remote Manipulator

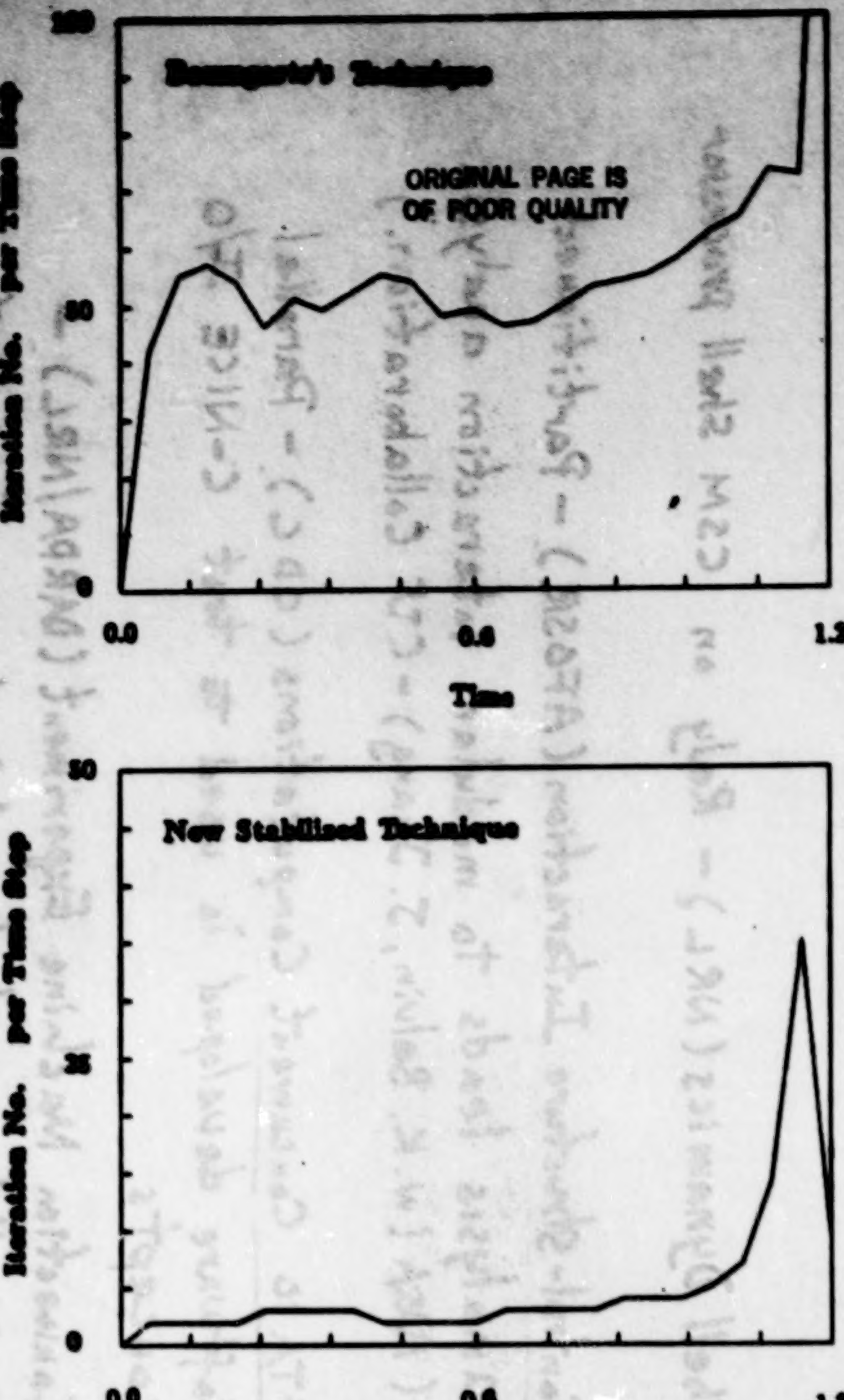

Fig.6 Performance of Two Stabilization Techniques

for Three-Link Remote Manipulator

(Solution Accuracy=10^{-6})

Related Research Activities to CSM at CU

- Shell Dynamics (NRL) – Rely on CSM Shell processor
- Control-Structure Interaction (AFOSR) – Partitioned analysis leads to modular interaction analysis (NASA (W. K. Belvin, J. Juang) – CU Collaboration.)
- ETA10 Concurrent Computations (CDC) – Parallel Software developed is used to test C-NICE I/O concepts
- Connection Machine Experiment (DARPA/NRL) – A Parallel Computational Mechanics Experiment

25

Future Plans (12/87 – 11/88)

- C-NICE :
  - Implement A First Version of Parallel I/O
  - Parallel Control for CRAY-II & Conn. M/C.
  - Source Code Management System (TIM)
- Concurrent Applications Software Tools :
  - Further Experiments with FORCE/CRAY-II UNICOS Multitasking to solve nonlinear dynamics problems.
- Multibody Dynamics :
  - Transform research modules of constraint solver, flexible beams, joints, topology mapping schemes, partitioned procedure into an experimental processor & attempt to implement it into CSM/Testbed.

Future Plans – Cont'd

- Multibody Dynamics :
  - Implement the 5 modules on the Alliant/8 and refine partitioned procedures.

N89

29810

UNCLAS

MULTI-GRID FOR STRUCTURES ANALYSIS

By
Albert F. Kascak
Structural Dynamics Branch, NASA LeRC

Introduction

In structural analysis the amount of computational time necessary for a solution is proportional to the number of degrees of freedom times the bandwidth squared. In implicit time analysis, this must be done at each discrete point in time. If, in addition, the problem is nonlinear, then this solution must be iterated at each point in time. If the bandwidth is large, the size of the problem that can be analyzed is severely limited.

The multi-grid method is a possible algorithm which can make this solution much more computationally efficient. This method has been used for years in computational fluid mechanics. It works on the fact that relaxation is very efficient on the high frequency components of the solution (nearest neighbor interactions) and not very good on low frequency components of the solution (far interactions). The multi-grid method is then to relax the solution on a particular model until the residual stops changing. This indicates that the solution contains the higher frequency components. A coarse model is then generated for the lower frequency components to the solution. The model is then relaxed for the lower frequency components of the solution. These lower frequency components are then interpolated to the fine model.

In computational fluid mechanics the equations are usually expressed as finite differences. To generate a coarse model, the grid size is just doubled and a Green's integral theorem is used to obtain the forcing function on the coarse grid. To transfer the lower frequency solution back to the fine grid, linear interpolation is used.

In structural dynamics the equations are usually expressed as finite elements. Neighbor elements need not be connected. The process of condensing a fine model into a coarse model and interpolating the low frequency solution to the fine model is not clear.

OBJECTIVE: IMPLICIT TIME MARCH SOLUTION OF NONLINEAR STRUCTURAL DYNAMICS

- o BEAM (MULTI-SHAFT, COMBINED LATERAL, TORSIONAL, AND AXIAL ANALYSIS)
- o PLATE (BLADE VIBRATION WITH COULOMB DAMPING))
- o 3-D (SPACE STRUCTURES ANALYSIS)

Objective

The objective of this work is to use an implicit time march solution to study nonlinear structural dynamics. The work will be done in three phases. The first phase will be a beam structure. This will have application in a multi-shaft, combined lateral, torsional, and axial rotor dynamic analysis. The second phase will be a plate structure. This will have application in bladed disk vibration with Coulomb damping. The third phase will be a full 3-D structure. This will have application in space structures.

NUMERICAL INTEGRATION

LET $R(t)$ BE AN n ELEMENT VECTOR OF NODAL DISPLACEMENTS AND

$$V(t) = \dot{R}\ , \quad A(t) = \dot{V}$$

MODIFIED TAYLOR SERIES

$$R(t) = R(0) + V(0)t + \frac{1}{2} A(0)t^2 + \frac{1}{6} \alpha \dot{A}(\xi)t^3$$

$$V(t) = V(0) + A(0)t + \frac{1}{2} \beta \dot{A}(\xi)t^2$$

$$A(t) = A(0) + \dot{A}(\xi)t$$

WHERE

$$0 \leq \xi \leq t$$

AND; α AND β ARE DETERMINED SO THAT THE METHOD IS NUMERICALLY STABLE AS $t \rightarrow \infty$

Numerical Integration

The numerical integration method is based on a Nordsieck-like method. The displacement, velocity, and acceleration are defined at an initial time. A modified Taylor series is used to calculate the displacement, velocity, and acceleration at the advanced time. The Lagrange's remainder term, the time derivative of the acceleration, is calculated from the equations of motion at the advanced time. Alpha and beta are constants determined so that the method is stable as time approaches infinity.

This method of integration for a first order differential equation is Gear's method (Gear, 1971). Zeleznik (1979) showed that this method could be used on higher order equations. Kascak (1980) showed that for a third order integrator used on a linear second order differential equation the method is unconditionally stable.

NUMERICAL STABILITY

$$MA + CV + KR = F$$

$$\left(tM + \frac{1}{2}\beta t^2 C + \frac{1}{6}\alpha t^3 K\right)\mathring{A}(\xi) = F - \left(M + tC + \frac{1}{2}t^2 K\right)A(0) - (C + tK)V(0) - KR(0)$$

$$\text{AS } t \to \infty \qquad \mathring{A}(\xi) \approx -\left(\frac{3}{\alpha t}\right)A(0)$$

$$R = R(0) + V(0)t$$

$$V = V(0) + \left(1 - \frac{3}{2}\left(\frac{\beta}{\alpha}\right)\right)A(0)t$$

$$A = \left(1 - \left(\frac{3}{\alpha}\right)\right)A(0)$$

$$\text{LET } \alpha = 3 \text{ AND } \beta = 2 \;\therefore\; R = R(0) + V(0)t$$

$$V = V(0)$$

$$A = 0$$

Numerical Stability

The numerical stability of this method can be examined by substituting the displacement, velocity, and acceleration into the linear equations of motion and solving for the time derivative of the acceleration. As time approaches infinity the dominate term on both the right and left side of the equation has the stiffness matrix as a pre-multiplier. The time derivative of the acceleration is proportional to the initial acceleration divided by the time. If this is substituted into the modified Taylor series, and alpha is set to 3 and beta is 2: the acceleration is zero and the velocity is constant. The eigenvalues become zero and one.

ITERATIVE SOLUTION

GIVEN: $R(0),\ V(0),\ A(0),$ AND $\dot{A}(\xi) \sim \dot{A}^{(0)}$

THEN: $R^{(0)} = R(0) + V(0)t + \frac{1}{2} A(0)t^2 + \frac{1}{2} \alpha \dot{A}^{(0)} t^3$

$V^{(0)} = V(0) + A(0)t + \frac{1}{2} \beta \dot{A}^{(0)} t^2$

$A^{(0)} = A(0) + \dot{A}^{(0)} t$

LET: $\dot{A}(\xi) = \dot{A}^{(0)} + \Delta \dot{A}$

THEN: $R(t) = R^{(0)} + \frac{1}{6} \alpha \Delta \dot{A} t^3$

$V(t) = V^{(0)} + \frac{1}{2} \beta \Delta \dot{A} t^2$

$A(t) = A^{(0)} + \Delta \dot{A} t$

Iterative Solution

If the initial displacement, velocity, acceleration, and an initial estimate of the time derivative of the acceleration are given, then an estimate of the advanced displacement, velocity, and acceleration is given by the modified Taylor series. The correction to the time derivative of the acceleration can be found from the equations of motion.

NONLINEAR EQUATION OF MOTION

$$0 = F(R, V, A, t)$$

WHERE F IS AN n ELEMENT VECTOR SUM OF THE STATIC AND DYNAMIC FORCES

THEN: $$0 = F\left(R^{(0)} + \frac{1}{6}\alpha\Delta\dot{A}t^3,\ V^{(0)} + \frac{1}{2}\beta\Delta\dot{A}t^2,\ A^{(0)} + \Delta\dot{A}t, t\right)$$

OR: $$0 = F(\Delta\dot{A})$$

Nonlinear Equations of Motion

The nonlinear equations of motion are the sum of both the static and dynamic forces for each element. As such, the equations are functions of the displacement, velocity, acceleration, and time. If the modified Taylor series is substituted into the equations of motion using the iterative form, then the equations of motion become a function of the correction to the time derivative of the acceleration.

LINEARIZED EQUATION OF MOTION

$$0 = F^{(0)} - B\Delta\mathring{A}$$

WHERE

$$F^{(0)} = F(R^{(0)}, V^{(0)}, A^{(0)}, t)$$

$$B = \frac{1}{6}\alpha t^3 K + \frac{1}{2}\beta t^2 C + tM$$

$$K = -\frac{\partial F}{\partial R}, \quad C = -\frac{\partial F}{\partial V}, \quad M = -\frac{\partial F}{\partial A}$$

$$\therefore \; B\Delta\mathring{A} = F^{(0)}$$

Linearized Equations of Motion

To solve for the correction, the equations of motion are linearized about the estimated values. The instantaneous stiffness, damping, and mass are defined by the various partial derivatives wth respect to displacement, velocity, and acceleration. If the linearization is done numerically, the stiffness, damping, and mass don't have to be calculated. The numerical differentiation of the correction to the time derivative of the acceleration is all that is needed.

This solution procedure is equivalent to the Newton-Raphson technique. The numerical differentiation and the solution of the linearized equations of motion are computationally time consuming, although straight-forward. The multi-grid technique could potentially be orders of magnitude faster. The linearized equations of motion will be the basis for generating a coarse model from a fine model.

STATIC CONDENSATION

$$\left[\begin{array}{c:c} B_{11} & B_{12} \\ \hdashline B_{21} & B_{22} \end{array}\right]\left[\begin{array}{c} \Delta\dot{\mathring{A}}_1 \\ \hdashline \Delta\dot{\mathring{A}}_2 \end{array}\right] = \left[\begin{array}{c} F_1^{(0)} \\ \hdashline F_2^{(0)} \end{array}\right]$$

$$\left(B_{11} - B_{12}B_{22}^{-1}B_{21}\right)\Delta\dot{\mathring{A}}_1 = F_1^{(0)} - B_{12}B_{22}^{-1}F_2^{(0)}$$

$$\Delta\dot{\mathring{A}}_2 = B_{22}^{-1}\left(F_2^{(0)} - B_{21}\Delta\dot{\mathring{A}}_1\right)$$

$$\text{LET } B^{(1)} = B_{11} - B_{12}B_{22}^{-1}B_{21}, \quad F^{(1)} = F_1^{(0)} - B_{12}B_{22}^{-1}F_2^{(0)}$$

$$\therefore B^{(1)}\Delta\dot{\mathring{A}}_1 = F^{(1)}$$

$$\text{IF } F_2^{(0)} = 0 \Rightarrow \Delta\dot{\mathring{A}}_2 = -B_{22}^{-1}B_{21}\Delta\dot{\mathring{A}}_1 \text{ (INTERPOLATOR)}$$

Structural Condensation

If the linearized equation set is partitioned into nodes belonging to a coarse model (the top partition) and the nodes eliminated from the fine model (the bottom partition), then structural condensation can be used to solve for the coarse model. In addition, the structural condensation process can be used to interpolate the solution from the coarse model to the fine model. If the higher frequency part of the solution is found on the fine model and the lower frequency part of the solution is found on the coarse model, then the resultant forces must be zero. Thus the solution for the nodes eliminated from the fine model can be found.

FINE-TO-COARSE MODEL TRANSFORMATION

$$\Phi = \begin{bmatrix} I \\ \hline -B_{22}^{-1}B_{21} \end{bmatrix} \Rightarrow \Delta\dot{A} = \Phi\Delta\dot{A}_1$$

COARSE-TO-FINE MODEL TRANSFORMATION

$$\theta = \left[\begin{array}{c|c} I & -B_{12}B_{22}^{-1} \end{array}\right] \Rightarrow F^{(1)} = \theta F^{(0)}$$

$$\therefore\ B\dot{A} = F^{(0)} \Rightarrow \theta B\Phi\Delta\dot{A}_1 = \theta F^{(0)}$$

OR

$$B^{(1)}\Delta\dot{A}_1 = F^{(1)}$$

Fine-to-Coarse and Coarse-to-Fine Model Transformations

The fine-to-coarse model transformation is a rectangular matrix which averages the force from the fine model to the coarse model. The upper partition is an identity matrix and the lower partition is defined in the structural condensation process. The coarse-to-fine transformation interpolates the correction of the time derivative of the acceleration from the coarse to fine model. In the symmetric case, the fine-to-coarse transformation is the transpose of the coarse-to-fine transformation.

NONLINEAR CONDENSATION

$$0 = F(\Delta\mathring{A}) \Rightarrow 0 = \theta F(\Phi\Delta\mathring{A}_1)$$

RELAXATION

$$0 = \theta F^{(0)} - D\Delta\mathring{A}_1 \Rightarrow \Delta\mathring{A}_1 = D^{-1}F^{(1)}$$

Nonlinear Condensation

The nonlinear condensation process transforms the independent variables from the coarse model to the fine model and the dependent variables from the fine to coarse model. Thus the resultant forces are relaxed on the coarse model. This would only require the inversion of a diagonal matrix. The corrections on the coarse model are then interpolated to the fine model. The linearization of the equations of motion is not needed in the solution process, but only needed to define the transformations.

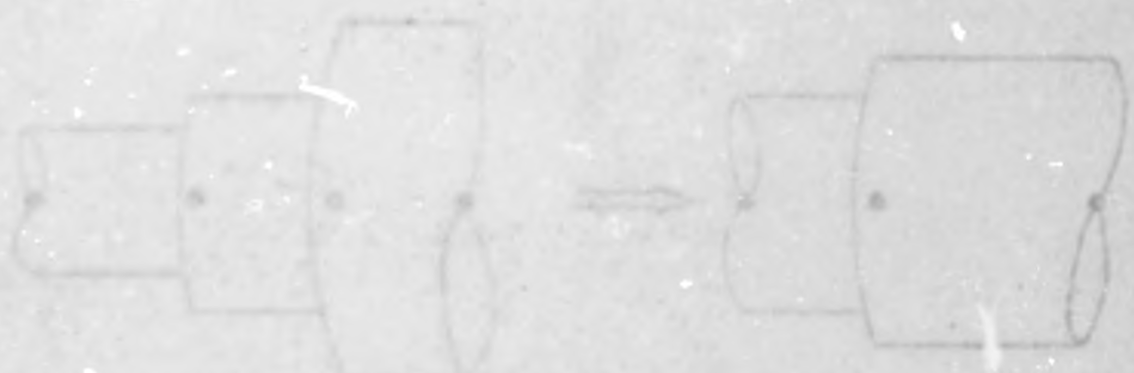

LOCAL STRUCTURAL CONDENSATION

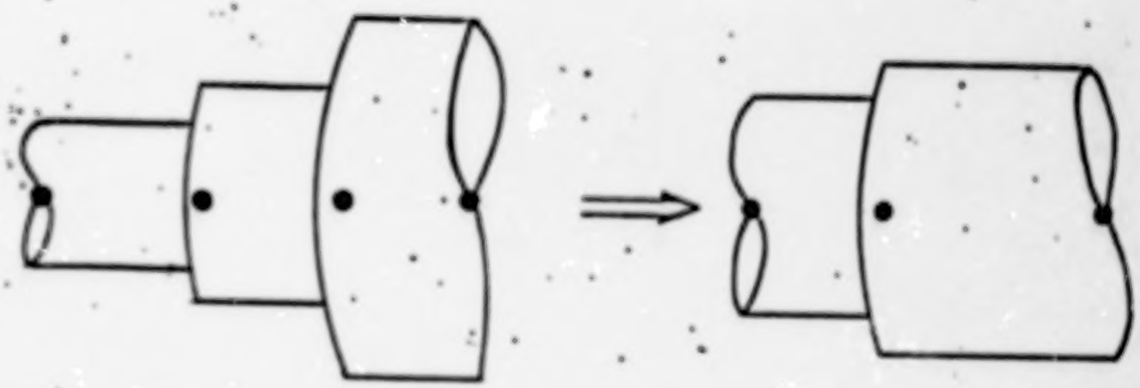

B IS BLOCK TRIDIAGONAL -- INCLUDES NEAREST NEIGHBOR INTERACTION, NEGLECT FAR INTERACTION

Local Structural Condensation

The linearization of the equations of motion and the structural condensation process require a considerable amount of computational time. Multi-grid via relaxation is most efficient on nearest neighbor interactions. Thus only a partial linearization of the equations of motion is necessary. The equations of motion only have to be linearised with respect to the node under consideration and its nearest neighbors. Applying condensation to this local interaction model results in local structural condensation. In the case of a beam, this linearization results in a block tridiagonal matrix and the structural condensation results in a coarse model in which every other node is removed from the fine model.

$$
\begin{pmatrix}
V_1 & W_1 & & & & & & & \\
U_2 & V_2 & W_2 & & & & & \bigcirc & \\
 & U_3 & V_3 & W_3 & & & & & \\
 & & U_4 & V_4 & W_4 & & & & \\
 & & & U_5 & V_5 & W_5 & & & \\
 & & & & U_6 & V_6 & W_6 & & \\
\bigcirc & & & & & U_7 & V_7 & W_7 & \\
 & & & & & & U_8 & V_8 & W_8 \\
 & & & & & & & U_9 & V_9
\end{pmatrix}
\begin{pmatrix}
\Delta\dot{A}_1 \\ \Delta\dot{A}_2 \\ \Delta\dot{A}_3 \\ \Delta\dot{A}_4 \\ \Delta\dot{A}_5 \\ \Delta\dot{A}_6 \\ \Delta\dot{A}_7 \\ \Delta\dot{A}_8 \\ \Delta\dot{A}_9
\end{pmatrix}
=
\begin{pmatrix}
F_1 \\ F_2 \\ F_3 \\ F_4 \\ F_5 \\ F_6 \\ F_7 \\ F_8 \\ F_9
\end{pmatrix}
\qquad B\Delta\dot{A} = F^{(0)}
$$

$$
\left(\begin{array}{cccc|ccccc}
V_2 & \bigcirc & & & U_2 & W_2 & & \bigcirc & \\
 & V_4 & & & & U_4 & W_4 & & \\
\bigcirc & & V_6 & & \bigcirc & & U_6 & W_6 & \\
 & & & V_8 & & & & U_8 & W_8 \\
\hline
W_1 & & \bigcirc & & V_1 & & & & \\
U_3 & W_3 & & & & V_3 & & \bigcirc & \\
 & U_5 & W_5 & & & & V_5 & & \\
\bigcirc & & U_7 & W_7 & \bigcirc & & & V_7 & \\
 & & & U_9 & & & & & V_9
\end{array}\right)
\left(\begin{array}{c}
\Delta\dot{A}_2 \\ \Delta\dot{A}_4 \\ \Delta\dot{A}_6 \\ \Delta\dot{A}_8 \\ \hline \Delta\dot{A}_1 \\ \Delta\dot{A}_3 \\ \Delta\dot{A}_5 \\ \Delta\dot{A}_7 \\ \Delta\dot{A}_9
\end{array}\right)
=
\left(\begin{array}{c}
F_2 \\ F_4 \\ F_6 \\ F_8 \\ \hline F_1 \\ F_3 \\ F_5 \\ F_7 \\ F_9
\end{array}\right)
\qquad
\left(\begin{array}{c|c}
B_{11} & B_{12} \\ \hline B_{21} & B_{22}
\end{array}\right)
\left(\begin{array}{c}
\Delta\dot{A}_1 \\ \hline \Delta\dot{A}_2
\end{array}\right)
=
\left(\begin{array}{c}
F_1^{(0)} \\ \hline F_2^{(0)}
\end{array}\right)
$$

C-5

Beam Example

If the tridiagonal equation set is re-ordered into even-numbered in both the fine and coarse model (top) and odd-numbered just in the fine model (bottom), then the structural condensation has a simple form. In the re-ordered equation set, the block matrices on the diagonal are diagonal. The inversion of these block matrices is trivial.

$$-B_{22}^{-1}B_{21} = \begin{pmatrix} T_1 & & & \\ S_2 & T_2 & & \\ & S_3 & T_3 & \\ & & S_4 & T_4 \\ & & & S_5 \end{pmatrix} \qquad \begin{array}{l} T_L = -V_{2L-1}^{-1}W_{2L-1} \\ \\ S_L = -V_{2L-1}^{-1}U_{2L-1} \end{array}$$

$$-B_{12}B_{22}^{-1} = \begin{pmatrix} X_1 & Y_1 & & & \\ & X_2 & Y_2 & & \\ & & X_3 & Y_3 & \\ & & & X_4 & Y_4 \end{pmatrix} \qquad \begin{array}{l} X_L = -U_{2L}V_{2L-1}^{-1} \\ \\ Y_L = -W_{2L}V_{2L+1}^{-1} \end{array}$$

$$B_{11} - B_{12}B_{22}^{-1}B_{21} = \begin{pmatrix} V_1^{(1)} & W_1^{(1)} & & \\ U_2^{(1)} & V_2^{(1)} & W_2^{(1)} & \\ & U_3^{(1)} & V_3^{(1)} & W_3^{(1)} \\ & & U_4^{(1)} & V_4^{(1)} \end{pmatrix} \qquad \begin{array}{l} V_L^{(1)} = V_{2L} + X_LW_{2L-1} + Y_LU_{2L+1} \\ \\ U_L^{(1)} = +X_LU_{2L-1} \\ \\ W_L^{(1)} = +Y_LW_{2L+1} \end{array}$$

$$\Delta\dot{A}_{2L} = \Delta\dot{A}_L^{(1)} \quad , \quad \Delta\dot{A}_{2L-1} = S_L\Delta\dot{A}_{L-1}^{(1)} + T_L\Delta\dot{A}_L^{(1)}$$

$$F_L^{(1)} = F_{2L} + X_LF_{2L-1} + Y_LF_{2L+1}$$

Solution of Beam Example

The solution for the non-identity partition of both transformations is tridiagonal. The non-identity partition of the fine-to-coarse transformation is also lower triangular. The non-identity partition of the coarse-to-fine transformation is also upper triangular.

ACCALERATION PARAMETER

$\epsilon\ (\ |\lambda|\ )$ - based on local coefficients

$$\lambda = \frac{(\Delta \dot{\vec{A}})^T D (\Delta \dot{\vec{A}})}{(\Delta \dot{\vec{A}})^T (\Delta \dot{\vec{A}})}$$

(Rayleigh Quotient)

Acceleration Parameter

Normally the relaxation technique can be improved by using a weighted average of the previous and calculated values of the corrections to the solution (over relaxation). The rate of convergence of the high frequency components can be improved at the expense of the low frequency components. To do this an estimate of highest frequency eigenvalue is needed. The Rayleigh quotient is a good method to estimate the highest eigenvalue (at least in the symmetric case). In addition, the highest eigenvalue should be a strong function of the nearest neighbors; therefore, local linearization could be used in the Rayleigh quotient.

MULTI GRID METHOD

- o RELAX ON FINE GRID TO GET HIGH FREQUENCY COMPONENT
- o CALCULATE RESIDUAL ON FINE GRID
- o CHECK RESIDUAL FOR SOLUTION
- o CHECK CHANGE IN RESIDUAL FOR CHANGE IN GRID
- o STATIC CONDENSE TO COARSE GRID
- o RELAX ON COARSE GRID TO GET LOW FREQUENCY COMPONENT
- o INTERPOLATE LOW FREQUENCY TO FINE GRID

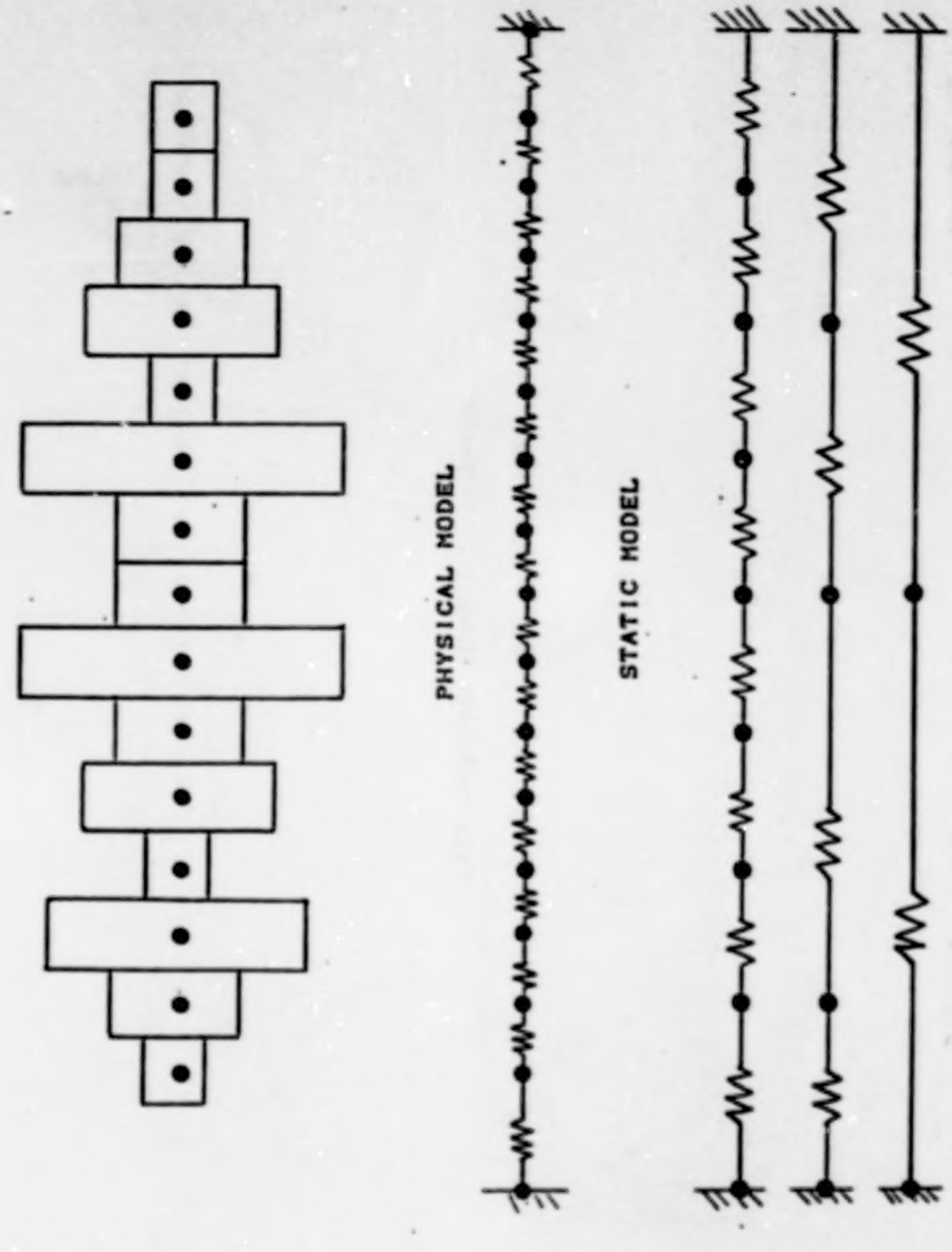

PAGE 1161 INTENTIONALLY BLANK

PRECEDING PAGE BLANK NOT FILMED

Multi-Grid Method

In summary, the multi-grid method for structural dynamics is first to relax the equations of motion on the fine grid to obtain the high frequency components of the solution. Then calculate the norm of the residual on the fine model. Next check to see if the norm is small enough for a solution. If not, check to see if the norm has changed significantly from the previous iteration. If the norm has changed, then relax the solution until the norm stops changing. This indicates that the high frequency components on this model have been found.

To find the lower frequency components of the solution, local structural condensation is used to generate a coarse model. On the coarse model, relaxation is used to generate the lower frequency components of the solution. These lower frequency components are interpolated to the fine grid where the norm of the residual is calculated. Based on this norm, either a solution is found, more relaxation is needed, or a coarser model is needed. The process is repeated until a solution is found.

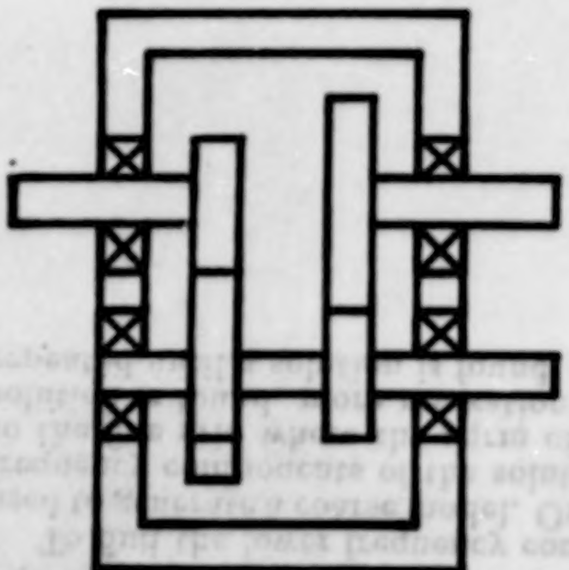

PHYSICAL MODEL

NONLINEAR FINITE ELEMENT MODEL

Multi-Grid Analysis Applied to Transmission Dynamics

Transmission dynamics is a case of nonlinear structural dynamics. Physically a transmission is composed of gears, shafts, bearings, seals, and a case. The case and the shafts can be modeled by finite element methods. The bearings and seals are modeled by special programs developed in tribology and other areas. Gear interactions are developed for some kind of gears, but not for others. Thus, a transmission can be modeled by a number of linear and nonlinear finite elements. As a first approximation, a transmission can be modeled as a beam structure. The transmission can be analyzed as a multi-shaft, combined lateral, torsional, and axial rotor dynamic system.

SPECIAL ASPECTS

- Gyroscopic and gear forces cause nonlinear lateral and torsional coupling.

- Gear tooth pass frequencies are high frequency forcing functions. This implies a need for a fine structural model.

- Gear - gear interactions cause a wide band width.

Special Aspects

Special aspects complicate the dynamic analysis of transmissions. Gyroscopic and gear forces cause nonlinear lateral and torsional coupling. Gear tooth passing frequencies are high frequency forcing functions. This implies a need for a fine structural model. Gear-gear interactions cause the system to have a wide bandwidth.

GEAR TOOTH INTERACTION

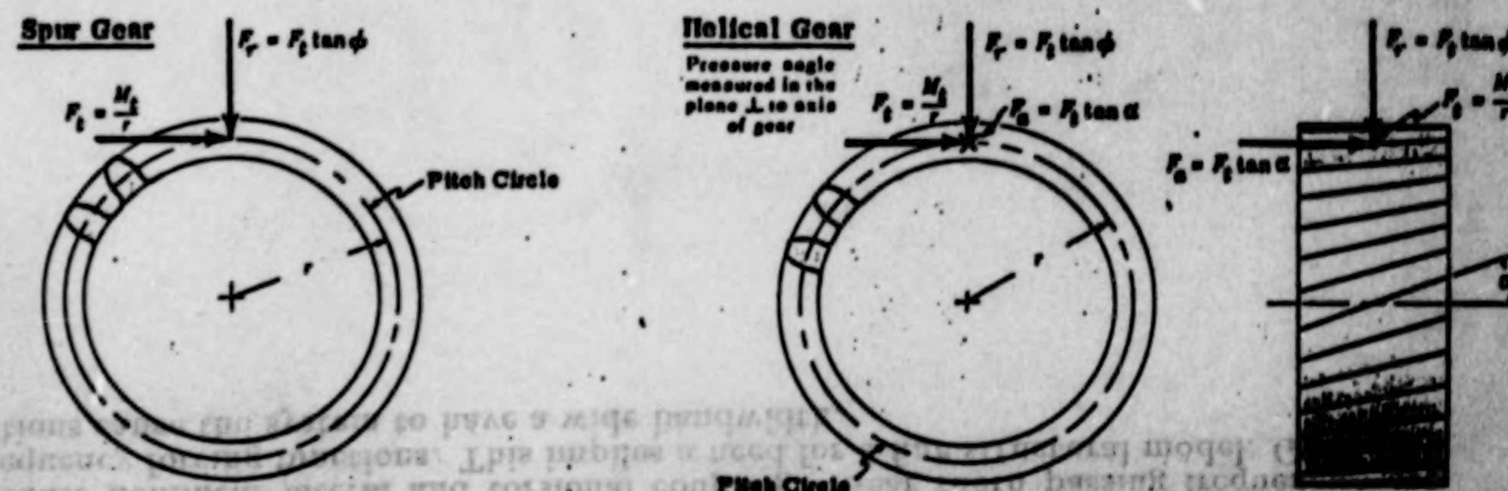

Gear Tooth Interaction

Consider gear tooth interaction. For any gear set the line of force does not pass through the gear centers. In the case of spur gears any perturbation of the radial force will result in a perturbation of the tangential force and vice versa. In the case of helical or spiral gears any perturbation of the radial force will result in perturbations of both the axial and tangential forces. This results in a nonlinear coupling between the axial, tangential, and radial directions.

GEAR TOOTH MODEL

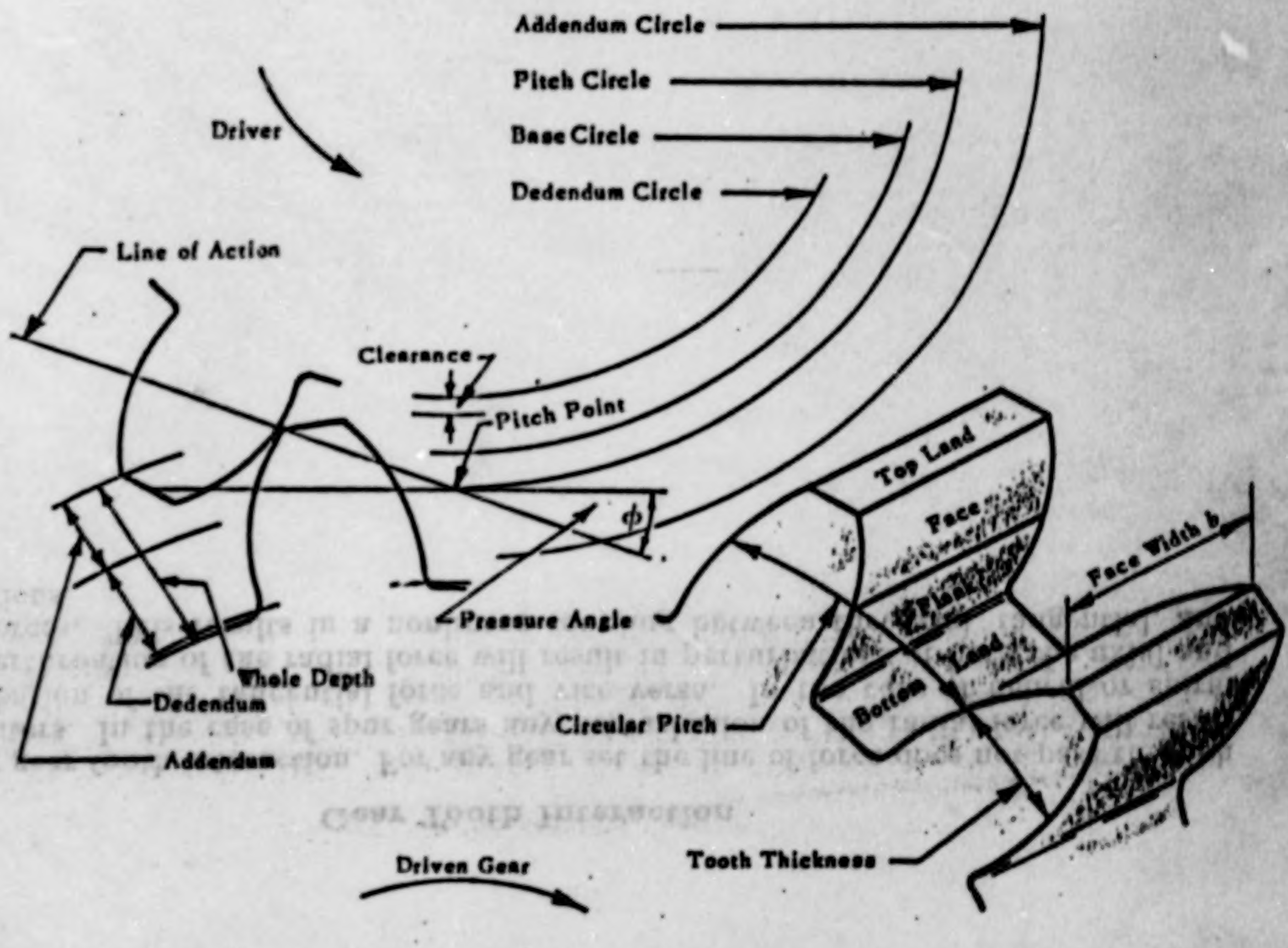

ORIGINAL PAGE IS
OF POOR QUALITY

Gear Tooth Model

Consider the gear tooth interactions of a spur gear set. The contact point varies as the angle of the gear set varies. Machining errors cause the contact point to move. High torque can cause the teeth to bend. The number of teeth in contact varies as the torque varies. Negative torque can result in backlash. The force must be transmitted through the contact point. All these effects cause nonlinear time varying interactions between the spur gears set. For the other kind of gears the interaction is more complicated. Thus, gear tooth interactions cause high frequency forcing functions on the structure.

TYPICAL TRANSMISSION

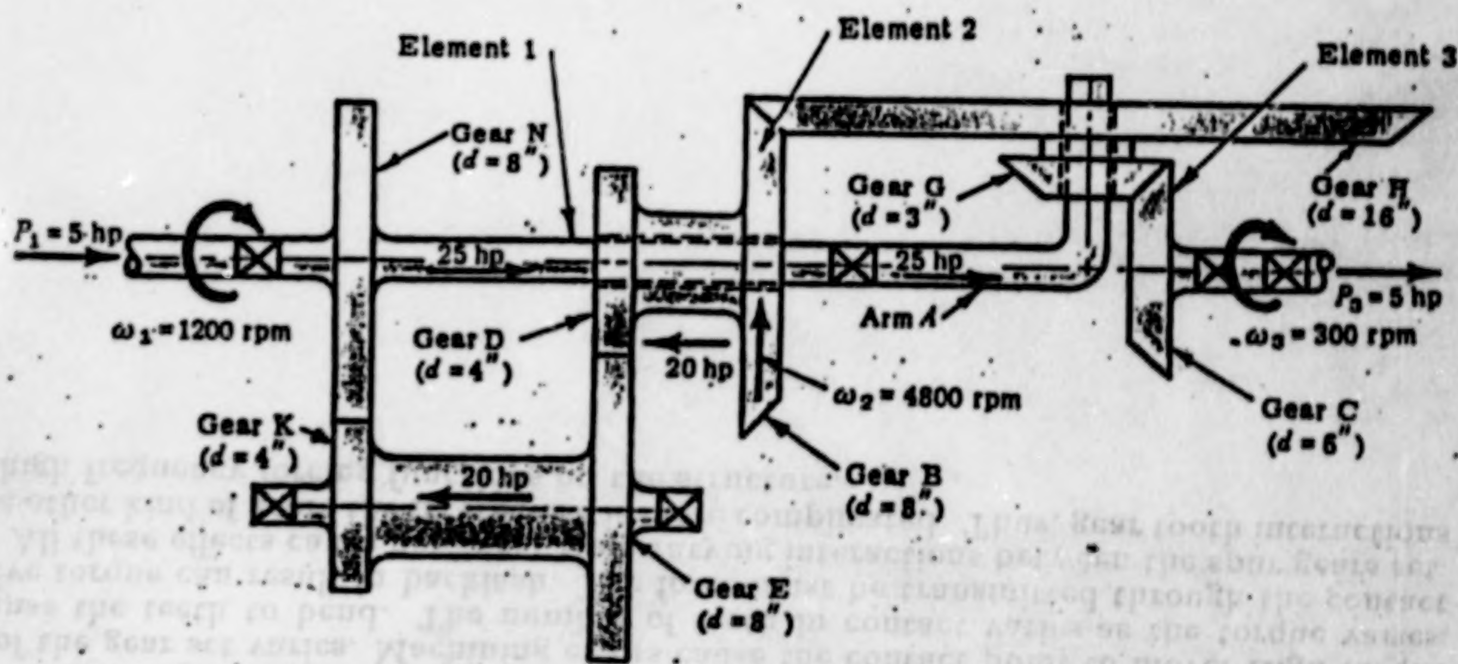

ORIGINAL PAGE IS
OF POOR QUALITY

Typical Transmission

In a typical transmission there are many gear sets. Each of these gear sets causes one location on the structure to interact with another point on the structure. Thus, far interactions are important and the structural model has a wide bandwidth.

Transmission Dynamic Analysis

Complete transmission dynamic analyses are rare in the open literature. David and Mitchell (1986) have used a modal balance technique. The problem with modal techniques is that the nonlinearities cause the set of modes not to be closed. This results in side bands around the tooth passing frequency. Whenever a solution is found, it is not known whether all of the important modes in the solution have been included. Also, superfluous modes tend to overwhelm the solution technique. The time march multi-grid method should eliminate these problems.

APPLICATION OF MULTIGRIDDING TECHNIQUES TO STRUCTURAL ANALYSIS USING A PARALLEL TRANSPUTER ARRAY

A. F. KASCAK (ANALYSIS)

L. J. KIRALY (ARCHITECTURE)

E. H. MEYN (HARDWARE)

J. D. GUPTILL (SOFTWARE)

Application of Multi-Grid Techniques To Structural Analysis Using a Parallel Transputer Array

A large number of multi-grid computational steps can be done in parallel. A new parallel computing system based on the transputer chip has recently become available. The transputer chip is a self-contained high performance computer. Separate processors within the transputer chip perform normal computations, manage memory, perform floating point arithmetic functions, and manage communications with other transputers concurrently. Many transputers can be linked together to form a parallel processing computer network by simply connecting serial communication links between transputers. A team has been assembled to apply the multi-grid technique to this transputer array.

OBJECTIVE

TIME MARCH SOLUTION OF NONLINEAR STRUCTURAL DYNAMICS

- o BEAM (MULTI-SHAFT - COMBINED LATERAL, TORSIONAL AND AXIAL ANALYSIS)
- o PLATE (BLADE VIBRATION WITH COULOMB DAMPING)
- o 3-D (SPACE STRUCTURES ANALYSIS)

RELATED WORK

- o MULTIGRID ANALYSIS USED IN FLUID DYNAMICS BUT NOT IN STRUCTURAL DYNAMICS
- o TRANSPUTER USED IN STRUCTURAL STATICS, (SPARTA)
- o TRANSPUTER USED IN GRAPHICAL DISPLAY, G. K. ELLIS (ICOMP)

Objective

The objective of this research is to take the serial codes developed for multi-grid technique applied to the beam, plate, and 3-D brick elements and apply them to the parallel transputer array.

Related Work

The multi-grid analysis has been used in fluid dynamics for years, but not in structural dynamics. The transputer is currently being applied to static structural problems using a direct or wave front technique. In addition, the transputer is being used to process graphical displays. This graphical display work is being done on a transputer test bed system. The test bed system is designed to be electronically reconfigured into a variety of different equivalent architectures so that the interplay between algorithms and architectures can be fully explored.

APPROACH

USE "OCCAM" PARALLEL PROGRAMMING LANGUAGE AND ELECTRONICALLY RE-CONFIGURE ARCHITECTURE TO ASSESS VARIOUS APPROACHES TO STRUCTURAL MULTIGRID ANALYSIS

- NUMERICAL STABLE TIME INTEGRATION
- LOCAL STRUCTURAL CONDENSATION TO OBTAIN INTERPOLATION FROM COARSE TO FINE MODEL AND AVERAGE FINE TO COARSE MODEL
- RELAX EACH NODE WITH ONE CPU FOR EACH DEGREE OF FREEDOM

Approach

The approach is to use an "OCCAM" parallel programming language (specifically designed for the transputer) and the test bed (with electronically reconfigurable architectures) to assess their application to structural dynamic multi-grid analysis. Areas which can profit from parallel computations are the time step advancement, the coarse-to-fine and fine-to-coarse transformations, and the relaxation process.

POTENTIAL IMPACT

- o DEMONSTRATION OF A NEW APPROACH TO STRUCTURAL DYNAMIC SIMULATIONS WITH A RECONFIGURABLE PARALLEL ARCHITECTURE WHICH CAN DRAMATICALLY REDUCE THE COST AND COMPUTING TIME

Potential Impact

The multi-grid method, although used for years in fluid dynamics, now offers a new approach to nonlinear structural dynamics. The computing time does not depend on the cube of the number of degrees of freedom. Thus, dramatic reductions in computing time are possible. In addition, the relaxation process is applicable to parallel computation. Thus, the method is very attractive for future computers.

References

David, J. W. and Mitchell, L. D., 1986, "Linear Dynamic Coupling in Geared Rotor Systems", *Transactions of the ASME, Journal of Vibration, Acoustics, Stress, Reliability in Design*, Vol. 108, pp. 171-176.

Gear, C. W., 1971, *Numerical Initial Value Problems in Ordinary Differential Equations*, Prentice-Hall Inc.

Kascak, A. F., 1980, *The Response of Turbine Engine Rotors to Interferences Rubs*, NASA TM-81518.

Zeleznik, F. J., 1979, "Personal Communication at the Lewis Research Center, NASA".

NASA

Report Documentation Page

1. Report No. NASA CP-10012, Part 3	2. Government Accession No.	3. Recipient's Catalog No.
4. Title and Subtitle NASA Workshop on Computational Structural Mechanics - 1987		5. Report Date February 1989
		6. Performing Organization Code
7. Author(s) Nancy P. Sykes, Editor		8. Performing Organization Report No.
		10. Work Unit No. 505-63-01-10
9. Performing Organization Name and Address NASA Langley Research Center Hampton, VA 23665-5225		11. Contract or Grant No.
		13. Type of Report and Period Covered Conference Publication
12. Sponsoring Agency Name and Address National Aeronautics and Space Administration Washington, DC 20546-0001		14. Sponsoring Agency Code

15. Supplementary Notes

Nancy P. Sykes: Analytical Services and Materials, Inc., Hampton, Virginia.

16. Abstract

This conference publication contains the proceedings of the Workshop on Computational Structural Mechanics held at NASA Langley Research Center, November 18-20, 1987. The workshop was sponsored jointly by NASA Langley Research Center and NASA Lewis Research Center.

The workshop was organized into the following three sessions:

(1) Concurrent Processing Methods and Applications
(2) Advanced Methods & Testbed/Simulator Development
(3) Computational Dynamics

17. Key Words (Suggested by Author(s))	18. Distribution Statement
Parallel Processing Computational Dynamics Testbed Computational Structural Mechanics	Unclassified - Unlimited Subject Category 39

19. Security Classif. (of this report)	20. Security Classif. (of this page)	21. No. of pages	22. Price
Unclassified	Unclassified	428	A19

END

DATE

FILMED

DEC 6 1989